Identification And Characterisation Of Novel Iron Acquisition Mechanisms in *Sinorhizobium meliloti* 2011 and *Pseudomonas aeruginosa.*

Páraic Ó Cuív

Ph D. 2003

Identification And Characterisation Of Novel Iron Acquisition Mechanisms in *Sinorhizobium meliloti* 2011 and *Pseudomonas aeruginosa*.

Thesis

Presented for the Degree of

DOCTOR OF PHILOSOPHY

by Páraic Ó Cuív

under the supervision of Michael O'Connell, B. Sc., Ph.D.

School Of Biotechnology

Dublin City University

August 2003

I hereby certify that this material, which I now submit for assessment on the programme of study leading to the award of Degree of Doctor of Philosophy, is entirely my own work and has not been taken from the work of others save and to the extent that such work has been cited and acknowledged within the text of my own work.

Signed: Pádraic Ó Cuív ID No: 95458328

Date: 17th - MF - 2003

Acknowledgements

Ba mhaith liom buíochas ó chroí a ghabháil leis an Dr. Michael O'Connell as an gcabhair agus treoir i rith an tionscanamh Ph.D seo. Thug sé an saoirse dom mo chuid smaointe a fhorbairt agus mo chuid oibre a dhéanamh go neamspleach, ach choinnigh se dírithe ar an bpríomh aidhm i gcónaí mé. Buíochas freisin as ucht na ndeiseanna a fuair mé taisteal thar lear le ceithre bliana anuas.

Ba mhaith liom buíochas a ghabháil le chuile dhuine a bhí sa saotharlann liom le cheithre bliana anuas, go mór mhór an Dr. Paul Clarke a chuir comhairle orm ó lá go lá agus a bhí in-ann smaoineamh ar bhreis oibre dom chuile lá. Ba mhaith liom buíochas a ghabháil le Roman as ucht an chraic agus na leabhra agus le Caroline....Tiocfaidh do lá! Ba mhaith liom aitheantas a thabhairt freisin do fhoireann Scoil An Bhiththeicneolaíocht. Chomh maith leis seo, ba mhaith liom aitheantas ar leith a thabhairt do mhicléinn Scoil An Bhiththeicneolaíocht, go mór mhór dóibh súid a rinne an chéim liom.

Buíochas ar leith do na leaids a bhí ina gcónaí liom le h-ocht mbliana anuas; Ado, Mike, James agus Johnny (Refresher); agus i Phibsboro le Colm (Candyman), Darragh (Gimli), Michelle agus Joanne. Buíochas mór le Pat a thosaigh an chéim liom ar an lá ceanna ocht mbliana ó shin, a thosaigh an iarchéim liom ar an lá céanna cheithre bliana ó shin, agus a chriochnaigh liom ar an lá céanna, ag an am céanna, sa seomra céanna ar an dara lá de mhí Mhéan Fómhair 2003. Ta chuile eachtra spóirt, polatíocht agus rl. pléite againn ar ár siúlóid laethúil agus tá mé tar éis foghlaim faoi 'Protein Purification' gan é a dhéanamh fiú!

Ba maith liom buíochas a ghabháil le mo chlann uilig go mór mhór Mamó, Máire agus Bríd as ucht an bhia, lóistín agus an comhrá. Ba mhaith liom buíochas a ghabháil freisin le Brían, Emer agus Éamon. Réitigh Brian mo chuid béilithe dom agus thug sé a charr ar iasacht dom nuair a bhí mé fé bhrú ama agus rinne sé cinnte gur thug mé aire dom féin. Go raibh míle maith agat. Buíochas freisin Emer agus Éamon as ucht na cuairteanna agus glaochanna teileafón. Ba maith liom buíochas mór millteach a ghabháil le Daid agus Mam as ucht an tacaíocht uilig thar na blianta; ó'n gcéad lá a shúil mé isteach sa naíscoil i gCorr na Móna go dtí anois agus me críochnaithe san ollscoil. Ni bheith me in-ann é a dhéanamh gan bhur gcuid tacaíochta agus grá.

Míle buíochas dóibh súid uilig a thug cabhair dom ar an óiche deireannach. Bhí sibh iontach!

Faoi dheireadh, ba mhaith liom buíochas faoi leith a ghabháil le Carmel. Bhi tú i gconaí le grá, tacaíocht agus misneach a thabhairt dom nuair nach raibh cursaí ag dul go maith. Bhi a fhios agat freisin, níos fearr ná mé féin, cén uair a bhi briseadh ag teastáil uaim. Go raibh míle maith agat as ucht chuile rúd a rinne tú dom. Ni dhéanfaidh mé dearmad ar choíche.

Ta an thráchtas seo tiomnaithe do mo chlann agus cairde agus dóibh súid nach bhfuil linn níos mó, go mór mhór Papó, Mícheal agus Michael.

Just to see what would happen.

Table Of Contents

Chapter 1

List of Tables

List Of Figures

Abstract

All known microorganisms with the exception of *lactobacilli* display an absolute requirement for iron. Although iron is the fourth most abundant element on earth, it is rapidly oxidised at neutral pH forming insoluble hydroxides. To overcome this limitation, microorganisms have developed a plethora of mechanisms to acquire iron. *Sinorhizobium meliloti* 2011, the endosymbiont of *Medicago sativa*, produces one known siderophore, rhizobactin 1021. Due to the high demand for iron in the nodule, the iron acquisition mechanisms of *S. meliloti* 2011 have been subject to particular interest.

Rhizobactin 1021 is structurally similar to aerobactin, which is produced by various pathogenic bacteria. In *E. coli*, aerobactin is transported at the inner membrane via the *fhu* system. The *fhu* system of *E. coli* was found to be sufficient to allow the transport of rhizobactin 1021 accross the inner membrane. A *fhuC* mutant was found to be defective in the transport of rhizobactin 1021. A novel permease, RhtX, was identified in *S. meliloti* and found to be involved in rhizobactin 1021 transport. Heterologous expression of RhtX in an *E. coli fhuC* mutant restored rhizobactin 1021 utilisation, but not aerobactin utilisation. A homologue of RhtX was identified in the opportunistic human pathogen *P. aeruginosa*. Mutation of the gene, *fptX*, was found to result in a deficiency in pyochelin utilisation in *P. aeruginosa*.

P. aeruginosa was found to be capable of utilising the xenosiderophores rhizobactin 1021, schizokinen and aerobactin. A receptor mediating the transport of these siderophores was identified and characterised.

S. meliloti 2011 has also been found to be capable of acquiring iron from haem compounds, a characteristic generally found only amongst pathogens. A number of putative haem acquisition loci were identified in *S. meliloti* 2011 and were subject to analyses. The protein encoded by Smc02726 was identified as the receptor for haemin and haemoglobin under free living conditions.

Chapter 1

Introduction

1.1: Introduction

Almost all-living organisms have an absolute nutritional requirement for iron. Iron is an essential cofactor of many enzymes and is intimately involved in processes including the catalysing of enzymatic reactions, electron transport and nitrogen fixation. Although iron is the fourth most abundant element on earth, being exceeded only by aluminium, silicon and oxygen, it is not readily available in the environment. Iron was present in its ferrous form in the environment before the evolution of photosynthetic organisms. As the atmosphere became more strongly oxidising upon the production of oxygen by these organisms, the available iron in the atmosphere was converted to its ferric form. The solubility of the Fe(III) ion at physiological pH is limited by its tendency to hydrolyse and polymerise to form insoluble $Fe(OH)_3$. At pH 7 the concentration of ferric iron is approximately 10^{-17} M (Neilands *et al.*, 1987), a value to low to support microbial growth. As pH lowers, Fe(III) becomes more soluble, and is available in sufficient concentration to support the normal growth rates of microorganisms. However as most microorgansims grow at or near neutral pH, iron is not sufficiently available in soluble form. In biological systems host iron-binding compounds such as transferrin and ferritin impose similar restriction on the availability of iron for microbial assimilation.

To combat the low availability of external iron, microorganisms have evolved high affinity uptake systems that allow for the acquisition of iron from the environment. This affinity uptake system involves the production of chelators, termed siderophores to solubilise iron. Siderophores (Greek for iron bearers) are defined as low-molecular weight (500-1000 Daltons), virtually ferric specific ligands that facilitate iron uptake from the environment (Neilands, 1981). The efficient absorption of siderophores at low concentration is achieved by receptors in the cell envelope. Numerous siderophores have been isolated and characterised and the genes governing biosynthesis and utilisation have been sequenced. Iron acquisition may also occur by the direct acquisition of iron from iron containing proteins such as haem and transferrin. This ability, which is common amongst but not limited to pathogens, broadens the range of iron sources available to bacteria.

1.2: Classes and Structures of Microbial Siderophores

There is a significant amount of structural variety between the siderophores produced by various microorgansims. However most siderophores can be classified according to their main chelating groups, which are generally either hydroxamates or catecholate/phenolates. Hydroxamates type siderophore can be synthesised by both fungi and bacteria, but in general, bacteria produce only catecholates/phenolates.

1.2.1: Catecholates

Catecholate siderophores consist of three repeating units of 2,3-dihydroxybenzoic acid (DHBA) or sometimes salicylic acid, linked via amino acid or amino alkane residues forming either a cyclic or linear molecule.

Enterobactin

Enterobactin is regarded as the prototypical siderophore of the catechol type. The siderophore was isolated from *Salmonella typhimurium* (Pollack and Neilands, 1970) and *Escherichia coli* (O'Brien and Gibson, 1970) and named enterobactin and enterochelin respectively, although the former term is generally used. Enterobactin is a cyclic triester of 2,3-dihydroxybenzoyl serine with the strongest affinity for iron of any chelator known with a formation constant (K_f) of 10^{52} (Figure 1.1). The triester backbone structure is very susceptible to hydrolysis resulting in a reduction in affinity for Fe(III) as the pH is lowered. At a pH below 7, iron is held less firmly than in trihydroxamates. Enterobactin production has been demonstrated in most enterobacteriaceae, with strains unable to produce enterobactin often able to utilise it (Persmark *et al*, 1989).

Linerar Catechols With 2-Hydroxyphenyloxazoline

Agrobactin, produced by the gram negative phytopathogen *Agrobacterium tumefaciens*, is a linear tricatecolamide siderophore (Ong *et al.*, 1979). It consists of three residues of 2,3-dihydroxybenzoic acid, a threonyl group in the form of an oxazoline ring and a permidine chain (Figure 1.1). *Paracoccus denitrifians* (Tait, 1975; Peterson and Neilands, 1979) and the human pathogen *Vibrio cholerae* (Griffiths *et al.*, 1984) also produce linear catecholate siderophores termed parabacin and vibriobactin respectively. In parabactin the *meta*-hydroxyl group of the middle

catechol ring is absent. Vibriobactin has two oxazoline rings and a nonspermidine backbone.

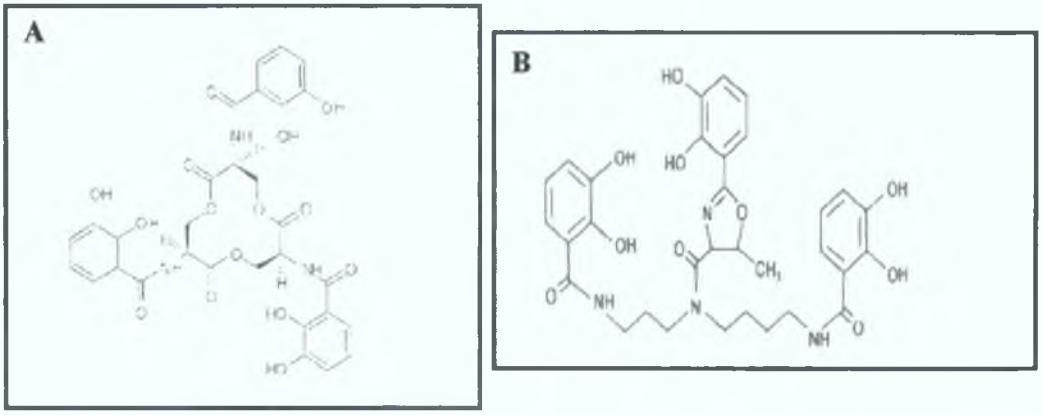

Figure 1.1: Structure Of Enterobactin (A) (reviewed by Roosenberg *et al*, 2000) **and Agrobactin (B)** (Höfte, 1993)

Catechols With A Hydroxypheylthiazoline Group

Two siderophores have been reported which contain a hydroxyphenylthiazoline group. Pyochelin isolated from *Pseudomonas aeruginosa* (Cox *et al.*, 1981) possesses a hydroxyphenylthiazoline group linked to a thiazolidine carboxylic acid group (Figure 1.2). Pyochelin has a very low iron binding capacity ($K_f = 5*10^5$; Cox and Graham, 1979), and forms 2:1 complexes with Fe(III). Pyochelin is however extremely active in iron transport. *Pseudomonas putida, Pseudomonas stutzeri* and *Pseudomonas maltophila* do not produce pyochelin but appear to express a ferripyochelin binding protein when grown in iron-low medium (Sokol, 1984).

Anguibactin, a siderophore isolated from the fish pathogen *Vibrio anguillarum* has also been found to contain a hydroxyphenylthiazoline group and forms a 1:1 complex with Fe(III) (Jalal *et al.*, 1989). *Acinetobacter baumanii* was found to produce a siderophore that was similar to anguibactin, and was termed acinetobactin (Figure 1.2). The only difference between the siderophores is that acinetobactin contains an oxazoline ring compared to a thiazoline ring for anguibactin (Yamamoto *et al*, 1994).

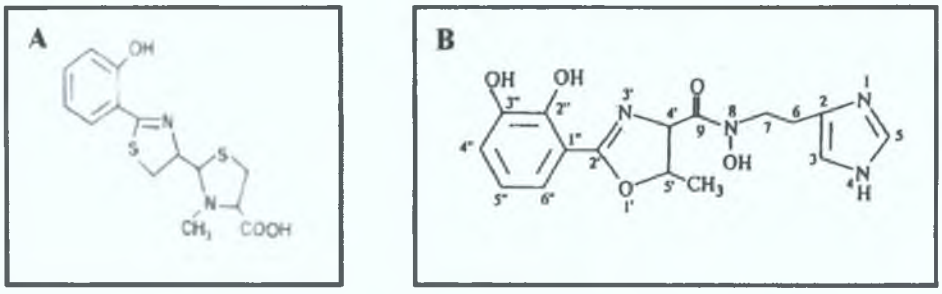

Figure 1.2: Structure Of Pyochelin (A)(Höfte, 1993) **and Acinetobactin** (B)(Yamamoto *et al*, 1994).

1.2.2: Hydroxamates

Most hydroxamate siderophores contain three secondary hydroxamate groups. Each hydroxamate group provides two oxygens which form a bidentate ligand with iron, resulting in a hexadentate octahedral complex with Fe(III) for each siderophore.

Citrate Hydroxamates

Citrate hydroxamates possess two hydroxamate groups, which have substituted the distal carboxyl groups of citric acid. The ferric iron is co-ordinated by two hydroxamates and the α-hydroxycarboxylate group of citric acid.

Aerobactin is a siderophore, which has been isolated from many common clinical enterobacteriaceae such as *E. coli*, *Enterobacter cloacae*, *Enterobacter aerogens*, *Shigella* spp and *Salmonella* spp (Gibson and Magrath, 1969). The two primary carboxyls of the citric acid in aerobactin are substituted with N-acetyl-N-hydroxylysine (Figure 1.3). Aerobactin forms a hexacoordinate complex with Fe(III), with a (K_f) of 10^{23}. Aerobactin genes can be chromosomal or plasmid encoded. Aerobactin has been found to play a role in virulence (Maritnez *et al.*, 1990) and is associated with strains isolated from blood and urine. Arthrobactin, a siderophore produced by *Arthrobacter* spp contains two molecules of 5-(N-acetyl-N-hydroxy-amino)-1-aminopentoic acid linked to citric acid (Figure 1.3)(Neilands and Leong, 1986).

Schizokinen is a citrate hydroxamate produced by the gram-positive bacillus, *Bacillus megaterium* (Byers *et al.*, 1967). It is also produced by several cyanobacteria

including *Anabaena* spp (Clarke *et al.*, 1987). In schizokinen, citric acid is substituted with 1-amino-3-(N-hydroxy-N-acetyl)aminopropane (Figure 1.3).

Rhizobactin 1021, which is produced by *Sinorhizobium meliloti* 1021 is a citrate hydroxamate siderophore in which the distal carboxyl groups of the citrate molecule are amide linked to two different side chains, 1-amino-3-(N-hydroxy-N-acetyl)aminopropane and 1-amino-3-(N-hydroxy-N-(E)-2-decenylamino)propane (Persmark *et al*, 1993) (Figure 1.3). The pathogen *Acinetobacter haemolyticus* produces a similar siderophore to rhizobactin termed acinetoferrin. The siderophore consists of side chains of 1-amino-3-(N-hydroxy-N-2-octenylamino)propane which are amide linked to the carboxyl groups of the citrate molecule (Figure 1.3)(Okujo *et al*, 1994).

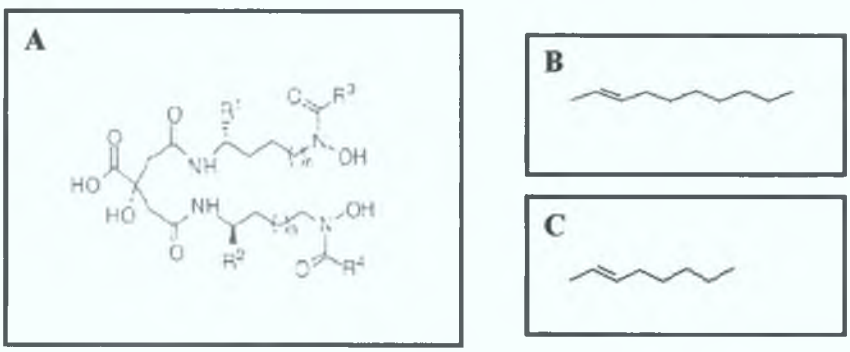

Figure 1.3: Structure Of Aerobactin (**A**; $R^1 = R^2 = COOH$; $R^3 = R^4 = H$; n = 2), **Arthrobactin** (**A**; $R^1 = R^2 = H$; $R^3 = R^4 = H$; n = 2), **Schizokinen** (**A**; $R^1 = R^2 = H$; $R^3 = R^4 = H$; n = 0), **Rhizobactin 1021** (**A**; $R^1 = R^2 = H$; $R^3 = H$; $R^4 =$ **B**; n = 0) **and Acinetoferrin** ($R^1 = R^2 = H$; $R^3 = R^4 =$ **C**; n = 0) (reviewed by Roosenberg *et al*, 2000).

Ferrioxamines

Ferrioxamines are a group of siderophores typically produced by Actinomycetes. Ferrioxamines are trihydroxamates with repeating units of 1-amino-ω-N-hydroxaminoalkane (pentane or butane) and succinic or acetic acid (Neilands and Leong, 1986). Ferrioxamines exist in cyclic or open chain form. The methane sulfonate salt desferrioxamine B, produced by *Streptomyces pilus* has been produced commercially by CIBA-Geigy as Desferal®. Desferal® is used for deferration therapy (Höfte, 1993).

Other Hydroxamates

The potential human pathogen *Pseudomonas cepacia* produces a cyclic monohydroxamate called cepabactin. Cepabactin is also produced by other non-fluorescent pseudomonads (Höfte, 1993).

Alcaligin, produced by *Alcaligenes denitrificans* produces a cyclic dihydroxamate siderophore that chelates Fe(III) at a ratio of 3:2. A similar cyclic dihydroxamate bisucaberin, is produced by the salt water bacterium *Alteromonas haloplanktis* (Höfte, 1993).

1.2.3: Carboxylate

A number of siderophores have been detected in bacteria that contain neither phenol/catecholate or hydroxamate functional groups. These siderophores have been termed carboxylates. The development of the EDDHA-Luria Broth bioassay (Ong *et al.*, 1979; Smith and Neilands, 1984) and the universal assay for siderophore detection (Schwyn and Neilands, 1987) has facilitated the detection of siderophores that are neither catecholates nor hydroxamates.

Rhizobactin

Rhizobactin was discovered when it was found that *Rhizobium meliloti* DM4 (now *Sinorhizobium meliloti* DM4) could be made iron deficient in culture, but the Arnow and Csaky reagents gave negative results for catechol and hydroxamate siderophores. However, the development of the less restrictive EDDHA-Luria Broth bioassay (Smith and Neilands, 1984) allowed for its isolation. Rhizobactin is an amino poly(carboxylic acid) with ethylenediaminedicarboxyl and hydroxycarboxyl moieties as iron chelating groups (Smith *et al.*, 1985).

Other Carboxylates

A number of other siderophores are also classified as carboxylate siderophores. Staphyloferrin A is a siderophore produced by *Staphylococcus hyicus* DSM 20459. The siderophore consists of one D-ornithine residue linked by two amide bonds to two citric acid residues (Höfte, 1993).

The human pathogen, *Proteus mirabilis*, was found to produce α-hydroxyisovaleric acid in low iron media. Also the mugineic acids phytosiderophores produced by plants can also be classified as carboxylate siderophores (Höfte, 1993).

1.2.4: Citrate

Although citrate fails to meet the definition of a siderophore, it is none the less capable of acting as an iron source for bacteria. Citrate functions as a siderophore for a number of organisms including *E. coli* and *Bradyrhizobium japonicum* (Guerinot *et al*, 1990). It is thought that ferric dicitrate is the form utilised by bacteria as an iron source (Hussein *et al*, 1981).

1.2.5: Mycobactin

Mycobactins are hybrids of the hydroxamate and phenol-catecholate classes of siderophores. Mycobactin contain a hydroxyphenyloxazoline ligand and linear and cyclic hydroxamate ligands. The siderophore contains substituents that vary according to the species. Mycobactin was originally isolated as a growth factor for *Mycobacterium paratuberculosis*. Mycobactin is a unique microbial siderophore in that it is both lipid-soluble and intracellular in its occurrence. Mycobactin has been isolated from *Mycobacterium*, *Nocardia* and *Rhodococcus* species. These bacteria are members of the nocardioform group of Actinomycetes (characterised by a thick lipodial cell envelope) that includes saprophytic soil organisms, animal and human parasites. Mycobactins appear to function as intracellular stores of iron (Ratledge, 1987).

1.2.6: Pyoverdine

Pyoverdine siderophores are yellow/green fluorescent water-soluble chromopeptides. All pyoverdines possess the same type of chromophore derived from 2,3-diamino-6,7-dihydroxy quinolone. The three bidentate chelating groups that bind Fe(III) are the catechol group of the chromopore, the hydroxamate group of N^{δ}-hydroxyornithine and either an α-hydroxy acid of hydroxyaspartic acid or the hydroxamate group of a second N^{δ}-hydroxyornithine. The peptide chain of the siderophore differs among strains by number and composition of amino acids. Chelation of Fe(III) involves the catecholate group of the chromophore and the two hydroxamate moieties of the

hydroxyaminopropyl residues of the peptide chain. Pyoverdine siderophores are typically produced by fluorescent pseudomonads, but siderophores with very similar structures have been detected in iron low cultures of *Azotobacter vinelandii* and *Azomonas macrocytogenes* (Höfte, 1993).

Pyoverdines have been studied extensively because of their antagonistic action on phytopathogenic fungii and minor bacterial pathogens. Studies suggest that pyoverdines are antagonistic through chelation of iron from the environment of the target pathogen (Buyer and Leong, 1986; Loper and Buyer, 1991), although it is possible that pyoverdines with different peptide chains could inhibit growth of other microorgansims by acting as peptide antibiotics (Hancock and Chapple, 1999).

1.2.7: Fungal Siderophores

All fungal siderophores so far studied are of the hydroxamate type and contain an N^{δ}-hydroxyornithine moiety.

Rhodotorulic Acid

Rhodotorulic acid (RA) was initially isolated from the supernatants of iron deficient cultures of the yeast *Rhosotorula pilinanae*. At pH 7 the iron complex is dimeric, with the fromula $Fe_2(RA)_3$ (Höfte, 1993).

Dimerum Acid

Dimerum Acid (DA) is a dihydroxamate derivative of rhodotorulic acid and forms $Fe_2(DA)_3$ complexes. It is produed by important phytopathogeic fungi such as *Verticillum dahliae*, which causes wilt diseases in a variety of plants (Höfte, 1993).

Coprogens

Coprogens are trihydroxymate derivatives of rhodotorulic acid with a linear ligand structure. Coprogen was first isolated from a culture of the fungus *Pilobolus* and has since been isolated from *Penicillium* spp and *Neurospora crassa* (Höfte, 1993).

Ferrichromes

Ferrichromes was one of the first siderophores to be isolated in nature, being initially isolated from *Ustilago sphaerogena*. Ferrichromes are cyclic peptides that contain a tripeptide of N^{δ}-acyl- N^{δ}-hydroxyornithine and a variable content of glycine, serine or alanine. Most of the ferrinchromes studied are hexapeptides. Ferrichrome is produed by a wide range of fungi such as *Aspergillus* spp, *Ustilago* spp, *Penicillum* spp, and various yeasts (Winkelman and Huschka, 1987). Ferrichrome have been found to be an effective iron donor in every fungal system studied to date, even when not synthesised by the organism (Adjimani and Emery, 1987). Ferrichrome is commonly used as a siderophore by bacteria, although the bacteria are apparently unable to synthesise the compound themselves. Ferrichrome uptake by *E. coli* has been found to be dependent on the FhuA outer membrane protein (Coulton *et al.*, 1983).

Siderophore thus consist of a group of compounds with diverse structures that are iron chelating and that promote growth under conditions of iron limitation. The diverse chemical structures of siderophores possibly reflect the environment in which they function, and may also be seen as an adaptation by the bacterium to the ecological niche that it occupies.

1.3: Siderophore Chemical Synthesis And Antibiotic Siderophore Conjugates

While most antibiotics diffuse into bacteria, gram-negative bacteria are less susceptible to antibiotics, a property conferred upon the bacterium by the presence of the outer membrane, which acts as a permeability barrier. If however the antibiotic is actively transported into the periplasm, it forms a concentration gradient into the cytoplasm thereby lowering the antibiotic minimum inhibitory concentration (MIC). A number of naturally occurring antibiotics that mimic siderophores have been reported. Albomycins are iron-chelating antibiotics that mimic the transport of ferrichrome and are attached via a serine spacer to a toxic moiety. Following internalisation into the cytoplasm the toxic group has to be cleaved to be biologically active (Braun, 1999). Siderophores can also behave as antibiotic agents by depriving essential iron from competing organisms and thereby limiting their growth. Siderophore analogues may also function by blocking siderophore receptor sites with non-functional siderophore derivatives.

The existence of naturally occurring siderophore antibiotic derivatives prompted investigations into the chemical synthesis of novel siderophore conjugates. The attachment of toxic compounds to siderophores results in a new form of drug delivery in which the conjugate is actively transported via the organisms own iron transport system and is referred to as 'Trojan Horse' drug delivery. The active transport of the conjugates is potentially very effective for the delivery of toxic groups that may be effective against certain biochemical targets, but that are therapeutically ineffectual because of low the permeability of the cell.

The synthesis of siderophores can proceed by processes known as semisynthesis or total synthesis. Semisynthesis involves the induction of microorganisms to synthesise and excrete siderophores in excess of their own dry cell weight (reviewed by Roosenberg *et al*, 2000). However, while many siderophores are readily produced through fermentation, many of the common siderophores have no suitable groups that are suitable for the conjugation of antimicrobial agents. The development of total synthesis of siderophores and siderophore derivatives has enabled this problem to be partially overcome. The limiting factor in the rational design of siderophore antibiotic conjugates is the minimal structural requirements for siderophore transport and the

mode of linkage between the siderophore and the antibiotic. While the total synthesis of naturally occurring siderophores is challenging, a number of siderophores have been synthesised (reviewed by Rosenberg *et al*, 2000).

The ability to synthesise siderophores has enabled the generation of siderophore probes for the elucidation of iron uptake mechanisms. The ability of *M. paratuberculosis* to utilise various iron chelates appended to a citric acid platform was evaluated and a number of new structural elements were identified that stimulated growth (Wang and Phanstiel, 1998; Guo *et al*, 2002). Such siderophore analogues and platforms can act as a structural scaffold to which various antibiotics can be conjugated. Similarly the design and synthesis of artificial siderophores and siderophore analogues has enabled a broader understanding of how microorganisms recognise and utilise siderophores (reviewed by Rosenberg *et al*, 2000).

Siderophore antibiotic conjugates consist of a general structure of an antibiotic, which is usually linked to the siderophore by a spacer (Figure 1.4). The intact conjugate, the released drug or the iron chelation properties of the siderophore moiety may cause the biological activity of the conjugate.

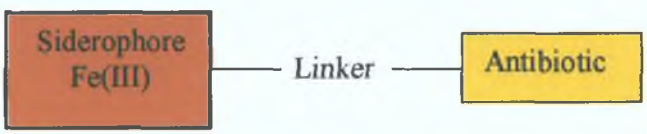

Figure 1.4: General Structure Of A Siderophore Antibiotic Conjugate.

The extensive use of β-lactam antibiotics has resulted in widespread resistance amongst previously susceptible microoganisms. A number of microorganisms such as *P. aeruginosa* also display an intrinsic resistance to β-lactam antibiotics. Thus, the antimicrobial effects of siderophore antibiotic conjugates have been examined. The conjugation of a β-lactam antibiotic to the citrate based siderophore arthrobactin resulted in growth inhibition of an indicator *E. coli* strain. The inhibition was shown to result from the action of the antibiotic portion of the conjugate and enhanced activity was observed under iron deplete conditions (Ghosh and Miller, 1993). Kline

et al (2000) described the synthesis of novel siderophore β-lactam conjugates. The antimicrobial properties of the conjugates were tested against a panel of *E. coli*, *P. aeruginosa* and *Staphylococcus aureus* strains and most of the conjugates showed very good activity against their cellular targets. *In vivo* tests with *P. aeruginosa* using siderophore β-lactam conjugates increased the survival of infected mice from two to seven days (reviewed by Budzikiewicz, 2001).

Siderophore β-lactam conjugates based on diamino acids and dipeptides were synthesised and showed high *in vitro* activity against the gram negative bacterial pathogens *P. aeruginosa*, *E. coli*, *Klebsiella pneumoniae*, *Serratia marcesens* and *Stenotrophomonas maltophilia* (Wittmann *et al*, 2002). Similar conjugates with acylated bis-catecholates siderophores based on secondary diamino acids and related compounds also showed strong antibacterial activity against *P. aeruginosa*, *E. coli*, *K. pneumoniae*, *S. marcesens* and *S. maltophilia* (Heinisch *et al*, 2002).

Investigations into the mechanisms of resistance to siderophore antibiotic conjugates revealed that the resistance was due to mutations in the cognate outer membrane siderophore receptor(s). To avoid the generation of such mutants, various 'cocktails' of siderophore antibiotics conjugates were analysed for their antimicrobial affects. Analysis of *E. coli* indicated that mutants appeared after an extended period of time, however, the mutant strain was unable to grow under iron limiting conditions mimicking human serum (Minnick *et al*, 1992). The mechanism of resistance was determined and the mutant strain was found to be lacking in both catechol and hydroxamate type siderophore receptors. This observation led to the development of mixed siderophores that contained both catechol and hydroxamate moieties. It was hypothesised that these siderophores would be utilised via both catechol and hydroxamate receptors and that any resulting mutants should be defective in both utilisation routes. Studies with mixed siderophore carbacephalosporin conjugates indicated that mutant selection was delayed, with the conjugate apparently being utilised via multiple pathways (Ghosh *et al*, 1996).

Rapid progress has been made in the rational design of siderophore antibiotic conjugates and in the understanding of their intracellular mechanism of action. The

use of siderophores to actively transport antibiotics into cells has resulted in a reprieve for a number of antibiotics. The use of vancomycin, a widely used antibiotic in the treatment of infections caused by gram-positive bacteria, had lead to increased resistance and a need to temper its use. Vancomycin was also ineffectual against gram-negative pathogens. A spermidine based catechol ligand and a mixed catechol and hydroxamate ligand was conjugated to vancomycin, and studies indicated that the conjugated antibiotic lost some activity against gram positive bacteria relative to the antibiotic itself, and that the activity against gram negative bacteria was similar to vancomycin itself. However under iron limiting conditions which mimic human serum, the spermidine based conjugate displayed enhanced activity against an antibiotic hypersensitive strain of *P. aeruginosa* (Ghosh and Miller, 1996).

Diarra *et al* (1996) suggested the use of a multitude of species directed or broadly active conjugates following the examination of siderophore antibiotic conjugate efficacy against various pathogens. A further development in siderophore antibiotic conjugate design has been the synthesis of a siderophore analogue that allows the conjugation of several different antibiotics (Figure 1.5). The artificial siderophore, a trihydroxymate that mimics the natural siderophore rhodotorulic acid (Section 1.2.7), can be envisioned as a 'multiwarhead' conjugate, with the drugs targeting different processes within the cell (Murray and Miller, 2002).

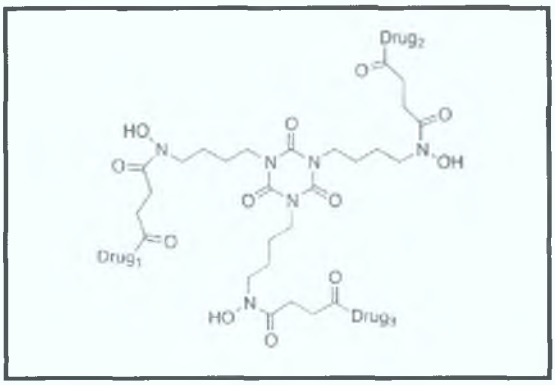

Figure 1.5: 'Multiwarhead' Siderophore Antibiotic Conjugate (Murray and Miller, 2003)

1.4: Active Transport Of Ferrisiderophores In Gram Negative Bacteria

Gram-negative bacteria are enclosed by an outer membrane exposed to the extracellular environment and an inner membrane that serves to contain the bacterial cytoplasm and provide a stable physiological environment. The cell membrane provides protection from substances, both biological and chemical, to the bacteria. The membranes however, hinder the passage of essential nutrients into the cytoplasm. Many of the nutrients required for the efficient growth of Gram-negative bacteria diffuse through outer membrane protein channels termed porins, and into the periplasmic space between the outer and inner membrane or through the outer membrane by lipid bilayer diffusion. Essential nutrients are then actively transported across the inner membrane into the cytoplasm. The process of active transport is driven by the hydrolysis of adenosine triphosphate (ATP) or by an ion electrochemical potential across the inner membrane.

As mentioned previously, iron is an essential nutrient for almost all bacteria, and its acquisition presents bacteria with a difficulty. Bacteria have evolved various strategies to acquire this precious metal, including the production of the chemical iron chelators, siderophores (Section 1.2). Siderophores are released by the bacterium into the extracellular environment and are subsequently transported as ferrisiderophore complexes. As these complexes are too large to diffuse through the outer and inner membranes, they have to be actively transported into the cell. The following sections describe the active transport of ferrisiderophore complexes across the outer and inner membranes, the release of iron from the complex within the cell, the secretion and recycling of siderophores, the storage of the acquired iron in an inert form and the mechanisms of regulation employed.

1.5: Ferrisiderophore Receptors

Ferrisiderophore complexes are too large to diffuse into the bacterial cell, and consequently they have to be actively transported. In gram-negative bacteria, specific receptors for the ferrisiderophore complexes have been identified in the outer membrane. Ferrisiderophore receptors also serve as entry points for various bacteriophages, colicins and antibiotics, which are actively transported into the cell. For this reason, ferrisiderophore receptors are generally induced only under iron limiting conditions and are not present under iron sufficient conditions. Bacteria often possess multiple outer membrane ferrisiderophore receptors that provide specificity for different siderophores. Bacteria are often endowed with the ability to utilise heterologous or xenosiderophores. Heterologous siderophores or xenosiderophores may be defined as siderophores that may be utilised, but are not synthesised by a particular bacteria. The ability of bacteria to utilise xenosiderophores confers a competitive advantage on the bacteria and enables them to occupy extended ecological niches.

The amino acid sequences of ferrisiderophore receptors show homology to other bacterial outer membrane proteins. Outer membrane proteins have in general hydrophobic residues at positions 3,5,7 and 9 of the ten C-terminal amino acids. Ferrisiderophore receptors and other outer membrane proteins are synthesised with a signal sequence that targets the proteins to the outer membrane. The signal sequence is cleaved upon secretion into the periplasm. Ferrisiderophore receptors and other outer membrane proteins have numerous membrane-spanning amphipathic β-sheets that are thought to facilitate transport across the inner membrane (Nikaidi and Saier, 1992). The C-terminal region has been shown to form a membrane spanning β-sheet involved in the incorporation of the outer membrane proteins into the outer membrane (Struyvé *et al*, 1991).

E. coli K-12 possess at least six outer membrane receptors that enable the utilisation of several siderophores (Guerinot, 1994). The crystal structures of three of the receptors, FhuA (Ferguson *et al.*, 1998; Locher *et al.*, 1998), FepA (Buchanan *et al.*, 1999) and FecA (Ferguson *et al*, 2002) have been determined. The FhuA protein

functions as the outer membrane receptor for ferrichrome, FepA functions as the outer membrane receptor for enterobactin and FecA functions as the outer membrane receptor for ferricitrate. Structural analysis of the three proteins indicated that they are all structurally similar. The proteins were found to form a β-barrel, approximately 70 Å in height, with 22 antiparallel β-strands connected by short turns in the periplasm and external loops that extend above the cell surface. The β-barrel has an elliptical shape, with dimensions of approximately 35 Å by 47 Å, which are caused by the right-handed twists of the β-strands. The angle of the β-strands to the axis is approximately 45°. In contrast to structurally similar porins, the β-barrel channel of siderophore receptors is closed. A globular domain derived from approximately the first 160 amino acids at the N-terminus is positioned in the pore towards the periplasmic end of the barrel. For this reason the globular domain is referred to as the 'cork' or 'plug'. The plug domain consists of a mixed four-stranded β-sheet with short interspersed α-helices and connecting loops. The β-sheet is orientated approximately 45° relative to the membrane, so that it blocks the direct passage of siderophores through the outer membrane (Figure 1.6).

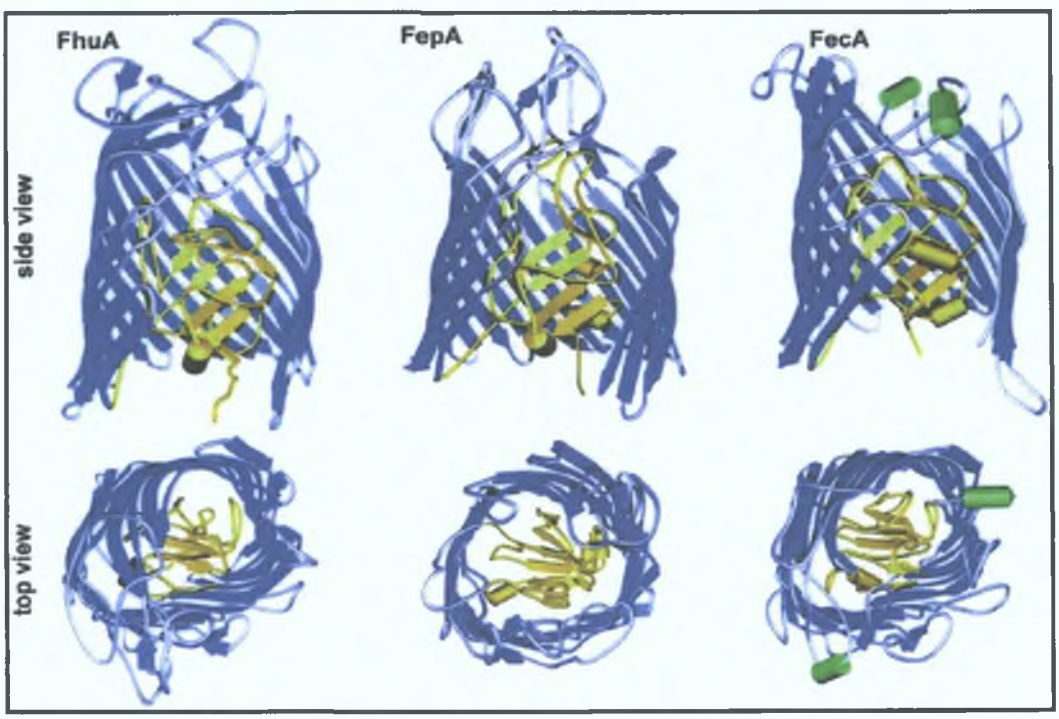

Figure 1.6: Crystal Structures Of FhuA, FepA And FecA. In the side views, a portion of the β-strands (blue) was deleted to improve the view on the globular central domain (cork; yellow). The view from outside the cell (top view) illustrates the closure of the β-barrel channel by the cork domain. The N-terminal segments of the proteins, FhuA1-18, FepA1-10, FecA1-79 are not seen in the crystal structure which suggests a flexible structure (Braun and Braun, 2002).

The plug domain of FhuA and FecA contain three loops, termed apices A, B and C, that extend above the plane of the outer membrane and which have been shown to be important for ligand binding (Locher *et al*, 1998; Ferguson *et al*, 2000; Ferguson *et al*, 2001; Ferguson *et al*, 2002). The FepA plug domain contains two equivalent loops (Buchanan *et al*, 1998). The plug domain of FhuA, FepA and FecA also serve to delineate two pockets within the β-barrels of the proteins. Located above the plug domain and open to the solvent is the extracellular pocket. The residues lining these pockets impart a specific electrostatic charge that are tailored to their specific siderophores. Below the plug domain and exposed to the periplasm is the periplasmic pocket (reviewed by Ferguson and Deisenhofer, 2002).

The crystal structures of FhuA with bound ferrichrome and FecA with bound ferric citrate have been solved (Ferguson *et al*, 1998; Ferguson *et al*., 2002). The crystal structures of FhuA in complex with the siderophores ferricrocin (Ferguson *et al*, 1998) and phenylferricrocin (Ferguson *et al*, 2000) and with the antibiotics albomycin (Ferguson *et al*, 2000) and rifamycin CGP4832 (Ferguson *et al*, 2001) have also been solved and provide an insight into the ligand transport process. For FhuA transport, a single ligand is bound non-covalently within the extracellular pocket of the protein beyond the outer membrane. The ligands, which are all ferri hydroxymates with the exception of rifamycin CGP4832, are bound in identical orientations with the ferric ion buried and with the peptide components of the ligands solvent accessible within the pocket. The compounds, although chemically dissimilar, form van der Waals and electrostatic contacts with common side chains of FhuA. Most of the interactions between the protein and ligand form with apices A, B and C within the plug domain. Additional contacts between the ligand and FhuA occur with residues located in the β-barrel.

The binding of the ligands to FhuA and FecA causes small local translations of the plug apices A, B and C on the extracellular side of the plug. The translations are accompanied by large structural translations on the periplasmic side of the outer membrane. In the liganded structure, an N-terminal segment located within the periplasmic pocket of the protein, termed the switch helix, unwinds to assume a flexible extended conformation. The unwinding of the switch helix signals the

presence of a receptor bound ligand in the periplasm, such that energised TonB proteins can distinguish between unliganded and liganded receptors. The N-terminal regions of the ferric siderophore receptors are not seen in the crystal structures indicating the presence of a flexible structure.

Analysis of the crystal structure of FecA indicated the presence of a second gate primarily composed of the external loops of the β-barrel. Upon binding of the ligand, this second gate closes behind it preventing access to the external milieu. Ferguson *et al* (2002) (reviewed by Postle, 2001) proposed a model for iron transport via FecA: (i) The siderophore complex is adsorbed by low affinity sites on the external loops of the β-barrel. (ii) The siderophore is transferred to its high affinity binding site where it forms electrostatic interactions with the globular domain and numerous charged residues within the β-barrel and extracellular loops. (iii) The external loops reposition themselves closing the external pocket of the barrel and consequently favouring directed transport by disrupting the low affinity binding site and shielding the high affinity site from the solvent. (iv) A TonB dependent conformational change in the globular domain allows the release and transport of the ligand into the periplasmic space.

Although the structural mechanism of the final energy dependent transport stage has not been determined, two models have been proposed (Ferguson *et al*, 1998; Locher *et al*, 1998; Buchanan *et al*; 1999). In the first proposal, an energised TonB molecule induces cooperative structural changes within the plug domain and/or barrel, that may eject the plug domain with bound siderophore into the periplasm (Usher *et al*, 2001). Alternatively, the plug domain may remain inside the β-barrel, and both domains undergo allosteric transitions that lead to the opening of an underlying transmembrane channel within the receptor through which the siderophore permeates into the periplasm by a surface diffusion mechanism (Ferguson *et al*, 1998).

1.6: The TonB Complex

Siderophore mediated iron uptake across the outer membrane is an energy dependent process. There is no known energy source within the outer membrane or within the adjacent periplasmic space to drive the translocation of siderophores into the periplasm. The outer membrane cannot be energised by an electrochemical potential because it contains open protein channels and high-energy metabolites, such as ATP, have not been found in the periplasm. Gram-negative bacteria therefore couple the electrochemical charge gradient, or proton motive force, of the cytoplasmic membrane with siderophore transport across the outer membrane (Bradbeer, 1993).

Although TonB homologues have been identified in many bacteria, the TonB protein of *E. coli* is the best characterised. The TonB protein contains three domains that function in activity of the protein as an energy transducer (Traub *et al*, 1993; Larsen *et al*, 1996). The 26 kDa TonB protein of *E. coli* contains a hydrophobic sequence at its N-terminus, which functions as an uncleaved export signal sequence, and which anchors the protein in the cytoplasmic membrane (Postle and Skare, 1988). The second domain contains proline-rich repeats, suggesting a structure that spans the periplasmic space (Hannavy *et al*, 1990). Synthetic peptides corresponding to the proline rich domain were shown by nuclear magnetic resonance to be capable of spanning the periplasm (Evans *et al*, 1986; Brewer *et al*, 1990). Deletion of this domain did not significantly affect TonB activity. The only noticeable effect of the deletion was a reduced ability to adsorb phage ϕ80, in a medium of high osmolarity that expands the periplasmic space. This finding suggested that contact between the TonB protein and the FhuA receptor was impaired (Larsen *et al*, 1993). The crystal structure of the C-terminal domain of TonB has been determined and shown to form a cylinder composed of two intertwined subunits with six β-strands that form a large β-sheet, that physically interact with the TonB-boxes of outer membrane receptors (Moeck and Letellier, 2001; Chang *et al*, 2001).

The TonB protein is known to interact with several outer membrane receptors. The presence of conserved domains within these outer membrane receptors with which TonB could interact would therefore be expected. A conserved motif termed the

'TonB box' has been found to be conserved amongst TonB dependent receptors. The TonB box is a hydrophobic, 5-7 amino acid segment, found close to the N-terminus of TonB dependent outer membrane receptors (Postle, 1993). Evidence suggests that it is the conformation of the TonB box rather than some specific amino acid sequence that dictates recognition of the receptor by TonB and therefore productive energy coupling interactions (Kadner, 1990; Larsen *et al*, 1997). Substitutions in the TonB box impair receptor activity, but such effects can be suppressed by complementary substitutions in TonB, suggesting that the TonB box, which is predicted to be located in the periplasm, physically interacts with the TonB protein (Heller *et al*, 1988; Schöffer and Braun, 1989; Günter and Braun, 1990; Bell *et al*, 1990). *E. coli* treated *in vivo* with synthetic peptides corresponding to the TonB box affected several processes including growth in low iron media, ϕ80 infection and killing by colicins B and Ia (Tuckman and Osburne, 1992). Interactions between the TonB box and the region around residue 160 of the TonB protein is supported by *in vivo* cross-linking experiments (Cadieux and Kadner 1999; Cadieux *et al*, 2000).

Analysis of the outer membrane receptors FhuA and FepA indicate that other regions of the outer membrane receptors are also involved in TonB interactions (Braun *et al*, 1999; Scott *et al*, 2001; Killmann *et al*, 2002). FhuA and FepA mutants lacking the globular domain, including the TonB box, displayed TonB dependent activity for their ligands. The data indicate the presence of sites of interaction between the β-barrel of the outer membrane receptors and TonB. Synthetic peptides corresponding to the region around residue 160 of TonB impaired ferrichrome transport into cells expressing wild type FhuA and a globular domain deletion mutant, indicating that this TonB region is also involved in the interaction of TonB and the β-barrel of FhuA (Killmann *et al*, 2002).

Two further motifs designated TonB region II and TonB region III have also been shown to be conserved amongst TonB dependent receptors (Bitter *et al*, 1991; Ankenbauer and Quan, 1994). TonB region II is typically located towards the C-terminal of the receptor. Region III is typically located at a distance of approximately 100 amino acids from the N-terminal TonB box. It is possible that these domains are involved in interactions with the TonB protein.

TonB's biological function, stability and its association with the cytoplasmic membrane is dependent upon two additional cytoplasmic membrane proteins, ExbB and ExbD which have unusual membrane topologies (Eick-Helmerich and Braun, 1989; Larsen *et al*, 1999). Mutants in the *exb* locus were found to overproduce enterobactin and to be partially tolerant to colicin B (Eick-Helmerich and Braun, 1989). Sequencing revealed two genes, *exbB* and *exbD*, which were essential for the Exb-related activity. The N-terminus of the ExbB protein is predicted to be located in the periplasm. The protein is predicted to span the cytoplasmic membrane thrice, with the majority of the protein located in the cytoplasm (Kampfenkel and Braun, 1993b; Karlsson *et al*, 1993). The ExbD protein is anchored by its N-terminal end in the cytoplasmic membrane while the remainder of the protein is located primarily in the periplasm (Kampfenkel and Braun, 1992; reviewed by Braun, 1995).

Evidence for an interaction between TonB and ExbB comes from analysis of proteolytic degradation and *in vivo* crosslinking studies. The TonB protein was degraded by proteolysis when it was overexpressed relative to ExbB (Fischer *et al*, 1989). Crosslinking studies indicated an interaction between TonB and ExbB *in vivo* (Skare *et al*, 1993; Jaskula *et al*, 1994; Larsen *et al*, 1994). Studies using antibodies directed against TonB also indicated that ExbB was involved in the stabilisation of TonB (Skare and Postle, 1991). A fusion protein containing the N-terminal membrane spanning residues of TonB fused to β-lactamase interfered with native TonB activity, indicating that the fusion protein was competing with native TonB for the binding of another component (Karlsson *et al*, 1993). Another fusion protein containing the hydrophobic N-terminus of the TetA tetracycline resistance protein fused to TonB was also affected in TonB activity (Jaskula *et al*, 1994). A mutation in the transmembrane region of TonB rendered TonB inactive, and prevented the formation of the TonB complex (Larsen *et al*, 1994). The results indicated that the N-terminal region of TonB anchors the protein in the cytoplasmic membrane and is essential for TonB activity and the interactions between TonB and ExbB. The ExbD protein was shown to interact with ExbB and TonB (Braun *et al*, 1996), while both ExbB and ExbD were shown to form homomultimers *in vivo* (Higgs *et al*., 1998). Quantification of the individual components of the TonB-ExbBD complex indicates that they are present at a ratio of one TonB: two ExbD : seven ExbB in cells grown

under various conditions of iron limitation (Higgs *et al*, 2002a). The ratios indicated that the ExbB multimers alone could constitute the proton translocater that energises TonB, leaving ExbD to participate with other ExbB multimers in the recycling of TonB after an energy transduction event (Higgs *et al*, 2002a). This hypothesis would be consistent with the topologies of the two proteins in which the prominent domain of ExbB occupies the cytoplasm while the prominent domain of ExbD occupies the periplasm. As previously described, mutants in *exbB* and *exbD* show a reduction in all TonB dependent activities (Skare *et al*, 1993; Ahmer, 1995). The residual level of TonB activity results from the presence of TolQ and TolR, which show strong amino acid homology to ExbB and ExbD, and which are functional analogues of the ExbBD proteins of *E. coli*. The TolQR proteins confer a 'leaky' TonB phenotype on the *E. coli exb* mutants (Braun, 1989; Eick-Helmerich and Braun, 1989; Braun and Herrmann, 1993; Kampfenkel and Braun, 1993a). Homologues of ExbB and ExbD have been identified in *P. aeruginosa* and have been shown to be inessential for TonB mediated iron acquisition (Zhao and Poole, 2000). The expression of *tolQR* was shown to be iron regulated (Lafontaine and Sokol, 1998), however, efforts to generate mutants in *tolQR* failed, indicating that *tolQR* mutations were lethal in this organism (Dennis et al, 1996; Zhao and Poole, 2000).

The transfer of energy from the cytoplasmic membrane to the outer membrane by the TonB-ExbBD complex possibly occurs by a cooperative transition. The ExbBD complex is likely to constitute the proton translocation apparatus, which couples chemiosmotic potential with a series of conformational changes in TonB. The transition of TonB is believed to involve three stages: uncharged, charged and discharged (Larsen *et al*, 1999). Following unwinding of the switch helix, and the transition to the liganded receptor conformation, TonB preferentially interacts via the C-terminal of the TonB box and possibly other side chains found in the β-barrel domain of TonB-dependent receptors (Braun *et al*, 1999; Merianos *et al*, 2000). This association occurs independently of the energised state of the TonB-ExbBD complex (Letain and Postle, 1997; Howard *et al*, 2001, Moeck and Letellier, 2001), but is enhanced in the presence of the ligand (Skare *et al*, 1993; Moeck *et al*, 1997; Cadieux and Kadner, 1999; Moeck and Letellier, 2001; Larsen and Postle, 2001). Upon forming a complex with the outer membrane receptor, TonB releases stored energy

and assumes the discharged conformation. Energy transduction leads to allosteric changes within the receptor, such that the binding site is affected leading to a reduction in binding affinity, and subsequent release of the ligand as previously described (Figure 1.7).

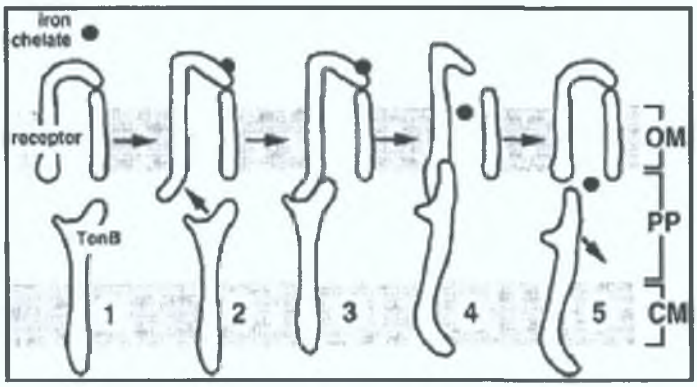

Figure 1.7: Mechanism Of TonB Energy Transduction. TonB-dependent translocation of ferric iron chelates across the outer membrane (OM). A prototypical high-affinity receptor within the OM is depicted before its interaction with ligand from the external milieu and with TonB from the periplasm (PP)(step 1). Binding of a cognate chelate induces TonB-independent conformational changes in the receptor (step 2) in surface and periplasmically exposed loops. These latter changes indicate ligand occupancy and so promote TonB to contact the receptor physically and preferentially (step 3). TonB transduces pmf-derived energy, in this scheme represented as a conformational change (step 4) enabling further alterations in surface-exposed loops of the receptor, such that its affinity for ligand is decreased, and ligand enters an underlying pore domain. TonB dissociates from the receptor (step 5) to be recycled by the cytoplasmic membrane (CM) ExbB-ExbD complex; extramembranous loops of the high-affinity receptor attain their preligand-loaded conformations. Horizontal arrows are intended to depict a progression of conformational changes in the siderophore receptor as opposed to its lateral movement within the OM. In this model, TonB is depicted as being embedded within the CM.

The absence of virtually all TonB dependent outer membrane receptors failed to prevent localisation of TonB to the outer membrane (Higgs *et al*, 2002b). The identification of two additional non-receptor proteins with which TonB interacts at the outer membrane suggests that the association of TonB with the outer membrane may be mediated through proteins that provide docking sites for TonB prior to or following the energy transduction event (Higgs *et al*, 2002b)

While TonB proteins have generally only been implicated in import processes across the outer membrane, there is also evidence to suggest that TonB or TonB like proteins may have a role in export. The TonB1 protein of *P. aeruginosa* can complement *tonB* mutations in *E. coli* and *P. putida* WCS358 (Poole *et al*, 1996) with regards to import. However, analysis of multidrug resistance in *P. aeruginosa* which is afforded in part by the operation of the multidrug efflux system encoded by *mexA-mexB-oprM* (Poole

et al, 1993a; Poole, *et al*, 1993b; Gotoh *et al*, 1995; Li *et al*, 1995), was found to be compromised in a *tonB1* deletion strain. The TonB1 protein of *P. aeruginosa* contains an unusual N-terminal sequence (Poole *et al*, 1996) that has been shown to be essential for activity of the protein (Zhao and Poole, 2002). Analysis of TonB chimeras in *P. aeruginosa* indicated that the protein was able to interact with a range of 'receptors' and that the N-terminal sequence may be involved in other cellular processes yet to be identified (Zhao and Poole, 2002). A TonB-like protein identified in *Aeromonas hydrophilia* was also shown to play a role in export of the aerolysin exotoxin (Howard *et al*, 1996). This suggests that energy-dependent export might occur at the level of the outer membrane and that it might be mediated by TonB.

Analysis of the *tonB*, *exbB* and *exbD* genes in bacteria indicated that the genetic organisation is not conserved. The *exbB* and *exbD* genes of *E. coli* are linked, but not with tonB (reviewed by Ratledge and Dover, 2000). The *tonB* gene of *Rhizobium leguminosarum*, which also contains an unusual N-terminal, is similarly unlinked to the *exbBD* genes (Wexler *et al*, 2001). In contrast the *exbB*, *exbD* and *tonB* genes are linked in *Haemophilus influenzae* (Jarostk *et al*, 1994), *Pasteurella multocid*a (Bosch *et al*, 2002) and *B. japonicum* (Nienaber *et al*, 2001). A second *tonB* gene in *P. aeruginosa* is also linked to the *exbBD* genes (Zhao and Poole, 2000), while in *V. cholera*, two-linked *tonBexbBD* systems which are physically separated from each other, are present (Occhino *et al*, 1998). While the arrangement of the genes indicates that they form an operon, this has only been confirmed for *V. cholera* (Occhino *et al*, 1998). Analysis of the *P. multocida tonB-exbBD* system indicated that the genes were independently transcribed (Bosch *et al*, 2002). While *E. coli* encodes only one TonB protein, in several organisms, more that one putative *tonB* gene has been identified (Occhino *et al*, 1998; Zhao and Poole, 2000). The *tonB* genes in several of these organisms are linked to specific iron utilisation genes, and only affect iron utilisation by these systems (Occhino *et al*, 1998; Neinaber, 2001).

The effect of mutations in *tonB* in various pathogens has been assessed. Mutations in *tonB* of *Salmonella enterica* serovar Typhimurium and *S. enterica* serovar Typi (Tsolis *et al*, 1996; Gorbacheva *et al*, 2001), *S. dysenteria*e (Reeves *et al*, 2000), *V. cholera* (Henderson and Payne, 1994; Seliger *et al*, 2001), *P. aeruginosa* (Takase *et al*, 2000b), *H. influenzae* (Jarosik *et al*, 1994), *Bordetella pertussis* (Pradel *et al*,

2000) and uropathogenic *E. coli* (Torres *et al*, 2001) resulted in an avirulent or attenuated phenotypes in animal models. It is not clear whether the abrogation of virulence is due to a loss of all TonB dependent transport systems, or the loss of a particular system. Nonetheless, the results underlined the importance of TonB in the virulence capabilities of several pathogens.

1.7: Transport Of Ferrisiderophore Complexes Into The Cytoplasm

Following the internalisation of a ferrisiderophore complex by an outer membrane siderophore receptor, the complex must be transported across the periplasmic space and subsequently across the inner membrane into the cytoplasm. The transport of ferrisiderophore complexes into the cytoplasm is mediated by periplasmic binding protein dependent transport (PBT) systems, a subclass of the ABC superfamily of transport proteins. The PBT systems consist of a periplasmic binding protein, a transmembrane diffusion complex consisting of one or two different polytopic integral membrane proteins and one or two hydrophilic membrane associated ATP hydrolases that supply the system with energy (Nikaido and Saier, 1992; reviewed by Köster, 2001)(Figure 1.8).

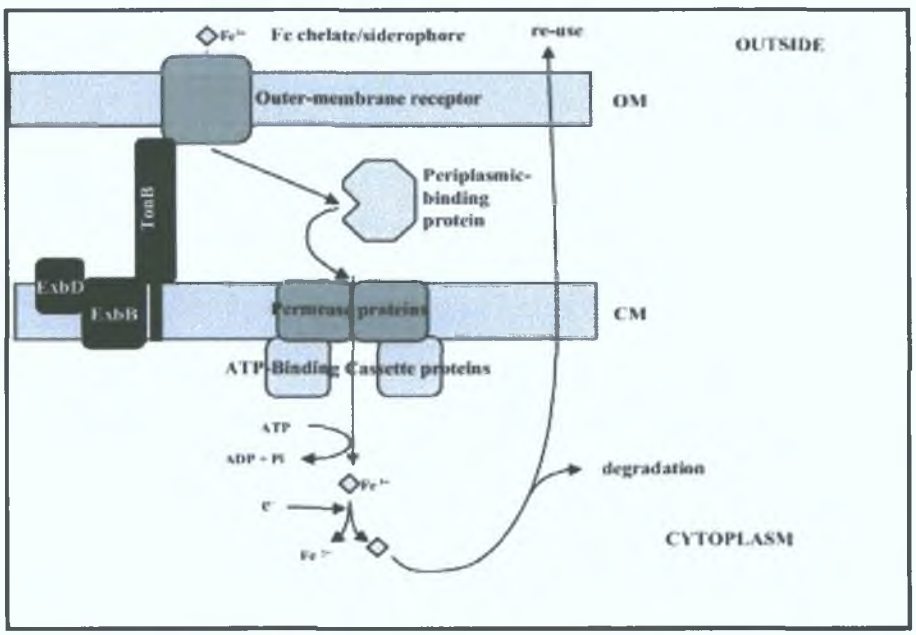

Figure 1.8: Generalised Siderophore Mediated Iron Acquisition. Iron bound siderophore binds to its cognate receptor in the outer membrane (OM) resulting in a conformational change. Energy transduced by the TonB complex results in the release of the siderophore into the periplasm where it is bound by a periplasmic binding protein and transported to a transport system located in the cytoplasmic membrane (CM). Energy in the form of ATP is used to mediate transport across the cytoplasmic membrane where the iron is subsequently released from the siderophore. The siderophore is subsequently degraded or recycled (Andrews *et al*, 2003).

The majority of PBT transport systems were identified by sequence analysis, and their biochemistry and substrate specificity were subsequently analysed. *E. coli* K-12 encodes three PBT systems; one each for the transport of ferric catechols, ferric citrate and ferric hydroxamates. The PBT system for the transport of ferric enterobactin, a

catechol, consists of the periplasmic binding protein FepB, the highly hydrophobic inner membrane proteins FepD and FepG and the cytoplasmic membrane associated ATPase FepC (Chenault and Earhart, 1991; Shea and McIntosh, 1991). The PBT system for the transport of ferric dicitrate consists of the periplasmic binding protein FecB, the highly hydrophobic integral inner membrane proteins FecC and FecD and the cytoplasmic membrane associated ATPase FecE (Staudenmaier *et al*, 1989). Ferric dicitrate itself is not internalised into the cytoplasm. The iron molecule is removed from the dicitrate moiety in the periplasm, and is transported directly into the cytoplasm (Hussein *et al*, 1981).

The PBT system for the transport of ferric hydroxamates, which is encoded by the *fhuBCD* system, is the most characterised transport system of this type and serves as a model system for the analysis of inner membrane siderophore transport. The PBT system for the transport of ferric hydroxamates consists of the periplasmic binding protein FhuD, the hydrophobic inner membrane protein FhuB and the cytoplasmic membrane associated ATPase FhuC.

The periplasmic binding protein FhuD is synthesised with a typical export signal sequence, and is processed and targeted to the periplasmic space. The FhuD protein acts to deliver ferri hydroxamates released from the outer membrane receptor to its inner membrane transport system. The FhuD protein has been shown to bind a wide range of hydroxamate siderophores including ferrichrome, coprogen, rhodotorulic acid, ferrioxamine B, aerobactin and schizokinen (Köster and Braun, 1990; Köster, 1997; Braun *et al*, 1998). The crystal structure of FhuD has been solved (Clarke *et al*, 2000), and it has been shown that similarly to other periplasmic binding proteins, FhuD possesses a bilobal structure giving it a 'kidney bean' shape. In contrast however, FhuD does not contain the flexible hinge region found in these proteins, and does not appear to undergo the major opening and closing movements that are characteristic of other periplasmic binding proteins. The ligand-binding site of the protein is located within a shallow pocket between the two lobes. The binding of the ligand is mediated by hydrophobic and hydrophilic interactions between the iron centre of the ligand and the residues in the binding pocket. The ligand backbone does not interact directly with the FhuD protein, which possibly explains the ability of FhuD to bind different hydroxamate siderophores.

The inner membrane protein FhuB is an extremely hydrophobic polytopic membrane protein. The protein has been shown to consist of 10 membrane spanning regions, with the N- and C- termini located in the cytoplasm (Groeger and Köster, 1998). The FhuB protein consists of two major domains, FhuB[N] and FhuB[C], that display significant homology to each other. Both domains of FhuB, which are connected by a short linker region are essential for function and deletion of either domains results in the abrogation of activity. The heterologous expression of the two domains of FhuB resulted in a restoration of ferric hydroxamate uptake, indicating that the two domains were functional even when produced as two distinct polypeptides (Köster and Braun, 1990). Two conserved regions found in the N- and C- termini of FhuB have also been shown to be important for the transport of ferric hydroxamates (Köster and Bohm, 1992).

The FhuC protein is a cytoplasmic membrane associated protein. The FhuC protein is an ATPase which energises the translocation of the ferrisiderophore complex from the periplasm to the cytoplasm. The FhuC protein contains two highly conserved motifs termed Walker A and Walker B. These two motifs function as two ATP-binding motifs (reviewed by Nikaido and Hall, 1998). Mutations in these motifs resulted in a loss of activity indicating that FhuC functions as an ATP hydrolase (Schultz-Hauser *et al*, 1992).

The genes encoding the Fhu system are iron regulated and constitute an operon organised *fhuACDB*. The translational coupling of the genes may reflect the importance of guaranteeing the proper stoichiometry of the transport components. While no interaction has been detected between the periplasmic binding protein and the outer membrane receptor, such an interaction would probably be favourable to transport efficiency. However, such an interaction is not necessary for the periplasmic release of a ferrisiderophore complex from the outer membrane receptor as shown by the accumulation of aerobactin in the periplasm of an *E. coli fhuD* mutant (Wooldridge *et al*, 1992). Analysis of FhuD indicated that the protein interacted with FhuB even in the absence of a bound ligand. The addition of FhuD to spheroplasts protected FhuB from proteolysis and cross-linking experiments also indicated a physical interaction between FhuD and FhuB (Rohrbach *et al*, 1995). Competitive peptide mapping using peptides corresponding to different regions of

FhuB also suggested a direct interaction between FhuD and FhuB (Mademidis *et al*, 1997). The FhuC protein interacts with FhuB at the two conserved domains found in the N- and C- termini of the proteins (see above). FhuB proteins with only one of the two domains are still able to interact with FhuC. Immunoelectron microscopy with anti FhuC antibodies showed FhuB mediated association of FhuC with the inner membrane (Schultz-Hauser, 1992). It is of interest to note that one of the predicted interaction sites between FhuD and FhuB is located on a cytoplasmic loop close to a binding for FhuC. It is possible that a direct interaction between ligand bound FhuD and FhuC could lead to release of the ligand and transport of the ferri hydroxamate to the cytoplasm via FhuB (Mademidis *et al*, 1997).

1.8: Iron Release From Ferrisiderophore Complexes And Siderophore Recycling

Once a ferrisiderophore has been internalised into the cytoplasm, the iron must be released from the complex and reduced to the metabolically active Fe(II). The process of iron release is thought to involve reduction of the siderophore complexed iron. Siderophores have a much higher affinity for ferric iron than for ferrous iron, thus the reduction of iron to its ferrous state facilitates its release from the ferrisiderophore complex.

Ferrisiderophore reductases have been identified in several different species of bacteria including *B. megaterium* (Arceneaux and Byers, 1980), *E. coli* (Fischer *et al*, 1990), *P. aeruginosa* (Cox, 1980a) and *Mycobacterium smegmatis* (Brown and Ratledge 1975; Ratledge, 1971). In all cases the reductant involved in the reaction was NADH or NADPH. Several ferrisiderophore reductases have been found to be stimulated by the addition of a flavin mononucleotide (FMN) and a divalent metal cation (generally Mg^{2+}). Several enzymes with ferric reductase activity have been identified e.g. flavin reductase, sulfite reductase, but there is no strong evidence to suggest that these enzymes play any major physiological role in iron metabolism (Fontecave *et al*, 1994). Reductive activity should not therefore be taken as implying the presence of a specific ferric reductase.

The ferrisiderophore reductases of *B. megaterium* (Arceneaux and Byers, 1980) and *E. coli* (Fischer *et al*, 1990) have been partially purified and show broad substrate specificity. Two ferrisiderophore reductases were identified in *E. coli*, a membrane bound reductase and a soluble reductase. The soluble 26 kDa ferrisiderophore reductase was found to reduce every siderophore tested including, carrier free Fe(III), aerobactin, schizokinen, arthrobactin, ferrichrome and several other hydroxymate type siderophores, as well as two synthetic analogues of enterobactin and ferridicitrate irrespective of whether or not it could be used by the bacterium.

In *E. coli*, the release of iron from enterobactin requires the Fes protein which is encoded within the enterobactin regulon (Pierce *et al*, 1983). The Fes protein is thought to function by hydrolysing the ester bonds of internalised ferrienterobactin. The protein is then thought to reduce the iron in a sequential step. The breakdown

products of enterobactin, linear monomer, dimer and trimer dihydroxybenzoyl -serine (DHBS) diffuse out of the cell and can act as a weak siderophores which are utilised by the Cir/Fiu receptors (Hantke, 1990). The result of the activity of the Fes enzyme is that the enterobactin molecule can only be used once. For each atom of iron internalised by enterobactin, one enterobactin molecule is degraded.

The FhuF protein of *E. coli* was initially identified as being required for ferrioxamine B utilisation, and was assumed to be a transport protein. Subsequent analysis indicated that FhuF was a cytoplasmic ferredoxin like protein thought to act as a ferrioxamine B reductase in the release of iron from the internalised ferri-siderophore (Muller *et al*, 1998; Patzer and Hantke, 1999).

Once the iron has been removed from the siderophore, the siderophore may be recycled or degraded as described previously for enterobactin. The ability to recycle siderophores possibly confers a competitive advantage on the microorganisms, as the cell does not expend energy continually synthesising new siderophore molecules. Similarly, bacteria can reuse xenosiderophores that they do not themselves synthesise. A number of siderophores have been shown to be recycled. Aerobactin, a siderophore produced by various pathogenic strains of *E. coli* has been shown to be reused an average of three times (Braun *et al*, 1984). Analysis of fluorescent conjugates of ferrichrome also indicated that the siderophore was recycled in *Ustilago maydis* and *Pseudomonas putida* (Ardon *et al*, 1997; Nudelman *et al*, 1998). This is in contrast to ferrichrome utilisation in *E. coli* where deferri-ferrichrome is acylated resulting in inactivation (Hartmann and Braun, 1980). Analysis of ferrichrome utilisation in *U. maydis* indicated that the ferrichrome fluorescence was located in vesicles within the cell, suggesting that ferrichrome possibly acts as an iron storage molecule (Ardon *et al*, 1997; Ardon *et al*, 1998). In *P. aeruginosa*, the peptidic siderophore pyoverdine has also been shown to be recycled (Schalk *et al*, 2002).

1.9: Secretion Of Siderophores

Siderophores, antibiotics and metal transporting agents are produced by many microorganisms and often confer a competitive advantage on the organisms that produce then (Dreschel and Jung, 1998; Demain and Fang, 2000). The environmental release of these compounds, which can be structurally quite distinct, generally requires an active efflux device. The release of charged molecules typically requires three components; an active membrane pump belonging to the RND (resistance nodulation division) family (Saier *et al*, 1994), a membrane fusion protein (MFP) that links the pump to the outer membrane (Dinh *et al*, 1994), and an outer membrane channel for release (Nikaido, 1996, Putman *et al*, 2000). These transport proteins are involved in the symport, antiport and uniport of various substrates, including antibiotics (Marger and Saier, 1993). Such proteins have generally only been analysed as multidrug exporters, resulting in their more general function as metabolite exporters to be overlooked. The size and charge of most siderophores all but excludes the possibility of passive diffusion across the cell membrane. This necessitates the need for a siderophore secretion apparatus or a transport pump. Despite extensive characterisation and analysis of the mechanisms of siderophore utilisation systems, the membrane secretion apparatus for the transport of these molecules into the environment have not been clearly identified or characterised.

A putative operon was identified in *P. aeruginosa*, which appeared to encode an efflux system involved in the export of the siderophore pyoverdine (Poole *et al*, 1993a). The efflux system, MexAB-OprM, was also found to function as a multidrug efflux pump as overexpression of the operon increased the resistance of *P. aeruginosa* to several antibiotics including chloramphenicol, tetracycline and nalidixic acid (Poole *et al*, 1993b). While MexAB-OprM may play a role in the export of pyoverdine, evidence suggests that it may be more generally involved in the export of secondary metabolites and antibiotics (Poole, 1994; Li *et al*, 1995). An operon, PA2389-PA2390-PA2391, was identified within the pyoverdine *pvd* gene cluster and was predicted to encode an efflux system. Mutants in these genes produced significantly reduced levels of pyoverdine, indicating that they were defective in secretion of the siderophore (Oschsner *et al*, 2002b). It is possible that this system

represents the primary exporter for pyoverdine, while the MexAB-OprM system may act as a more general export system for pyoverdine.

A protein identified in *M. smegmatis* was implicated in siderophore secretion. ExiT was predicted to be a member of the ABC transporter family classically represented by the haemolysin exporter, HlyB, of *E. coli* (reviewed by Higgins, 1992). The ExiT protein was predicted to be a membrane protein with twelve putative transmembrane domains. A signature ATP binding cassette was identified near the C-terminal of the protein. An *exiT* mutant did not produce exochelin, nor did it accumulate the siderophore internally. It was suggested that synthesis and export of the siderophore might be coupled so as to avoid any toxic effects of free siderophore in the cell (Zhu *et al*, 1995).

Analysis of the enterobactin operon of *E. coli* lead to the identification of a 43 kDa membrane protein with homology to the major facilitator superfamily (MFS) class of proton motive force dependent membrane efflux systems (Chenault and Earhart, 1991; Shea and McIntosh, 1991; Pao *et al*, 1998). Analysis of the protein, designated EntS, indicated that it was involved in the export of enterobactin but not of its breakdown product, 3-dihydroxy-N-benzoyl-L-serine, which can also function as a siderophore (Section 1.8)(Furrer *et al*, 2002).

Several MFS type proteins have been identified in other siderophore regulons. Encoded within the alcaligin gene island of *B. pertussis* is a protein with homology to MFS type proteins (Brickman and Armstrong, 1999). Two proteins encoded within a region involved in siderophore biosynthesis and transport in *A. baumannii* also show homology to MFS and RND type efflux proteins (Dorsey *et al*, 2003). The involvement, if any of these proteins in siderophore export remains to be elucidated.

1.10: Novel Mechanisms For Outer Membrane Siderophore Transport

The transport of ferrisiderophores is thought to involve the translocation of the siderophore from an extracellular environment to an intracellular environment by the processes described in the previous sections. Analysis of several siderophore utilisation systems has indicated that the transport mechanism might be more complex than originally thought.

Pyoverdine, a fluorescent siderophore produced by *P. aeruginosa* is transported at the outer membrane by its cognate receptor FpvA. Although it is generally accepted that siderophore receptors only bind ferrisiderophores (Figure 1.9 (a)), FpvA purified from a pyoverdine producing strain of *P. aeruginosa* co-purified with deferri-pyoverdine. It was subsequently shown that this process also occured with intact cells. Further examination indicated that iron free pyoverdine was displaced by iron bound pyoverdine at the outer membrane (Figure 1.9 (b)). The process of displacement appeared to be regulated by TonB as a *P. aeruginosa tonB1 tonB2* mutant failed to mediate the replacement of pyoverdine with iron bound pyoverdine (Schalk *et al*, 2001). The results indicates the involvement of TonB in initial binding and replacement as well as subsequent transport for iron bound pyoverdine as TonB does not appear to affect deferri-pyoverdine binding. The results also suggest that the FpvA binding site of pyoverdine differs from that of iron bound pyoverdine. After the transport of ferripyoverdine into the cytoplasm, the iron is released and the pyoverdine is secreted into the external environment (Schalk *et al*, 2002). The strong binding of pyoverdine to FpvA possibly results in faster iron delivery to the organism. Pyoverdine bound to FpvA can extract Fe^{3+} from the medium and deliver it to the cell immediately, whereas pyoverdine released into the medium must first bind Fe^{3+} and then diffuse through the media to bind FpvA.

In contrast to other characterised iron utilisation systems, a large variety of structurally different siderophores that serve as iron sources are though to be transported via a single transporter across the outer membrane of *A. hydrophilia* (Stinzi *et al*, 2000). Competition studies indicated that structurally unrelated siderophores bind at the same time as amonabactin, a siderophore produced by *A.*

hydrophilia, to the outer membrane receptor. The iron is then transferred to amonabactin by an as yet unknown mechanism (Figure 1.9 (c)).

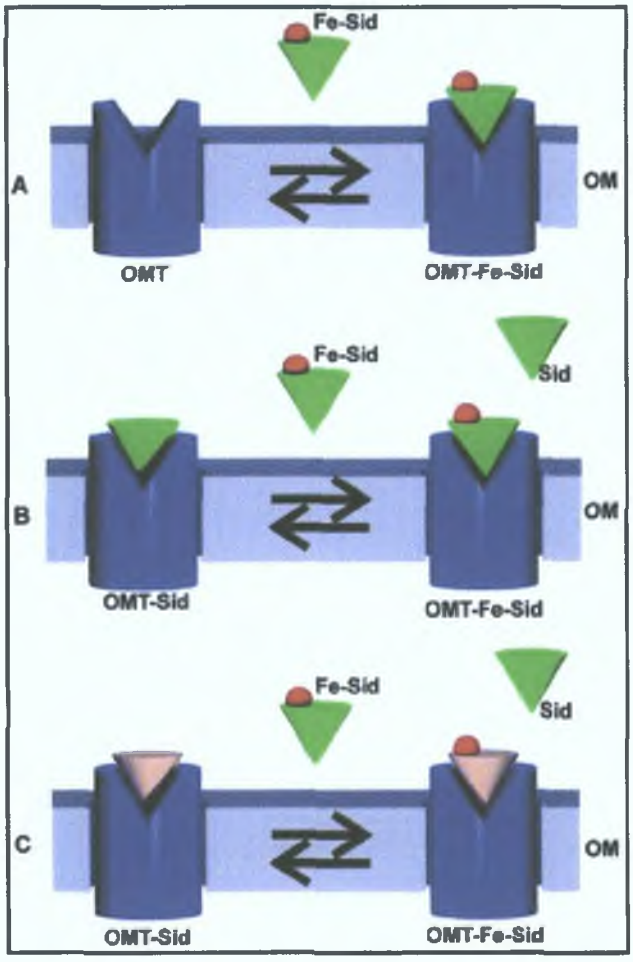

Figure 1.9: Mechanisms Of Siderophore Transport. A: Ferric (red) siderophore (green)(Fe-Sid) binds to the outer membrane transport protein (blue)(OMT) and is transported as such across the outer membrane (OM). B: Ferric pyoverdine displaces pyoverdine at the FpvA transport protein of *P. aeruginosa*. C: Different ferric siderophores supply iron to the siderophore bound to the transport protein of *A. hydrophila*. OMT-Fe-Sid, ferric siderophore bound to an outer membrane transport protein (Braun and Braun, 2002).

1.11: Iron Storage

With the exception of lactobacilli, all microorganisms require iron for growth. Although it is important that bacteria acquire sufficient iron to support growth, it is also important that the cell maintains the acquired iron in a non-toxic form. It is vital for cell survival that cellular iron be inhibited from reacting with the reactive oxygen species that are produced from aerobic metabolism. To overcome this dilemma, microorgansims have developed mechanisms of depositing iron intracellularly in a safe and bioavailable form within iron storage proteins (Andrews, 1998). Three types of iron storage proteins have been discovered in bacteria: Ferritins, which are also found in eukaryotes and are well characterised, bacterioferritins, which are haem containing proteins found only in eubacteria and Dps proteins, which are only found in prokaryotes. The storage proteins are distantly related and display many structural and functional similarities.

1.11.1: Ferritin

Ferritins have been isolated from both eukaryotes and prokaryotes and are well characterised. The ferritin molecule consists of a protein coat surrounding an inorganic iron core. The structure of these proteins provides them with their iron storage capability. Ferritins are composed of twenty-four identical subunits that assemble to form a hollow spherical structure. Each subunit folds to form a four α-helix bundle. The central cavity acts as an iron storage reservoir that can store between 2000-3000 iron atoms per 24-mer. Iron is taken up into ferritin in a ferrous state, but is stored in the central cavity in the oxidised ferric state. Specific sites within the ferritin molecule termed the ferroxidase centre catalyse the ferrioxidation step. These sites are located within the central regions of the individual subunits.

An *E. coli* mutant in the ferritin A (FtnA) gene, *ftnA* was isolated, and showed a reduced rate of growth under iron limiting conditions (Abdul-Tehrani *et al*, 1999). The growth defect was only observed when the wild type and mutant strains were grown in iron replete media and subsequently transferred to iron deplete media. It was demonstrated that there was an approximate 50% reduction in stationary phase iron content following the growth under iron replete conditions. It was thus

concluded that ferritin acts as an iron store accumulating iron during post-exponential growth in iron replete media to act as an intracellular source of iron during subsequent growth under iron deplete conditions. Expression of *ftnA* is induced by iron and by post exponential growth.

1.11.2: Bacterioferritin

Bacterioferritins (Bfr) are more common in bacteria than ferritins, yet their physiological function is unclear. Bacterioferritins are structurally similar to ferritins: They are also composed of twenty four identical subunits that assemble to form a hollow sphere whose central cavity can store between 2000-3000 iron atoms per 24-mer. Unlike ferritins however, bacterioferritins contain haem generally in the form of protoporphyrin IX. There are normally 12 haem groups per 24-mer located at each of the 12 two fold interfaces between subunits. The haem iron atom is located towards the inner surface of the protein shell, with the haem exposed to the central storage cavity. The function of the haem group is unclear, but evidence suggests that it is involved in the release of iron from bacterioferritin by facilitating reduction of the iron core (Andrews *et al*, 1995).

Many bacterioferritin genes, *bfr*, are associated with a gene, *bfd* encoding a ferredoxin known as Bfd (Bacterioferritin associated ferredoxin). The *bfd* gene is induced by conditions of iron limitation and taken with evidence that it interacts specifically with Bfr and that Bfd contains an Fe-S domain, it suggests a role for Bfd in iron release from Bfr (Quail *et al*, 1996; Garg *et al*, 1996). No phenotypes are associated with *bfr* mutants of *E. coli*.

1.11.3: Dps

Although Dps (DNA binding protein from starved cells) proteins are smaller that either ferritins or bacterioferritins, they show considerable structural similarity. They are composed of twelve identical subunits that assemble to form a hollow sphere. The central iron storage cavity can store approximately 500 iron atoms per 12-mer. The conserved amino acid residues found in ferritins and bacterioferritins are not conserved in Dps proteins. These proteins bind iron at a site located at a two-fold interface between subunits (Ilari *et al*, 2000). The mechanism of iron oxidation therefore varies from that of ferritins and bacterioferritins.

The Dps protein was initially identified in *E. coli* and was found to be induced in stationary phase by σ^S, which is a stationary phase sigma factor and a global regulator in bacteria encoded by *rpoS*. Dps was found to be a non-specific DNA binding protein with a role in the protection of DNA from redox stress (Almiron *et al*, 1992). Subsequent analysis of Dps indicated that the primary function of the protein was in the protection of DNA from hydroxyl free radicals (Zhao *et al*, 2002). It is likely that the Dps protein of *E. coli* does not primarily function in iron storage.

1.12: Regulation Of Siderophore Mediated Iron Acquisition

While iron is essential for growth of most microorganisms, excess iron can have deleterious effects due to its ability to catalyse the generation of free radicals. Bacteria therefore exert a fine control over the intracellular concentration of iron. The control of intracellular iron is generally regulated by the controlled expression of genes involved in iron acquisition and storage. Genes can be repressed in iron replete conditions or derepressed under conditions of iron depletion. In *E. coli* and many other bacteria this regulation is mediated by the Ferric Uptake Regularor (Fur) protein (reviewed by Hantke, 2001). Genes are repressed under iron replete conditions by the interaction of Fur with the promoter regions of the genes of interest (Bagg and Neilands, 1987). Under iron deplete conditions Fur dissociates from the promoters, and positive regulatory elements are induced (Crosa, 1997).

1.12.1: The Fur Regulon

Fur is considered a global regulator or iron metabolism genes as it is the chief protein involved in the regulation of iron acquisition genes. A *fur* mutant was initially identified by its phenotype in *S. typhimurium* (Ernst *et al*, 1978) and *E. coli* (Hantke *et al*, 1984). The mutant was identified by its constitutive expression of genes involved in siderophore biosynthesis and utilisation. The Fur protein of *E. coli* was identified and shown to be a homodimer composed of 17 kDa subunits (Coy and Neilands, 1991) that acted as a transcriptional repressor of iron-regulated promoters by virtue of its Fe^{2+} dependent DNA binding activity. The Fur protein was shown to bind one ferrous ion per subunit, but other ions such as Co(II), Cd(II), Cu(II) and Mn(II) were also found to be bound by Fur. The concentration of these ions *in vivo* however is insufficient to be of any relevance in the Fur interaction (Bagg and Neilands, 1987). The Fur protein of *E. coli* contains one zinc ion per dimer, possibly at a site located in the C-terminal half of the subunit (Jacquarnet *et al*, 1998; Althaus *et al*, 1999), however, this site is not conserved in all bacteria, and the zinc ion is apparently not required for function (Lewin, 2002). The N-terminal half of the protein contains a helix-turn-helix motif that confers on the protein the ability to bind DNA (reviewed by Hantke, 2001)

The isolation of purified Fur protein enabled the analysis of the interaction of the Fur complex and iron-responsive promoters of *E. coli*. The Fur complex was found to bind generally between the –35 and –10 sites of the promoters of iron regulated genes. Fur binding was found to correlate with the presence of a 19 bp palindromic consensus sequence known as the Fur box (Figure 1.10 (A))(de Lorenzo *et al*, 1988a). It should be noted that this sequence is deduced and that the exact sequence is not found anywhere in the *E. coli* genome sequence. Examination of Fur binding by DNase I footprinting revealed that Fur protected a region larger than the Fur box, indicating that Fur interacts with DNA outside the Fur box (Escolar *et al*, 2000). The Fur protein was also shown to stimulate binding at weak secondary binding sites adjacent to the primary binding site of the aerobactin biosynthesis operon promoter and Fur dimers were shown to wrap around the double helix extending into regions that do not match the Fur box consensus sequence (de Lorenzo *et al*, 1988a; Le Cam *et al*, 1994). Such binding lead to a re-interpretation of the Fur box sequence as three repeats of 6 bp (Figure 1.10 (B))(Escolar *et al*, 1998) which was then further refined to be overlapping 13 bp motifs (Figure 1.10 (C))(Lavrrar *et al*, 2002) indicating the dynamic functionality of Fur binding (Figure 1.10).

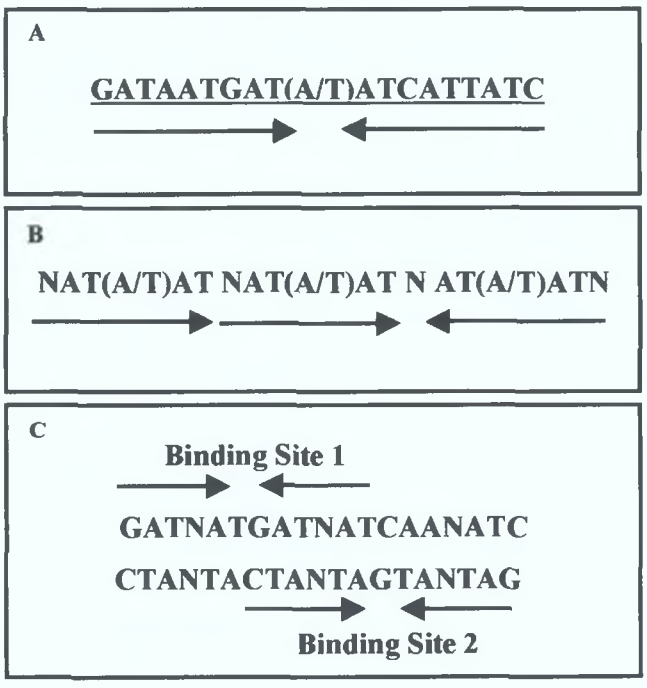

Figure 1.10: Models of Fur Consensus Sequence. The possible binding site models are discussed in the text.

The Fur protein appears to exist as a dimer in solution regardless of the presence or absence of Fe^{2+} (Coy and Neilands, 1991; reviewed by Escolar *et al*, 1999). The C-terminal of the protein has implicated in dimerisation while the N-terminal region of the protein has been shown to function in DNA binding and deletion of this domain abolishes the ability of the protein to bind DNA (Coy and Neilands, 1991; Stojiljlovic and Hantke, 1995; reviewed by Escolar *et al*, 1999). The Fur protein is quite abundant in *E. coli* in contrast with the generally low concentration of other regulators. It is possible that this is due to the tendency of Fur to polymerise along DNA or that Fur may act as a buffer, binding free Fe^{2+} ions in the cell. The *fur* gene appears to form an operon with *fldA*, which has been shown to be essential and encodes a flavodoxin. It is possible that FldA functions to maintain cytosolic free iron in a reduced state in order to provide Fe^{2+} to the Fur protein (Zheng *et al*, 1999).

Although the main function of the Fur protein is to regulate genes involved in iron acquisition Fur also appears to regulate genes that do not appear to be directly involved in iron acquisition. In *Salmonella*, *fur* mutants display an increased sensitivity to acids (Hall and Foster, 1996), while *E. coli fur* mutants are unable to grow on non-fermentable carbon sources, indicating a deficiency in respiration (Hantke, 1987). The degenerate nature of the Fur box sequence also allows for the sequential expression of various genes. Under conditions of iron limitation, *E. coli* expresses iron-regulated genes in sequence depending on the level of iron stress (Klebba *et al*, 1982). In *E. coli*, *fhuF* and *fhuA* are amongst the earliest genes to be expressed under conditions of iron limitation, while *fepA*, *fiu* and *cir* induction require a greater level of iron stress. The difference in gene expression may be explained by analysis of the Fur boxes located in the promoters of the individual genes: The *cir* promoter contains two well conserved Fur boxes while the *fhuA* promoter only contains one poorly conserved Fur box (Coulton *et al*, 1986; Griggs and Konisky, 1989). The relatively poor Fur box in the *fhuA* promoter leads to relatively weak binding of Fur in comparison to the *cir* Fur box. This feature of differential expression has been used to develop an *in vivo* assay to allow for the detection of Fur boxes in cloned fragments of DNA (Stojilikovic *et al*, 1994).

Fur homologues have been discovered in many other bacteria (reviewed by Crosa, 1997; reviewed by Hantke, 2001). In several bacteria, including *P. aeruginosa*,

Nesserria meningitides and *Synechococcus*, the *fur* gene appears to be essential (reviewed by Escolar *et al*, 1999). This indicates that Fur possibly regulates essential cellular processes. Global analysis of iron regulated genes in *P. aeruginosa* indicated the presence of many genes that were induced by conditions of iron limitation, some of which are likely to be regulated by Fur (Ochsner *et al*, 2002). Similar analysis in *B. subtilus* enabled the identification of genes that are induced under conditions of iron limitation, and that are regulated by Fur (Baichoo *et al*, 2002). The global analysis indicates that a wide variety of cellular processes are regulated by iron availability.

1.12.2: Small Regulatory RNAs-*ryhB*

As described previously, bacteria respond to conditions of iron limitation by inducing genes involved in iron acquisition, while repressing proteins involved in iron storage in a process mediated by the Fur complex. The Fur protein also appears to induce iron storage proteins and some iron-dependent proteins under conditions of iron repletion (Gruer and Guest, 1994; Dubrac and Touati, 2000). The Fur protein appears to regulate this induction indirectly by direct regulation of a small 90 nucleotide small RNA (sRNA) termed *ryhB*. Fur represses the synthesis of *ryhB*, which in turn negatively regulates the synthesis of at least six proteins that bind iron in the cell including bacterioferritin and ferritin. The *ryhB* RNA appears to function by binding to regions within a mRNA which are complementary to the *ryhB* sequence, which indicates that *ryhB* functions as an antisense RNA. The production of sRNA's to regulate proteins is advantageous to the cell as it does not require the synthesis of a protein to post-transcriptionally regulate the mRNA. Also, because sRNA's may also act on an existing mRNA it should exert its effect faster than regulation at the level of the promoter, which would also leave the existing message intact. For Fur, *ryhB* may also function to allow Fur to act as a positive regulator for a small subset of genes. Genome wide analysis has enabled the identification of further sRNAs and it is possible the sRNAs play an integral part in the regulation of iron homeostasis systems. Figure 1.11 shows the mechanism of *ryhB* function.

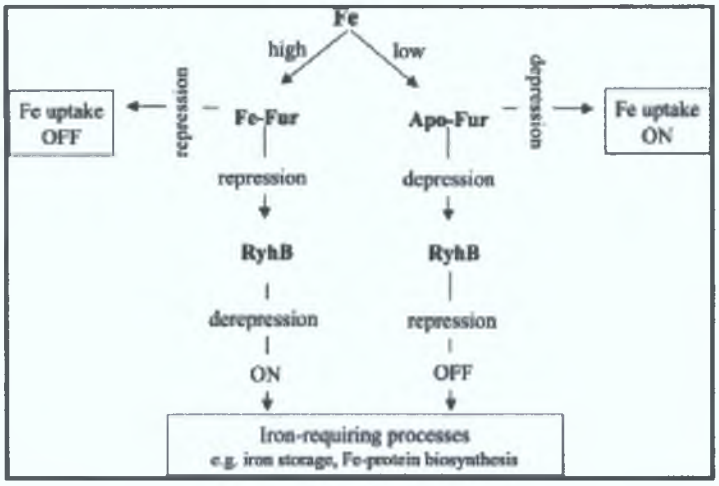

Figure 1.11: Roles of Fur and *ryhB* in mediating Fe-dependent gene regulation in *E. coil* (Andrews *et al*, 2003).

1.12.3: Hfq

The *ryhB* sRNA requires the Hfq RNA-binding protein for function. Hfq is an RNA-binding protein that has been found to participate in many RNA transactions in the cell including mRNA stability, mRNA polyadenylation and translation (Wassarman *et al*, 2001). An *E. coli hfq* mutant exhibited pronounced pleiotropic phenotypes including decreased growth rate, UV sensitivity, osmosensitivity and increased cell length (Tsui *et al*, 1994). The phenotype of the mutant is similar to that caused by a σ^S mutant. It was subsequently shown that Hfq positively regulates *rpoS* expression post-transcriptionally (Muffler *et al*, 1996). The production levels of more than 30 proteins are affected in a *hfq* mutant strain. In approximately half the cases, the changes are independent of σ^S (Muffler, 1997). Hfq appears to stimulate RNA-RNA pairing, indicating that it acts as a general RNA chaperone (reviewed by Gottesman, 2002).

1.12.4: Other Regulators

Intensive screening of organisms of interest has resulted in the identification of apparently novel regulators and novel mechanisms of regulation. Similarly, in a number of studies, evidence suggests the presence of additional regulators that have yet to be identified. The plethora of regulatory mechanisms identified possibly reflects the importance of iron for normal cell function.

An iron responsive regulator termed RirA (**R**hizobial **i**ron **r**egulator) was identified in the symbiotic nitrogen fixing bacterium *R. leguminosarum* bv. *viciae*. Mutations in *rirA* caused high-level constitutive transcription of at least eight operons whose transcription is normally iron regulated (Todd *et al*, 2003). The mechanism of RirA function is not known, but analysis of the N-terminal region indicates that the region has significant matches to transcriptional regulators. Analysis of the *rpoI* (Yeoman *et al*, 1999) and *hmuPSTUV* (Wexler *et al*, 2001) promoter regions revealed the presence of a conserved 10-mer AAACTTGACT. However the lack of any other conserved sequence in the promoter regions of any other gene affected by RirA indicates that it may act by some other unknown mechanism. Close homologues of RirA have been identified in the near rhizobial relatives, *Sinorhizobium*, *Agrobacterium* and *Mesorhizobium*. A close homologue has also been identified in the important pathogen *Brucella*. An *rirA* mutant was unaffected in nodule formation and symbiotic nitrogen fixation.

As mentioned previously, *V. anguillarum* produces a catechol siderophore termed anguibactin (Section 1.2.1). The siderophore is transported via a PBT system that includes the outer membrane receptor FatA and the periplasmic binding protein FatB. A chromosomally encoded Fur homologue negatively regulates the expression of FatA under iron replete conditions (Tolmasky *et al*, 1994). An antisense RNA (RNAα) that was encoded in the *fatB* region was identified and found to be transcribed only under iron replete conditions (Waldbeser *et al*, 1993). The RNAα molecule was found to affect the stability of *fatA* and *fatB* mRNA transcripts (Waldbeser *et al*, 1993; Waldbeser *et al*, 1995). The data suggests that there are two levels of regulation: The first is at the transcriptional level and the second level is post-transcriptional and is regulated by the RNAα.

In high GC-content Gram-positive bacteria the DtxR protein mediates global iron regulation. The protein was initially identified in *Corynebacterium diphtheriae* as a repressor of toxin repressor (Boyd *et al*, 1990). The DtxR proteins regulate genes similar to those regulated by Fur in many Gram-negative bacteria including siderophore biosynthesis genes and oxidative stress response genes. Although the Fur and DtxR proteins do not display any sequence homology they do display a number of

structural similarities. The N-terminal of both proteins contain a DNA binding domain while the central domain appears to be involved in metal binding and dimerisation. In contrast to Fur, the DtxR protein contains a carboxy domain of unknown function.

B. japonicum coordinates haem biosynthesis with iron availability, in a process that is regulated by the Irr (Iron response regulator) protein, which is a member of the Fur family of transcriptional regulators (Hamza *et al*, 1998). Irr-mediated regulation ensures that the production of porphyrin does not exceed iron availability. Irr is subject to complex post-transcriptional modification: It is degraded when bound to haem, which is delivered by the enzyme ferrochelatase, resulting in an increase in haem biosynthesis (Qi *et al*, 1999: Qi and O'Brian, 2002). Homologues of Irr have been identified in *S. meliloti*, *R. leguminosarum* and *Mesorhizobium loti*.

Random mutagenesis of *S. meliloti* 2011 led to the identification of two mutants that were affected in iron acquisition (Lynch, PhD Thesis 1999). One of the mutants was defective in all types of iron acquisition examined, whereas the second mutant was defective in siderophore production and in all types of iron acquisition examined. The mutants are similar to mutants isolated by Fabiano *et al* (1995), which are also defective in iron acquisition. The molecular basis of the iron acquisition defect remains to be elucidated but the broad phenotype observed suggests a regulatory defect.

Phase variation is a process by which the diversification of a single bacterial population occurs into differentiated subpopulations. Phase variation is an important process, as phenotypical differentiation can allow the establishment of specific ecological niches. Phase variation is thought to occur via a mechanism of slipped-strand mispairing. This process is believed to occur during DNA replication, where DNA polymerase 'slips' on a string of repeated nucleotides in the templated DNA, resulting in the addition or deletion of one repeat unit in the daughter strand (Levinson and Gutman, 1987). This can occur within an open reading frame, resulting in a frameshift mutation, or in the promoter region of a gene causing differences in promoter-strength transcription. The FetA protein of *Neserria gonorrhoeae*, which functions as an outer membrane receptor for ferrienterobactin (Carson *et al*, 1999),

was found to be regulated by phase variation. The difference in expression was found to correlate with the number of cytosine residues found in the promoter region of *fetA*, the alteration of which leads to a drastic reduction in gene expression (Carson *et al*, 2000). Anti FetA antibodies commonly occurs in infected patients, and phase variant regulation of the receptor may enable the bacterium to evade the host immune response. The bacterium *Pseudomonas fluorescens* F113 undergoes phase variation during colonization of the alfalfa rhizosphere (Sánchez-Contreras *et al*, 2002). Variants displayed altered colony morphology and differences in motility. The production of a number of extracellular factors including siderophore and exoprotease production was also affected. Analysis indicated that phase variation of the described traits was due to mutations in the *gacA/gacS* system, which co-ordinately regulates the production of secondary metabolites (Blumer *et al*, 1999) and *sss*, a site specific recombinase required for competitive root colonisation by *P. fluorescens* (Dekkers *et al*, 1998).

Analysis of *R. leguminosarum* and *B. japonicum* suggest the presence of further unidentified regulators. A laboratory strain of *R. leguminosarum* was found to have acquired a mutation that affected iron responsive gene regulation (de Luca *et al*, 1998). Although the phenotype associated with this strain was similar to that described for an *rirA* mutant, the mutation was found to be unrelated to this gene (Todd *et al*, 2002). A pallindromic repeat sequence was identified between the *hmuR* and *hmuT* genes of *B. japonicum*. Mutagenesis of the repeat sequence led to a drastic reduction in *hmuT* and *hmuR* gene expression. The reduction in expression was shown to be unrelated to the activity of the Irr or Fur protein, suggesting regulation by an as yet unidentified regulator (Nienaber *et al*, 2001).

1.13: Haem Acquisition In Bacteria

Haem performs several different functions such as acting as a prosthetic group for several proteins and acting as a cofactor to mediate oxygen transport. The iron chelated in the porphyrin ring can also act as an iron source for the growth of bacteria. Pathogenic bacteria encounter an environment that is essentially iron deplete. Virtually all host iron is bound to haemoglobin, transferrin and lactoferrin (reviewed by Payne, 1993; reviewed by Litwin and Calderwood, 1993; reviewed by Crosa, 1997). To overcome these conditions of iron limitation, many microorgansims have developed acquisition systems to obtain iron from the various haem proteins found in the host.

Haem comprises a metal chelated ion, generally iron, in a porphyrin ring. When the bound iron is in the reduced Fe^{2+} state, the compound is referred to as haem, while when it is in the oxidised Fe^{3+} state, the compound is referred to as haemin. Similarly to ferrisiderophore complexes, the size of haem in solution limits its ability to traverse the outer membrane of bacteria. Haem compounds therefore have to be actively transported into cells in an energy dependent manner. The best-characterised mechanism by which bacteria acquire haem is by direct binding of haem or haem compounds to specific outer membrane receptors (Figure 1.12A).

The energy for transport across the outer membrane protein is provided by the action of TonB and in several cases specific *tonB* genes have been found to be associated with outer membrane haem receptors (Occhino *et al*, 1998; Nienaber *et al*, 2001). Inactivation of these *tonB* genes did not abolish all TonB dependent functions indicating that these proteins are partially redundant. Haem outer membrane receptors have been shown to contain several highly conserved domains that may be important for function (Bracken *et al*, 1999; Wandersman and Stokiljkovic, 2000; Nienaber *et al*, 2001).

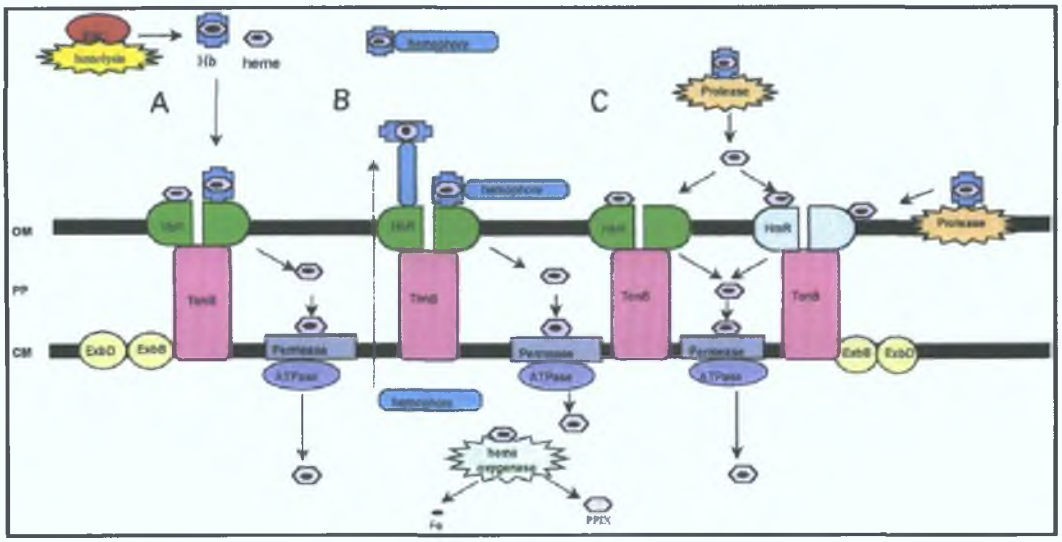

Figure 1.12: Microbial mechanisms for haem capture (Genco and Dixon, 2001). Red blood cells (RBCs) are degraded by a bacterial haemolysin, resulting in the liberation of haemoglobin (Hb) and haem (Hm). Although not depicted, it is well accepted that, once released, haem is bound to albumin and haemopexin. Haem may be transported into the bacterial cell by several mechanisms.

A. Direct binding of haemoglobin to a specific TonB-dependent outer membrane receptor; Hb and Hm are proposed to bind to discrete sites on the receptor.

B. Capture of haemoglobin and haemopexin by secreted proteins (haemophores), which deliver the haemoglobin or haemopexin to a specific TonB-dependent outer membrane receptor; the Hb receptor may bind the Hb-bound haemophore through either the Hb or the haemophore.

C. Degradation of haemoglobin, haemopexin and human serum albumin by bacterial proteases, resulting in the liberation of haem. Bacterial proteases can be either membrane bound or secreted. Haem is subsequently bound by TonB-dependent haem/haemoglobin receptors and transported into the periplasm. Energy for the transport of iron or haem across the outer membrane into the periplasmic space is provided by TonB in association with the ExbB and ExbD proteins. The transport process through the cytoplasmic membrane is not well described but appears to occur via an ABC transport system composed of a cytoplasmic membrane-associated permease and an ATPase. Within the cytoplasm, haem is degraded by a haem oxygenase.

Haem acquisition systems can be generally separated into three categories based on the factors involved in acquisition mechanism. The largest category comprises systems that are similar to the systems described for the acquisition of ferrisiderophores. They involve a specific TonB dependent outer membrane receptor and a PBT system required for transport through the inner membrane. The best-studied examples of this type of system include the HemR-HemSTUV system of *Yersinia enterocolitica* (Stokiljkovic and Hantke, 1992), the HmuRSTUV system of *Yersinia pestis* (Hornburg *et al*, 1996; Thompson *et al*, 1999) and the PhuR-PhuSTUVW system of *P. aeruginosa* (Ochsner *et al*, 2000).

The haem acquisition systems in the second category consist of a TonB dependent outer membrane receptor, an extracellular haem binding protein and an ABC export system, also referred to as a type I secretion system. The secreted proteins function to extract haem from haemoglobin and haemopexin and to deliver the haem complex to the outer membrane haem receptor (Figure 1.12 (B)). The best-characterised example of this systems is the HasA system of *S. marcesens* (Létoffé *et al*, 1999), however similar systems have been identified in *P. aeruginosa* and *P. fluorescens* (Létoffé *et al*, 1998; Létoffé *et al*, 2000). The HasR receptor of *S. marcesens* can transport free haem or haem from haemoglobin, but the presence of HasA greatly enhances transport.

The third category involves haem-binding outer membrane lipoproteins. The best-studied examples of this system are found in *H. influenzae* type *b* (Hanson *et al*, 1992) and *H. influenzae* Rd (Reidl and Mekalanos, 1996).

The release of iron from haem in the cytoplasm is thought to be achieved by the degradation of the haem molecule. In the gram positive bacterium *C. diphtheriae*, this release has been shown to be mediated by haem oxygenase (Chu *et al*, 1999). Haem oxygenases from eukaryotic cells have been shown to be involved in the oxidative degradation of haem through cleavage of the porphyrin ring. The role of haem oxygenases in the release of iron from haem in other organisms remains to be confirmed.

The acquisition of haem from host haem protein complexes can also be enhanced by the action of extracellular proteases and haemolysins that degrade host haem proteins (Figure 1.12 (C)). Several microorganisms have been shown to produce efficient haemolysins and proteases. *P. aeruginosa*, an opportunistic human pathogen secretes several extracellular factors that facilitate the acquisition of haem. *P. aeruginosa* produces an extracellular protein, termed exotoxin A which has broad cytotoxic activity towards eukaryotic cells under conditions of iron limitation (Vasil *et al*, 1977). *P. aeruginosa* also produces the heat labile haemolysin, phospholipase C (Berka and Valil, 1992). Similarly the pathogen *V. cholera* El-Tor produces a cytotoxic haemolysin, HlyA under conditions of iron limitation (Stoebner and Payne, 1988; Menzl *et al*, 1996). *S. marcesens* has also been shown to produce a

haemolysin, ShlA under conditions of iron limitation (Poole and Braun, 1988). The ability of haemolysins and various other toxins to release iron and haem compounds from host cells broadens the sources of iron available to various pathogens, and possibly contributes to pathogenecity of the organism.

1.14: Siderophore Mediated Iron Acquisition In *E. coli*

The *E. coli* K-12 bacterium is the most studied and characterised microorganism, and is generally regarded as being a model organism. The entire genome of the microorganism has been sequenced and the techniques for its genetic manipulation are well established. Consequently, the mechanisms of iron acquisition in *E. coli* have been examined in detail. *E. coli* K-12 has been found to synthesise and utilise the catechol siderophore, enterobactin. The bacterium has also been shown to transport a wide variety of heterologous siderophores or xenosiderophores. Various pathogenic strains of *E. coli* have been shown to harbour plasmids that confer upon the bacterium the ability to synthesise and utilise the citrate hydroxamate siderophore, aerobactin. The various siderophore acquisition mechanisms identified in *E. coli* are shown in Figure 1.13.

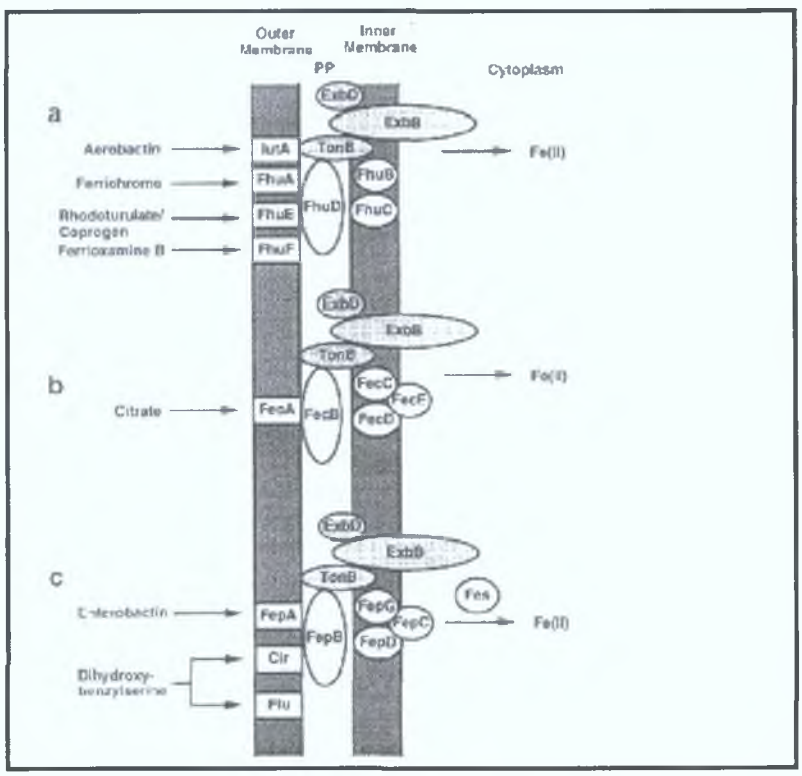

Figure 1.13: Siderophore Acquisition Systems Of *E. coli* (Guerinot, 1994). As described previously (Section 1.8), FhuF is not thought to function as an outer membrane receptor.

1.14.1: Enterobactin

Enterobactin, a catechol siderophore first isolated from *E. coli* and *S. typhimurium*, is widely produced by members of the Enterobacteriacae (1.2.1). The genes encoding enterobactin biosynthesis and transport are clustered on the *E. coli* chromosome in a large 22 Kb region, and are arranged into six individual gene cluster operons (Earhart, 1996; reviewed by Crosa and Walsh, 2002). The synthesis of enterobactin is performed by non-ribosomal peptide synthesases (NRPS). NRPS are multimodular enzymes that produce peptide products of a particular sequence without an RNA template. Enterobactin is synthesised by a fork in the aromatic amino acid pathway. Chorismic acid, an aromatic amino acid precursor, is converted into enterobactin by a series of reactions involving the enterobactin biosynthesis proteins. The biosynthesis of enterobactin may be broken into two parts; Initially chorismic acid is converted to 2,3-dihydroxybenzoic acid (DHB) by the enzymes EntC, EntB and EntA (Walsh *et al*, 1990). Subsequently, enterobactin is synthesised from DHB and L-serine by EntD, EntE and EntF and the C-terminal aryl carrier of EntB, which is a bifunctional protein (Gehering *et al*, 1997; reviewed by Crosa and Walsh, 2002). The acquisition of enterobactin by *E. coli* is mediated by the FepA outer membrane receptor and a PBT system consisting of FepBCDG (Section 1.5 and 1.7). Secretion of the siderophore has been found to be primarily dependent on the EntS protein (Section 1.9)(Furrer *et al*, 2002).

1.14.2: Ferric citrate

Although it is thought that *E. coli* does not produce citrate in sufficient quantities to drive iron uptake, the bacterium nonetheless encodes proteins that allow for high affinity acquisition of the ferric citrate molecule. The ferric citrate transport system consists of an outer membrane receptor protein, FecA and a PBT consisting of FecBCDE (Section 1.5 and 1.7). The outer membrane receptor FecA is a dual function protein: The protein binds and transports ferric citrate and it is also required to initiate transcription of the *fecABCDE* transport operon, but not the regulatory genes *fecIR* which encode an extra cytoplasmic sigma factor (ECF) and a transmembrane sensor respectively (Härle *et al*, 1995; Ochs *et al*, 1995; Angerer *et al*, 1995; Kim *et al*, 1997). The transport of ferric citrate and the initiation of transcription requires the proton motif force of the cytoplasmic membrane as transduced by TonB. Transport of the siderophore is not required to initiate

transcription (Zimmermann *et al*, 1984). The binding of ferric citrate to FecA initiates a signal transduction cascade in which the cytoplasmic membrane spanning protein, FecR, interacts with the N-terminal of FecA and subsequently activates the extra cytoplasmic function (ECF) sigma factor, FecI, to bind to the *fecA* promoter thereby inducing transcription (reviewed by Visca *et al*, 2002).

1.14.3: Xenosiderophores

E. coli K-12 produces the catechol siderophore enterobactin, whose breakdown products can also function as weak siderophores (Section 1.9). Various pathogenic strains of *E. coli* have also been found to synthesise the citrate hydroxamate siderophore aerobactin. Despite this, of the six outer membrane siderophore receptors produced by *E. coli* K-12, three act as receptors for heterologous siderophores. FecA functions as a receptor for ferric citrate which can be considered to be a xenosiderophore, FhuA functions as a receptor for ferrichrome and FhuE functions as a receptor for coprogen and rhodotorulic acid (Figure 1.13). The ability of the bacterium to utilise xenosiderophores in not unusual, and it may confer an advantage to the bacterium when grown in a competitive environment.

1.14.4: Aerobactin

Certain clinical isolates of *E. coli* containing the plasmid pColV-K30 were found to encode a high affinity iron acquisition system independent of the enterobactin system (Williams, 1979). The siderophore, a hydroxamate, was isolated and shown to be aerobactin (Warner, 1981). As mentioned previously, aerobactin is a citrate hydroxamate siderophore originally isolated from *Aerobacter aerogenes* (now *Klebsiella pneumoniae*) (Section 1.2.2)(Gibson and Magrath, 1969). The siderophore has also been found to be synthesised by various *Shigella* spp. (Lawlor and Payne, 1984) and some *Salmonella* spp (McDougall and Neilands, 1984). In *E. coli* the utilisation of aerobactin is mediated by the IutA outer membrane receptor and the FhuCDB inner membrane iron transport system (Figure 1.13 and Section 1.7).

1.14.5: Aerobactin And Virulence

E. coli strains containing the pColV-K30 plasmids were characterised by their ability to cause disseminating infections in experimental animals. Although the plasmid also encoded the bacteriocin colicin V as well as the aerobactin regulon, it was shown that

the virulence characteristic could be attributed to the plasmid encoded aerobactin system rather than the bacteriocin or chromosomally encoded enterobactin system (Williams and Warner, 1980). The virulence of the *E. coli* pColV-K30 strains, which also produce enterobactin, was found to be greatly enhanced by the presence of the aerobactin system. The ability of aerobactin to have such a dramatic effect on virulence compared to enterobactin was surprising as enterobactin has a much higher affinity for Fe(III) than aerobactin ($K_f = 10^{52}$ for enterobactin compared to 10^{23} for aerobactin). These values however refer to fully deprotonated ligands, and probably do not accurately reflect the relative ability of these compounds to compete for iron at physiological pH. Aerobactin also has a number of other advantages over enterobactin *in vivo*. Enterobactin is relatively unstable and poorly soluble. While enterobactin deferrates transferrin more rapidly than aerobactin at neutral pH, the relative rates are reversed in the presence of serum albumin. The aromatic nature of enterobactin also causes it to adhere to proteins removing it from circulation (Konopka and Neilands, 1984). This characteristic of enterobactin causes it to act as a hapten inducing the production of anti enterobactin antibodies that can inhibit enterobactin utilisation (Moore and Earhart, 1981). Pathogenic *E. coli* also secrete aerobactin more rapidly than enterobactin (Der Vartanian, 1988), and aerobactin also promotes bacterial growth at concentrations some 500-fold lower that enterobactin (Williams and Carbonetti, 1986). The ability of aerobactin to be recycled (Braun *et al*, 1984) while enterobactin molecules deliver an iron atom and are subsequently hydrolysed by the Fes enzyme (Section 1.8)(O'Brien *et al*, 1971) possibly explains this discrepancy in the relative growth promoting effects. Finally, aerobactin channels iron directly into iron-dependent metabolism rather than releasing it into an intracellular 'labile pool' (Williams and Carbonetti, 1986).

Aerobactin has been found to be unimportant in the virulence of surface or intracellular pathogens. Aerobactin mutants of *Shigella flexneri*, a pathogen which multiplies within the intestinal cells of its human host, showed a reduction in the ability to cause intestinal fluid accumulation and to grow in the extracellular compartments of the host (Nassif *et al*, 1987), but were able to invade and multiply in epithelial cells to the same extent as the parent strain (Lawlor *et al*, 1987). The lack of a consistent effect of siderophore mutations on virulence suggest that iron acquisition mechanisms may be different between pathogens that grow intracellularly

and pathogens that grow in the blood or extracellular spaces. In an intracellular environment, pathogens may be able to utilise the large amounts of host iron compounds present thereby removing the dependency on a functional siderophore mediated iron acquisition system.

1.14.5: Genetic Analysis Of The Aerobactin Regulon

The aerobactin regulon have been shown to be both plasmid and chromosomally encoded. In *E. coli*, the aerobactin regulon has been found to be encoded on the pColV-K30 plasmid (Section 1.14.4) while in a number of other organisms the regulon is chromosomally encoded (McDougal and Neilands, 1984; Purdy and Payne, 2002). The entire aerobactin mediated iron acquisition system of pColV-K30 was cloned and found to be organised as an operon consisting of four biosynthesis genes, *iucABCD* (iron uptake chelate) and the outer membrane receptor gene *iutA* (iron uptake transport). As previously described, the enterobactin regulon located on the *E. coli* chromosome consists of six transcriptional units encoded over an approximate 22 Kb region. The aerobactin regulon consists of a single polycistronic operon spanning 8.3 Kb and arranged *iucABCDiutA*. The relatively small size of the operon in comparison to the enterobactin system lead to the study of aerobactin biosynthesis and transport as a model siderophore acquisition system.

The biosynthesis of aerobactin requires the four genes of the biosynthesis operon. The biosynthesis is initiated by the hydroxylation and acetylation of lysine. Two molecules of N^6-acetyl-N^6-hydroxylysine are then condensed with the primary carboxyls of citrate to yield aerobactin.

An insertion element, IS1 was found to flank the ColV aerobactin regulon in *E. coli* with two distinct replication regions overlapping the IS1 elements. Analysis of the IS1 elements indicated that they were both active and that the entire aerobactin system could undergo transposition like events (de Lorenzo *et al*, 1988b). The transposition like events possibly allow the spread of aerobactin genes amongst ColV plasmids and other members of the F1 incompatibility group. Analysis of the aerobactin regulons in *Shigella* indicated they were also bounded by IS elements forming pathogenicity islands (Moss *et al*, 1999; Vokes *et al*, 1999; Purdy and Payne, 2001).

Analysis of the promoter region upstream of *iucA* revealed the presence of two transcriptional start sites: A major transcriptional start site (P1) and a minor transcriptional start (P2) located approximately 50 bp upstream from P1. Transcription initiating at P1 was not detected following growth in high iron conditions, while specific RNA was detected in cells grown under conditions of iron depletion. A transcriptional fusion of the aerobactin promoter indicated that repression of aerobactin biosynthesis occurred by iron at the transcriptional level (Bindereif and Neilands, 1985). It was subsequently shown that the negative regulation of the aerobactin operon was mediated by the Fur protein (de Lorenzo *et al*, 1988a). DNA footprinting experiments performed with purified Fur protein showed that Fur first protected a sequence in the vicinity of the –35 region of the P1 promoter, and this was designated the primary binding site. An additional secondary binding site was located downstream of the –10 region (de Lorenzo *et al*, 1987). The regulation of the aerobactin regulon by Fur has been extensively studied and serves as a model for Fur mediated iron regulated promoters.

The biosynthesis proteins of aerobactin, IucA, IucB, IucC and IucD have been found to be present at different levels in *E. coli* (de Lorenzo *et al*, 1986) with IucA>IucC≥IucD>IucB. As the aerobactin regulon is arranged in an operonic structure with one mRNA molecule encoding the biosynthesis genes, some form of posttranscriptional control must be acting to alter the level of expression of the individual proteins. Analysis of the nucleotide sequence directly upstream of the individual genes revealed the potential for the formation of stable stem-loop mRNA structures (Martinez *et al*, 1994). The potential mRNA secondary structure at the gene junctions may account for the different levels of expression of the genes. The lack of non-coding sequence also indicates that the genes are translationally coupled. Sequence analysis indicated that there is a frameshift between *iucB* and *iucC* and also between *iucC* and *iucD*. In order to translate the aerobactin mRNA therefore, the ribosomes must effect two frameshifts. It is possible that these features of the mRNA account for the differential expression of the aerobactin genes.

1.15: Siderophore Mediated Iron Acquisition In *P. aeruginosa*

P. aeruginosa is a ubiquitous gram-negative rod. It is an opportunistic human pathogen that causes severe and often fatal infections, particularly in immuno-compromised patients. The ability of *P. aeruginosa* to thrive in a variety of environments is reflected in the size of its genome, which at 6.3 Mb is one the largest microbial genomes sequenced to date. Indeed, the *P. aeruginosa* genome is only 1.3 Mb smaller than the single celled eukaryote, *Saccharomyces cerevisiae*. In comparison to many other microorganisms that need to only acquire iron from the limited ecological niches to which they are limited, *P. aeruginosa* uses a plethora of acquisition systems to acquire this precious metal. The genome of *P. aeruginosa* has been fully sequenced (Stover *et al*, 2000) revealing the presence of up to 34 putative TonB dependent outer membrane receptors (Köster, 2001). The virulence of *P. aeruginosa* has been correlated with its ability to acquire iron, and consequently *P. aeruginosa* represents a model organism for the analysis of iron acquisition by a pathogen.

1.15.1: Pyoverdine

P. aeruginosa produces two known siderophores under conditions of iron limitation: pyoverdine and pyochelin (reviewed by Cornelis and Matthijs, 2002; reviewed by Poole and McKay, 2003). Pyoverdine, which is the primary siderophore of *P. aeruginosa*, is characterised by its fluorescence, which is conferred upon the molecule by a conserved dihyroxyquinoline chromophore (Section 1.2.6). Pyoverdine also contains a short peptide of variable length that possibly explains the specificity of pyoverdine utilisation amongst fluorescent pseudomonads. The genes involved in the biosynthesis of pyoverdine in the *P. aeruginosa* PA01 strain are located within a region of the chromosome referred to as the *pvd* locus (Tsuda *et al*, 1995). A separate operon, *pvcABCD*, located elsewhere on the chromosome has also been implicated in biosynthesis of the pyoverdine chromophore (Stintzi *et al*, 1996, 1999). The *pvd* locus appears to be involved in non-ribosomal peptide synthesis of the peptide moiety, although a *pvd* gene has been implicated in chromophore biosynthsis (Mossialos *et al*, 2002). Mutants defective in the twin arginine translocation system (TAT) are defective in pyoverdine production, indicating that some of the proteins involved in pyoverdine biosynthesis must be exported (Ochsner *et al*, 2002a).

The production of pyoverdine in *P. aeruginosa* requires the product of the *pvdS* gene, which encodes an ECF sigma factor (reviewed by Visca *et al*, 2002). PvdS is required for the expression of several *pvd* genes (Wilson *et al*, 2001; Ochsner *et al*, 2002b) as well as the *pvc* genes although PvdS regulation of the *pvc* system is indirect and is mediated throught PtxR, a positive regulator of the LysR family (Hamood *et al*, 1996). PvdS is also required for the production of several virulence factors including exotoxin A (Ochsner *et al*, 1996), the endoprotease PrpL (Wilderman *et al*, 2001) as well as several other iron regulated non-siderophore genes (Ochsner *et al*, 2002b). Although the *pvd* genes are iron regulated, they lack Fur boxes, and the iron regulation appears to be mediated via PvdS, whose production is Fur regulated.

The outer membrane receptor for pyoverdine, FpvA is inducible under conditions of iron limitation and shows homology to TonB dependent outer membrane receptors. The FpvA protein contains a long and unusual signal sequence and it was shown that export of FpvA to the outer membrane was TAT dependent (Ochsner *et al*, 2002a). FpvA contains an N-terminal sequence similar to that found in the *E. coli* ferric citrate receptor, FecA. The N-terminal sequence of FecA is not involved in transport, but is involved in FecA dependent *fecA* gene expression in conjunction with FecIR (Section 1.14.2). Similarly, the N-terminal sequence of FpvA is not required for pyoverdine utilisation, but is required for FpvA-mediated pyoverdine biosynthesis (Shen *et al*, 2002). The binding of ferripyoverdine to FpvA transduces a signal to the cytoplasmic membrane spanning antisigmafactor FpvR. The signal is transduced to PvdS, whose activity is regulated by FpvR, and PvdS subsequently stimulates the production of pyoverdine and the virulence factors exotoxin A and PrpL (Lamont *et al*, 2002). The production of FpvA has been shown to be induced by its cognate siderophore pyoverdine (Gensberg *et al*, 1992). The induction of *fpvA* gene expression was found to be dependent on ferripyoverdine and FpvI, an ECF sigma factor required for *fpvA* gene expression (Rédly and Poole, 2003). Thus, FpvA is a member of a branched signalling pathway involving the cytoplasmic membrane spanning antisigmafactor, FpvR, which directly regulates the activity of two ECF sigma factor proteins, PvdS and FpvI (Figure 1.14)(Beare *et al*, 2003).

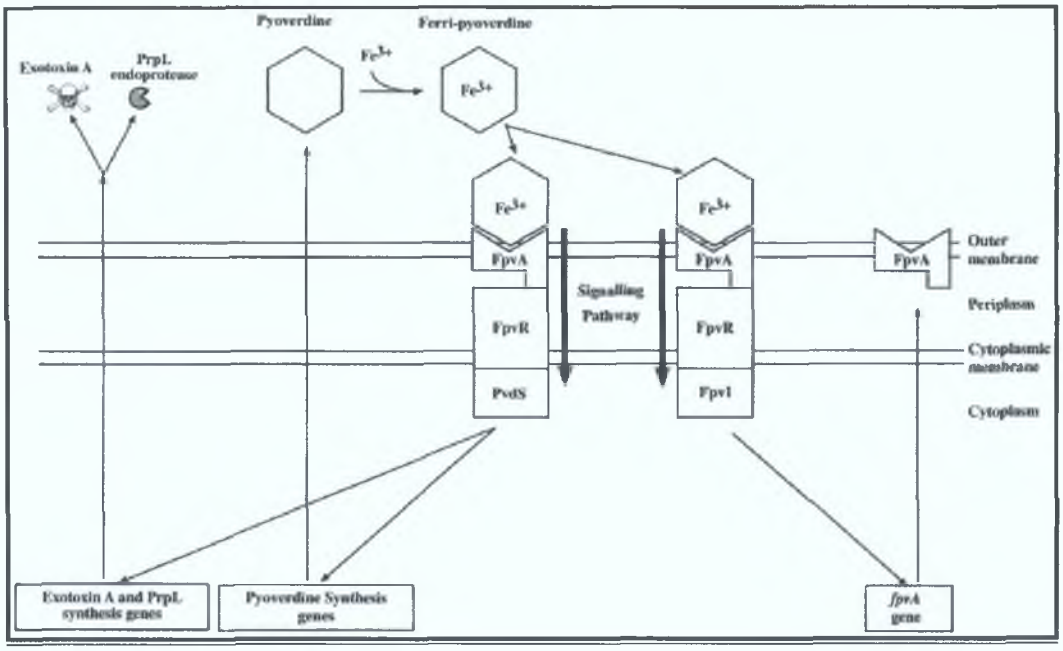

Figure 1.14: Model of the Fpv signalling system. Ferripyoverdine complexes bind the FpvA receptor protein, transmitting a signal to the FpvR protein that otherwise suppresses the activity of PvdS and FpvI. PvdS and FpvI then bind core RNA polymerase. RNA polymerase containing PvdS expresses genes required for the synthesis of pyoverdine, PrpL endoprotease and exotoxin A (Lamont *et al*, 2002), and RNA polymerase containing FpvI expresses the *fpvA* gene (Beare *et al*, 2003).

1.15.2: Xenosiderophore Utilisation

As mentioned previously, analysis of the genome sequence of *P. aeruginosa* indicated that 34 putative TonB dependent receptors were encoded within the genome (Köster, 2001). The ligands for many of these putative receptors are unknown, but *P. aeruginosa* has been shown to utilise several xenosiderophores. The ability of *P. aeruginosa* to utilise enterobactin and its breakdown products 2,3-dihydroxybenzoic acid and N-(2,3-dihyroxybenzoyl)-L-serine has been reported (Liu and Shokrani, 1978; Poole *et al*, 1990; Screen *et al*, 1995). The utilisation of enterobactin is mediated by the outer membrane receptor PfeA. Expression of *pfeA* requires the products of the *pfeRS* operon, which encodes a two component regulatory system (Dean and Poole, 1993). A *P. aeruginosa pfeA* mutant displays low-level utilisation of enterobactin indicating the presence of a second enterobactin outer membrane receptor (Dean *et al*, 1996). A putative inner membrane iron transport system for enterobactin has been identified from analysis of the genomic sequence, but its role if any in enterobactin utilisation remains to be confirmed. The ability of *P. aeruginosa* to utilise ferric citrate and the known virulence factor, aerobactin has also been

reported (Liu and Shokrani, 1978; Cox, 1980b; Harding and Royt, 1980). *P. aeruginosa* has also been shown to utilise the fungal siderophores desferrichrysin, desferrirubin, coprogen and deferrioxamine (Meyer, 1992). Ferrioxamine B utilisation has been found to be dependent on the FiuA outer membrane receptor which is under the control of the FpvIR like gene products, FiuIR (Vasil and Ochsner, 1999). The plethora of inducible siderophore receptors in *P. aeruginosa* possibly indicates that xenosiderophores utilisation is a common feature of pseudomonads and is indicative of their wide environmental distribution.

1.15.3: Haem Utilisation

Similarly to many other pathogens, *P. aeruginosa* is characterised by its ability to acquire iron from haem and haem-containing proteins. *P. aeruginosa* encodes two distinct haem acquisition systems; the *phu* and *has* loci (Ochsner *et al*, 2000). As previously described, haem acquisition systems can be separated into three categories (Section 1.13). The largest category into which the *phu* system of *P. aeruginosa* falls consists of an outer membrane receptor, PhuR and a PBT system, PhuSTUVW. Expression of the *phu* system was induced under conditions of iron limitation, and was directly mediated by the Fur protein (Ochsner *et al*, 2000). Deletion of *phuR* or *phuSTUV* greatly reduced growth on of *P. aeruginosa* on haem sources although residual growth was observed. This residual growth was attributed to the *has* system.

The *has* system encodes an outer membrane receptor, HasR and an extracellular haem binding protein, HasA. The system is iron regulated, with the regulation mediated by the Fur protein. The HasA protein is similar to the HasA haemophore produced by *S. marcesens* (Létoffé *et al*, 1998) and the HasA haemophore of *P. fluorescens* (Létoffé *et al*, 2000). Release of HasA in *S. marcesens* and *P. fluorescens* requires the presence of a type I secretion system encoded by *hasDEF* (Létoffé *et al*, 1994; Idei *et al*, 1999). Homologues of *hasDEF* have been identified downstream of *hasRA* in *P. aeruginosa*, but their role in haemophore secretion has yet to be confirmed. The *has* system thus represents a second category haem acquisition system consisting of an outer membrane receptor, an extracellular haem binding protein and a type I secretion system (Section 1.13). Deletion of *hasR* significantly reduced utilisation of haemin and haemoglobin as iron sources (Ochsner *et al*, 2000). Haem iron is released by the action of PigA, a haem oxygenase, which causes oxidative cleavage of the molecule.

The *pigA* gene is required for the utilisation of haem as an iron source (Ratliff *et al*, 2001).

1.15.4: Pyochelin

While *P. aeruginosa* produces two siderophores, pyoverdine is the primary siderophore and pyoverdine producing strains tend to produce little pyochelin (Heinrichs *et al*, 1991). There thus appears to be a hierarchy of siderophore usage by *P. aeruginosa*. Pyochelin is a low affinity but active siderophore of *P. aeruginosa* (Cox, 1980b). Pyochelin is formed by a condensation reaction of salicylate and two cysteinyl residues and binds Fe(III) in a 2.1 ratio (Cox and Graham, 1979). Pyochelin also chelates Zn(II), Cu(II), Co(II), Mo(VI) and Ni(II) and has been implicated in the delivery of Co(II) and Mo(IV) to *P. aeruginosa* cells (Visca *et al*, 1992). Pyochelin has been shown to acquire iron from transferrin (Siyrosachati and Cox, 1986) and to act as a virulence factor (Cox, 1982; Takase *et al*, 2000a). Pyochelin has been implicated in catalysing the formation of tissue-damaging free radicals (reviewed by Poole and McKay, 2003).

The pyochelin regulon appears to be localised to a single region of the *P. aeruginosa* chromosome. The genes for the biosynthesis of pyochelin and its intermediates salicylate and dihydroaeruginoate, have been identified and are arranged in two separate operons; *pchDCBA* and *pchEFGHI*, although *pchHI* do not encode proteins that are involved in the biosynthesis of the siderophore. The protein products of the biosynthesis genes have been characterised (Serino *et al*, 1995; Serino *et al*, 1997; Reimmann *et al*, 1998; Reimmann *et al*, 2001) and a mechanism for the biosynthesis of pyochelin has been proposed (reviewed by Crosa and Walsh, 2002). The ferripyochelin receptor gene, *fptA* is located directly downstream of the *pchEFGHI* operon, and is transcribed from a separate promoter (Heinrichs and Poole, 1996). The FptA protein is a 75 kDa TonB dependent outer membrane receptor. The *fptA* gene is inducible by human respiratory muscous *in vitro* (Wang *et al*, 1996a) and expression of the gene has been detected *in vivo*, indicating a role in *in vivo* iron acquisition possibly in lung infections (Wang *et al*, 1996b). Expression of both biosynthesis operons and *fptA* is iron regulated and mediated by the Fur protein (Ochsner and Vasil, 1996; Serino *et al*, 1997; Reimmann *et al*, 1998). The AraC type regulator, encoded by *pchR*, is also Fur regulated (Heinrichs and Poole, 1993; Ochsner and

Vasil, 1996), and is required for expression of *fptA* and the biosynthesis genes (Heinrichs and Poole, 1996; Reimmann *et al*, 1998). Expression of *fptA* is repressed in the absence of pyochelin, however expression is promoted in the presence of the siderophore in a process that is mediated by PchR (Heinrichs and Poole, 1996). Similarly, expression of *pchDCBA* and *pchEFGHI* are repressed in the absence of siderophore and derepressed in its presence in a process mediated by PchR (Reimmann *et al*, 1998). These results appear to indicate that pyochelin acts as a signal molecule to induce expression of the relevant genes possibly by interacting with PchR. Two partially conserved heptameric repeat sequences CGAGGGA and CGTGGAT were identified upstream of the –35 region of the *fptA* promoter, and were also found to be conserved upstream of the *pchR* gene, indicating that they possibly act as a binding site for PchR (Heinrichs and Poole, 1996). FptA mutants show reduced *fptA* gene expression indicating that ferripyochelin binding to FptA leads to a signal transduction cascade that enables PchR to act as a repressor or activator. It is likely however that the defect in ferripyochelin uptake in an *fptA* mutant negatively affects PchR induced expression of the *fptA* gene assuming ferripyochelin interacts directly with PchR.

1.16: Iron Acquisition In Plants

Similarly to bacteria, plants also display a requirement for iron. Plants can be divided into two groups depending on the strategy employed to acquire iron. Dicotyledons and non-grass monocotyledons employ a mechanism of enzymatic reduction of ferric iron to the ferrous state to facilitate iron uptake. This acquisition strategy is generally referred to as strategy I. Graminaceous plants (grasses) employ a strategy that involves the production and utilisation of phytosiderophores in a strategy referred to as strategy II.

1.16.1: Dicotyledons And Non-Grasses

The acquisition of iron by Strategy I is a complex process that is ultimately dependent upon a system of iron reduction. The acquisition of iron in the ferrous state has been shown to be a relatively efficient process in plants. Most families of angiosperms with the exception of the Gramineae have been shown to employ an iron acquisition mechanism in which the reduction of ferric iron to the ferrous state is obligatory (Römheld, 1987). The roots of dicotyledenous plants have been shown to have a short zone that can be extended during conditions of iron limitation, where ferric chelates are reduced (Römheld, 1987). Iron chelated in the soil by organic compounds produced by both prokaryotic and eukaryotic organisms are reduced releasing the iron from the complex and generating free ferrous iron which is available to the plant.

The solubility of ferric iron is increased as the pH is lowered. Dicotyledons and non-grasses have been found to acidify the rhizosphere leading to a concomitant drop in pH. The ability of plants to acidify the rhizosphere is thought to be mediated by an ATP-dependent pump that extrudes protons into the rhizosphere. Grasses do not excrete protons and it is thought that the extrusion of protons is linked with ferric-chelate reductase activity (Welkie and Miller, 1993).

Iron bioavailabiltiy is also increased by the presence of phenolic compounds in the rhizosphere. As the pH drops with the secretion of protons, the plasma membrane can become permeable leading to a release of low molecular weight substances. The increased levels of organic compounds can lead to increased growth of

microorganisms and a reduction in the local oxygen concentration. The reduction in oxygen levels results in the mean lifetime of Fe(III) ions in the steady state of reduction and oxidation being shorter. It is thought that secreted organic compounds enhance the effectiveness of ferric reductases by solubilising iron in the rhizosphere (Welkie and Miller, 1993). Several plant phenolics have also been shown to promote the release of iron from ferritin (Boyer *et al*, 1990).

The acquisition of iron by strategy I is therefore a complex mechanism dependent on a reduction system, the efficiency of which is linked inexorably to soil pH and the presence of organic compounds.

1.16.2: Grasses

Members of the Gramineae employ a different strategy, termed strategy II for the acquisition of iron under iron limiting conditions. Although grasses only represent a small fraction of plant species, they include many species that are important crops, and are therefore commercially important. Grasses have been shown to grow under iron limiting conditions and must therefore encode iron acquisition mechanisms. Grasses have been found to acquire iron via mechanisms that are comparable to the siderophore mediated iron acquisition systems of bacteria. Grasses have been found to produce natural chelators of iron termed phytosiderophores. Phytosiderophores are low molecular weight compounds with an affinity for iron. They are synthesised and secreted by the plant root and are taken up into the root by a specific uptake system.

Cultured oat and rice plants were shown to produce iron-chelating compounds, the release of which for oat plants was greatly enhanced under iron limiting conditions (Takagi *et al*, 1984). The compound, which was identified as mugineic acid functions in a similar way to microbial siderophores. Mugineic acid forms a stable complex with Fe(III) in an octahedral configuration which facilitates the recognition of the complex by a high affinity uptake system. The secretion of mugineic acid was increased under iron limiting conditions and decreased upon the addition of exogenous iron.

A number of phytosiderophores have been isolated from grasses. Multiple phytosiderophores have also been found to be produced by individual grasses. The

ability of crops to secrete phytosiderophores has been shown to correlate with efficiency of iron acquisition.

The mechanisms of iron acquisition between grasses and non-grasses has been shown to differ. In both cases however, plants have evolved effective strategies to satisfy their requirement for iron. The identification of plant genes involved in iron acquisition and metabolism may be of commercial importance.

1.17: Iron Uptake By Rhizobia

Rhizobia are found free living in the soil or in a nitrogen fixing symbiosis with a suitable leguminous host. Due the importance of many iron containing enzymes and proteins in nitrogen fixation, the iron acquisition mechanisms of rhizobia have been subject to particular interest. Investigations on the mechanisms of iron acquisition have generally focused on those systems that function in a free-living state. A number of iron acquisition systems have been identified and characterised.

1.17.1: Siderophore Mediated Iron Transport In Rhizobia

The development of the CAS assay (Schwyn and Neilands, 1987) has provided a relatively simple way of determining siderophore production by bacteria of interest. The assay has also been modified and has resulted in a further extension of its uses (Milagres *et al*, 1999; Machuca and Milagres, 2003). Rhizobia, in common with other bacteria have been found to produce siderophores, many of which appear to be strain specific. Rhizobia have been found to produce a variety of siderophores including: carboxylates (Smith *et al*, 1985), catechols (Modi *et al*, 1985; Patel *et al*, 1988; Roy *et al*, 1994), citrate (Guerinot *et al*, 1990), hydroxymates (Persmark *et al*, 1993; Dilworth *et al*, 1998) and anthranilate (Rioux *et al*, 1986).

An analysis of siderophore production by root nodule bacteria revealed that all the strains tested gave a positive result for the CAS assay (Carson *et al*, 1992). Further analysis of rhizobia field isolates revealed that most of the strains tested produced siderophores as determined by the CAS plate assay (Fabiano *et al*, 1994). A number of the siderophores produced by rhizobia have been identified. *S. meliloti* DM4, an agronomically important strain and the endosymbiont of alfalfa was found to produce a carboxylate type siderophore termed rhizobactin (Smith *et al*, 1985)(Section 1.2.3). *Rhizobium leguminosarum* was found to produce anthranilate, which was suggested to function as a siderophore (Rioux *et al*, 1986).

Similarly to *E. coli*, rhizobia have been shown to produce iron regulated outer membrane proteins in response to iron limitation. Root nodule bacteria isolated from various plants have been shown to produce iron regulated proteins, ranging in size from 64 to 94 kDa, in response to iron limitation (Fabiano *et al*, 1994). *Rhizobium*

GN1 was also observed to produce iron repressible outer membrane proteins and a siderophore biosynthesis mutant was shown to utilise exogenously supplied siderophore (Jadhav and Desai, 1994). In *S. meliloti*, siderophore mediated iron transport was found to correlate with the presence of a specific iron regulated outer membrane protein (Reigh and O'Connell, 1993).

Many rhizobial strains are not genetically well characterised and the components involved in siderophore biosynthesis and utilisation have yet to be identified. For this reason, investigations into siderophore production and acquisition have focused on the well-studied and genetically characterised strains, *S. meliloti* 2011, *R. leguminosarum* biovar *viciae* J251 and *B. japonicum* USDA110.

1.17.2: Rhizobactin 1021

S. meliloti 2011 produces one known siderophore termed rhizobactin 1021. Rhizobactin 1021 is characterised by the presence of an (E)-2-decanoic acid residue (Persmark *et al*, 1993), and is chemically similar to aerobactin and schizokinen (Section 1.2.2). The rhizobactin 1021 regulon of *S. meliloti* 2011 was identified and found to be encoded on the pSyma megaplasmid (Barloy-Hubler *et al*, 2000; Lynch *et al*, 2001). The rhizobactin 1021 regulon was found to consist of at least eight genes, six of which showed homology to siderophore biosynthesis genes, one of which showed homology to siderophore outer membrane receptors, and one of which showed homology to transcriptional regulators of the AraC type. Transposon insertion mutants in the genes of interest were generated and their phenotypes were analysed (Lynch, PhD Thesis 1999; Lynch *et al*, 2001). The biosynthesis genes were determined to form an operon, which was regulated by iron and the AraC type regulator, RhrA. Transcription of *rhtA* was found to be positively regulated by RhrA.

1.17.3: Vicibactin

R. leguminosarum biovar *viciae* produces a novel hydroxamate siderophore termed vicibactin (Dilworth *et al*, 1998). Vicibactin is a cyclic hydroxamate with three moieties each of D-3-hydroxybutyric acid and N^2-acetyl-N^2-hydroxy-D-ornithine linked by alternating amide and ester bonds. Vicibactin is utilised in *R. leguminosarum* by a system that is homologous to the Fhu system of *E. coli*. Mutants in the *fhu* system (arranged *fhuDCB* in *R. leguminosarum*) were found to be defective

in vicibactin utilisation. A *fhuA* homologue found adjacent to the *fhuDCB* system was found to be a pseudogene (Stevens *et al*, 1999). The gene encoding the outer membrane receptor for vicibactin, *fhuA* was identified and mutated (Yeoman *et al*, 2000). A cluster of eight genes, *vbsGSO*, *vbsADL*, *vbsC* and *vbsP* was identified in a region located downstream of *fhuA* and were found to be involved in the biosynthesis of vicibactin (Carter *et al*, 2002). Transcription of *vbsGSO* and *vbsADL* required the closely linked gene, *rpoI* (Yeoman *et al*, 1999). Transcription of *fhuA* and *fhuDCB* was found to be independent of *rpoI* (Stevens *et al*, 1999; Yeoman *et al*, 2000).

1.17.4: Haem Utilisation By Rhizobia

The ability of bacteria to acquire iron from haem and haem compounds is generally considered a characteristic of pathogenic bacteria (Lee, 1995; Genco and Dixon, 2001). However analysis of various rhizobial species indicated that the bacteria were capable of utilising haem and haem containing compounds as iron sources (Noya *et al*, 1997). The ability of rhizobia to utilise haem compounds is of interest due to the importance of the haem compound leghaemoglobin in symbiosis.

1.17.5: *S. meliloti*

As previously described, the ability of *S. meliloti* to utilise haem compounds was analysed (Noya *et al*, 1997). Analysis of *S. meliloti* 242 indicated that the bacterium was capable of utilising haem, haemoglobin and leghaemoglobin as iron sources. *S. meliloti* mutants affected in siderophore production were also found to be defective in the utilisation of haem and haemoglobin (Fabiano *et al*, 1995). Random mutagenesis of *S. meliloti* 2011 also led to the identification of two mutants affected in haem utilisation (Lynch, PhD Thesis 1999). Genomic sequencing of *S. meliloti* 1021 identified two putative haem receptors, Smc04205 and Smc02726, and a putative inner membrane iron transport system, *hmuPSTUV* (Gailbert *et al*, 2001). Analysis of an iron regulated outer membrane protein in *S. meliloti* 242 indicated that it was similar to Smc02726 and was capable of binding haemin (Battistoni *et al*, 2002). The effect if any of these genes on nodulation and symbiotic nitrogen fixation remains to be elucidated.

1.17.6: *R. leguminosarum*

The ability of *R. leguminosarum* to utilise haem has been documented (Noya *et al*, 1997). Wexler *et al* (2001) described the identification of a putative inner membrane haem transport system that was located adjacent to the *R. leguminosarum tonB* gene. Mutants in the inner membrane haem transport system, designated *hmuPSTUV*, showed slightly reduced growth with haem as the sole iron source, indicating the presence of an alternative system for the utilisation of this compound. An insertion in the *tonB* gene resulted in an abolition of haem utilisation as an iron source. The gene organisation of the *hmu* locus of *R. leguminosarum* was similar to that of the *hmu* locus of *S. meliloti* 1021 (Wexler *et al*, 2001; personal observation). Mutations in *tonB* or the *hmu* system did not affect nodulation or symbiotic nitrogen fixation.

1.17.7: *Bradyrhizobium japonicum*

The ability of *B. japonicum* to utilise haem compounds has been described (Noya *et al*, 1997). A haem uptake system was identified in *B. japonicum* and found to consist of a cluster of nine putative genes (Nienaber *et al*, 2001). Identified were a putative inner membrane iron transport system encoded by *hmuTUV* and a haem receptor, *hmuR*. Also identified were genes whose protein products were predicted to encode TonB and ExbBD homologues as well as two other genes encoding proteins of unknown function. Analysis indicated that HmuR and the TonB-ExbBD system were required for haem utilisation, but that the HmuTUV system was dispensable for utilisation of the same compound. The TonB-ExbBD system also appeared to be specific for haem utilisation, as siderophore utilisation remained unaffected in a deletion mutant. The nodulation and symbiotic nitrogen fixation properties of the mutants were similar to wild type (Nienaber *et al*, 2001).

1.18: Iron And The *Rhizobium*-Legume Symbiosis

Iron is an essential element in an effective symbiosis between rhizobia and the leguminous host. Iron is a cofactor of many of the enzymes involved in the symbiosis such as nitrogenase, ferredoxin and leghaemoglobin. A number of these proteins are also abundant: Water-soluble non-leghaemoglobin iron has also been found in large quantities in nodule extracts (Wittenberg *et al*, 1996). The importance of iron in symbiosis is underlined by the presence such large quantities of iron and iron containing proteins in the nodule.

1.18.1: The *Rhizobium*-Legume Symbiosis

Sinorhizobium, *Rhizobium* and *Bradyrhizobium* are characterised by their ability to induce nitrogen fixing nodules on suitable leguminous hosts. Leguminous plants have been shown to produce attractants that result in a chemotactic response from the rhizobia towards the plant roots (Bergman *et al*, 1988). The chemotactic response results in large populations of rhizobia in the rhizosphere. When bacteria come into contact with the surface of the root, they alter the growth of the epidermal root hairs resulting in the curling of the root hairs (Libbenga and Harkes, 1973). As this occurs, the cells of the root cortex under the epidermis begin dividing trapping bacteria in curled root hairs or between a hair and another cell. The bacteria proliferate and infect the outer plant cells and the infection proceeds by the development of an infection thread that is surrounded by the cell membrane and a cellulosic wall (Callaham and Torrey, 1981). Cell division in the plant cell root establish the body of the nodule while the infection thread penetrates target cells in the nodule. Within the infected tissue, bacteria are released into the plant cytoplasm, and are enveloped by plant plasma membrane (Robertson *et al*, 1978).

In various rhizobial species, common and host-specific nodulation (*nod*) genes have been identified which determine infection and nodulation of specific hosts (reviewed by Fisher and Long, 1992). With the exception of *nodD*, which is constitutively expressed, most *nod* genes are not expressed in cultured cells. Expression is induced upon exposure to plant exudates (Mulligan and Long, 1985) and this induction depends on the NodD protein. Many of the inducing molecules that have been purified from plant exudates have been identified as flavonoids, which are three

ringed aromatic compounds. The protein products of the *nodABC* genes are required for both root hair curling and for cell division, while the protein products of *nodFE*, *nodH*, and *nodLMN*, which are involved in host selection affect the location and tightness of root hair curling and the efficiency and persistence of cell division (reviewed by Long, 1989). The basic structure of Nod factors seems to be a β-1,4-linked oligomer of *N*-acetylglucosamine with an *N*-acyl n-substitution on the non-reducing end (reviewed by Fischer and Long, 1992). Individual rhizobial strains may make a family of factors that vary slightly in length and/or substitution. Substitutions usually differ when factors from different species are compared, which may account for host range distinctions between species and biovars of rhizobia.

After the initiation of infection, bacteria must complete the penetration and subsequent release into the host cells. This process requires the presence of specific bacterial surface components and plant components that include amongst them neutral glucans, lipopolysaccharides and charged heteropolysaccharides. Possible roles for the extracellular polysaccharides include signalling, osmotic regulation and recognition which function to present and/or disguise the bacterium during invasion.

In *Rhizobium*, the genes for nitrogen fixation are generally divided into two groups: The *nif* genes refer to those with homologues in free-living nitrogen fixing systems such as *Klebsiella*, while *fix* genes refer to those required for symbiotic nitrogen fixation, but whose function is not known to be analogous to any free living system. Both *nif* and *fix* mutants induce nodule formation, but they do not fix nitrogen. The symbiotic activation of the *nif* genes is dependent on NifA (Szeto *et al*, 1987). Redox-dependent control of *nifA* expression occurs in response to *fixL* and *fixJ* which encode a two-component regulatory system that is oxygen responsive (Merrick, 1992).

1.18.2: Iron And Nodule Formation

The concentration of bioavailable iron in the soil varies greatly with pH and oxygen content. It is at this first level that iron can affect symbiosis. In order for nodulation to commence, *Rhizobium* must come into contact with the root of a suitable leguminous host. As such, the limiting factor in the initiation of nodulation is the

abundance of the bacterium in the rhizosphere. A bacterium that can compete effectively for the limited iron available will be at a competitive advantage and consequently will predominate over those that are less competitive. Siderophore mediated iron acquisition system may confer a selective advantage in soils with a low amount of bioavailable iron. Similarly, the ability to utilise xenosiderophores may also confer a selective advantage on the bacteria. Rhizobia have for the most part therefore developed specific siderophore iron acquisition systems which function in the free-living state, and which allow for efficient colonisation of the rhizosphere.

Iron deficiency has been found to decrease nodule number and nodule mass in a number of legumes. Peanuts grown in severely iron deficient calcareous soils fail to nodulate until give foliar iron application. Plants treated with exogenous iron produce a greater number of excisable nodules and carry a greater nodule mass when compared to untreated plants. The mechanism by which iron affects nodule number and mass is unknown, however it has been suggested that the iron deficiency exerts a greater effect on the rhizobia which were consequently unable to acquire adequate amounts of iron from the plant (O'Hara *et al*, 1988).

1.18.3: Iron And Nodule Function

Bacteroids are enclosed in a membrane that is derived from the plant plasma membrane termed the peribacteroid membrane. More than one bacteroid may be enclosed by a single membrane generating a peribacteroid unit or symbiosome.

Nodules differ in morphology and vascularization depending on the plant host and they can therefore be grouped into two distinct groups: indeterminate and determinate nodules. Several legumes including alfalfa, clover and pea form indeterminate nodules. Indeterminate nodules have persistent meristems at their distal ends with nodule cells proximal to the meristem invaded by infection threads. The next region contains bacteroids and is the site of active nitrogen fixation. Dramatic changes in gene expression have been found to occur in a single cell layer adjacent to the start of this nitrogen fixation zone. The proximal end of the nodule is a senescence zone. A single nodule can thus represent the whole time course of nodule development (Figure 1.15).

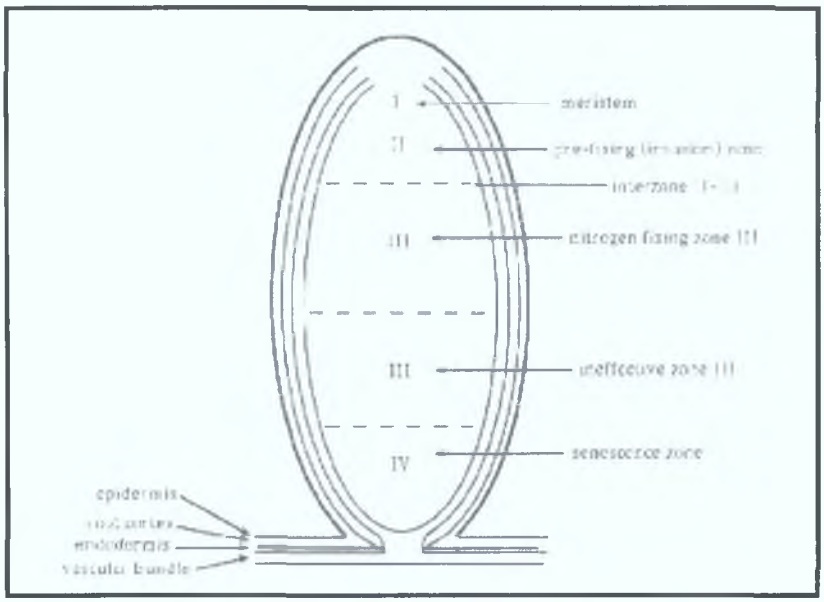

Figure 1.15: General Organisation Of An Indeterminate Root Nodule (Guerinot, 1993).

Determinate nodules, such as those of soybean and french bean, display only meristemic activity early in nodule development and once mitotic activity has ceased, nodule size increases by cell expansion rather than cell division. In contrast to indeterminate nodules, determinate nodules are not characterised by various development zones. This is advantageous for biochemical analyses as all the cells in the nodule are more or less the same age and can be viewed over a time course. In both determinate and indeterminate nodules, only about 60% of the cells in the mature nodule are infected (Guerinot, 1993). The role of a number of iron containing compounds in the functioning of the nodule has been examined and is discussed in detail below.

(i) Nitrogenase

The nitrogenase enzyme complex consists of two metalloproteins, which are highly conserved in sequence and structure in nitrogen-fixing bacteria. The protein containing the site of substrate reduction is the nitrogenase molybdenum-iron protein, which is also known as dinitrogenase or component I. The electron donor to the component I protein is the nitrogenase reductase or component II. Nitrogenase can constitute 10-12% of the total bacterial protein (Verma and Long, 1983). Although oxygen is required to allow for bacterial respiration, nitrogenase itself is irreversibly

inactivated by oxygen. It is therefore essential that the oxygen level in the nodule is adequately buffered. This is facilitated by the action of leghaemoglobin.

(ii) Leghaemoglobin

The process of nitrogen fixation in the nodule is oxygen sensitive, which even at very low levels, irreversibly inhibits the nitrogenase enzyme complex. Oxygen however is required for bacterial respiration and the level of oxygen in the nodule is therefore tightly controlled. This nodule environment has an overall low oxygen level, but a high oxygen flux to the bacteria. The oxygen level is kept low by the high rate of bacterial respiration and also by an oxygen diffusion barrier in the inner cortex of the nodule. The diffusion of oxygen is mediated by leghaemoglobin, a symbiotic protein related to vertebrate globin. The leghaemoglobin protein is present at a high level in the nodule thus ensuring that most of the oxygen reaching the bacteria is carried by the protein (Guerinot, 1993). Leghaemoglobin is first detectable in the nodule prior to the detection of nitrogenase activity, with many types of leghaemoglobins present. The leghaemoglobins are encoded by various genes and vary in their oxygen affinities. The leghaemoglobin protein is composed of a haem moiety produced by the bacteria and an apoprotein produced by the plant. Leghaemoglobin therefore appears to be a truly symbiotic protein.

(iii) Haem biosynthesis

As previously mentioned, leghaemoglobin appears to be a truly symbiotic protein with the apoleghaemoglobin synthesised by the plant and the haem moiety synthesised by the bacterium. A *B. japonicum hemA* mutant defective in the δ-aminolevulinic acid (ALA) synthase enzyme that is involved in the first step of bacterial haem synthesis was found to form fully effective nodules on soybeans (Guerinot and Chelm, 1986). This result was in contrast to previous results for a *S. meliloti hemA* mutant, which was shown to form nodules that were incapable of nitrogen fixation on alfalfa (Leong *et al*, 1982). Further analysis using the broad host-range *S. meilioti* sp NGR234 indicated that *hemA* mutants formed nodules that did not fix nitrogen regardless of whether they were determinate or indeterminate nodules (Stanley *et al*, 1988). Sangwan and O'Brien (1991) showed that the *B. japonicum hemA* mutant was rescued by plant ALA utilisation by the bacteroids *in planta*.

A *B. japonicum hemH* mutant was found to produce nodules that did not fix nitrogen, contained few viable bacteria and did not express leghaemoglobin or apoprotein (Frustaci and O'Brian, 1992). The *hemH* mutation was not rescued by the plant and it thus seems that *hemH* is essential for normal nodule development.

(iv) Ferritin

The ferritin protein as previously described is an iron storage protein found in animals, plants and microorganisms. Ko *et al* (1987) reported an inverse correlation between the age of the nodule and the amount of ferritin present. Phytoferritin has also been found to disappear with the appearance of leghaemoglobin.

1.18.4: Siderophores And The Nodule

There is a high iron demand in the nodule and consequently the importance of iron acquisition mechanisms by siderophores *in planta* have been evaluated. Soybean nodules have been found to contain siderophores in the peribacteroid space, which vary depending on the infecting strain of *B. japonicum* (Wittenberg *et al*, 1996). The peribacteroid membrane has been shown to display reductase activity and is capable of reducing ferri citrate and allowing the passage of Fe(II) into the peribacteroid space (Le Vier and Guerinot, 1996). The reduced iron was not immediately transported into bacteroids and it was thus suggested that the peribacteroid space might function as an iron store with the iron possibly complexed by bacterial siderophores.

Analysis of the possible role of siderophores in iron acquisition in the nodule has generally been performed on genetically well-characterised strains of rhizobia. The examination of nodules formed by mutants defective in siderophore utilisation, production or iron regulation has been central to this elucidation.

The endosymbiont of alfalfa *S. meliloti* 1021 produces one known siderophore, rhizobactin 1021. Random transposon mutagenesis of *S. meliloti* 1021 led to the isolation of mutants defective in biosyntheis, utilisation and regulation of rhizobactin 1021 (Gill and Neilands, 1989). Nodule formation and nitrogen fixing ability was examined and in each case the mutant phenotype was indistinguishable from that of the parent strain. The level of nitrogen fixed by *S. meliloti* 1021 and a biosynthesis mutant isolated by Gill and Neilands (1989) indicated that the level fixed was greater

for wild type than for biosynthesis mutants (Barton *et al*, 1992). The growth and nitrogen fixing capability of alfalfa nodulated with *S. meliloti* 1021 mutants described by Gill and Neilands (1989) was examined by Barton *et al* (1996). After 18 days, wild type *S. meliloti* 1021 had the highest nitrogen fixing activity, with the lowest nitrogen fixing activity being recorded by the biosynthesis mutant. After 65 days, wild type *S. meliloti* 1021 and the rhizobactin 1021 utilisation mutants showed the highest nitrogen fixing activity, while the biosynthesis and regulatory mutants displayed a lower level of activity. The result indicated that the *S. meliloti* 1021 mutants defective in rhizobactin 1021 biosynthesis or regulation were defective in nitrogen fixation, or fixed nitrogen at a lower rate.

The region encoding the rhizobactin 1021 regulon was sequenced and mutants were generated by fragmented targeted mutagenesis (Lynch, PhD Thesis 1999; Lynch *et al*, 2001). A biosynthesis mutant and an outer membrane receptor mutant were examined for their ability to nodulate and fix nitrogen. Both mutants were found to be unaffected in either capability. Expression analysis indicated that the rhizobactin 1021 biosynthesis operon was not expressed in the nodule at a stage when *nifH* was actively expressed (Lynch *et al*, 2001).

S. meliloti 242 mutants were isolated that were defective in siderophore mediated iron acquisition (Fabiano *et al*, 1995). The mutants, which were classified as biosynthesis, transport or regulatory were found to form effective nodules, however significant differences were observed in the kinetics of nodulation of the wild type strain and the various mutants when examined under iron deplete conditions. The results indicated that iron and the high-affinity rhizobactin 1021 iron acquisition system might effect the early nodulation events in *S. meliloti* 242. *S. meliloti* 242 was found to encode homologues of *rhrA* and *rhtA* (Platero *et al*, 2003), possibly indicating that the organism encodes a regulon similar to the rhizobactin 1021 regulon of *S. meliloti* 1021. Mutants in *rhrA* and *rhtA* were similar to the parent strain as regards nodule formation and nitrogen fixing capability.

As previously described, anthranilate has been found to act as a siderophore in *R. leguminosarum* (Rioux *et al*, 1986). Anthranilate synthesase is encoded by the *trp*E(G) gene in *S. meliloti*, and is the first enzyme in the tryptophan biosynthesis

pathway. Mutants were isolated and were found to generate two classes of unusual elongated nodules on alfalfa that are distinguished by their extended invasion zones (Barsomian *et al*, 1992). Type A nodules were characterised by a pink colour at their base, were capable of limited nitrogen fixation and contained cells packed with bacteroids at their bases. Type B nodules did not have pink bases, did not fix nitrogen and did not contain bacteroids. Mutants defective in the later stages of tryptophan biosynthesis formed normal nitrogen fixing nodules indicating that *trp*E(G) but not other tryptophan biosynthetic genes are required for normal nodulation. Barsomian *et al* (1992) suggested that anthranilate or another derived factor might function as a siderophore *in planta*. However, anthranilate may also have a separate function unrelated to iron chelation. Anthranilate represents the first step in the synthesis of an indol ring similar to those found in plant hormones, and the disruption of the synthesis pathway may account for the nodule phenotype. The phenotype associated with the *trp*E(G) mutant can not therefore be conclusively attributed to a deficiency in iron acquisition.

The effect of *Rhizobium leguminosarum* biovar *viciae* vicibactin regulon mutants on nodulation and nitrogen fixing has also been examined. Mutants defective in vicibactin utilisation were found to be unaffected in nodulation and nitrogen fixing capability (Stevens *et al*, 1999; Yeoman *et al*, 2000). Similarly, vicibactin biosynthesis mutants were also unaffected (Carter *et al*, 2002) in their ability to induce nodulation and fix nitrogen. Mutants in the ECF sigma factor gene, *rpoI*, which regulates vicibactin biosynthesis, were also unaffected in nodulation and nitrogen fixing (Yeoman *et al*, 1999) indicating that vicibactin is not required for an effective symbiosis.

A number of rhizobial isolates do not produce siderophores, and consequently it is not surprising that a number of studies have shown that rhizobia defective in siderophore mediated iron acquisition produce functional nodules. Analysis of *S. meliloti* 1021 however indicates a correlation between nitrogen fixing activity and rhizobactin 1021 production.

Similarly, a *R. leguminosarum* biovar *viciae fhuA*::*gus* fusion was found to be expressed in the meristematic zone, but not in the mature nodules possibly indicating

a role for vicibactin during early nodule formation (Yeoman *et al*, 2000). The identification of siderophore bound in the peribacteroid space possibly indicates a role for the siderophore in the maintenance of an iron pool within the bacteroid. However, studies with siderophore biosynthesis mutants indicate that this iron pool is not essential for effective nodulation and nitrogen fixation. It is possible that the siderophore confers a competitive advantage on the bacteria when found free living in the soil. A genome wide analysis of iron acquisition genes that are expressed in the nodule should aid in the elucidation of how bacteria acquire this essential element *in planta*.

1.19: Summary

As described in the previous sections, microorganisms have developed numerous strategies for the acquisition of iron. These strategies range from the production of siderophores to the utilisation of haem compounds. In many instances, the principal mechanism of acquisition reflects an adaptation to the environmental conditions in which the microorganism is generally found.

This thesis examines siderophore utilisation in *S. meliloti* 2011, the endosymbiont of *Medicago sativa* and *P. aeruginosa*, an opportunistic human pathogen. The work describes the identification and characterisation of novel proteins involved in siderophore utilisation in these organisms.

The ability of *P. aeruginosa* to utilise several xenosiderophores and the identification and characterisation of a protein involved in their utilisation is also described. The ability of *S. meliloti* 2011 to utilise haem and haem proteins is also described and analysed.

Chapter 2

Materials And Methods

2.1: Bacterial Strains, Primer Sequences and Plasmids

The bacterial strains, primer sequences and plasmids used in this study are described in Tables 2.1, 2.2 and 2.3 respectively.

Table 2.1: Bacterial Strains.

Strain	Phenotype/Genotype	Source/Reference
Sinorhizobium meliloti		
2011	Wild type, Nod^+ Fix^+	Meade *et al*, 1982
2011str^r	Spontaneous high level streptomycin resistant derivative	This study
Rm818	pSyma cured strain	Gift from Dr. Michael F. Hynes
2011*rhrA*26	Tn*5lac* insertion in *rhrA*	Lynch *et al*, 2001
2011*rhtA*45	Tn*5lac* insertion in *rhtA*	Lynch *et al*, 2001
2011*rhbA*62	Tn*5lac* insertion in *rhbA*	Lynch *et al*, 2001
2011*orf1*43	Tn*5lac* insertion in *orf1*	Lynch, PhD Thesis 1999
2011*rhtX*43	Same as 2011*orf1*43	Lynch, PhD Thesis 1999
2011*rhtX*1	Ω-Km^R in *rhtX*	This study
2011Sma2335km	Km^R in Sma2335	This study
2011Smc04205km	Km^R in Smc04205	This study
2011Smc02726km	Km^R in Smc02726	This study
2011*hmuT*-km	Km^R in *hmuT*	This study
102F34	Does not produce or utilise rhizobactin 1021	Lynch, PhD Thesis 1999
Pseudomonas aeruginosa		
PA01	Wild type	Gift from Dr. Keith Poole
CDC5	PA01, *pwd-2*	Ankenbauer *et al*, 1986
DH119	CDC5, *pchR*	Heinrichs and Poole (1996)

Strain	Phenotype/Genotype	Source/Reference
DH143	CDC5, *fptA*	Heinrichs and Poole (1996)
PALS128-17	*pvdB*, *pchB* or *pchA*	Serino *et al*, 1985
K1040	PAO6609, *met-9011, amiE200 rpsL, pvd-9,* Δ*tonB*::ΩHg	Zhao *et al*, 1998
PA4218km	*pvd2*, Km^R in PA4218	This study
PA4219km	*pvd2*, Km^R in PA4219	This study
PA4220km	*pvd2*, Km^R in *fptB*	This study
PA4675km	*pvd-2, pchR,* Km^R in *chtA*	This study
PA1365km	*pvd-2, pchR,* Km^R in PA1365	This study
Escherichia coli		
INVαF'	F^-, *recA*1, *hsdR*17(r_k^-, m_K^+), *supE*44, Φ80d*lacZ*ΔM15, Δ(*lacZYA-argF*)U169	Invitrogen
DH5α	F^-, recA1, *hsdR*17(r_k^-, m_K^+), *supE*44, Φ80d*lacZ*ΔM15, Δ(*lacZYA-argF*)U169	Bethesda Research Laboratories
XL1-Blue	*recA*1, *hsdR*17(r_k^-, m_K^+), *supE*44, *lac*, [F', *proAB*$^+$ *lacI*^{q}, *lacZ*ΔM15::Tn10(Tet^R)]	Stratagene
BL21	F^-, *dcm*, *ompT*, $hsdS_B(r_B^- m_B^-)$ *gal*	Novagen
S17-1	*thi* pro *res*$^-$ *mod*$^+$ Sm^R Tp^R *recA1* RP4-2(Tc::Mu; Km::Tn7)	Simon, 1983
RK4375	*fhuC*::Tn*10*, *fepA9, aroE24*	*E. coli* Genetic Stock Centre. This study
H1443	K-12 strain, *aroB*	Goss *et al*, (1984)
EN307	H1443, pEN7	Gross *et al*, (1985)
GR36	H1443, pRG13	Gross *et al*, (1985)

Strain	Phenotype/Genotype	Source/Reference
Bacillus megaterium		
ATCC 19213, 91-02	Produces schizokinen	NCIMB

Table 2.2: Primer Sequences

Primer Name	Primer Sequence	Tm (°C)
Hemr-F	5' **GGG CCC** TCG ACG GCA CCG GGG GGG 3'	>75
Hemr-R	5' **GCG GCC GC**T TCA CTC GAA CCA CTC TAG AAC T 3'	72.1
HemR-F2	5' **AGA TCT** TGG GCG TCG GCG TCG GCC GAT CAT C3'	>75
HemR-R1	5' **GCG GCC GC**G CAA GCG ACG CAT GGA GGT TGA AGC CG 3'	>75
HmuT-F	5' **GTC GAC** GAA AGC GCC GTC CAC GAA AAG GTC GG 3'	74.6
HmuT-R	5' **GGA TCC** ACG ATC AAA AGC ACC GCG CCG AGG CT 3'	74.6
RhtX-F1	5' **CTC GAG** GCC GGG CAG TGG CAG TTT TCG ATG C 3'	74.8
RhtX-R1	5' **CTG CAG** TCA TCG TGA TCT TGA AGG ACG CGC TTT C 3'	71.9
RhbA-F	5' **GGG CCC** GTG ATT GTA AAG AGT TAG ACC GAG ATG 3'	71.9
RhbB-R	5' **GGA TCC** TTA TGG GCG TGC ATG ATG GGT CTC CAG 3'	73.2
RhtX-F	5' **AGA TCT** GTT GCC GAA GCC CTG CGG GTT 3'	71.0
RhtX-R	5' **AGA TCT** GGA AGG CGG AGG CGG AGA TGG C 3'	72.4
Kan-F	5' **GGG CCC** GAC GTT GTA AAA CGA CGG CCA GTG 3'	73.6
Kan-R	5' **GGG CCC** GGA AAC AGC TAT GAC CAT GAT TAC G 3'	70.8
Orf2APA-F	5' **GCG GCC GC**C GAT GGT CTG CTT CAC CCC CTC 3'	>75
Orf2-APA-R	5' **CCC GGG** CAT CCA GGC ATT CGG CCG CCG G 3'	>75
RhtA-F1	5' **GAA TCC** CCT GTT GAC GTT CGC ATG C 3'	66.3
RhtA-R1	5' **TCT AGA** TTA AAA AAC CTT TCT CAG CGA GAC CGC G 3'	72.5
RhrA-F	5' **GAA TTC** TCA AGC GGC GGC TGC CAG CC 3'	71.1
RhtA-R	5' **CTC GAG** CGC GGA ATC GCC CAC G 3'	69.6
FhuC-F	5' GAA TTC GTG CCC ATT TCA CAA GTT GGC TGT TAT GC 3'	69.5
FhuD-F	5' GAA TTC CTG CAC CTG TGA GTT TTG TTT ATT GAT GAG 3'	68.4
FhuD-R	5' GGA TCC TCA CGC TTT ACC TCC GAT GGC GTT ATC C 3'	73.1
FhuB-R	5' GGA TCC TTA ACG GCT CTG CTT TCT CAA CCA ATA GAT AA 3'	68.4

Restriction sites are in bold type and underlined.

Table 2.3: Plasmids

Plasmid	Description	Source/Reference
pCR2.1	PCR Cloning Vector: Amp^R, Km^R, *lacZα*	Invitrogen
pUC18	Cloning Vector, Amp^R, *lacZα*	Amersham Pharmacia
pUC4K	Ap^R, Source of Km^R cassette	Amersham Pharmacia
pHP45-ΩKm	Ap^R, Source of Ω-Km cassette	Frada *et al*, 1987
pJQ200ks+	Gm^r, *sacB*, *mob*	Quandt and Hynes (1993)
pSUP104	Tc^r, *mob*	Priefer *et al*, 1985
pBBR1MCS-5	Gm^R, *mob*	Kovach *et al*, 1997
pRK600	Cm^R, pRK2013 Nm::Tn9, provides transfer functions	Finan *et al*, 1986
pRG13	Cm^R, carrying *iutBACD*	Gross *et al* (1985)
pEN7	Ap^R, carrying *iutA*	Gross *et al* (1985)
pST-Blue	Cloning Vector: Amp^R, Km^R, *lacZα*	Novagen
pOC4K	pUC4K, Ap^S	This study
	Cosmid vectors	
pPOC1	Cosmid isolated from *S. meliloti* 2011 genebank	This study
pPOC3	Cosmid isolated from *S. meliloti* 2011 genebank	This study
pMO 012405	Contains chromosomal region encoding *fptX*	Pseudomonas Genetic Stock Centre
pMO 010918	Contains chromosomal region encoding *chtA*	Pseudomonas Genetic Stock Centre
pMO 010141	Contains chromosomal region encoding PA1365	Pseudomonas Genetic Stock Centre

Plasmid	Description	Source/Reference
	pUC18 And pST-Blue Derived Vectors	
pUC6 0 E/E	6 Kb E/E subclone of pMO 010918	This study
pUC8 5 E/E	8 5 Kb E/E subclone of pPOC1	This study
pUC3 5 E/B	3 5 Kb E/E subclone of pUC8 5E/E	This study
pUC8 8 E/E	8 8 Kb E/E subclone of pMO012405	This study
pUC3 6 E/B	3 6 Kb E/B subclone of pUC8 8 E/E	This study
pUC3 6K E/B	Km^R insertion in pUC3 6 E/B	This study
pST3 6 E/B	3 6 Kb E/B subclone of pUC3 6 E/B	This study
	pCR2.1 Derived Vectors	
pCR2 7 A/N	2 7 Kb A/N product encoding Smc04205 for mutagenesis	This study
pCR2 2 N/Bg	2 2 Kb N/Bg product encoding Smc02726 for mutagenesis	This study
pCR2 2 S/B	2 2 Kb S/B product encoding *hmuT* for mutagenesis	This study
pCR2 0 Bg/Bg	2 0 Kb Bg/Bg product encoding *rhtX* for mutagenesis	This study
pCR2 0 N/Xm	2 0 Kb N/Xm product encoding Sma2335 for mutagenesis	This study
pCR3 6K E/B	3 6 Kb E/B subclone of pUC3 6K E/B	This study
pCR2 4 E/Xb	2 4 Kb E/Xb product encoding *rhtA*	This study
pCR2 9 E/X	2 9 Kb E/X product encoding *rhrA*	This study
pCR1 3 X/P	*rhtX* for expression	This study
pCR2 9 A/B	*rhbAB* for expression	This study
pPC3 5	pCR2 1 carrying *fhuCDB* for expession	This study
pPC2 9	pCRP2 1 carrying *fhuCD* for expression	This study

Plasmid	Description	Source/Reference
pPC2 0	pCR2 1 carrying *fhuDB* for expression	This study
pOCAPA-K	Km^R cassette as an *Apa*1 fragment	This study
	pJQ200ks+ Derived Vectors	
pOC2 7 A/N	2 Kb A/N subclone of pCR2 7 A/N	This study
pOC2 7K A/N	Km^R insertion in pOC2 7 A/N	This study
pOC2 2 N/Bg	2 Kb N/Bg subclone of pCR2 2 N/Bg	This study
pOC2 2K N/Bg	Km^R insertion in pOC2 2 N/Bg	This study
pOC2 2 S/B	2 Kb S/B subclone of pCR2 2 S/B	This study
pOC2 2K S/B	Km^R insertion in pOC2 2 S/B	This study
pOC200	pJQ200 with the *Bam*H1 site in the MCS destroyed	This study
pOC3 4 X/Xm	3 4 Kb X/Xm subclone of pUC6 0 E/E	This study
pOC3 4K X/Xm	Km^R insertion in pOC3 4 X/Xm	This study
pOC4 0 A/B	4 0 Kb A/B subclone of pMO 010141	This study
pOC4 0K A/B	Km^R insertion in pOC4 0 A/B	This study
pOC2 0 Bg/Bg	2 0 Kb Bg/Bg subclone of pCR2 0 Bg/Bg	This study
pOC2 0-ΩK Bg/Bg	Ω-Km^R insertion in pOC2 0 Bg/Bg	This study
pOC2 0 N/Xm	2 0 Kb N/Xm suclone of pCR2 0 N/Xm	This study
pOC2 0K N/Xm	Km^R insertion in pOC2 0 N/Xm	This study
pOC3 6 X/Xm	3 6 Kb X/subclone of pUC8 8 E/E	This study
pOC3 6K X/Xm	Km^R insertion in pOC3 6 X/Xm	This study
pOC3 6 P/Xb	3 6Kb P/Xb subclone of pST3 6 E/B	This study
pOC3 6K P/Xb	Km^R insertion in pOC3 6 P/Xb	This study

Plasmid	Description	Source/Reference
pOC3 6K B/Xb	3 6 Kb B/Xb subclone of pCR3 6K E/B	This study
	pSUP104 Derived Vectors	
pSUP2 4 E/Xb	pSUP104 carrying the region encoding *rhtA*	This study
pPOC5	pSUP104 carrying the region encoding *rhrA* and *rhtA*	This study
	pBBR1MCS-5 Derived Vectors	
pPOC6	pBBR1MCS-5 carrying *rhbAB* for expression	This study
pPOC4	pBBR1MCS-5 carrying *rhtX* for expression	This study

2.2: Microbiological Media

Solid complex media contained 15 g/L Oxoid No 3 agar Solid minimal media contained 15 g/L Oxoid No 1 purified technical agar Tryptone and yeast extract were from Oxoid Other chemicals were from Sigma Chemicals Co Ltd and BDH Chemicals Ltd All chemicals were analar grade All glassware used for low iron media was washed in 2 M HCl and rinsed in ultra pure deionized water All minimal and low iron media were prepared in ultra pure water Distilled water was used to prepare complex media and sterilisation was achieved by autoclaving at 15 lb/in^2 for 20 min

- **Preparation Of Ultra Pure Water For Low Iron Media**

A cation exchange column was prepared using Amberhte 200 resin and distilled water The Amberhte 200 resin is a strongly acidic cation exchange resin that efficiently chelates divalent metal ions A reservoir of water was prepared and inflow was mediated by means of a capillary tube In order to prevent the column from running dry, the rate of outflow was adjusted to equal the rate of inflow One column volume of water was allowed to flow through and was discarded The column was then ready for the preparation of ultra pure water Water prepared in this manner was used in the preparation of CAS media

- **TY Medium (Beringer, 1974)**

Used for the routine culturing of *Sinorhizobium* strains

Tryptone	5 g
Yeast Extract	3 g
$CaCl_2$ $2H_2O$	0 7 g

Adjusted to pH 7 0 with NaOH and volume brought to 1 L with dH_2O The solution was then sterilised by autoclaving

- **Luria Bertani Broth (LB)**

Used for the routine culturing of *E. coli* and *P. aeruginosa* strains.

Tryptone	10 g
Yeast Extract	5 g
NaCl	10 g

Adjusted to pH 7.0 with NaOH and volume brought to 1 L with dH_2O. The solution was then sterilised by autoclaving.

- **Psi Broth**

After making LB and autoclaving as described above, $MgSO_4$ and KCl were added to a final concentration of 4 mM and 10 mM respectively.

- **SOB Medium**

Tryptone	20 g
Yeast Extract	5 g
NaCl	0.5 g
KCl	2.5 mM
dH_2O	1 L
pH	7.0

After autoclaving, the solution was allowed to cool to 55°C and sterile solutions of $MgCl_2$ (1 M) and Mg_2SO_4 (1 M) were added to final concentrations of 10 mM.

- **SOC Medium**

After making SOB as above, 7.2 ml of 50% sterile glucose was added to give a final concentration of 20 mM.

- **Chrome Azurol S (CAS) medium (Schwyn and Neilands, 1987)**

Used to detect the production of siderophores by bacterial strains.

Pipes	30.24 g
Sucrose	2 g
KH_2PO_4	0.03 g
H_2O	875 ml
pH	6.8 (with a 50% (w/w) NaOH soln.)

This solution was autoclaved separately. After cooling, 10 ml deferrated casamino acids (10%) and 10 ml of a solution containing biotin, thiamine and panthothenic acid (10 mg/l of each) were added. Also added were 10 ml $MgSO_4.7H_2O$ solution (0.2 M) and 7.8 ml $CaCl_2.H_2O$ solution (1 M). The dye solution was finally added along the glass wall with enough agitation to achieve mixing without the generation of foam. The dye solution was prepared as follows: 60.5 mg CAS was dissolved in 50 ml Pipes (1 mM, pH 5.6) and mixed with 10 ml of an iron(III) solution (1 mM $FeCl_3$, 10 mM HCl). While stirring, this solution was slowly added to 72.9 mg HDTMA dissolved in 40 ml pipes pH 5.6. The resultant dark blue liquid was autoclaved.

Casamino acids for this medium were deferrated according to the method described by Waring (1942). The casamino acids were dissolved in 200 ml of ultra pure water and filtered into a glass-stoppered separatory funnel. 8-OH quinolone (5 mg) was dissolved in 1 ml of chloroform, poured into the funnel, shaken vigorously and allowed to stand for 5 min. Approximately 3 ml of chloroform were poured into the funnel, shaken vigorously for 1 min and then rotated for 30 sec to cause droplets of chloroform containing 8-OH quinolone-iron complexes to coalesce and settle. The chloroform layer was drawn off and the casamino acid solution was washed twice with 3 ml aliquots of chloroform. The whole extraction was repeated 3 times. The procedure removed all contaminating iron.

- **Jensen Plant Media (Jensen, 1942)**

Used for nodulation analysis of *Medicago sativa*.

Agar No. 3	7.5 g
dH_2O	550 ml

Following autoclaving solutions of K_2HPO_4, $MgSO_4$ and NaCl were added to a final concentration of 0.2%. Also added was $CaHPO_4$ to a final concentration of 0.1% and $FeCl_3$ to a final concentration of 0.01%. Each of these solutions was autoclaved separately.

- **Low-Iron Media**

All low-iron media was prepared with ultra-pure water and supplemented with the appropriate concentration of 2,2' dipyridyl.

2.3: Solutions and Buffers

- **TE Buffer**

Tris-HCl	10 mM
Na_2-EDTA	1 mM
pH	8 0

- **TES Buffer**

Tris-HCl	10 mM
Na_2-EDTA	1 mM
NaCl	50 mM
pH	8 0

- **Lysis Buffer**

Tris-acetate pH 7 8	40 mM
Sodium acetate	20 mM
EDTA	1 mM
SDS	1%

- **STET Buffer *(Holmes and Quigley, 1981)***

Tris-HCl	50 mM (5 ml of 1 M solution)
Na_2-EDTA	50 mM (10 ml of 0 5 M solution)
Triton X-100	5% (v/v)
Sucrose	8% (w/v)
dH_2O	to 100 ml
pH	8 0

- **Solutions For The 1,2,3 Method (*Birnboim and Doly, 1979*) And Cosmid DNA Preparation**

Solution 1

Glucose	1 ml (of 0 5 M solution)
Na_2-EDTA	1 ml (of 0 1 M solution)
Tris-HCl	0 25 ml (of 1 M solution)
dH_2O	to 10 ml

Solution 2

NaOH	2 ml (of 1 N solution)
SDS	1 ml (of 10% solution)
dH_2O	to 10 ml

made up fresh every month and stored at room temperature

Solution 3

Potassium acetate	3 M
pH	4 8

To 60 ml of 5 M Potassium acetate, 11 5 ml of glacial acetic acid and 28 5 ml of dH_2O was added The resulting solution was 3 M with respect to Potassium and 5 M with respect to acetate

- **50X Tris Acetate EDTA (TAE) Buffer**

EDTA	100 ml (of 0 5 M solution)
Glacial Acetic Acid	57 1 ml
Tris	242 g
dH_2O	to 1 L
pH	8 0

diluted to 1X with dH_2O before use

- **Gel Loading Dye (6X)**

Bromophenol Blue	0.25%
Xylene Cyanol	0.25%
Ficoll (Type 400)	15%

Made in dH_2O and stored at room temperature following autoclaving.

- **TB Buffer For Competent Cells (*Inoue et al, 1990*)**

Pipes	10 mM
$CaCl_2$	15 mM
KCl	250 mM
pH with KOH	6.7

Once the pH had been adjusted, $MnCl_2$ was added to a final concentration of 55 mM. The solution was then filter sterilised through a 0.45 μm sterile filter and stored at 4°C.

- **TFB1 Buffer For Competent Cells**

RbCl	100 mM
$MnCl_2$	50 mM
Potassium acetate	30 mM
$CaCl_2$	10 mM
Glycerol	15%
pH	5.8

The solution was filter sterilised through a 0.45 μm sterile filter and stored at 4°C.

- **TFB2 Buffer For Competent Cells**

MOPS	10 mM
RbCl	10 mM
$CaCl_2$	75 mM
Glycerol	15%
pH with KOH	6.8

The solution was filter sterilised through a 0.45 μm sterile filter and stored at 4°C.

- **Solutions For Southern Blot Analysis**

20X SSC

NaCl	175.83 g
Trisodium citrate	88.2 g
pH	7.0
dH_2O	to 1 L

Denaturing Solution

NaCl	87.66 g
NaOH	20 g
dH_2O	to 1 L

Neutralising Solution

NaCl	87.66 g
Tris	121.1 g
pH	8.0
dH_2O	to 1 L

Washing Buffer

Maleic acid	11.61 g
NaCl	8.76 g
Tween 20	0.3% (v/v)
pH	7.5 (with solid NaOH)
dH_2O	to 1 L

Maleic Acid Buffer

Maelic acid	11.61 g
NaCl	8.76 g
pH	7.5 (with solid NaOH)
dH_2O	to 1 L

Detection Buffer

Tris	12.11 g
NaCl	5.84 g
pH	9.5
dH_2O	to 1 L

Denhardt's Solution (50X)

Ficoll (Type 400)	5 g
Polyvinylpyrrolidone	5 g
BSA (Pentax Fraction V)	5 g
dH_2O	500 ml

Salmon Sperm DNA

Salmon sperm DNA was dissolved in water at a concentration of 10 mg/ml, and mixed until dissolved. The DNA was sheared by passing it several times through an 18-gauge hypodermic needle. The DNA was boiled for 10 minutes, dispensed into small aliquots and stored at -20°C.

Prehybridisation Solution

SSC	6X
SDS	0.5% (w/v)
Denhardt's solution	5X
Salmon sperm DNA (10 mg/ml)	1 ml

Salmon sperm DNA was prepared by boiling for 5 min and chilling quickly in an ice water bath.

Hybridisation Solution

Prehybridisation solution was prepared as above and denatured labelled probe was added (Section 2.28).

Blocking Stock Solution (10X)

Blocking Reagent	10% (w/v)

The blocking reagent was dissolved under constant stirring in Maleic acid buffer and heated to 65°C. The solution remained opaque. To prepare 1X blocking solution, the blocking stock solution was diluted with Maleic acid buffer.

Antibody Solution

The antibody was centrifuged at 10,000 rpm for 5 min before each use. The antibody was diluted 1:5000 (150 mU/ml) in blocking solution.

2.4: Antibiotics

Antibiotics used were from Sigma Aldrich Co. Ltd. Antibiotics were prepared to a concentration of 100mg/ml and stored in the dark at -20°C unless otherwise indicated.

- **Ampicillin** was prepared in dH_2O and used at a final concentration of 100 µg/ml in solid and liquid broth for both *P. aeruginosa* and *E. coli*.
- **Chloramphenicol** was prepared in ethanol and used at a final concentration of 20 µg/ml in both solid and liquid media.
- **Tetracycline** was prepared in 50% ethanol at a concentration of 10 mg/ml. Tetracycline was used at a final concentration of 10 µg/ml for *S. meliloti* and

E. coli in both solid and liquid media. It was used at a final concentration of 50 μg/ml for *P. aeruginosa* in both solid and liquid media.

- **Kanamycin** was prepared in dH_2O. For *S. meliloti*, kanamycin was used at a final concentration of 100 μg/ml in solid media and 50 μg/ml in liquid broth. For *P. aeruginosa*, kanamycin was used at a final concentration of 500 μg/ml in solid media. For *E. coli*, kanamycin was used at a final concentration of 30 μg/ml in both solid and liquid media.
- **Neomycin** was prepared in dH_2O and used at a final concentration of 100 μg/ml in solid media and 50 μg/ml in liquid broth for *S. meliloti*.
- **Gentamicin** was prepared in dH_2O. For *P. aeruginosa*, gentamicin was used at a final concentration of 50 μg/ml in both solid and liquid media. For *S. meliloti* and *E. coli* gentamicin was used at a final concentration of 20 μg/ml in both solid and liquid media.
- **Streptomycin** was prepared in dH_2O and used at a final concentration of 1 mg/ml in solid media for *S. meliloti*.

2.5: Storing and Culturing Bacteria

Strains were stored as glycerol stocks. A 1 ml aliquot of a late log phase culture was added to 0.5 ml of sterile 80% glycerol in a microfuge which was then mixed and stored at -20°C. A duplicate set of long term socks were stored at -80°C. Where hosts were harbouring plasmids, the appropriate antibiotic was added to the stock medium. Working stocks were stored on plates at 4°C.

2.6: Plasmid Preparation By The 1,2,3 Method

This method was described by *Birnboim and Doly* (1979). A 1.5 ml aliquot of a bacterial culture grown in selective media was pelleted at 13,000 rpm in a microfuge and the supernatant was removed. The pellet was resuspended by vortexing in 100 μl of solution 1 and was then left for 5 min at room temperature. Then 200 μl of solution 2 was added, the tube was mixed by inversion and placed on ice for 5 min.

Then 150 µl of solution 3 was added, the tube was mixed by inversion and placed on ice for 10 min. A clot of chromosomal DNA formed and was pelleted by centrifugation at 13,000 rpm in a microfuge for 10 min. The supernatant was placed into a fresh tube and 450 µl of phenol chloroform isoamylalcohol (25:24:1) was added and mixed by vortexing. After centrifugation at 13,000 rpm for 5 min the aqueous layer was removed to a fresh tube and an equal volume of isopropanol was added. After mixing, the tube was incubated at room temperature for 10 min. Then the tube was centrifuged at 13,000 rpm for 10 min to pellet the plasmid DNA. The pellet was washed with 70% ethanol, dried briefly in a vacuum dryer and resuspended in 50 µl of TE buffer. Plasmid DNA was stored at 4°C.

2.7: Plasmid Preparation By The Rapid Boiling Method

This method was described by *Holmes and Quigley* (1981) and used instead of the 1,2,3 procedure outlined above for the screening of large numbers of transformants. A 1.5 ml aliquot of an overnight culture was spun at 13,000 rpm in a microfuge for 5 min and the supernatant removed. The pellet was resuspended in 350 µl of STET buffer. A 20 µl aliquot of 10 mg/ml lysozyme solution (prepared fresh in STET buffer) was added and the microfuge tube incubated at 30°C for 10 min. The tube was then place in a boiling water bath for 60 sec and then spun at 13,000 rpm for 10 min. The supernatant was removed to a fresh tube and an equal volume of isopropanol was added. The tube was left at room temperature for 10 min and then the plamid DNA was pelleted by centrifugation at 13,000 rpm for 10 min. The pellet was washed with 70% ethanol, dried briefly in a vacuum dryer and then dissolved in 50 µl of TE buffer. Plasmid DNA was stored at 4°C.

2.8: Preparation Of Cosmid DNA

A 1.5 ml aliquot of a bacterial culture grown in selective media was pelleted at 13,000 rpm in a microfuge and the supernatant was removed. The pellet was resuspended by vortexing in 100 µl of solution 1 and was then left for 5 min at room temperature. Then 200 µl of solution 2 as added, the tube was mixed by inversion and placed on ice

for 5 min. Then 150 µl of solution 3 was added, the tube was mixed by inversion and placed on ice for 10 min. A clot of chromosomal DNA formed and was pelleted by centrifugation at 13,000 rpm in a microfuge for 10 min. The supernatant was placed into a fresh tube and 450 µl of phenol chloroform isoamylalcohol (25:24:1) was added and mixed by vortexing. After centrifugation at 13,000 rpm for 5 min the aqueous layer was removed to a fresh tube and a 2.5 volume of ice cold ethanol was added. After mixing, the tube was incubated on ice for 30 min. Then the tube was centrifuged at 13,000 rpm for 10 min to pellet the cosmid DNA. The pellet was washed with 70% ethanol, air dried and then dissolved in 10 µl of TE buffer. Cosmid DNA was stored at 4°C.

2.9: Preparation Of Total Genomic DNA from *Sinorhizobium*

A 1.5 ml aliquot of early stationary phase culture of *Sinorhizobium* spp. was pelleted at 13,000 rpm for 5 min. The cells were washed with 1.5 ml of TES buffer and resuspended in 700 µl of TE buffer. Lysozyme solution (20 mg/ml in TE) was prepared freshly and 50 µl was added and the suspension was incubated at 30°C for 20 min. A sarkosyl/pronase solution (10% sarkosyl in TE containing 5 mg/ml pronase) was prepared and 50 µl was added and the suspension incubated at 37°C for one hour. Lysis was evident by an increase in the viscosity of the suspension. Sodium acetate (70 µl of a 3 M solution) was added and mixed gently. Then 600 µl of phenol chloroform isoamylalcohol (25:24:1) was added and the suspension was mixed slowly by inversion for 5 min. After centrifugation at 13,000 rpm for 5 min the aqueous phase was removed to a fresh microfuge tube and 600 µl of phenol chloroform isoamylalcohol (25:24:1) was again added and mixed slowly by inversion for 5 min. Following centrifugation at 13,000 rpm for 5 min the supernatant was removed to a fresh microfuge tube. Phenol extraction was carried out by adding 700 µl of chloroform:isoamylalcohol (24:1), mixing by inversion for 5 min, followed by centrifugation at 13,000 rpm for 5 min. The aqueous layer was removed to a fresh microfuge tube and the DNA was precipitated with an equal volume of isopropanol and was evident in the suspension as a coiled thread. The microfuge tube was spun at 13,000 rpm for 10 min to pellet the DNA. The pellet was washed twice with 70%

ethanol, air dried and dissolved in 200 µl of TE buffer. Genomic DNA was stored at 4°C.

2.10: Rapid Preparation Of Gram Negative Bacterial Genomic DNA

This method was modified from that described by *Chen and Kuo* (1993) and used to prepare genomic DNA from *Pseudomonas* spp. A 1.5 ml aliquot of a bacterial culture was pelleted at 13,000 rpm in a microfuge and the supernatant was removed. The cell pellet was resuspended in 200 µl of lysis buffer and lysed by vigorous pipetting. Then 66 µl of 5 M NaCl solution was added, the tube was mixed by inversion and the viscous mixture was centrifuged at 13,000 rpm for 10 min at 4°C. The supernatant was transferred into a fresh tube and an equal volume of phenol chloroform was added and mixed gently by inversion 50 times. After centrifugation at 13,000 rpm for 5 min, the supernatant was removed to a fresh tube, an equal volume of chloroform was added and the tube was again mixed gently by inversion a further 50 times. Following centrifugation at 13,000 rpm for 3 min, the extracted supernatant was transferred to a fresh tube and precipitated with 2.5 volumes of ice cold ethanol. The pellet was washed twice with 70% ethanol, dried briefly in a vacuum dryer and redissolved in 50 µl of TE buffer. Genomic DNA was stored at 4°C.

2.11: Agarose Gel Electrophoresis For DNA Characterisation

DNA was analysed by running on agarose gels in a horizontal gel apparatus. Gels were prepared by dissolving agarose in 1X TAE buffer to the required concentration (typically 0.7-2%) and boiling until the solution became translucent. The 1X TAE buffer was also used as the running buffer. A tracker dye was incorporated into DNA samples to facilitate loading of samples. Mini-gels were frequently run at 140 Volts for 20-30 min or until the tracker dye had migrated the required distance while maxi gels were frequently run at 40 Volts overnight. Gels were stained by immersing in a bath of ethidium bromide for 20 min and then destained by immersing in a water bath for 10 min. Gels were then visualised on a UV transilluminator and photographed using a UV image analyser.

2.12: Preparation Of Ethidium Bromide

A 10 mg/ml stock solution of ethidum bromide was prepared by dissolution in dH_2O. The solution was stored in the dark at 4°C. A 100 µl aliquot of this stock solution was added to 1 L of dH_2O for staining agarose gels. Gloves were worn at all times when handling solutions containing ethidium bromide. Ethidum bromide waste was collected and filtered through a deactivating filter (Schleicher and Schuell). The clear liquid was disposed of normally and the solids contained in the filter were incinerated.

2.13: Isolation Of DNA From Agarose Gels

DNA was purified from agarose gels using a DNA Gel Purification Kit (Eppendorf). The kit was used according to the manufactures instructions. Briefly, the gel slice was excised with a sterile scalpel and weighed. Three volumes of gel solubilising buffer was added and the tube was incubated at 55°C until the gel slice had completely dissolved. One volume of isopropanol was added to the tube and mixed vigorously. Then, 800 µl of the solution was transferred into a spin cup and spun at 13,000 rpm for 1 min. The flow through was discarded and 750 µl of washing solution was added and spun for a further minute at 13,000 rpm. The flow through was again discarded and the cup was again spun at 13,000 rpm for 2 min. The spin cup was transferred to a fresh microfuge tube and 30 µl of TE was added. The cup was then spun at 13,000 rpm for 1 min to elute the DNA.

2.14: Southern Blot Analysis

Following electrophoresis, the gel was stained in a bath of ethidium bromide and photographed. The DNA was denatured by immersing the gel in a denaturing solution of 1.5 M NaCl/0.5 M NaOH and agitating gently at room temperature for 1 hour. The gel was subsequently immersed in a neutralising solution of 1 M Tris, pH 8.0/1.5 M, and incubated with gentle agitation at room temperature for a further hour. A gel tray was inverted in a bath of 20X SSC, and a sheet of Whatman 3 MM paper

cut to the with of the gel was soaked in the 20X SSC and placed on top of the gel tray, with the ends dipping into the solution forming a wick. Air bubbles were removed by gently rolling the Whatman paper with a glass rod. The gel was inverted and placed gently on top of the Whatman paper. A piece of nitrocellulose filter cut exactly to the size of the gel was placed onto the surface of 2X SSC and allowed to soak from beneath. The filter was immersed in the solution for a further 2 min, and then placed on top of the gel. Air bubbles were removed as described above. Three pieces of Whatman paper were cut to the size of the gel and two of them were soaked in 2X SSC and placed on top of the filter. The third piece was then placed on top. Air bubbles were removed as described above. A stack of paper towels approximately 20 cm high was placed on top of the Whatman paper, ensuring that the towels did not come into contact with the wicks, and a weight was placed on top. The transfer of DNA was allowed to proceed for approximately 12-24 hours.

Following the completion of the transfer, the paper towels and the Whatman paper on top of the gel was removed and the gel and the filter were place gel side up on a dry sheet of Whatman paper. The positions of the wells were marked on the filter, which was then soaked for 5 min in 6X SSC. The filter was allowed to dry at room temperature for 1 hour and it was subsequently placed between two sheets of Whatman paper and baked at 80°C for two hours to irreversibly bind the DNA to the filter. The filter was then wrapped in Whatman paper and stored until required.

The filter was placed in roller bottles and at least 20 ml of prehybridisation solution was added per 100 cm^2 of filter. The filter was incubated while rotating for 1 hour. The prehybridisation solution was removed and hybridisation solution was added. The filter was incubated rotating for at least 16 hours. Following hybridisation, the filter was washed twice at room temperature with 2X SSC/0.1% SDS for 5 min. The filters was subsequently washed twice at 65°C with periodic agitation with 0.1X SSC/0.1% SDS for 30 min.

Immunological detection was performed using the DIG DNA Labelling and Detection Kit from Roche. Briefly, a 100 cm^2 filter was washed in washing buffer for 5 min. The filter was then incubated in 100 ml of blocking solution, which was prepared freshly, for at least 1 hour. Then, the filter was incubated for 20 min with 20 ml of

antibody solution. The filter was washed twice for 15 min with washing buffer and then equilibrated for 5 min in 20 ml of detection buffer. The filter was incubated with 10 ml of colorsubstrate solution and incubated in the dark until colour development was complete. The colour reaction was stopped by washing with TE buffer.

2.15: *In silico* Analysis Of DNA And Protein Sequences

The BLAST (Altschul *et al*, 1997) programs at NCBI (www.ncbi.nlm.nih.gov) were used to identify homologous sequences deposited in GenBank. DNA and Protein sequences were aligned using the MultAlin program (Corpet, 1988), available at (http://prodes.toulouse.inra.fr/multalin/multalin.html), and the Genedoc program, available to download at (http://www.psc.edu/biomed/genedoc/). DNA sequences were analysed for potential promoter sequences using the BDGP Neural Promoter Prediction Program at (http://www.fruitfly.org/seq_tools/promoter.html). DNA sequences were analysed using the pDRAW32 program, available to download at (http://www.acaclone.com/). Protein sequences were analysed using the online analysis tools available at ExPASy Molecular Biology Server (http://us.expasy.org/). The location of proteins was predicted using PSORT (Nakai and Kanehisa, 1991) at (http://psort.nibb.ac.jp/). Putative signal sequences were predicted using the SignalP program (Nielsen *et al*, 1997) at (http://www.cbs.dtu.dk/services/SignalP/). Potential domains within putative proteins were identified using Pfam program (Bateman *et al*, 2002) at (http://www.sanger.ac.uk/Software/Pfam/index.shtml). The *S. meliloti* 1021 genome sequence was accessed at (http://sequence.toulouse.inra.fr/meliloti.html) and the *P. aeruginosa* PA01 genome sequence was accessed at (www.pseudomonas.com).

2.16: Preparation Of High Efficiency Competent Cells

This method was described by *Inoue et al* (1990). A frozen stock of the appropriate *E. coli* strain was thawed, streaked on LB agar and incubated at 37°C overnight. Approximately 10-12 large colonies were removed with an inoculating loop and inoculated into 250ml of SOB medium in a 2 L baffled flask. The culture was grown at 18°C with vigorous shaking (200-250 rpm) until an OD_{600} of 0.6 was reached. The

flask was then placed on ice for 10 min. The culture was transferred to a 250 ml centrifuge bottle and spun in a Beckman J2-21 centrifuge at 5,000 rpm and 4°C for 5 min. The pellet was resuspended in 80 ml of ice-cold TB buffer, placed on ice for 10 min and spun down as before. The cell pellet was gently resuspended in 20 ml of ice cold TB buffer and DMSO was added slowly with gentle swirling to a final concentration of 7%. After incubation in an ice bath for 10 min the cell suspension was dispensed in 1 ml aliquots into microfuge tubes. The cells were then flash frozen in liquid nitrogen and stored at -80°C. Cells prepared in this manner frequently gave transformation efficiencies of the order or 10^8-10^9 transformants/ug DNA which is comparable with those attainable by electroporation.

2.17: Transformation Of High Efficiency Competent Cells

A microfuge tube of cells prepared according to the procedure outlined in section 2.14 was allowed to thaw on ice and a 1-5 µl aliquot of plasmid preparation was added to 200 µl of the competent cells. The contents of the tube were briefly mixed and incubated on ice for 30 min. The cells were heat shocked at 42°C for 30s ec and then transferred back onto ice for 2 min. Then 0.8 ml of SOC medium was added and the cells were incubated at 37°C with vigorous shaking for 1 hour. A 100 µl aliquot of the resulting transformation mixture was plated on an appropriate selective media and the plates were incubated at 37°C overnight.

2.18: Preparation Of Competent Cells By RbCl Treatment

A frozen stock of the appropriate *E. coli* strain was thawed, streaked on LB agar and incubated at 37°C overnight. A single colony was picked and a 10 ml LB broth was inoculated and incubated at 37°C overnight. One ml of the overnight culture was added to 100 ml of LB broth and grown shaking at 37°C until an OD_{600} of 0.5 was reached. The flask was then placed on ice for 5 min. The culture was transferred to a centrifugation bottle and spun in a Beckman J2-21 centrifuge at 5,000 rpm and 4°C for 5 min. The cell pellet was carefully resuspended in 30 ml of ice cold TFB1 buffer, incubated on ice for 90 min and spun down as before. The cell pellet was gently

resuspended in 4 ml of ice cold TFB2 and the cell suspension was dispensed in 1 ml aliquots into sterile microfuge tubes. The cells were then flash frozen in liquid nitrogen and stored at -80°C.

2.19: Transformation Of Competent Cells Prepared By RbCl Treatment

A 10 µl aliquot of a ligation mixture was added to 100 µl of competent cells that had been allowed to thaw on ice. The cells were kept on ice for 20 min and were then heat shocked at 42°C for 90 sec. A 500 µl aliquot of Psi broth was added to the cells and they were incubated at 37°C for 60-90 min. A 100-200 µl aliquot of the resulting transformation mixture was then plated on appropriate selective media and plates were incubated at 37°C for 24 hours.

2.20: Iron Nutrition Bioassays To Detect Siderophore Utilisation

Siderophore utilisation bioassays were performed in media prepared with ultra pure water and supplemented with the appropriate concentration of 2,2' dipyridyl. Molten agar (1.5% with Oxoid No.1 purified technical agar) prepared in 25 ml aliquots, was inoculated with 200 µl of a stationary phase culture and the appropriate concentration of 2,2' dipyridyl (Stock solution 60 mM in ethanol), usually 2 mM for *P. aeruginosa*, 400 µM for *E. coli* and 300 µM for *S. meliloti*, and the mixtures were poured into sterile plates. Wells were cut out of the solid media, and 50 µl of the test solutions was pipetted into the wells. Growth was allowed to proceed for 24 to 48 hours, and plates were then examined for haloes of bacterial growth surrounding wells bearing test solutions.

Test solutions (concentrated culture supernatants) were prepared by adding 2,2' dipyridyl to the appropriate concentration to broth, usually 500 µM for *P. aeruginosa* and 300 µM for *E. coli*, *S. meliloti* and *B. megaterium*, and then inoculating with the relevant strain. Growth was allowed to proceed until late log phase. The culture was transferred in 1.5 ml aliquots to microfuge tubes and centrifuged at 13,000rpm for 3 min to pellet the cells. Cell free supernatants were transferred to fresh tubes and

concentrated in a vacuum dryer set to high temperature, and then resuspended in one tenth the original volume with ultra pure water. The samples were then pooled, filter sterilised through a 0.45 μm filter and stored in the dark at -20°C. All test solutions were prepared in this manner and in this thesis, shall be referred to by the appropriate siderophore name. Ferrichrome was purchased from Sigma Chemicals Co. Ltd. Ferrichrome was dissolved in ultra pure water to a final concentration of 0.5 mM, filter sterilised through a 0.45 μm filter and stored in the dark at -20°C. To analyse ferrichrome utilisation, 50 μl of a 0.05 mM ferrichrome solution was used.

2.21: Analysis Of Siderophore Production By The CAS Plate Assay

Cultures were grown until late log phase or early stationary phase and the OD_{600} was determined. Then individual culture ODs, as determined at OD_{600}, were adjusted to 1 OD unit in a microfuge tube. The culture was then pelleted by centrifugation at 13,000 rpm for 3 min. The cell pellet was resuspended in a 0.85% sterile saline solution and 10 μl was spotted onto the surface of a CAS plate. Growth was allowed to proceed for 24 to 48 hours, and the plate was then examined for haloes to determine siderophore production.

2.22: Bacterial Conjugation By Triparental Mating

S. meliloti was grown to late log phase in TY and LB broth respectively, while *E. coli* donors were grown to late mid log phase in LB broth. *E. coli* donors (0.75 ml) were mixed with an *E. coli* (0.75 ml) strain carrying the mobilising plasmid pRK600 (Simon *et al*, 1986). The mixture was pelleted at 13,000 rpm for 3 min, resuspended in 100 μl of fresh LB and then spotted onto the centre of an LB plate. Following incubation overnight at 37°C, the bacteria were resuspended in 3 ml of LB broth. Then 0.75 ml of the bacterial donor culture was mixed with 0.75 ml of the recipient culture and the culture was pelleted as above. The pellet was resuspended in 100 μl of TY broth and spotted onto the centre of a TY plate. Following incubation overnight, the bacteria were resuspended in 2 ml of TY broth and dilutions were plated on appropriate selective media. As controls, donor and recipient strains were spotted

separately on agar plates and carried through the procedure as outlined above. Donor and recipients strains were then plated on the appropriate selective media. For triparental matings involving *P. aeruginosa*, LB was used instead of TY.

2.23: Surface Sterilisation Of *Medicago sativa*

Medicago sativa seeds were washed with sterile water and then stood in ethanol for 5 min. The ethanol was poured off and the seeds were again washed with sterile water. The water was poured off and the seeds were stood in domestic bleach for 10 min. The bleach was then poured off and the seeds were washed four times with sterile water. The seeds were then spread on TY plates and incubated at room temperature in the dark for two days.

2.24: Nodulation Analysis of *Medicago sativa*

Two-day old seedlings were transferred to Jensen media and inoculated with approximately 10^5 *S. meliloti* by streaking on the surface of the media. The plants were incubated for 30 days, after which they were observed for nodulation and assayed for nitrogen fixation.

2.25: Analysis Of Nitrogen Fixation By Gas Chromatography

Nitrogen fixation was assayed by the acetylene reduction assay (Wacek and Brill, 1976). Nodules were excised and placed into a sterile suba sealed vessel. The atmosphere was then made 10% with respect to acetylene. Acetylene reduction was determined by gas chromatography using a Poropak N column and a flame ionisation detector following a 24 hour incubation period. The injector temperature was 70°C and the oven temperature was 120°C.

2.26: TA Cloning Of PCR Products

PCR reactions (Section 2.28) were routinely performed to amplify DNA fragments of interest. PCR products were routinely cloned using Original TA Cloning Kit vector pCR2.1 from Invitrogen. The diagram below shows the concept behind the TA Cloning method.

Figure 2.1: Principle Of TA Cloning

The method is dependent on the fact that thermostable polymerases like *Taq* DNA polymerase, which lacks 3'-5' exonuclease activity, leave 3' A-overhangs, which can subsequently be cloned into a vector with 3' T-overangs. PCR products generated with *Taq* DNA polymerase have a high efficiency of cloning in the TA Cloning system. Other thermostable polymerases like *Vent* and *Pfu*, which have 3'-5' exonuclease activity, do no leave these 3' A-overhangs.

PCR products were amplified using a standard PCR reaction mixture (Section 2.28) and using Red*Taq* DNA polymerase from Sigma. They were subsequently ligated with the TA pCR2.1 vector. The ligation was set up as follows;

Fresh PCR product	1 µl
pCR2.1 Vector (25 ng/ µl)	2 µl
10X Ligation Buffer	1 µl
Sterile dH_2O	5 µl
T4 DNA Ligase (4.0 Weiss units)	1 µl
Total Volume	10 µl

The reaction was then incubated at room temperature overnight. Following incubation, 2-5 µl of the ligation was used to transform either *E. coli* DH5α cells

prepared by the high efficiency method (Section 2.14) or *E. coli* INVαF' one shot competent cells that were supplied with the TA Cloning Kit.

To transform INVαF' cells, the cells were first thawed on ice. Then 2 µl of β-mercaptoethanol (0.5 M) was added and mixed gently with the pipette tip. Between 2-5 µl of the ligation reaction mixture was added to the cells and mixed gently with the pipette tip. The cells were incubated on ice for 20 min and then 250 µl of SOC media was added. The cells were incubated at 37°C for 1 hour. A 50 µl aliquot of the transformation mixture was plated on LB agar containing ampicillin (100 µg/ml) and X-gal to select for transformants and to test for α-complementation of β-galactosidase. In addition to an ampicillin resistance gene the TA pCR2.1 vector also contained a kanamycin resistance gene. Kanamycin (30 µg/ml) was thus used to select for transformants instead of ampicillin when PCR products amplified from ampicillin resistant plasmids were being cloned.

2.27: Testing For α-Complementation of β-Galactosidase

Selection of recombinant plasmids was made on the following basis for pUC based vectors and the pCR2.1 TA cloning vector. Transformants bearing plasmids with inserts, or PCR products in the case of TA cloning, were distinguished from transformants bearing recircularised plasmids without inserts by plating on media containing X-gal to test for α-complementation of β-galactosidase. Transformants harbouring plasmids with inserts did not express a functional *lacZα* gene product, which is the α peptide of β-galactosidase, and therefore appeared white on X-gal plates because α-complementation could not occur. Transformants harbouring recircularised plasmid DNA without any inserts expressed a functional *lacZα* gene product and thus appeared blue on X-gal plates because α-complementation of β-galactosidase occurred resulting in the cleaving of X-gal. White colonies were thus picked from plates and screened for the presence of inserts.

In order to test for α-complementation, transformations were plated on LB agar containing an appropriate antibiotic, usually ampicillin in the case of TA cloning, and X-gal as mentioned above. The X-gal was not incorporated into the media. Instead

60µl of a stock solution of X-gal (40mg/ml in dimethylformamide) was spread on the surface of premade LB agar plates containing ampicillin, and the plates were allowed to dry. The stock solution of X-gal was not filter sterilised. It was stored at -20°C and in the dark as it is light sensitive. Transformations were plated out on LB ampicillin X-gal plates and the plates were then incubated at 37°C for 12-16 hours. The plates were then removed from the incubator and stored at 4°C for several hours in order to allow colour development. White colonies were then picked off plates and screened for the presence of plasmids bearing inserts.

IPTG was not required in the media when transforming *E. coli* strains DH5α or INVαF' because these strains did not contain the $lacI^q$ allele. The *lacI* gene encodes the Lac repressor, which represses expression of the *lacZ* gene from the *lac* promoter. The level of LacI repressor in the *E. coli* strains DH5α or INVαF' is not sufficient to suppress the *lac* promoter on multicopy number plasmids. In contrast, the $lacI^q$ allele expresses a higher level of LacI repressor than the normal *lacI* gene. In strains bearing this allele, IPTG has to be used to induce expression and therefore has to be added to the media when testing for α-complementation. A stock solution of IPTG (100 mM) was prepared by dissolving IPTG in water. The solution was filter sterilised and stored at -20°C. A 40 µl aliquot of this stock solution was spread on the surface of pre-made LB agar plates along with X-gal when testing for α-complementation.

2.28: Enzymatic Reactions

- **Enzymes and Buffers**

All enzymes and their relevant buffers were obtained from Invitrogen Life Technologies®, New England BioLabs® or Sigma Corporation and were used according to the manufacturers instructions.

- **RNase**

RNase that was free of DNase was dissolved at a concentration of 10 mg/ml in 10 mM Tris-HCl (pH 7.5) and 15 mM NaCl. The solution was then dispensed into aliquots and stored at -20°C.

- **Klenow Reaction**

DNA	18 µl
dNTPs (0.5 mM)	1 µl of each
Klenow Buffer (10X)	3 µl
Sterile dH_2O	4 µl
Klenow (0.5 U/µl)	1 µl

The reaction was incubated at room temperature for 1 hour. The reaction mixture was then phenol extracted to remove the enzyme and the DNA was ethanol precipitated.

- **Bacterial Alkaline Phosphatase (BAP) Reaction**

This protocol allows for the dephosphorylation of DNA directly in restriction endonuclease buffer in the presence of restriction endonuclease. To a restriction endonuclease digest, 1 µl of BAP (150 U) was added and the reaction was incubated at 65°C for 1 hour. The reaction mixture was then phenol extracted to remove the enzyme and the DNA was ethanol precipitated.

- **Klenow Labelling Reaction**

Probes for Southern blots were prepared as follows: Restricted DNA was boiled for 5 min and then chilled quickly on ice water. A labelling reaction was then set up as follows;

DNA	15 µl
Hexanucleotide mix	2 µl
DNTP labelling mix	2 µl
Klenow enzyme	1 µl

As longer incubation times resulted in an increase in labelling efficiency, the mixture was generally incubated for up to 20 hours. The probe was denatured by boiling for 10 min and chilling quickly on wet ice.

- **Standard PCR Reaction Mixture**

Template DNA	1 µl
Primers (0.6 nm/µl)	1 µl of each
Buffer (10X)	5 µl
dNTP Mix (10 mM)	1 µl
Sterile dH_2O	40 µl
RedTaq DNA Polymerase	1 µl

- **Standard PCR Program Cycle**

Stage 1: **Step1:** 95°C for 10 min

Stage 2: **Step1:** 95°C for 1 min
Step2: Annealing Temperature for 30 sec
Step3: 72°C for 1 min for every Kb to be synthesised. (Stage 2 was usually repeated for 30 cycles)

Stage 3: **Step1:** 72°C for 10 min

- **1 Kb Molecular Marker**

NEB 1 Kb ladder used for Southern hybridisations.

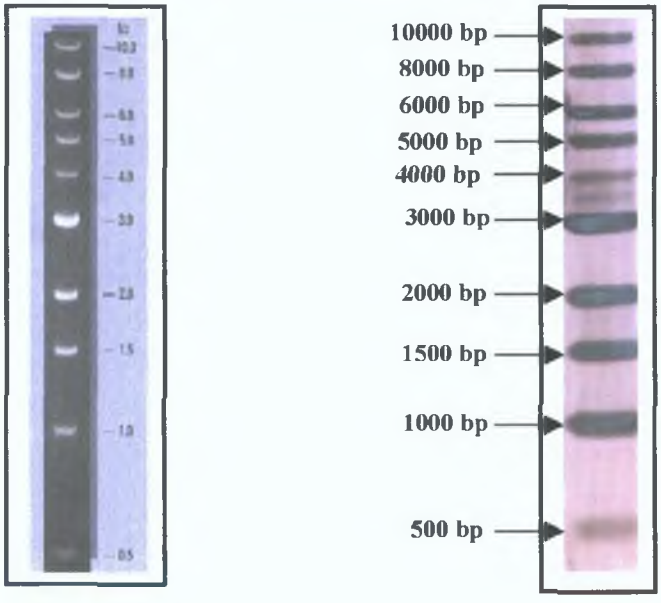

Chapter 3

Identification And Characterisation Of Novel Siderophore Utilisation Systems In *S. meliloti* 2011 and *P. aeruginosa*

3.1: Introduction

Sinorhizobium meliloti 2011 is a gram negative bacterium found free living in the soil, or as an endosymbiont of *Medicago sativa* (alfalfa) with which it forms a nitrogen fixing symbiosis. There is a high iron demand in the symbiosis due to the importance of many iron containing enzymes such as nitrogenase and ferredoxin which are involved in nitrogen fixation. Consequently, the methods of iron acquisition in rhizobia have been the subject of particular interest (Chapter 1).

S. meliloti 2011 has previously been shown to produce the siderophore rhizobactin 1021 under iron limiting conditions. The structure of rhizobactin 1021 has shown it to be a novel asymmetric citrate dihydroxymate siderophore (Chapter 1)(Persmark *et al.*, 1993). Siderophore mediated iron transport in *S. meliloti* was found to correlate with the presence of specific iron regulated proteins in the outer membrane (Chapter 1)(Reigh and O'Connell, 1993). Random mutagenesis of *S. meliloti* 2011 and *S. meliloti* 220-5 facilitated the isolation of mutants defective in siderophore production (Reigh, PhD Thesis)(Reigh and O'Connell, 1993). A Tn*5mob* containing *Eco*R1 fragment from a *S. meliloti* 220-5 mutant defective in siderophore uptake was cloned into pUC19 and this fragment was used to isolate by hybridisation the complementing cosmid, pGR30, from a gene bank of *S. meliloti* 2011. The introduction of pGR30 into *S. meliloti* 102F34, a strain deficient in the ability to synthesise or utilise rhizobactin 1021, conferred upon it the capacity to synthesise and utilise the said siderophore.

A 14.2 Kb region of pGR30 was sequenced and deposited at NCBI (Accession number AF110737). The sequence correlated with the sequence subsequently released as part of the *S. meliloti* 1021 genome project. Analysis of the sequence revealed the presence of ten ORF's with a high probability of being functional genes. Six of the ORF's showed homology to siderophore biosynthesis genes and were designated *rhbA*, *B*, *C*, *D*, *E*, and *F* respectively. The protein products of two further ORF's showed homology to regulatory and siderophore receptor proteins, and were designated *rhrA* and *rhtA* respectively (Lynch *et al*, 2001)(Lynch, PhD Thesis 1999). The protein product of the ninth ORF, designated *rhbG*, showed homology to siderophore biosynthesis proteins but, as yet, no function has been assigned to it. The

final ORF was partially sequenced, and the predicted protein product showed homology to signal transducers. This ORF was designated *orf1* (Lynch, PhD Thesis 1999). Figure 3.1 shows the position and orientation of the afore mentioned genes.

Figure 3.1: Organisation Of The Rhizobactin 1021 Regulon.

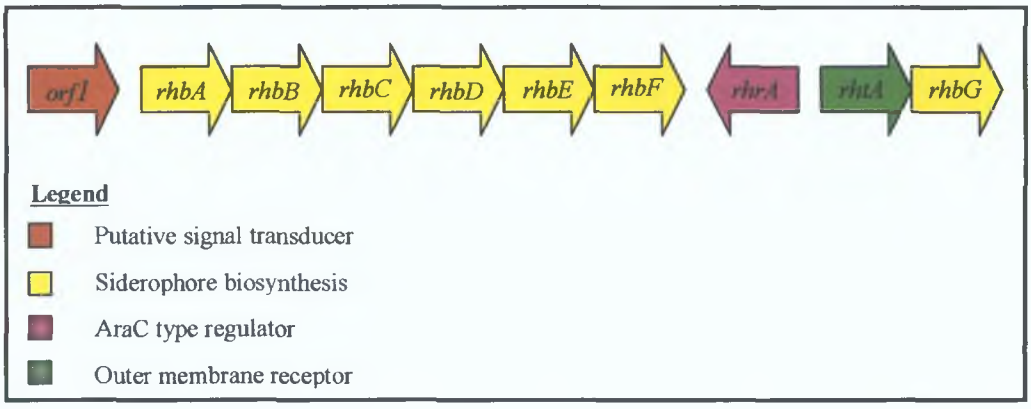

In order to determine the specific functions of the genes involved in rhizobactin 1021 biosynthesis, utilisation and regulation, transposon insertions were obtained by fragment-targeted mutagenesis and the mutated fragments were introduced into the chromosome of *S. meliloti* 2011 by allelic exchange (Lynch, PhD Thesis 1999; Lynch *et al*, 2001). The phenotypes of the various mutants constructed are described in Table 3.1. Phenotypic analysis involved the application of the CAS plate assay (Schwyn and Neilands, 1987)(Chapter 2) to assay siderophore production, the plate bioassay (Reigh and O'Connell, 1993)(Chapter 2) to determine siderophore utilisation and the analysis of outer membrane protein patterns by SDS-PAGE.

The phenotypes of *S. meliloti* 2011*rhbA*62, *S. meliloti* 2011*rhrA*26 and *S. meliloti* 2011*rhtA*45 were confirmed for use in the research presented in this thesis.

Table 3.1: Phenotypes Of *S. meliloti* Rhizobactin 1021 Regulon Mutants

S. meliloti Mutant	Mutated Gene	Halo on CAS medium	Rhizobactin 1021 utilisation	Outer membrane receptor protein
2011	Wild type	+	Yes	Abundant
2011 *rhbA*62	*rhbA*	-	Yes	Reduced
2011 *rhbC*2	*rhbC*	-	Yes	nt
2011 *rhbE*11	*rhbE*	-	Yes	Reduced
2011 *rhbF*104	*rhbF*	-	Yes	Reduced
2011 *rhbF*107	*rhbF*	-	Yes	Reduced
2011 *rhbG*25	*rhbG*	+	Yes	Abundant
2011 *rhrA*4	*rhrA*	-	No	None
2011 *rhrA*6	*rhrA*	-	No	None
2011 *rhrA*26	*rhrA*	-	No	None
2011 *rhtA*1	*rhtA*	+	No	None
2011 *rhtA*42	*rhtA*	+	No	None
2011 *rhtA*45	*rhtA*	+	No	None
2011 *orf1*43	*orf1*	-	No	Reduced

This chapter describes the characterisation of the region encoding the putative signal transducer, *orf1*, and an analysis of its role in rhizobactin 1021 utilisation. The identification and characterisation of a homologue of Orf1 in *P. aeruginosa* is also described.

3.2: Re-evaluation of the *S. meliloti* 2011*orf1*43 mutant phenotype

As previously described, an *orf1* mutant was generated and shown to be impaired in its ability to utilise rhizobactin 1021 and also in its ability to produce siderophore as determined by the CAS plate assay. Remarkably little information could be gained regarding the function of Orf1 using conventional sequence analysis. *In silico* analysis of Orf1 revealed limited sequence homology to YbtX, a protein of unknown function, encoded within the yersiniabactin siderophore regulon of *Y. pestis* (Fetherston *et al.*, 1999), and AmpG, a permease that functions in beta-lactamase induction in *E. coli*. The role of AmpG in cell wall recycling had previously been elucidated (Jacobs *et al.*, 1995), but no protein had previously been implicated as being involved in siderophore utilisation and secretion. Due to the mutant phenotype of *S. meliloti* 2011*orf1*43 and the limited sequence homology of Orf1 to known database proteins, it was decided to re-characterise the *S. meliloti* 2011*orf1*43 mutant phenotype in detail.

The original phenotype described for *S. meliloti* 2011*orf1*43 is as described in Table 3.1 (Lynch, PhD Thesis 1999). Examination of the *S. meliloti* 2011*orf1*43 mutant phenotype confirmed that the mutant was defective in rhizobactin 1021 utilisation, and had a reduced level of RhtA in the outer membrane compared to wild-type *S. meliloti* 2011. Analysis of siderophore production by the CAS plate assay however, indicated that siderophore biosynthesis was not totally abolished in *S. meliloti* 2011*orf1*43 as originally described, but that it was severely diminished (Figure 3.2).

Figure 3.2: Siderophore Production By *S. meliloti* 2011*orf1*43

In order to confirm that siderophore production was not abolished in *S. meliloti* 2011*orf1*43, siderophore was prepared from *S. meliloti* 2011*orf1*43 as described in Chapter 2, and used to cross feed mutants *S. meliloti* 2011*rhbA*62 and *S. meliloti*

2011*rhtA*45. *S. meliloti* 2011*rhbA*62 is impaired in its ability to synthesise rhizobactin 1021 but is unaffected in its siderophore utilisation capacity. *S. meliloti* 2011*rhbA*62 is used as an indicator strain for siderophore utilisation. *S. meliloti* 2011*rhtA*45 is impaired in its ability to utilise rhizobactin 1021. The results are described in Table 3.2.

Table 3.2: Analysis Of *S. meliloti* 2011*orf1*43 Siderophore Production

Concentrated Culture Supernatants	**Cross feeding of *Sinorhizobium* strains**	
	S. meliloti 2011*rhbA*62	*S. meliloti* 2011*rhtA*45
S. meliloti 2011	+++	-
S. meliloti 2011*rhbA*62	-	-
S. meliloti 2011*orf1*43	+	-

Analysis of the results indicated that siderophore prepared from *S. meliloti* 2011*orf1*43 could cross feed the indicator strain *S. meliloti* 2011*rhbA*62, but could not cross feed the control strain *S. meliloti* 2011*rhtA*45. Concentrated culture supernatants prepared in the same manner from *S. meliloti* 2011*rhbA*62 could not cross feed either mutant. Siderophore prepared from wild-type *S. meliloti* 2011 could only cross feed *S. meliloti* 2011*rhbA*62. The result indicated that *S. meliloti* 2011*orf1*43 was not abrogated in rhizobactin 1021 biosynthesis. Siderophore production however was severely diminished. The revised phenotype for *S. meliloti* 2011*orf1*43 is described in Table 3.3

Table 3.3: Revised Phenotype For *S. meliloti* 2011*orf1*43.

S. meliloti	**Mutated Gene**	**Halo on CAS medium**	**Rhizobactin 1021 utilisation**	**Outer membrane receptor protein**
2011	Wild type	++	Yes	Abundant
2011 *orf1*43	*orf1*	+	No	Reduced

Analysis of the result indicated that *orf1* possibly encoded a protein with a role in siderophore utilisation and secretion. On the basis of the phenotype of the mutant and the associated homology to YbtX, *orf1* was designated *rhtX* for ***rh***izobactin 1021 ***t***ransport.

3.3: Isolation Of Cosmids Complementing *S. meliloti* 2011*rhtX*43

The introduction of the cosmid pGR30 into *S. meliloti* 102F34, a strain which does not synthesis or utilise rhizobactin 1021, conferred upon the bacterium the ability to synthesis and utilise rhizobactin 1021. Restriction mapping of the cosmid indicated that the region upstream of *rhtX* was encoded on the cosmid. It was proposed to subclone and sequence the region upstream of *rhtX* in order to complete the open reading frame and also to determine if there were any further genes located upstream of *rhtX* that encoded proteins involved in the utilisation of rhizobactin 1021.

As previously described, a 14.2 Kb region of pGR30 had previously been subcloned and sequenced and the data was deposited at NCBI. Attempts were made to isolate pGR30 cosmid DNA with a view to subcloning the region upstream of *rhtX*, however numerous difficulties were encountered. Initial concerns centred on the nature of pGR30 as a cosmid. The cosmid pGR30 is based on the pBR325 replicon. The pBR325 replicon is a narrow host range mobilisable plasmid that cannot stably replicate in *S. meliloti*. In order to maintain the cosmid in *Sinorhizobium* therefore, it was necessary to generate a co-integrate with RP4, a broad host range self conjugative plasmid which is stably maintained in *Sinorhizobium*. Analysis indicated that the co-integrate was unstable and readily disassociated into smaller plasmids in *E. coli*. The formation of smaller plasmids often results in the deletion or rearrangement of sections of DNA. For this reason it was considered undesirable to subclone a fragment from pGR30. RP4 is a low copy number plasmid and is maintained at approximately 2-3 copies per cell. The low copy number of the resultant cosmid pGR30 meant that it was difficult to obtain sufficient cosmid DNA for subcloning. Finally, RP4 is a self-conjugative plasmid that can be stably maintained in *Sinorhizobium*, the RP4::pGR30 plasmid should be readily transmissible to a suitable *E. coli* host. However, all attempts to introduce a stable pGR30 into *E. coli* from *S. meliloti* failed.

To overcome these problems it was decided to mobilise a *S. meliloti* generated genebank into *S. meliloti* 2011*rhtX*43 in order to identify a more stable cosmid that complemented the mutation. A *S. meliloti* 2011 genebank (Freidman *et al.*, 1982) was kindly provided by Dr. Michael F. Hynes. The genebank was a pLAFR1 based cosmid bank. The pLAFR1 cosmid is a derivative of the low copy number broad host

range cloning vector pRK290 (Ditta *et al*, 1980) The pLAFR1 vector is approximately 21 6 Kb and confers tetracycline resistance which is suitable for selection in *S meliloti* 2011 The pLAFR1 vector encodes a unique *Eco*R1 site suitable for cloning or for adaptation by linkers and can be mobilised into and stably maintained within many gram-negative hosts The *Sinorhizobium* genebank was constructed using a partial *Eco*R1 digest of *S mehloti* and the mean insert size was determined to be 23 1 Kb

The pLAFR1 cosmid is mobilisable but as the cosmid does not encode transfer functions (*tra* genes), these have to be provided *in trans* The narrow host range plasmid pRK600 (Simon *et al*, 1986) encodes the necessary transfer functions, and was used for the mobilisation of the genebank The genebank was mobilised and mated *en masse* into *S meliloti* 2011*rhtX*43 by triparental mating as described in Chapter 2 Dilutions of the resulting mating mix were plated on TY agar containing neomycin, to counter select the *E coli* donor, and tetracycline to counter select the *S meliloti* recipient Individual colonies were subsequently spotted onto CAS agar plates and screened for restoration of siderophore production to the wild type level

Three transconjugants were identified that restored siderophore production in *S meliloti* 2011*rhtX*43 as determined by the CAS plate assay Examination of the transconjugants by the siderophore utilisation bioassay confirmed that the ability to utilise rhizobactin 1021 had been restored Cosmid DNA was prepared from the complemented *S meliloti* as previously described (Chapter 2) and transformed into *E coli* DH5α to facilitate large scale DNA preparation for analysis Cosmid DNA was analysed by restriction analysis and it was confirmed that they constituted three individual cosmids The cosmids were termed pPOC1, pPOC2 and pPOC3 As the transformation of large DNA fragments can result in deletions or rearrangements of DNA, each of the three cosmids was re-introduced into *S meliloti* 2011*rhtX*43 and the phenotypes of the transconjugants were analysed to confirm that the cosmids being analysed in *E coli* retained the complementary region The siderophore production of the transconjugants was analysed by the CAS plate assay The results revealed that pPOC2 did not complement the *rhtX* mutation to the same extent as the original pPOC2 isolate Further analysis by the siderophore utilisation bioassay indicated that the ability of the pPOC2 transconjugant to utilise rhizobactin 1021 had been abolished

Restriction analysis of pPOC2 indicated an approximate 1 Kb deletion within a 5 2 Kb *Bam*H1 fragment that encoded *rhtX*

Phenotypical analysis of the pPOC1 and pPOC3 transconjugants confirmed that they complemented the *rhtX* mutation to the same extent as the original cosmid isolates Due to the unknown nature of the pPOC2 deletion, it was decided to discontinue further study of this cosmid

3.4: Analysis Of The Complementing Cosmids pPOC1 And pPOC3

As previously described, the cosmids pPOC1 and pPOC3 were isolated on the basis of their ability to restore rhizobactin 1021 production and utilisation in *S. meliloti* 2011*rhtX*43. Jiping Li, a visiting student in the laboratory, had previously constructed a restriction map of the area encoding the rhizobactin 1021 regulon. Gill and Neilands (1989) had also described a restriction profile of the region. The sequence of the 14.2 Kb region (Lynch *et al*, 2001; Lynch PhD Thesis 1999) also enabled a highly detailed restriction map of the area to be constructed. Restriction analysis indicated that pPOC1 and pPOC3 comprised two individual cosmids that overlapped a region sufficient to complement the *rhtX* mutation and determined to be 8.5 Kb in length bounded by *Eco*R1 restriction sites.

It was decided to map the cosmids by complementation analysis in parallel with restriction analysis. The phenotypes of the transconjugants could be easily assayed by the CAS plate assay or the siderophore utilisation bioassay. The cosmids pPOC1 and pPOC3 were introduced into various rhizobactin 1021 regulon mutants. The transconjugants were assayed for the restoration of the relevant phenotype (Table 3.4).

Table 3.4: Complementation Analysis Of *S. meliloti*.

S. meliloti	Cosmid	Halo on CAS medium	Rhizobactin 1021 utilisation	Complementation
2011 wt		+	Yes	
	pPOC1	+	Yes	-
	pPOC3	+	Yes	-
2011*rhtX*43		+	No	
	pPOC1	+	Yes	Yes
	pPOC3	+	Yes	Yes
2011*rhbA*62		-	Yes	
	pPOC1	+	Yes	Yes
	pPOC3	+	Yes	Yes
2011*rhrA*26		-	No	
	pPOC1	+	Yes	Yes
	pPOC3	-	No	No
2011*rhtA*45		+	No	
	pPOC1	+	Yes	Yes
	pPOC3	+	No	No

The introduction of the cosmid pPOC1 into wild-type *S. meliloti* 2011 resulted in a marked increase in siderophore production as determined by the CAS plate assay (Figure 3.3). The introduction of pPOC3 also resulted in an increase in siderophore production although the increase was not as pronounced as for pPOC1. It was hypothesised that the increase in siderophore production was due to a copy number effect of the cosmid, which is maintained at approximately 5-8 copies per cell.

Analysis of the *S. meliloti* 2011*rhtX*43 pPOC1 transconjugant indicated that pPOC1 resulted in a restoration of siderophore production as determined by the CAS plate assay. In contrast, analysis of siderophore production by the *S. meliloti* 2011*rhtX*43 pPOC3 transconjugant by the CAS plate assay indicated that while siderophore production was restored, the level was below that produced by wild type *S. meliloti* 2011. The difference observed between the two transconjugants was initially confusing and is examined in more detail in Section 3.9 below.

The complementation results indicated that pPOC1 complemented the mutations in *S. meliloti* 2011*rhbA*62, *S. meliloti* 2011*rhrA*26 and *S. meliloti* 2011*rhtA*45. In contrast, pPOC3 did not complement any of the mutants with the exception of *S. meliloti* 2011*rhbA*62, where a slight increase in siderophore production was observed.

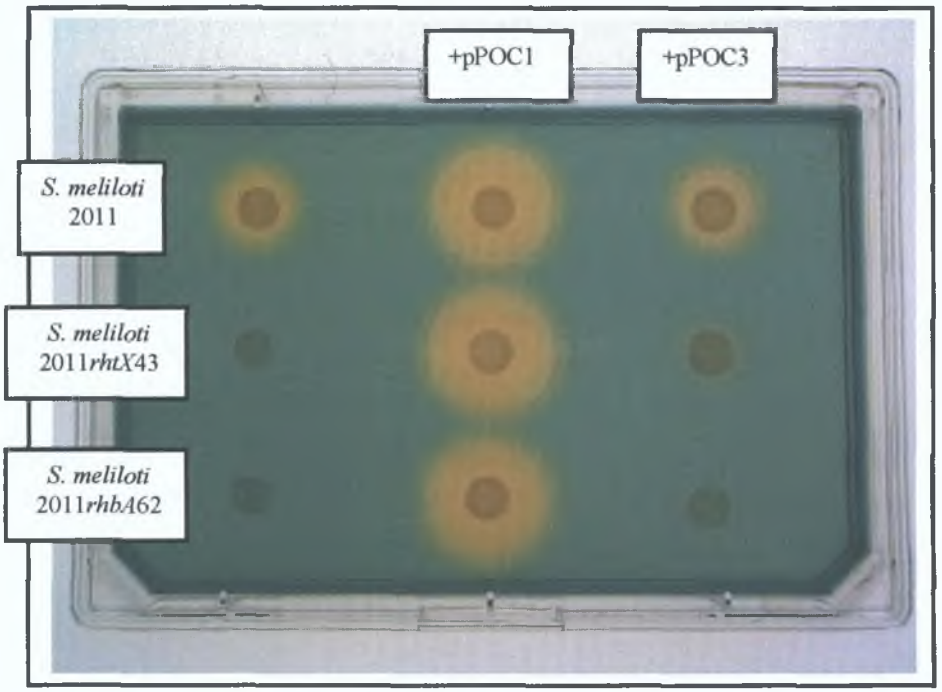

Figure 3.3: Analysis Of *S. meliloti* pPOC1 And pPOC3 Transconjugants. *S. meliloti* pPOC1 and pPOC3 transconjugants were spotted on CAS plates and analysed as described in Chapter 2. The orange halo indicates siderophore production.

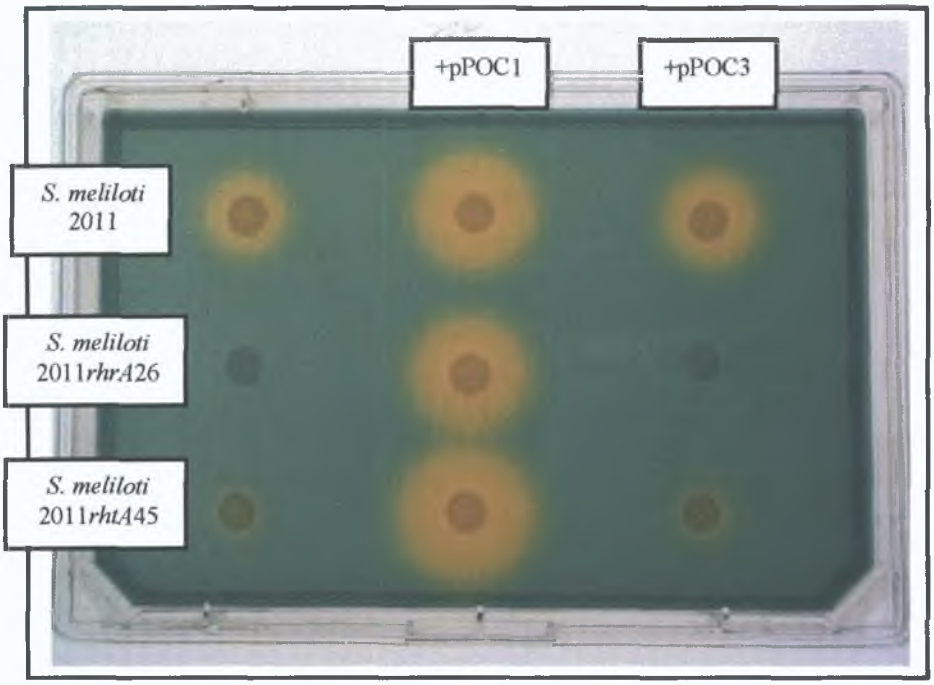

Figure 3.4: Analysis Of *S. meliloti* pPOC1 And pPOC3 Transconjugants. *S. meliloti* pPOC1 and pPOC3 transconjugants were spotted on CAS plates and analysed as described in Chapter 2. The orange halo indicates siderophore production.

Siderophore utilisation was analysed by the siderophore utilisation bioassay (Chapter 2). A strain of interest was seeded into iron-limited media and the ability of the strain to utilise various test compounds to alleviate the conditions of iron deficiency was examined. The iron chelator 2,2'dipyridyl was added to induce the conditions of iron limitation. The ability of *S. meliloti* 2011 to produce and utilise rhizobactin 1021 enables it to overcome the conditions of iron limitation resulting in growth throughout the plate (Figure 3.5 (A)). In comparison, *S. meliloti* 2011*rhtX*43 is unable to utilise rhizobactin 1021, and so does not grow throughout the plate (Figure 3.5 (B)). Both pPOC1 and pPOC3 therefore confer to varying degrees the ability to utilise rhizobactin 1021 on *S. meliloti* 2011*rhtX*43.

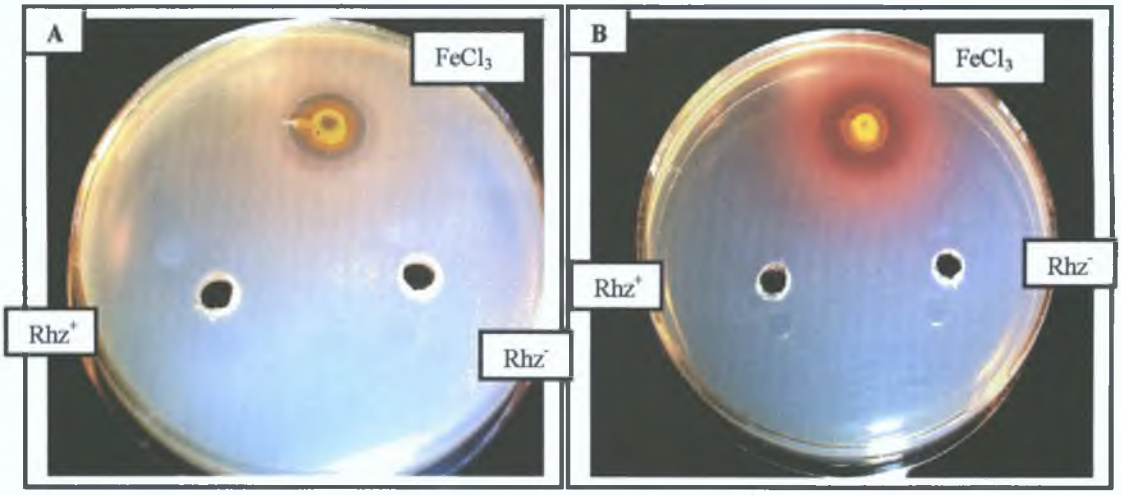

Figure 3.5: Rhizobactin 1021 Utilisation Bioassay Of *S. meliloti* 2011 (A) And *S. meliloti* 2011*rhtX*43 (B). Ferric chloride ($FeCl_3$) was used as a positive control. Concentrated culture supernatant containing rhizobactin 1021 (Rhz^+) was prepared as described in Chapter 2. A concentrated culture supernatant (Rhz^-) prepared from a rhizobactin 1021 biosynthesis mutant was used as a negative control.

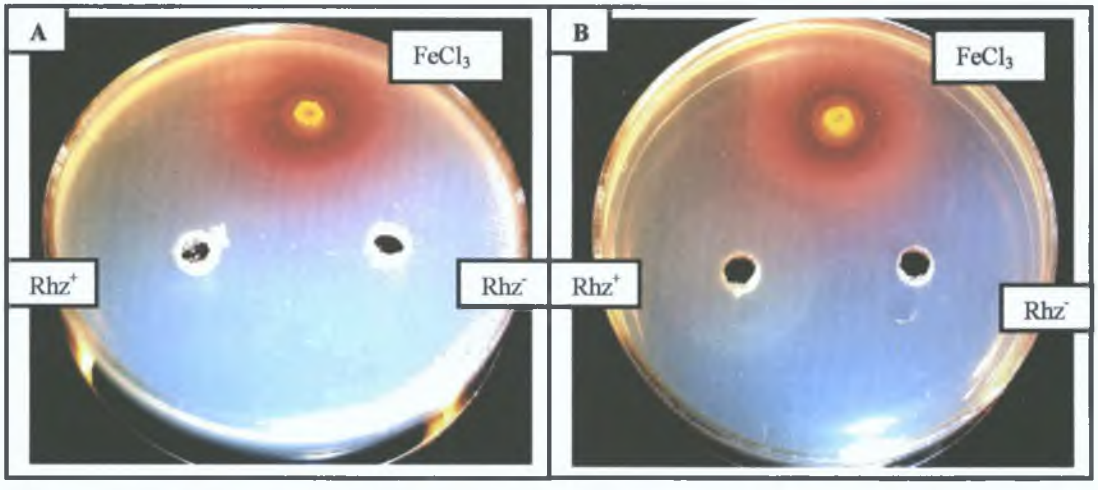

Figure 3.6: Rhizobactin 1021 Utilisation Bioassay Of *S. meliloti* 2011*rhtX*43 pPOC1 (A) and pPOC3 (B) Transconjugants. Ferric chloride ($FeCl_3$) was used as a positive control. Concentrated culture supernatant containing rhizobactin 1021 (Rhz^+) was prepared as described in Chapter 2. A concentrated culture supernatant (Rhz^-) prepared from a rhizobactin 1021 biosynthesis mutant was used as a negative control.

The introduction of pPOC1 and pPOC3 into *S. meliloti* 2011*rhtX*43 resulted in a restoration of rhizobactin 1021 utilisation as determined by the siderophore utilisation bioassay. However, analysis of the pPOC1 transconjugant indicated that the utilisation phenotype was similar to a wild type *S. meliloti* 2011 phenotype in that growth throughout the plate occurred. In contrast, the utilisation phenotype for the pPOC3 transconjugant was similar to that observed for a biosynthesis mutant where a halo of growth around the well containing the siderophore was observed. This result is discussed in Section 3.9.

Analysis of siderophore utilisation indicated that the *S. meliloti* 2011*rhrA*26 and *S. meliloti* 2011*rhtA*45 pPOC1 transconjugants were restored in rhizobactin 1021 utilisation. In contrast, pPOC3 did not result in a restoration of the rhizobactin 1021 utilisation phenotype in these strains.

The cosmids pPOC1 and pPOC3 were introduced into *S. meliloti* 102F34. *S. meliloti* 102F34 does not synthesise or utilise rhizobactin 1021. The introduction of pPOC1 into *S. meliloti* 102F34 conferred upon the strain the ability to synthesise rhizobactin 1021. However, the introduction of pPOC3 into *S. meliloti* 102F34 did not confer upon the strain the ability to synthesise rhizobactin 1021 (Figure 3.7). The introduction of pPOC1 into *S. meliloti* 102F34 conferred upon the strain the ability to utilise rhizobactin 1021, while in contrast pPOC3 did not confer upon the strain the ability to utilise rhizobactin 1021 (Table 3.5).

Table 3.5: Complementation Analysis Of *S. meliloti* 102F34

S. meliloti	Cosmid	Halo on CAS Medium	Rhizobactin 1021 Utilisation
102F34		-	-
102F34	pPOC1	+	+
102F34	pPOC3	-	-

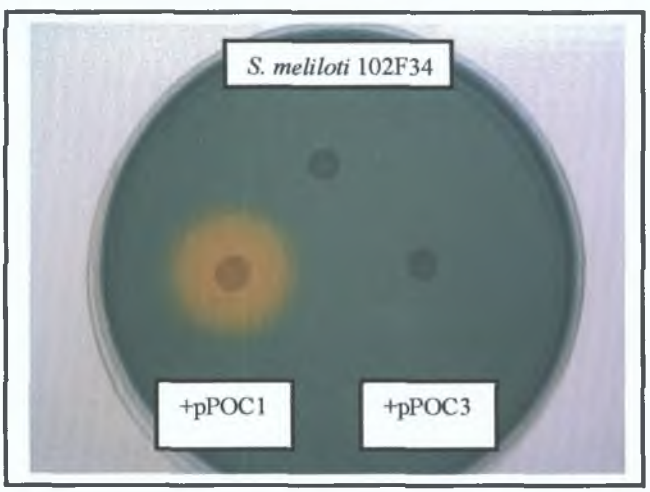

Figure 3.7: Analysis Of Siderophore Production By *S. meliloti* 102F34 -pPOC1 And -pPOC3 Transconjugants. *S. meliloti* 102F34 pPOC1 and pPOC3 transconjugants were spotted on CAS plates and analysed as described in Chapter 2. The orange halo indicates siderophore production.

3.5: Sequencing And *in silico* Analysis Of The *rhtX* Locus

Restriction analysis of pPOC1 and pPOC3 indicated that both cosmids contained an 8.5 Kb *Eco*R1 fragment which was predicted to encode *rhtX*. The cosmid pPOC1 was digested with *Eco*R1 and the 8.5 Kb fragment was gel purified and subcloned into bacterial alkaline phosphatase (BAP) treated pUC18. The clone, and all such subsequent clones were named according to the approximate size of the cloned fragment and the enzyme sites at either end e.g. pUC8.5 E/E is an 8.5 Kb *Eco*R1 fragment cloned into pUC18. A 3.5 Kb *Eco*R1/*Bam*H1 fragment was restricted from pUC8.5 E/E and subcloned into pUC18 generating pUC3.5 E/B. This plasmid pUC3.5 E/B was predicted to contain the 5' end of *rhtX* and the region directly upstream. The plasmid pUC3.5 E/B was partially sequenced resulting in 2.8 Kb of the sequence directly upstream of *rhtX*.

The genome sequence of *Sinorhizobium meliloti* 1021 was published in April 2001. A comparison of the sequence obtained from pUC3.5 E/B confirmed that the sequence correlated with the genome sequence with the exception of a dinucleotide repeat that is discussed in Section 3.8. Analysis of the genome sequence revealed the presence of a putative gene, Sma2335, upstream of *rhtX* and orientated in the opposite direction. Directly downstream of Sma2335 and orientated in the same direction was a putative *kdp* locus, encoding proteins predicted to be involved in potassium transport. The gene directly downstream of Sma2335, *kdpA*, was predicted to constitute an operon with *kdpBCD* and possibly two other genes. Analysis of the literature did not reveal any evidence to suggest that the protein products encoded by the *kdp* locus might be involved in siderophore mediated iron acquisition. Consequently, the *kdp* locus was not further analysed. A map of the region is shown in Figure 3.8.

Figure 3.8: Map Of The Cosmids pPOC1 And pPOC3 And The Region Encoding *rhtX*.

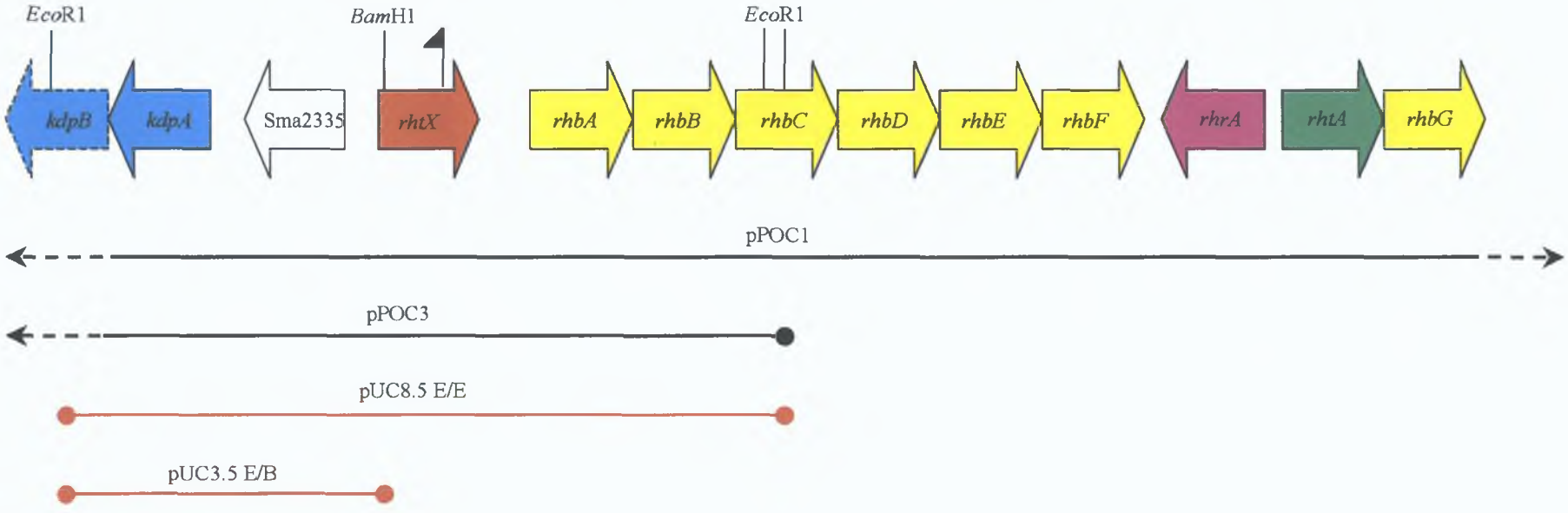

The biosynthesis genes (including *rhbG*) are coloured in yellow, while the *rhrA* and *rhtA* are coloured in pink and green respectively. The *rhtX* gene and the upstream Sma2335 gene are coloured in red and white respectively. The *kdp* genes are indicated in light blue. The dashed line for *kdpB* signifies the continuation of the *kdp* operon. The cosmid pPOC3 is predicted to end at one of the two *Eco*R1 sites encoded within *rhbC*. The orientation of the transposon insertion in *rhtX* is also indicated (↿). The dashed lines on the cosmids indicate that the cosmids extend to *Eco*R1 sites outside the range of this map. The plasmids pUC8.5 E/E and pUC3.5 E/B are indicated in red.

3.6: *In silico* Analysis Of *rhtX*

rhtX is located at position 1304824-1306116 of the *S. meliloti* 1021 pSyma megaplasmid. A putative ribosome binding site, TGGCA, was identified upstream of the predicted translational start site for *rhtX*. The protein predicted to be encoded by *rhtX* is 431 amino acids in length with a predicted molecular weight of 45.56 kDa and a pI of 9.84. The amino acid sequence of RhtX is shown below in Figure 3.9.

Figure 3.9: Amino Acid Sequence Of RhtX.

MLAAVVQGSDPIMTIAQTSPAVREGSTAAGAGRLYAVLGGLYLAQGIPTYLLLVALPP
LMRESGASRTAIGLFSLLMLPLVLKFAVAPLVDRWAPWPGLGHRRGWVVPTQLLVSAG
IASMALVEPDRAGTLFAIGICITLLSSVQDIATDGYAVRHLNGRTLAIGNAVQAGSIA
LGVIVGGTLTLVLFHKIGWRPTILLVACLSLLPLVAAIWMKDRAVASPEAPLRRRASL
FGFFRRPNAWMILAFALTYRASEGLVRGMEGSYLVDSKVPTEWIGYMSGAAAATAGLL
GALIAALIIRKAGLTATLILLGGLRSLCFLAFALNAFGIWPGIAVAMSASAFQTLIRY
MELVAIYSFFMASSSDDQPGTDFTILSCAELVVYLIGTSIAGYVADRFGYATLFSSAT
VISVLGIGLSVWMLERLKARPSRSR

The amino acid sequence of RhtX was compared against the NCBI database of protein sequences using the BLASTP program (Altschul *et al*, 1997). Analysis of the RhtX amino acid sequence indicated that the protein showed sequence homology to a family of proteins of unknown function. The most significant matches to RhtX identified using the BLASTP program and their associated predicted biochemical data are listed in Table 3.6.

Table 3.6: Proteins Displaying Significant Homology To RhtX.

Protein	Homologue	Molecular Mass (kDa)	Accession	Identity (%)*
Rrub1561	*Rhodospirillum rubrum*	47.25	ZP_00014546	26 (44)
All4027	Nostoc sp. PCC 7120	43.73	NP_488065	25 (45)
SMc02889	*S. meliloti* 1021	43.91	NP_384320	23 (40)
Y3421	*Y. pestis* KIM	49.31	AAM86970	22 (42)
YPO0772	*Y. pestis* CO92	47.73	CAC89621	22 (41)

*Identities (%) were calculated using the Genedoc program. Similarities are indicated in brackets.

The MultAlin (Corpet, 1988) and Genedoc programs were used to perform a global sequence alignment of RhtX and *R. rubrum* Rub1561, Nostoc sp. PCC7120 All4025, *S. meliloti* 1021 Smc02889, *Y. pestis* KIM Y3421 and *Y. pestis* CO92 YPO0772 (Figure 3.10).

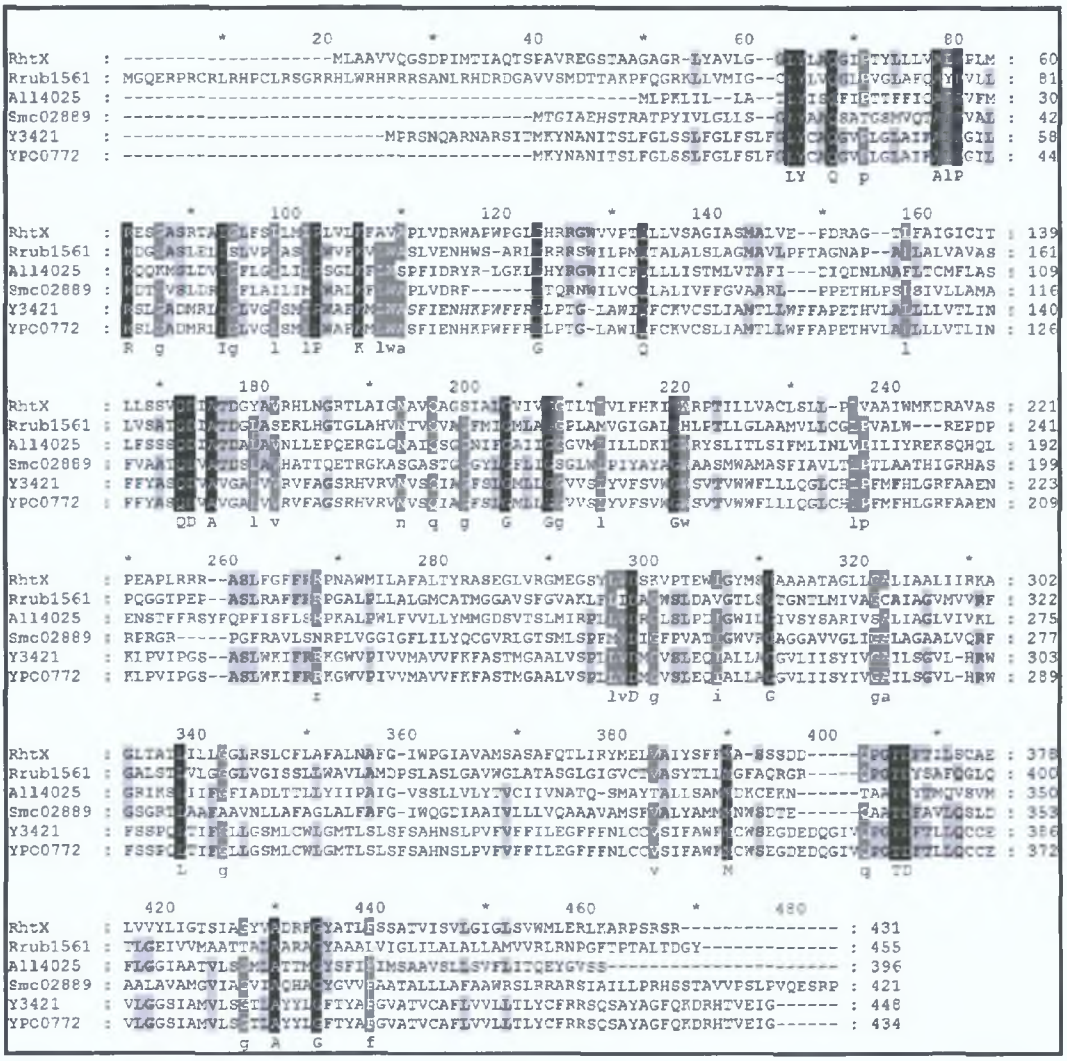

Figure 3.10: Multiple sequence alignment of RhtX; with *R. rubrum* Rub1561, Nostoc sp. PCC 7120 All4025, *S. meliloti* 1021 Smc02889 and *Y. pestis* KIM Y3421 and *Y. pestis* CO92 YPO0772. Black indicates 100% conservation, dark grey indicates 83% conservation and light grey indicates 66% conservation.

The amino acid sequence of RhtX was analysed using the PSORT program (Nakai and Kanehisa, 1991). The analysis indicated that the protein was predicted to be located in the inner membrane.

3.7: *In silico* analysis of Sma2335

Sma2335 is located at position 1304552-1304352 of the *S. meliloti* 1021 pSyma megaplasmid. A putative ribosome binding site, AGAGA, was identified upstream of the predicted translational start site for Sma2335. The protein predicted to be encoded by Sma2335 is 67 amino acids in length with a predicted molecular weight of 7.18 kDa and a pI of 9.69. The amino acid sequence of Sma2335 is shown below in Figure 3.11.

Figure 3.11: Amino Acid Sequence Of Sma2335.

MITLGPHSLSFLYVAAKPSQSIIDAARTHHPDLGSIWRMPMSDFLFLAAGIGGLAALA
LYARALSRL

The amino acid sequence of Sma2335 was compared against the NCBI database of protein sequences using the BLASTP program (Altschul *et al*, 1997). Analysis of Sma2335 indicated that the putative protein did not show homology to any protein in the NCBI database. The amino acid sequence of Sma2335 was subsequently compared against the NCBI database of protein sequences using the PSI-BLAST program (Altschul *et al*, 1997). PSI-BLAST, or Position Specific Iterated BLAST, uses an iterative search in which sequences found in one round of searching are used to build a score model for the next round of searching. Highly conserved positions receive high scores and weakly conserved positions receive scores near zero. The profile is used to perform subsequent BLAST searches, and the results of each iteration used to refine the profile. This iterative searching strategy results in increased sensitivity. Analysis indicated the Sma2335 did not display homology to any protein in the NCBI database

Analysis of Sma2335 using the PSORT program (Nakai and Kanehisa, 1991) indicated that the protein was predicted to be located in the inner membrane

3.8: Analysis Of *rhtX* And Sma2335 Promoter Region

Directly upstream of *rhtX*, and orientated in the opposite direction is a gene of unknown function, Sma2335, (Section 3.7; Figure 3.8). The intergenic region between *rhtX* and Sma2335 was examined in order to identify potential promoter sequences (Figure 3.12). A putative promoter was identified for *rhtX* using the Neural Promoter Prediction Program (Chapter 2). The *rhtX* promoter region was examined to identify any potential Fur boxes. A Fur box was identified which overlapped the putative *rhtX* promoter region. The putative Fur box exhibited 57% homology to the *E. coli* Fur consensus sequences.

A Post Doctoral researcher in the laboratory, Dr. Paul Clarke, identified a putative RhrA binding site in the *rhtX* and Sma2335 intergenic region. The putative binding site consists of a repeat of GTTCGC $(N)_{15}$ GTTCGC. The intergenic region between *rhrA* and *rhtA* was examined, and a similar repeat was identified. Analysis of the *rhtX* and *rhbA* intergenic region did not reveal the presence of a similar repeat, or of any sequences with homology to the putative binding sequence. The rhizobactin 1021 biosynthesis operon, *rhbABCDEF*, had previously been shown to be RhrA regulated. The identification of a putative RhrA binding site upstream of *rhtX* suggested that *rhtX* was also part of the *rhbABCDEF* operon.

An unusual CT repeating unit was identified in the region directly upstream of the Sma2335 translational start site. Analysis of the region using the sequence data available from the *S. meliloti* 1021 Genome Sequencing Project revealed that there were nineteen repeating CT units present. Analysis of the sequence data obtained from pUC3.5 E/B revealed that there were twenty repeating CT units present. The repeat found in the promoter region of Sma2335 is similar to that found in the promoter regions of genes that are regulated in part by phase variation. The significance and apparent variability of the CT repeat remains to be elucidated.

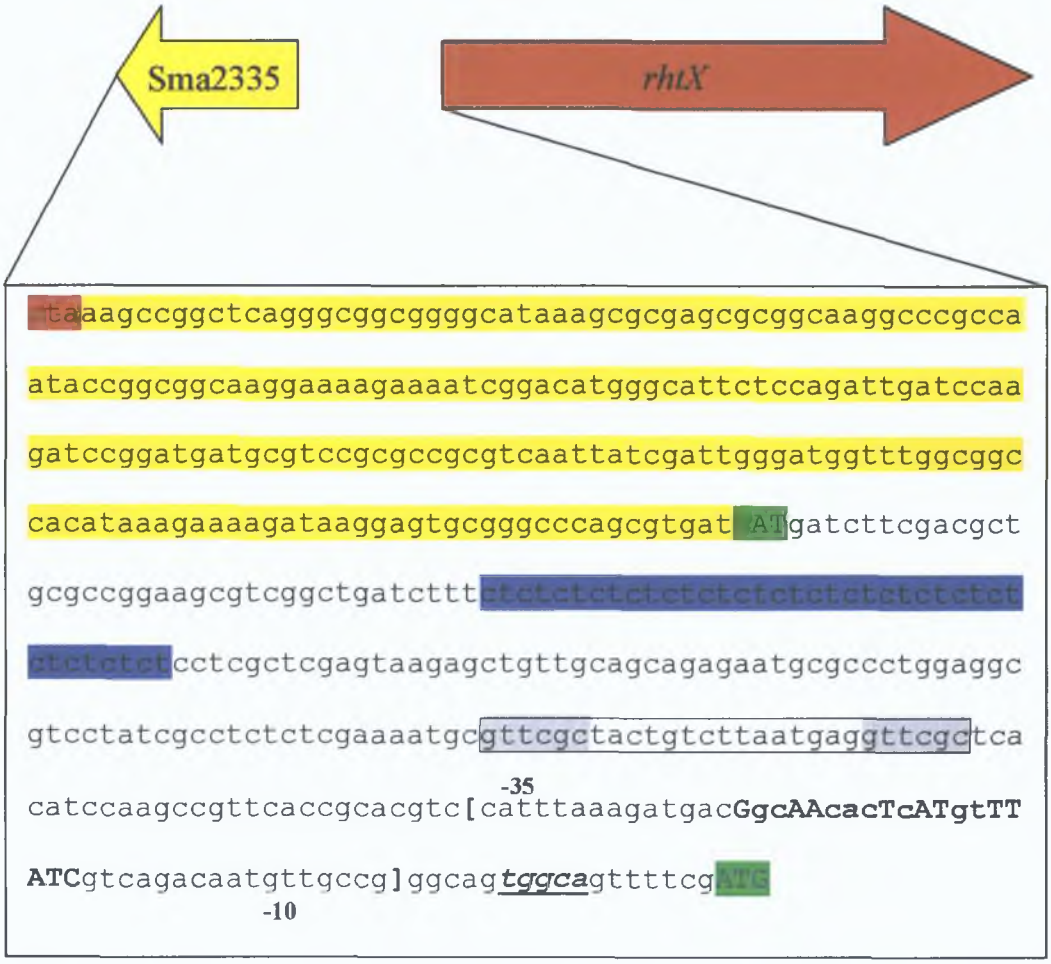

Legend

- Translational start codon
- Translational stop codon
- Open reading frame
- RhrA binding site. The potential binding sequence is boxed.
- CT repeat

[ ] Promoter. The –10 and –35 regions are indicated.

Fur Box: The Fur box is indicated in bold text. Conserved residues with the *E. coli* Fur consensus sequence are indicated in capitals.

RBS: The putative ribosome-binding site for *rhtX* is indicated in bold underlined italics.

Figure 3.12: Analysis Of Sma2335 And The Region Between Sma2335 And RhtX.

3.9: Questions Arising From The Complementation Analysis

Following the complementations undertaken and described in Section 3.4 the following results required explanation:

(a) As the pPOC3 cosmid did not complement the biosynthesis operon, was RhtX involved in the secretion of rhizobactin 1021?
(b) If RhtX is not involved in rhizobactin 1021 secretion, how does pPOC3 mediate the increased production of rhizobactin 1021 in *S. meliloti* 2011*rhtX*43?
(c) Was the transposon insertion in *rhtX* having a polar effect on the downstream *rhbABCDEF* biosynthesis operon?
(d) Was there a promoter located in the *rhtX/rhbA* intergenic region?

The sections below will describe the analysis of all of these possibilities.

3.10: Complementation Of *S. meliloti* 2011*rhtX*43

As previously described, the cosmids pPOC1 and pPOC3 were isolated by complementation of the *S. meliloti* 2011*rhtX*43 mutant phenotype. Analysis of the transconjugants by the CAS plate assay indicated that both cosmids lead to a restoration of siderophore production by *S. meliloti* 2011*rhtX*43. Mapping of the cosmids indicated that pPOC1 extended from a region upstream of *rhtX* to a region downstream of *rhbG*. Analysis indicated that pPOC3 extended from a region upstream of *rhtX* to one of two centrally located *Eco*R1 sites within *rhbC*, Section 3.4, Figure 3.8. The rhizobactin 1021 biosynthesis genes, *rhbABCDEF*, had previously been show to constitute an operon (Lynch *et al*, 2001). As pPOC3 did not encode the entire rhizobactin 1021 biosynthesis operon, the restoration of siderophore production in a *S. meliloti* 2011*rhtX*43 pPOC3 transconjugant was unexpected. This result made it necessary to consider that RhtX may have a role in siderophore secretion.

To determine whether RhtX functions in the secretion of rhizobactin 1021, it was decided to clone and express *rhtX* in *S. meliloti* 2011*rhtX*43. To overcome any titration effect due to RhrA regulation, it was decided to express the gene from an

independent promoter. It was decided to express *rhtX* from one of the broad host range pBBR1MCS series of vectors (Kovach *et al*, 1994; Kovach *et al*, 1995), which were a kind gift of Dr. Michael Kovach. The pBBR1MCS series of vectors contained a number of features, which made them suitable for the expression of *rhtX*. Five different versions of the vectors were available, each encoding a different antibiotic resistance. The vectors are broad host range and contain a *mob* site, which allows the vector to be introduced into a strain of interest by conjugation. Unlike other broad host range vectors expression vectors, the pBBR1MCS series of vectors are small. The plasmids contain the region encoding the multiple cloning site from pBluescript II KS+ which also allows a blue white screen for inserts. The region encoding the multiple cloning site encodes a *lac* promoter which can be utilised for the expression of proteins of interest. The pBBR1MCS vectors also encode an origin of replication that enables them to be stably maintained with narrow host range ColE1 and P15Abased plasmids and also with broad host range IncP, IncQ and IncW based plasmids.

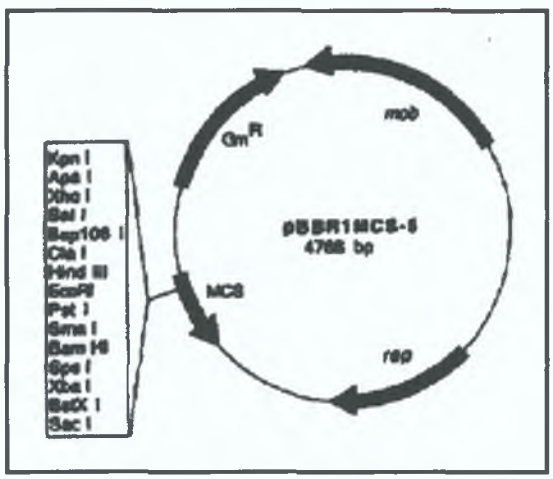

Figure 3.13: Map Of The Broad Host Range Plasmid pBBR1MCS-5. The origin of replication (*rep*), the mobilisation site (*mob*), the gentamicin resistance gene (Gm^R) and the multiple cloning site (MCS) are indicated.

As gentamicin is a suitable selection marker in *S. meliloti*, it was decided to clone *rhtX* into pBBR1MCS-5 and to express it under the control of the *lac* promoter. Two primers, RhtX-F1 and RhtX-R1 (Chapter 2) were designed to amplify *rhtX* from the *S. meliloti* 2011 genome. The forward primer RhtX-F1 was designed to incorporate a unique *Xho*1 site into the PCR product. The forward primer was also designed to incorporate the ribosome-binding site of *rhtX* into the PCR product. The reverse primer, RhtX-R1 was designed to incorporate a unique *Pst*1 site into the PCR product.

The unique *Xho*1 and *Pst*1 sites in the PCR product were added to allow for the subsequent cloning of *rht*X into the unique *Xho*1 and *Pst*1 sites of pBBR1MCS-5. The primer sequences are shown in Figure 3.14.

Figure 3.14: Primers For The Amplification Of *rhtX*.

*Xho*1

RhtX-F1: 5' CTC GAG GCC GGG CAG ***TGG CA***G TTT TCG ATG C 3'

*Pst*1

RhtX-R1: 5' CTG CAG TCA TCG TGA TCT TGA AGG ACG CGC TTT C 3'

Restriction sites are underlined and indicated in blue. The ribosome-binding site is highlighted and indicated in bold italics.

Total genomic DNA was prepared from *S. meliloti* 2011 as described in Chapter 2 and used as the template DNA in the PCR reaction. Following optimisation of the PCR reaction (Table 3.7), a specific 1.3 Kb PCR fragment was obtained and cloned into the pCR2.1 vector generating pCR1.3 X/P. The 1.3 Kb fragment was restricted from pCR2.1 X/P as an *Xho*1/*Pst*I fragment and cloned into *Xho*1/*Pst*1 restricted pBBR1MCS-5 generating pPOC4.

Table 3.7: PCR Reaction Conditions For The Amplification Of *rhtX*

PCR Conditions	
Annealing Temp	69°C
Annealing Time	1 min
Extension Time	2.0 min

The plasmid pPOC4 was introduced into *S. meliloti* 2011*rhtX*43 by triparental mating and the phenotype of the transconjugant was analysed. The results are indicated in Table 3.6 and Figure 3.15.

Table 3.8: Analysis Of *S. meliloti* 2011*rhtX*43 Transconjugants.

S. meliloti	Plasmid	Halo On CAS Plate	Rhizobactin 1021 Utilisation
2011	-	++++	+
2011	pPOC3	++++	+
2011	pPOC4	++++	+
2011 *rhtX*43	-	++	-
2011 *rhtX*43	pPOC3	+++	+
2011 *rhtX*43	pPOC4	+	+

To determine if RhtX was involved in secretion of rhizobactin 1021, the phenotype of the transconjugant was analysed by the CAS plate assay. Analysis of the phenotype revealed that in contrast to pPOC3, the introduction of pPOC4 into *S. meliloti* 2011*rhtX*43 did not result in increased siderophore production as analysed by the CAS plate assay. The result indicated that RhtX was not involved in rhizobactin 1021 secretion.

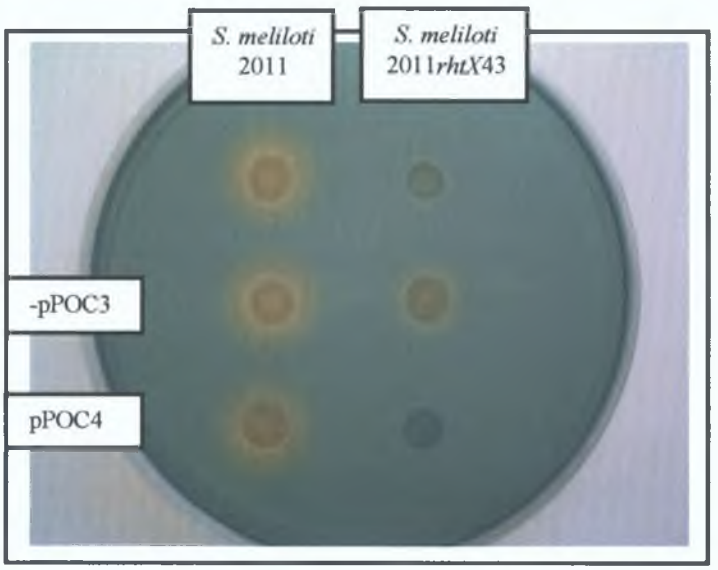

Figure 3.15: Analysis Of Siderophore Production By *S. meliloti* Transconjugants. *S. meliloti* pPOC3 and pPOC4 transconjugants were spotted on CAS plates and analysed as described in Chapter 2. The orange halo indicates siderophore production.

Analysis of the transconjugant by the siderophore utilisation bioassay indicated that the plasmid conferred upon the mutant the ability to utilise rhizobactin 1021 (Figure 3.16). The pPOC4 transconjugant did not exhibit growth throughout the plate, indicating that the wild type *S. meliloti* 2011 phenotype had not been restored. It was considered that the low level of siderophore production by *S. meliloti* 2011*rhtX*43 was

insufficient to allow it to overcome the conditions of iron limitation and to grow throughout the plate. The apparent reduction in siderophore production by the *S. meliloti* 2011*rhtX*43 pPOC4 transconjugant was possibly due to the ability of the transconjugant to utilise the produced siderophore thus preventing its extracellular accumulation. The siderophore utilisation phenotype observed was similar to the phenotype observed with the *S. meliloti* 2011*rhtX*43 pPOC3 transconjugant (Section 3.4). Previous analysis of the transconjugants by the siderophore utilisation bioassay had indicated that both cosmids conferred upon the mutant the ability to utilise rhizobactin 1021. However, the utilisation phenotypes conferred by both cosmids on *S. meliloti* 2011*rhtX*43 varied. The pPOC1 transconjugant showed a growth pattern that was similar to wild type *S. meliloti* 2011, with weak growth occurring throughout the plate. Analysis of the pPOC3 transconjugant revealed that growth only appeared to occur around the well containing rhizobactin 1021. As previously described, two putative RhrA binding sites had been identified in the rhizobactin 1021 regulon, in the *rhrA* and *rhtA* intergenic region, and also in the *Sma2335* and *rhtX* intergenic region. The cosmid pPOC1 had been shown by complementation and restriction analysis to encode both binding sites and RhrA. In contrast, pPOC3 was predicted to encode a putative RhrA binding site but the cosmid did not encode RhrA. As AraC type regulators are present in low abundance in the cell it was considered possible that pPOC3 was giving rise to a titration effect of RhrA.

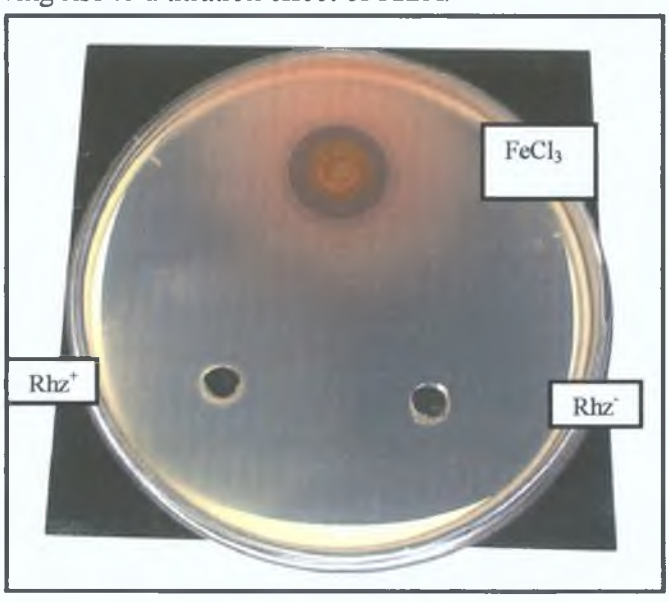

Figure 3.16: Rhizobactin 1021 Utilisation By *S. meliloti* 2011*rhtX*43 -pPOC4. Ferric chloride ($FeCl_3$) was used as a positive control. Concentrated culture supernatant containing rhizobactin 1021 (Rhz^+) was prepared as described in Chapter 2. A concentrated culture supernatant (Rhz^-) prepared from a rhizobactin 1021 biosynthesis mutant was used as a negative control.

3.11: Siderophore Production By *S. meliloti* 2011*rhtX*43

In order to explain the phenotype conferred by pPOC3 on *S. meliloti* 2011*rhtX*43, the effect of the transposon insertion in *rhtX* was examined in detail. As described previously, siderophore production by *S. meliloti* 2011*rhtX*43 was found to be severely diminished compared to wild type *S. meliloti* 2011. A putative RhrA binding site was identified upstream of *rhtX*. As *rhbABCDEF* had previously been shown to be positively regulated by RhrA, the identification of the putative binding site upstream of *rhtX* indicated that *rhtX* was part of the *rhbABCDEF* operon. Similarly, as no sequence resembling the putative RhrA binding site was identified in the region directly upstream of *rhbA*, it was considered unlikely RhrA was exerting its effect on *rhbABCDEF* transcription from this region.

Evidence from the literature indicated that promoter activity originating from Tn*5lac* had been detected in several rhizobial species (Wexler *et al*, 2001). It was considered that such promoter activity from the Tn*5lac* insertion in *S. meliloti* 2011*rhtX*43 would enable transcription of the *rhbABCDEF* operon and consequent biosynthesis of the siderophore. The cosmid pPOC3 had previously been shown to extend to one of two centrally located *Eco*R1 sites within *rhb*C. Analysis of the predicted biosynthesis pathway for rhizobactin 1021 (Lynch *et al.*, 2001) revealed that *rhbA* and *rhbB* were involved in the initial steps of the pathway, in the generation of 1,3 diaminopropane. It was hypothesised that the synthesis of 1,3 diaminopropane was a rate limiting step in the biosynthesis of rhizobactin 1021, and that the introduction of the extra copies of *rhbAB* on pPOC3 were sufficient to lead to an increase in siderophore production in *S. meliloti* 2011*rhtX*43.

In order to examine this hypothesis, it was decided to amplify *rhbAB* and to clone them onto the broad host range plasmid, pBBR1MCS-5 in order to express them under the control of the vector borne *lac* promoter. Two primers, RhbA-F and RhbB-R (Chapter 2) were designed to amplify *rhbAB* from *S. meliloti* 2011. The forward primer RhbA-F was designed to incorporate a unique *Apa*1 site into the PCR product. The forward primer was also designed to incorporate the ribosome-binding site of *rhbA* into the PCR product. The reverse primer, RhbB-R was designed to incorporate a unique *Bam*H1 site into the PCR product. The unique *Apa*1 and *Bam*H1 sites in the

PCR product were added to allow for the subsequent cloning of *rhbAB* into the unique *Apa*1 and *Bam*H1 sites of pBBR1MCS-5. The primer sequences are shown in Figure 3.17.

Figure 3.17: **Primers For The Amplification Of *rhbAB*.**

*Apa*1
RhbA-F: 5' GGG CCC GTG ATT GTA AAG AGT TAG ***ACC GA***G ATG 3'

*Bam*H1
RhbB-R: 5' GGA TCC TTA TGG GCG TGC ATG ATG GGT CTC CAG 3'

Restriction sites are underlined and indicated in blue. The ribosome-binding site is highlighted and indicated in bold italics.

Total genomic DNA was prepared from *S. meliloti* 2011 and used as the template DNA in the PCR reaction. Following optimisation of the PCR reaction (Table 3.9), a specific 2.9 Kb PCR fragment was obtained and cloned into the pCR2.1 vector generating pCR2.9 A/B. The 2.9 Kb fragment was restricted from pCR2.9 A/B as an *Apa*1/*Bam*HI fragment and cloned into *Apa*1/*Bam*H1 restricted pBBR1MCS-5 generating pPOC6.

Table 3.9: PCR Reaction Conditions For The Amplification Of *rhbAB*

PCR Conditions	
Annealing Temp	68°C
Annealing Time	1 min
Extension Time	3.5 min

The plasmid pPOC6 was introduced into *S. meliloti* 2011*rhtX*43 by triparental mating and the phenotype of the transconjugant was analysed. The results are shown in Table 3.10.

Table 3.10: Analysis Of *S. meliloti* 2011*rhtX*43 Transconjugants.

S. meliloti	Plasmid	Halo On CAS Plate
2011	-	++++
2011	pBBR1MCS-5	++++
2011	pPOC6	+++
2011 *rhtX*43	-	+
2011 *rhtX*43	pBBR1MCS-5	+
2011 *rhtX*43	pPOC6	++

Analysis of the transconjugants by the CAS plate assay indicated that there was an increase in siderophore production. The result indicated that the increase in siderophore production by the *S. meliloti* 2011*rhtX*43 pPOC3 transconjugant was due to an effect of RhbAB.

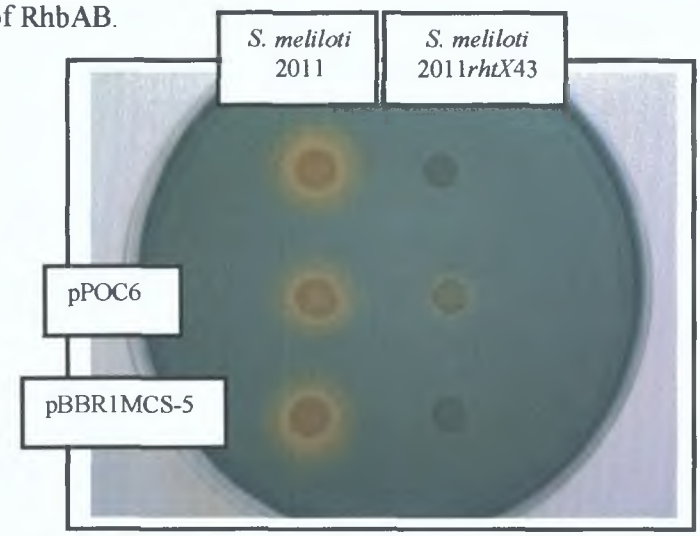

Figure 3.18: Siderophore Production By *S. meliloti* 2011*rhtX*43 Transconjugants. *S. meliloti* pPOC6 and pBBR1MCS-5 transconjugants were spotted on CAS plates and analysed as described in Chapter 2. The orange halo indicates siderophore production.

The phenotype of the *S. meliloti* 2011*rhtX*43 -pPOC6 transconjugant was not identical to that described for the pPOC3 transconjugant. It was considered possible that over-expression of the two proteins while under conditions of iron limitation may have affected siderophore production. A reduction in siderophore production for *S. meliloti* 2011 overexpressing *rhbAB* compared to *S. meliloti* 2011 suggested that this was likely. The *lac* promoter is usually de-repressed by the addition of the lactose analogue, IPTG to the medium. Analysis indicated that the *lac* promoter was not fully repressed in *S. meliloti*, even when the cells were grown in the absence of IPTG, and that the cells were therefore continually over-expressing RhbAB. The result indicated

however that the large halo affect conferred by pPOC3 on *S. meliloti* 2011*rhtX*43 was due to an effect of *rhbA* and *rhbB*. In order to determine where transcription of the rhizobactin 1021 biosynthesis operon was originating, it was decided to construct a polar mutation in *rhtX*. The construction of a polar mutation would confirm if *rhtX* constituted part of the *rhbABCDEF* operon as well as determining if there was a promoter in the *rhtX/rhbA* intergenic region. The polar mutation would also indicate if the Tn*5lac* insertion in *S. meliloti* 2011*rhtX*43 had promoter activity on *rhbABCDEF*.

3.12: The Mutagenesis Of *S. meliloti*

The era of genome sequencing had heralded an advent for the rapid targeted mutagenesis of microorganisms. The traditional method of laborious mutagenesis by transposon-based systems is gradually being replaced by site-specific mutagenesis by restriction site mobilisation elements or mutagenesis cassettes. The availability of genomic sequences has allowed the rapid targeted mutagenesis of genes of interest. A broad range of mutagenesis cassettes encoding different antibiotic resistances and reporter genes have been constructed allowing for various types of mutations to be constructed (Alexeyev *et al*, 1995; Becker *et al*, 1995).

Site-specific cassette mutagenesis is facilitated by the use of suicide vectors, which allow for selection of the insertion of the mutated fragment of interest into the chromosome by recombination. In *Rhizobium*, the suicide vectors are generally delivered by conjugation from *E. coli* using a *mob* based system. The transfer functions are provided *in trans* in the donor, resulting in the high frequency transfer of the suicide vector. The absence of a broad host range replication function on the plasmid results in a suicide effect and facilitates the selection of recombination events at a detectable frequency.

To determine the effects of specific genes on rhizobactin 1021 biosynthesis, regulation and utilisation, mutants were generated in various genes of interest. The suicide vector pJQ200ks (Quandt and Hynes, 1993) was used to introduce mutated fragments of interest into the genome of *S. meliloti*. The pJQ200ks vector has a number of features that facilitates the generation of cassette mutants. Firstly, the vector encodes gentamicin resistance, which is a suitable marker for selection in *Rhizobium*. Secondly, the multiple cloning site of pJQ200ks is extensive and allows for cloning of a range of DNA fragments. Thirdly, pJQ200ks encodes a *mob* (*oriT*) site, which facilitates the mobilisation of the plasmid into a strain of interest. Finally the *sacB* gene facilitates the isolation of mutants that have undergone a second recombination event eliminating the vector from the chromosome. A map of pJQ200ks is shown in Figure 3.19.

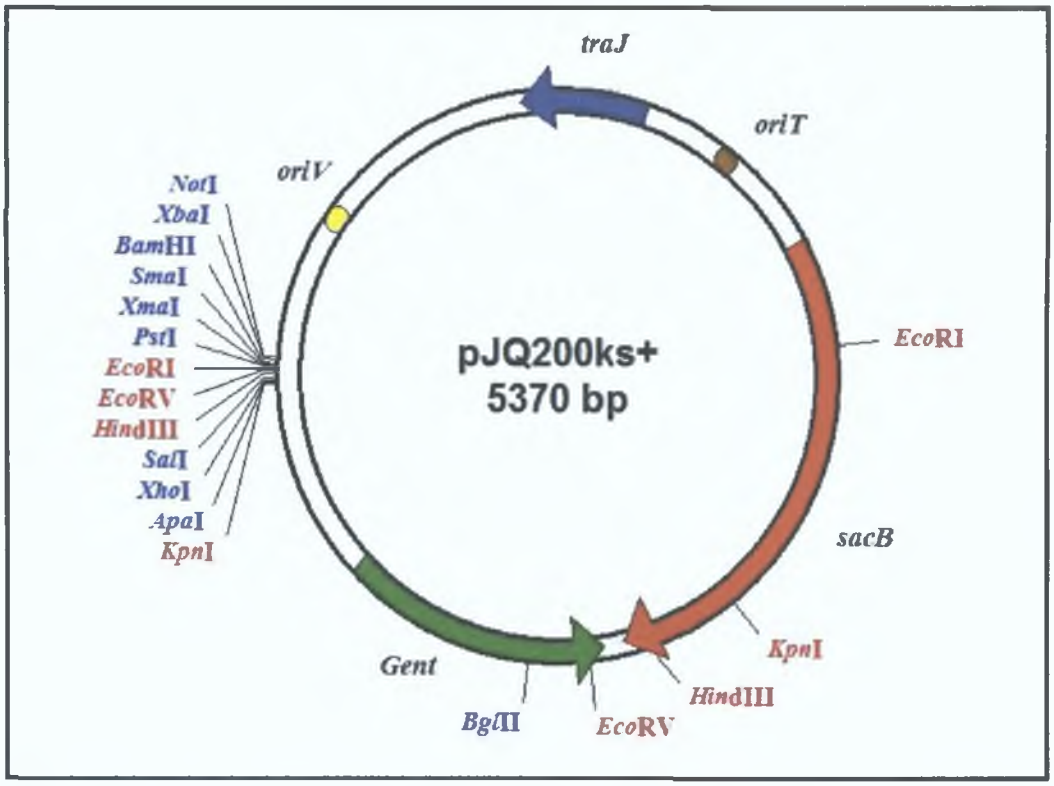

Figure 3.19: Map Of The Suicide Vector pJQ200ks. The gentamicin resistance gene (*Gent*), the *sacB* gene (*sacB*), the mobilisation site (*oriT*) and the origin of replication (*oriV*) are indicated.

The generation of cassette mutants is greatly facilitated by the use of PCR. However, PCR can result in Taq DNA polymerase generated point mutations that can potentially affect the interpretation of the mutant phenotype analysis. In general, for mutagenesis, approximately 2 Kb, 1 Kb on either side of the restriction site of interest, is amplified. The 1 Kb region provides homology to allow for efficient recombination of the mutated DNA fragment to occur. As it is not feasible to sequence each amplified 2 Kb fragment to ensure that no point mutations are present, where possible the fragment to be mutated should be cloned directly from a cosmid or plasmid source thereby avoiding the use of PCR.

The proceeding sections describe the construction of various cassette mutants of *S. meliloti* 2011 and their subsequent phenotypical analysis.

3.13: Generation Of A Streptomycin Resistant Strain Of *S. meliloti* 2011

As previously described, the suicide vector pJQ200ks encodes a *mob* site that allows for high efficiency mobilisation into the strain of interest. The vector is introduced into *S. meliloti* 2011 by triparental matings, and consequently, it is necessary to be able to counter select the *E. coli* donor. A rifampicin resistant strain of *S. meliloti* had previously been generated (Lynch *et al.*, 1999) to facilitate the counter selection of *E. coli* donors during triparental matings. Several problems were encountered with the use of rifampicin however. Rifampicin affects RNA synthesis by inhibiting the action of RNA polymerase. Spontaneous *E. coli* resistant rifampicin mutants occur at a low frequency, and the concentration of rifampicin used in the triparental mating consequently had to be elevated. Rifampicin however, does not readily dissolve at high concentrations, and there is therefore a limit to the amount of rifampicin that can be added to the media. Rifampicin is prepared in methanol, and as methanol is toxic to microbiological cultures, the amount of methanol added to the agar must be kept to a minimum. Rifampicin is also light sensitive and the red colour that it confers to the agar can obscure culture growth.

In order to overcome this problem, it was decided to generate a streptomycin resistant mutant of *S. meliloti* 2011. Streptomycin functions by inhibiting ribosomal function. In contrast to rifampicin, spontaneous streptomycin resistant mutants occur at a low level. Also, streptomycin readily dissolves in water and can be used at high concentrations.

S. meliloti 2011 is a spontaneous streptomycin resistant derivative of *S. meliloti* SU47. It was decided to increase the minimum inhibitory concentration of streptomycin of *S. meliloti* 2011 in order to select it during mutagenesis. *S. meliloti* 2011 was grown until early stationary phase and then plated on TY agar containing 500 μg/ml of streptomycin and incubated until single colonies developed. A single colony was then inoculated into TY broth, grown until early stationary phase and then plated on TY agar containing 1 mg/ml of streptomycin. A single colony was purified and used for the subsequent experiments using streptomycin as a selectable marker.

3.14: The Mutagenesis of *rhtX* Using An Antibiotic Resistance Cassette

Detailed sequence analysis of the *rhtX* gene sequence revealed the presence of a unique *Bam*H1 site within the gene into which an antibiotic resistance cassette could be inserted. Two primers, RhtX-F and RhtX-R (Chapter 2), were designed to amplify a 2.0 Kb region of the *S. meliloti* 2011 genome encoding *rhtX*, with the *Bam*H1 site centrally located. The forward primer and reverse primer, RhtX-F and RhtX-R were designed to incorporate unique *Bgl*II sites into the PCR product. The unique *Bgl*II sites in the PCR product were added to allow for the subsequent cloning of the 2.0 Kb fragment into the unique *Bam*H1 site of pJQ200ks (Section 3.12). As *Bgl*II and *Bam*H1 have compatible cohesive ends, the cloning of the 2.0 Kb *Bgl*II/*Bgl*II fragment into *Bam*H1 restricted pJQ200ks would result in the destruction of the vector borne *Bam*H1 site leaving only the unique *Bam*H1 site within *rhtX*.

Figure 3.20: **Primers For The Amplification Of A Region Encoding *rhtX*.**

*Bgl*II
RhtX-F: 5' AGA TCT GTT GCC GAA GCC CTG CGG GTT 3'

*Bgl*II
RhtX-R: 5' AGA TCT GGA AGG CGG AGG CGG AGA TGG C 3'

Restriction sites are underlined and indicated in blue.

Total genomic DNA was prepared from *S. meliloti* 2011 and used as the template DNA in the PCR reaction. Following optimisation of the PCR reaction (Table 3.11), a specific 2.0 Kb PCR fragment was obtained and cloned into the pCR2.1 vector generating pCR2.0 Bg/Bg. The 2.0 Kb fragment was restricted from pCR2.0 Bg/Bg as a *Bgl*II/*Bgl*II fragment and cloned into *Bam*H1 restricted pJQ200ks generating pOC2.0 Bg/Bg. As it was necessary to generate a polar mutation in *rhtX*, a plasmid harbouring a kanamycin cassette with well-characterised transcriptional terminators was obtained. The plasmid, pHP45-ΩKm (Fellay *et al*, 1987), was a kind gift from Dr. John Foster. The kanamycin cassette from pHP45-ΩKm was excised as a *Bam*H1 fragment and inserted into the unique *Bam*H1 site of pOC2.0 Bg/Bg generating pOC2.0ΩK Bg/Bg.

Table 3.11: PCR Reaction Conditions For The Amplification Of The Region Encoding *rhtX*

PCR Conditions	
Annealing Temp	71°C
Annealing Time	1 min
Extension Time	2.5 min

The plasmid pOC2.0ΩK Bg/Bg was introduced into *S. meliloti* 2011 by triparental mating and transconjugants were selected for on TY containing streptomycin and gentamicin. Second recombinants were selected by growing a single first recombinant without antibiotic selection in TY broth until early stationary phase had been reached and then by plating on TY agar containing 5% sucrose and kanamycin. Individual colonies were then screened for kanamycin resistance and gentamicin sensitivity. A potential mutant was identified in this way and selected for further analysis.

The genomic sequence in the region encoding *rhtX* was examined to identify restriction sites that were deemed suitable for the confirmation of the potential mutant by Southern blot analysis (Chapter 2). The kanamycin cassette was inserted into a *Bam*H1 site encoded within an 8.5 Kb *Eco*R1/*Eco*R1 fragment (Figure 3.21) as a *Bam*H1 fragment. Digestion of the mutant genomic DNA with *Eco*R1 and *Bam*H1 would generate three fragments as indicated in Figure 3.22. The plasmid pOC2.0ΩK Bg/Bg was labelled as described in Chapter 2 and used as a probe.

Figure 3.21: Analysis Of The Region Encoding *rhtX* In *S. meliloti*.

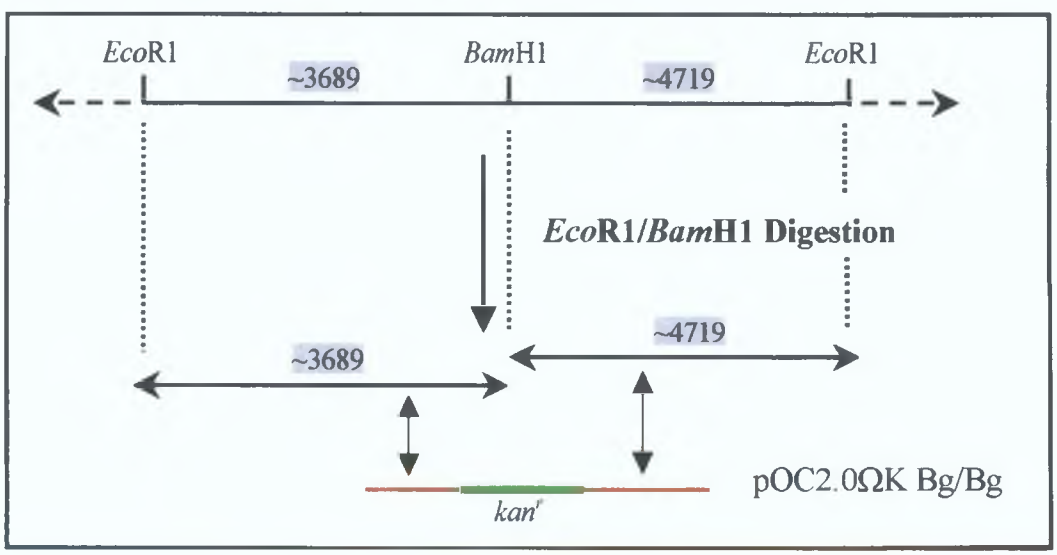

The predicted sizes of the digested fragments are highlighted in grey. The labelled probe is indicated in red, while the kanamycin cassette is highlighted in green. Regions of homology between the labelled probe and the digested fragments are indicated

Figure 3.22: Analysis Of The Region Encoding *rhtX* In A Potential Mutant

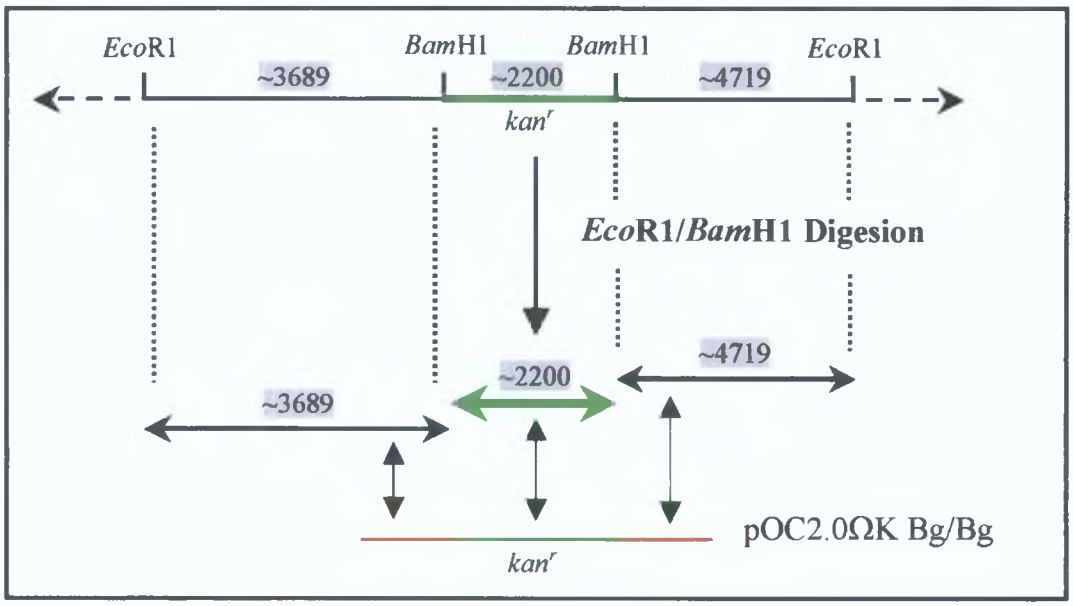

The predicted sizes of the digested fragments are highlighted in grey. The labelled probe is indicated in red, while the kanamycin cassette is highlighted in green. Regions of homology between the labelled probe and the digested fragments are indicated.

Genomic DNA was prepared from *S. meliloti* 2011 and the potential mutant (Chapter 2), restricted with *Eco*R1 and *Bam*H1, transferred to nitrocellulose and probed with labelled plasmid as described in Chapter 2. Examination of the hybridisation result appeared to indicate that the kanamycin cassette had integrated correctly into the chromosome. However analysis of the blot indicated that the hybridisation signal for the 4.7 Kb band was not as strong as for the other two bands (Figure 3.23).

Figure 3.23: Southern Blot Analysis Of *S. meliloti* 2011 And *S. meliloti* 2011*rhtX*1.

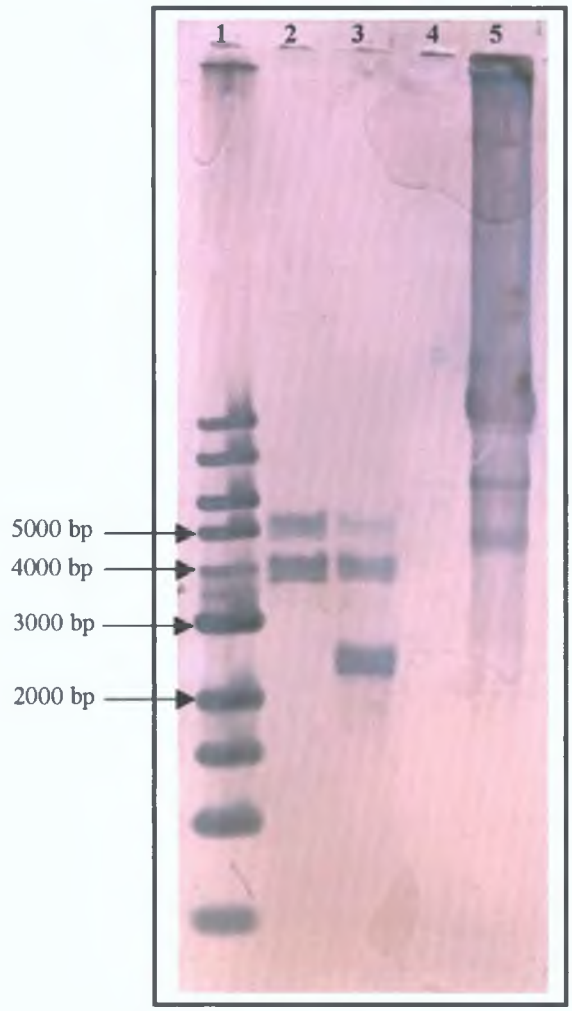

Legend

Lane 1: 1 Kb ladder (Section 2.28)

Lane 2: *S. meliloti* 2011 *Eco*R1/*Bam*H1

Lane 3: *S. meliloti* 2011*rhtX*1 *Eco*R1/*Bam*H1

Lane 5: pOC2.0ΩK Bg/Bg

To eliminate the possibility that the mutant was not correctly constructed and that the the 4.7 Kb band was the result of carry over, the blot was repeated using the plasmid pUC8.5 E/E as a probe. Probing using this plasmid should result in two hybridisation bands of 4.7 Kb and 3.6 Kb. Analysis of the blot indicated that the expected bands were present, indicating that the mutant was correctly constructed (Figure 3.24).

Figure 3.24: Southern Blot Analysis Of The Region Encoding *rhtX* In *S. meliloti* 2011 and *S. meliloti* 2011*rhtX*1.

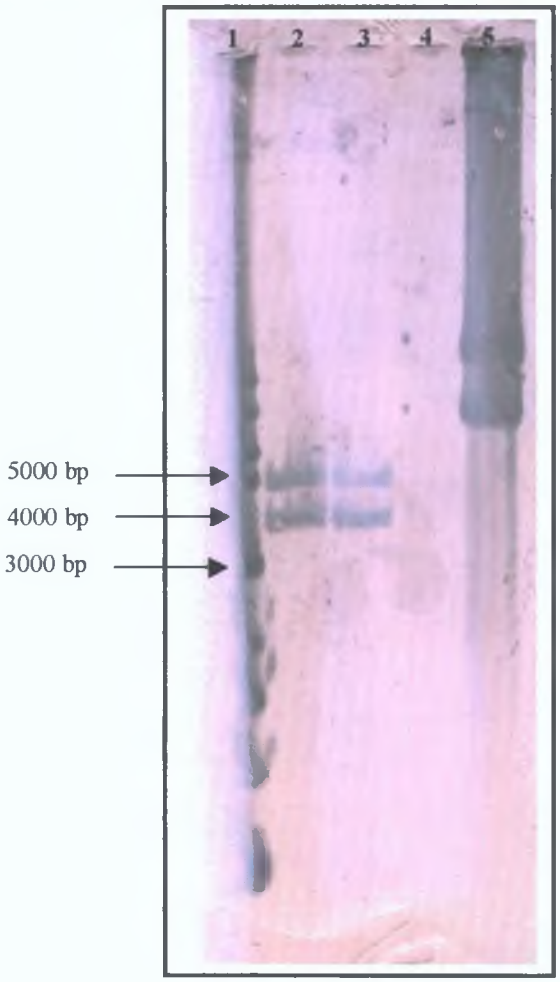

Legend

Lane 1: 1 Kb ladder (Section 2.28)

Lane 2: *S. meliloti* 2011 *Eco*R1/*Bam*H1

Lane 3: *S. meliloti* 2011*rhtX*1 *Eco*R1/*Bam*H1

Lane 5: pUC8.5 E/B

The mutant strain was named *S. meliloti* 2011*rhtX*1. The phenotypic characterisation of the *S. meliloti* 2011*rhtX*1 is described in Section 3.17-3.20.

3.15: Construction Of pOCAPA-K For Use In The Mutagenesis Of Sma2335

Cassette mutagenesis is a powerful tool for the elucidation of gene function. Cassette mutagenesis allows for the targeted mutagenesis of genes of interest. Cassette mutagenesis is however restricted, unlike transposon mutagenesis, by the availability of suitable restriction sites for the insertion of the cassette. In small genes, it can be difficult to identify a restriction site suitable for the insertion of a cassette. Sma2335, located upstream of *rhtX*, is predicted to be a small gene of 204 bp. Sma2335 encodes a limited number of restriction sites suitable for the insertion of a mutagenesis cassette. Analysis of the gene revealed the presence of a unique *Apa*1 site located close to the predicted translational start site that was deemed suitable for the insertion of a mutagenesis cassette.

The plasmid pUC4K (Vieira And Messing, 1982) encodes a kanamycin cassette that is bounded by five commonly used restriction enzymes, *Eco*R1, *Bam*H1, *Sal*1, *Hinc*II and *Pst*1. The presence of these sites enable the cassette to be cloned into similar restriction sites, or sites that are cleaved by restriction enzymes that produce compatible cohesive ends to the enzymes bounding the cassette. Cloning of the cassette however is limited to the sites bounding it. In order to overcome this problem and to increase the usefulness of the cassette, it was decided to amplify the cassette and to incorporate a restriction site of interest into the cassette, enabling it to be cloned into a wider variety of restriction sites.

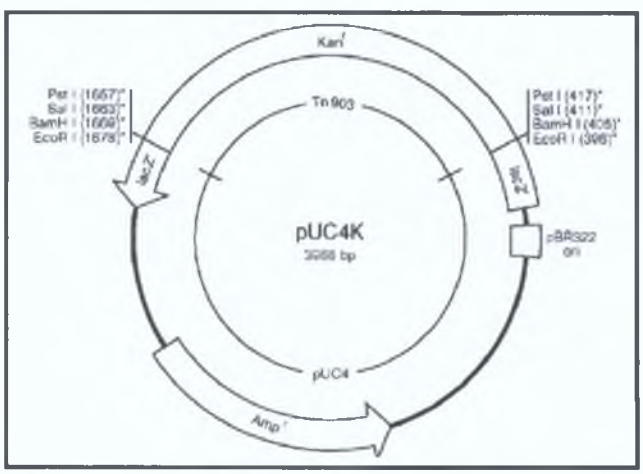

Figure 3.25: Map Of The pUC4K Plasmid Carrying The Kanamycin Cassette. The kanamycin cassette (Kan^r), bounded by *Eco*R1, *Bam*H1, *Sal*1 and *Pst*1 restriction sites is indicated.

In order to mutate Sma2335, it was decided to amplify the kanamycin cassette from pUC4K as an *Apa*1 restriction fragment and to insert it into the unique *Apa*1 site of the gene. Two primers were designed for the amplification of the region encoding the kanamycin cassette of pUC4K (Figure 3.26). By substituting the *Apa*1 site on the primers for a site of interest, the cassette could be adapted to make it suitable for cloning into a greater range of restriction sites.

Figure 3.26: Primers For The Amplification Of A Region Encoding The Kanamycin Cassette Of pUC4K.

*Apa*1
Kan-F: 5' GGG CCC GAC GTT GTA AAA CGA CGG CCA GTG 3'

*Apa*1
Kan-R: 5' GGG CCC GGA AAC AGC TAT GAC CAT GAT TAC G 3'

Restriction sites are underlined and indicated in blue.

The plasmid pUC4K was used as a template in the PCR reaction. Following optimisation of the reaction (Table 3.12) a 1.3 Kb PCR product was obtained.

Table 3.12: PCR Reaction Conditions For The Amplification Of The Region Encoding The Kanamycin Cassette Of pUC4K

PCR Conditions	
Annealing Temp	65°C
Annealing Time	30 sec
Extension Time	2.0 min

A ligation was set up with the pCR2.1 vector, but several attempts to isolate the required clone failed. In several cases, it was found that the pUC4K template DNA had been transformed from the ligation mixture. The plasmid pUC4K, similarly to the pCR2.1 vector, encodes both kanamycin and ampicillin resistance. As the amplified cassette was to be cloned in the pCR2.1 vector, it was decided that it would be preferable if it were possible to counter select the pUC4K plasmid in the subsequent transformation

In order to be able to counter select the pUC4K template DNA, it was decided to delete the ampicillin resistance of pUC4K. Restriction analysis of the pUC4K plasmid enabled the identification of three *Dra*1 sites located within the ampicillin resistance gene. The region between the *Dra*1 sites was deleted and the subsequent vector was called pOC4K. *E. coli* INVαF' harbouring pOC4K was confirmed to be kanamycin resistant and ampicillin sensitive.

The plasmid, pOC4K, was used as the template in the PCR reaction. A PCR reaction was performed as previously described (Table 3.12). Again, several attempts to isolate the required clone failed. Analysis indicated that a small non-specific PCR product was being amplified, possibly by non-specific annealing of the primers. The annealing temperature of the reaction was increased to 68°C, in order to increase the specificity of binding. The increase in temperature led to a decrease in the yield of the 1.3 Kb PCR product, but the PCR product appeared to be specific. A plasmid containing the required 1.3 Kb *Apa*1 fragment was isolated and termed pOCAPA-K. Restriction analysis of pOCAPA-K indicated that one of the primers had bound non-specifically. To ensure that the cassette still encoded kanamycin resistance, the cassette was restricted from pOCAPA-K as an *Apa*1 fragment and cloned into the unique *Apa*1 site of pJQ200ks. The resulting plasmid was kanamycin resistant indicating that the cassette was still functional and suitable for use in mutagenesis.

3.16: The Mutagenesis Of Sma2335

Sequence analysis of the Sma2335 gene sequence revealed the presence of a unique *Apa*1 site within the gene into which an antibiotic resistance cassette could be inserted. Two primers, Orf2APA-F and Orf2APA-R (Chapter 2), were designed to amplify a 2.0 Kb region of the *S. meliloti* 2011 genome encoding Sma2335, with the *Apa*1 site centrally located. The forward primer Orf2APA-F was designed so as to incorporate a unique *Not*1 site into the PCR product. The reverse primer, Orf2APA-R was designed to incorporate a unique *Xma*1 site into the PCR product. The unique *Not*1 and *Xma*1 sites in the PCR product were added to allow for the subsequent directional cloning of the 2.0 Kb fragment into *Psp*OM1/*Xma*1 restricted pJQ200ks (Section 3.12). *Psp*OM1 is an isoschizomer of *Apa*1. As *Psp*OM1 and *Not*1 have compatible cohesive ends, the cloning of the 2.0 Kb *Not*1/*Xma*1 fragment into *Psp*OM1/*Xma*1 restricted pJQ200ks would result in the destruction of the vector borne *Psp*OM1, and consequently the *Apa*1 site, leaving only the unique *Apa*1 site within Sma2335.

Figure 3.27: **Primers For The Amplification Of A Region Encoding Sma2335.**

*Not*1
Orf2APA-F: 5' GCG GCC GCC GAT GGT CTG CTT CAC CCC CTC 3'

*Xma*1
Orf2APA-R: 5' CCC GGG CAT CCA GGC ATT CGG CCG CCG G 3'

Restriction sites are underlined and indicated in blue.

Total genomic DNA was prepared from *S. meliloti* 2011 and used as the template DNA in the PCR reaction. Following optimisation of the PCR reaction (Table 3.13), a specific 2.0 Kb PCR fragment was obtained and cloned into the pCR2.1 vector generating pCR2.0 N/Xm. The 2.0 Kb fragment was restricted from pCR2.0 N/Xm as a *Not*1/*Xma*1 fragment and cloned directionally into *Psp*OM1/*Xma*1 restricted pJQ200ks generating pOC2.0 N/Xm. The kanamycin cassette from pOCAPA-K was excised as an *Apa*1 fragment and inserted into the unique *Apa*1 site of pOC2.0 N/Xm generating pOC2.0K N/Xm.

Table 3.13: PCR Reaction Conditions For The Amplification Of The Region Encoding Sma2335.

PCR Conditions	
Annealing Temp	70°C
Annealing Time	1 min
Extension Time	2.5 min

The plasmid pOC2.0K N/Xm was introduced into *S. meliloti* 2011 by triparental mating and transconjugants were selected on TY containing streptomycin and gentamicin. Second recombinants were selected by growing a single first recombinant without antibiotic selection in TY broth until early stationary phase had been reached and then by plating on TY agar containing 5% sucrose and kanamycin. Individual colonies were then screened for kanamycin resistance and gentamicin sensitivity. A potential mutant was identified in this way and selected for further analysis.

The genomic sequence in the region encoding Sma2335 was examined to identify restriction sites that were deemed suitable for the confirmation of the potential mutant by Southern blot analysis (Chapter 2). The kanamycin cassette from pOCAPA-K was inserted into an *Apa*1 site encoded within a larger 6.1 Kb *Apa*1/*Eco*R1 fragment (Figure 3.28) as an *Apa*1 fragment. Digestion of the mutant genomic DNA with *Apa*1 and *Eco*R1 would generate three fragments as indicated in Figure 3.29. The plasmid pOC2.0K N/Xm was labelled as described in Chapter 2 and used as a probe.

Figure 3.28: Analysis Of The Region Encoding Sma2335 In *S. meliloti*.

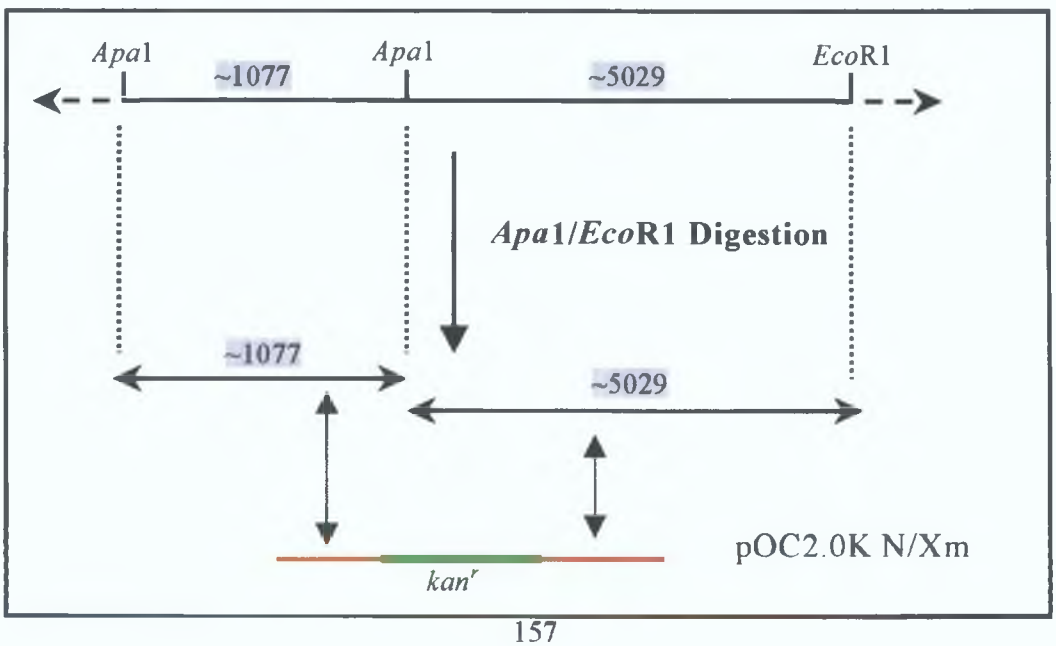

The predicted sizes of the digested fragments are highlighted in grey. The labelled probe is indicated in red, while the kanamycin cassette is highlighted in green. Regions of homology between the labelled probe and the digested fragments are indicated

Figure 3.29: Analysis Of The Region Encoding Sma2335 In A Potential Mutant

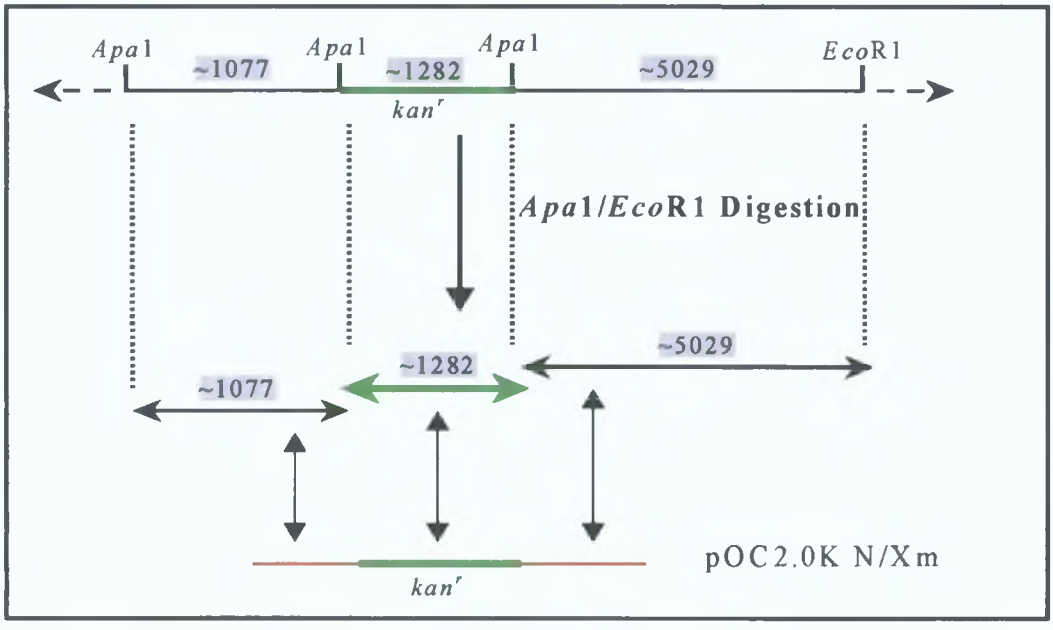

The predicted sizes of the digested fragments are highlighted in grey. The labelled probe is indicated in red, while the kanamycin cassette is highlighted in green. Regions of homology between the labelled probe and the digested fragments are indicated.

Genomic DNA was prepared from *S. meliloti* 2011 and the potential mutant (Chapter 2), restricted with *Apa*1 and *Eco*R1, transferred to nitrocellulose and probed with labelled plasmid as described in Chapter 2. Examination of the hybridisation result indicated that the kanamycin cassette had correctly integrated into the chromosome of *S. meliloti* (Figure 3.30).

Figure 3.30: Southern Blot Analysis Of *S. meliloti* 2011 And *S. meliloti* 2011Sma2335km

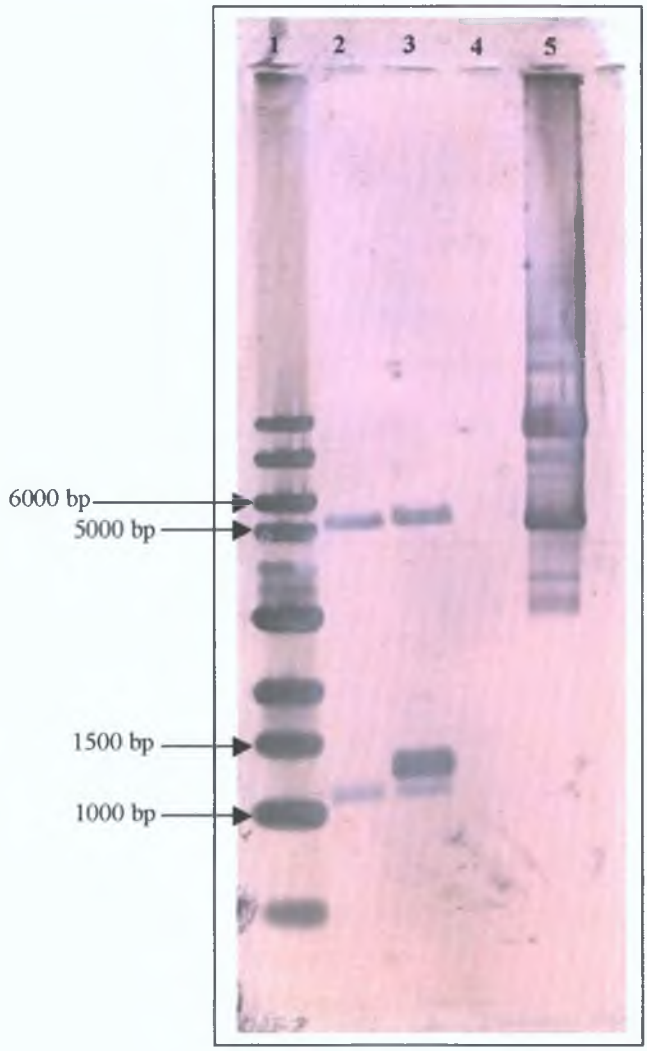

Legend

Lane 1: 1 Kb ladder (Section 2.28)

Lane 2: *S. meliloti* 2011 *Apa*1/*Eco*R1

Lane 3: *S. meliloti* 2011Sma2335km *Apa*1/*Eco*R1

Lane 5: pOC 2.0K N/Xm

The mutant strain was named *S. meliloti* 2011Sma2335km. The phenotypic characterisation of the *S. meliloti* 2011Sma2335km is described in Section 3.17-3.19.

3.17: Analysis Of *S. meliloti* 2011 Growth Under Low Iron Conditions

S. meliloti 2011 produces the siderophore rhizobactin 1021 under low iron conditions. *S. meliloti* 2011 mutants defective in biosynthesis or utilisation of the siderophore would be expected to show restricted growth under low iron conditions compared to wild type *S. meliloti* 2011. The chelator 2,2'dipyridyl displays an affinity for iron, and at high concentrations effectively removes available iron from the growth medium. The ability of the *S. meliloti* 2011 mutants to grow on TY agar under low iron conditions was evaluated. *S. meliloti* 2011 cultures were grown until early stationary phase and a range of dilutions were then plated on TY agar with increasing concentrations of 2,2'dipyridyl. Only plates where single colonies were clearly discernable were used in the analysis of the growth phenotype under low iron conditions. The results are shown in Table 3.14.

Table 3.14: Growth Of *S. meliloti* 2011 Mutants Under Low Iron Conditions.

S. meliloti	**Genotype**	**Concentration of 2,2'dipyridyl (μM)**			
		0	**100**	**200**	**300**
2011		+++	+++	+++	++
2011*rhtX*1	*rhtX*	+++	++	+	-
2011Sma2335km	Sma2335	+++	+++	+++	++

+ = Colony formation after 72 hour incubation

Analysis of the result indicated that *S. meliloti* 2011 showed strong growth at all concentrations of 2,2'dipyridyl tested. Growth at a concentration of 300 μM was slightly restricted. Analysis of *S. meliloti* 2011*rhtX*1 indicated that growth at a concentration of 200 μM 2,2'dipyridyl was severely restricted. Growth appeared to be completely inhibited at a concentration of 300 μM 2,2'dirpyridyl. Analysis of *S. meliloti* 2011Sma2335km indicated that growth in both cases was comparable to wild type *S. meliloti* 2011.

3.18: Analysis Of Siderophore Production By *S. meliloti* 2011 Mutants

The ability of *S. meliloti* 2011 mutants to produce siderophore was analysed by the chrome azurol S (CAS) plate assay. The distinctive orange halo around the colony can be used to indicate the effect of the mutation on siderophore production.

S. meliloti 2011 mutants were spotted onto CAS plates along with wild type culture as previously described, (Chapter 2). The size and intensity of the halos produced are shown in Table 3.15.

Table 3.15: Analysis Of Siderophore Production By *S. meliloti*

S. meliloti	**Genotype**	**Halo**
2011	Wild type	++
2011*rhtX*1	*rhtX*	-
2011Sma2335km	*Sma2335*	++

++ = Wild type halo, - = No halo

Analysis indicated that *S. meliloti* 2011*rhtX*1 was not producing any siderophore. The result indicated that the omega cassette element in *rhtX* was having a polar effect on the downstream biosynthesis genes. This indicated that there was no promoter in the *rhtX/rhbA* intergenic region and the *rhtX* was part of the *rhbABCDEF* operon. Similarly the result also indicated that the low level transcript of *rhbABCDEF* in *S. meliloti* 2011*rhtX*43 was probably due to promoter activity from Tn*5lac*. Analysis of *S. meliloti* 2011Sma2335km indicated that the mutant was unaffected in siderophore production as determined by the CAS plate assay.

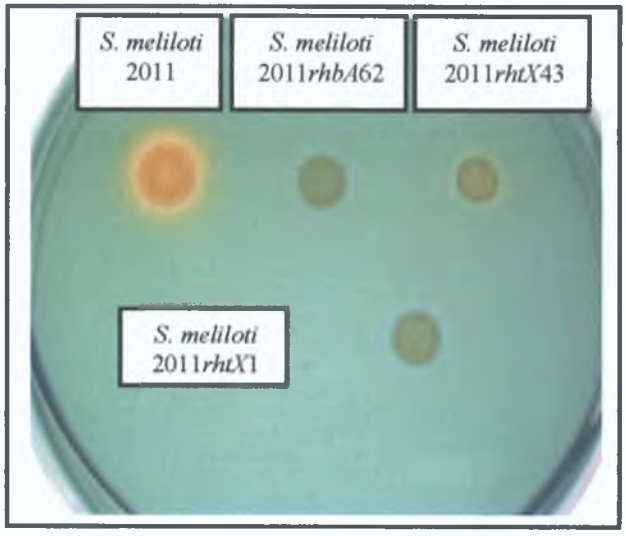

Figure 3.31: Analysis Of Siderophore Production by *S. meliloti* 2011*rhtX*1. *S. meliloti* 2011 mutants were spotted on CAS plates and analysed as described in Chapter 2. The orange halo indicates siderophore production.

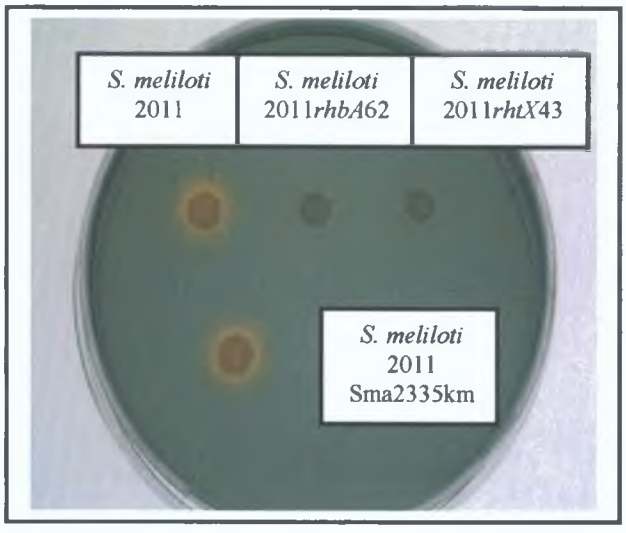

Figure 3.32: Analysis Of Siderophore Production by *S. meliloti* 2011 Sma2335km. *S. meliloti* 2011 mutants were spotted on CAS plates and analysed as described in Chapter 2. The orange halo indicates siderophore production.

3.19: Analysis Of Siderophore Utilisation By *S. meliloti* 2011 Mutants

The ability of the *S. meliloti* 2011 mutants to utilise rhizobactin 1021 was analysed by iron nutrition bioassays. *S. meliloti* 2011 defective in siderophore biosynthesis but unaffected in siderophore utilisation show a characteristic halo of growth around a well containing the siderophore of interest.

Iron nutrition bioassays were performed on the *S. meliloti* mutants as previously described (Chapter 2). As previously described in Section 3.17, growth of *S. meliloti* 2011 was found to be inhibited at a concentration of 300 μM 2,2'dipyridyl. The iron nutrition bioassays were therefore performed using a concentration of 300 μM 2,2'dipyridyl. Three wells were cut out of the test plates, which were seeded with the various strains, and the test solutions were added to individual wells. As a positive control, 50 μl of $FeCl_3$ was added to one of the wells. Rhizobactin 1021 was prepared from *S. meliloti* 2011 grown under iron deplete conditions as previously described (Chapter 2), and was added to one of the wells. As a negative control, *S. meliloti* 2011*rhbA*62, a siderophore biosynthesis mutant, was grown under iron deplete conditions, and the culture supernatant was prepared in a similar manner to that described for rhizobactin 1021 containing supernatants. A sample of this solution was added to the final well. The results of the iron nutrition bioassays are indicated in Table 3.16 below.

Table 3.16: Analysis Of Siderophore Utilisation In *S. meliloti*

S. meliloti	**Genotype**	**Rhizobactin 1021 Utilisation**
2011	Wild type	+
2011*rhtX*1	*rhtX*	-
2011Sma2335km	*Sma2335*	+

S. meliloti 2011 exhibited a pattern of growth throughout the plate. This strain was capable of producing and utilising rhizobactin 1021 and was therefore able to overcome the conditions of iron limitation. Stronger growth of *S. meliloti* 2011 was observed around the well containing rhizobactin. Examination of results indicated that *S. meliloti* 2011*rhtX*1 was not growing throughout the plate, which was as expected as

it does not synthesise rhizobactin 1021. Furthermore, it did not produce a halo of growth around the well containing rhizobactin 1021. The result indicated that *S. meliloti* 2011*rhtX*1 was defective in rhizobactin 1021 utilisation. The results indicated that the *S. meliloti* 2011Sma2335km was unaffected in rhizobactin 1021 utilisation. The mutant exhibited a pattern of growth throughout the plate, which was characteristic of wild type *S. meliloti* 2011.

3.20: Effects Of Rhizobactin 1021 Regulon Mutants On Symbiotic Nitrogen Fixation

S. meliloti 2011 is the endosymbiont of *Medicago sativa* (alfalfa). There is a high iron requirement in the symbiosis due to the presence of many iron-containing enzymes (Chapter 1). Although mutants in rhizobactin 1021 biosynthesis had previously been reported to be affected in symbiotic nitrogen fixation (Chapter 1), subsequent analysis indicated that rhizobactin 1021 biosynthesis and utilisation mutants were unaffected in symbiotic nitrogen fixation (Lynch *et al.*, 2001)(Chapter 1). The effect on symbiotic nitrogen fixation by further rhizobactin 1021 regulon mutants was examined. The ability of the rhizobactin 1021 utilisation mutant *S. meliloti* 2011*rhtX*43 to nodulate and fix nitrogen was examined. Previous analysis had indicated that *rhtX* constituted part of the *rhbABCDEF* operon. The *rhbABCDEF* genes had previously been shown to be positively regulated by RhrA (Lynch *et al*, 2001). The ability of *S. meliloti* 2011*rhrA*26 to nodulate and fix nitrogen was examined Table 3.17.

Table 3.17: Effect Of Rhizobactin 1021 Regulon Mutants On Symbiotic Nitrogen Fixation

Strain	Phenotype
S. meliloti 2011	Nod^+ Fix^+
S. meliloti 2011*rhtX*43	Nod^+ Fix^+
S. meliloti 2011*rhrA*26	Nod^+ Fix^+

Nod = Nodulation Fix = Nitrogen Fixation

Analysis of the results indicated that all the mutants tested formed effective nodules and were capable of symbiotic nitrogen fixation. This indicated that the rhizobactin 1021 regulon mutants were unaffected in symbiotic nitrogen fixation. The results indicated that the rhizobactin 1021 regulon was inessential for symbiotic nitrogen fixation. Analysis of *S. meliloti* 2011*rhtX*1 on plants nodulation indicated that the mutant induced nodule formation that was comparable that induced by *S. meliloti* 2011. The nodules displayed a red hue indicating the presence on leghaemoglobin. The plants were comparable in growth to those nodulated by *S. meliloti* 2011 indicating an effective symbiosis.

3.21: Analysis Of Rhizobactin 1021 Utilisation In A pSyma Cured Strain

The rhizobactin 1021 regulon is encoded on the pSyma megaplamid of *S. meliloti* 1021 (Lynch *et al*, 2001). As previously described, the cosmid pPOC1 was found to complement all mutations isolated in the rhizobactin 1021 regulon. The introduction of the cosmid into *S. meliloti* 102F34, a strain that does not produce or utilise rhizobactin 1021 conferred upon this bacterium the ability to produce and utilise the said siderophore. Analysis of the region upstream of *rhtX* and downstream of *rhbG* indicated that there were no proteins encoded in these regions that displayed homology to proteins involved in iron transport. The absence of a clearly identifiable periplasmic binding protein and an ATPase, common components of inner membrane transport systems raised the possibility that these proteins might be encoded on a different region of the genome.

The pSyma megaplasmid is predicted to encode two putative iron acquisition systems (Barnett *et al*, 2001). In order to investigate the possibility that these systems or other uncharacterised proteins were involved in rhizobactin 1021 acquisition, it was decided to analyse rhizobactin 1021 utilisation in the pSyma-cured strain, *S. meliloti* Rm818. The cosmid pPOC1 was introduced into *S. meliloti* Rm818 by triparental mating and the ability of the transconjugant to utilise rhizobactin 1021 was analysed by the iron nutrition bioassays. The results are described in Table 3.18.

Table 3.18: Analysis Of Rhizobactin 1021 Utilisation In *S. meliloti* Rm818.

S. meliloti	**Genotype**	**Rhizobactin 1021 Utilisation**
2011	-	+
Rm818	pSyma cured	-
Rm818 +pPOC1	pSyma cured, pPOC1	+

The result indicated that the introduction of pPOC1 into *S. meliloti* Rm818 conferred upon the bacterium the ability to utilise rhizobactin 1021. The result indicated that the region of pSyma encoded in pPOC1 was sufficient to allow for rhizobactin 1021 utilisation and that no other proteins encoded by the pSyma plasmid was involved in rhizobactin 1021 utilisation.

The ability of the *S. meliloti* Rm818 pPOC1 transconjugant to synthesise and secrete rhizobactin 1021 was analysed by the CAS plate assay.

3.19: Analysis Of Rhizobactin 1021 Production By *S. meliloti* Rm818.

S. meliloti	Genotype	Halo
2011	-	++
Rm818	pSyma cured	-
2011 +pPOC1	pPOC1	++++++
Rm818 +pPOC1	pSyma cured, +pPOC1	+++++

The result indicated that siderophore production by the *S. meliloti* Rm818 +pPOC1 transconjugant was slightly reduced in comparison to a *S. meliloti* 2011 +pPOC1 transconjugant. This is possibly due to a growth defect of the *S. meliloti* Rm818 strain due to the pSyma deletion. Also, *S. meliloti* 2011 would encode an extra copy of the rhizobactin 1021 regulon in comparison to *S. meliloti* Rm818. The result indicated that excluding the region of pSyma encoded by pPOC1, no other proteins encoded by pSyma are involved in the biosynthesis or secretion of rhizobactin 1021.

3.22: Re-Constitution Of A Rhizobactin 1021 Utilisation System In *S. meliloti* 102F34

As previously described, *S. meliloti* 102F34 does not produce or utilise the siderophore rhizobactin 1021. Analysis of *S. meliloti* 102F34 transconjugants that had received pPOC1 indicated that the cosmid was sufficient to allow rhizobactin 1021 synthesis and utilisation in *S. meliloti* 102F34 and in the *S. meliloti* 2011 pSyma cured strain *S. meliloti* Rm818. Sequence analysis of the region encoded by pPOC1 indicated that with the exception of RhtA and RhtX, no other proteins encoded by pPOC1 were likely to be involved in rhizobactin 1021 utilisation. In order to determine if RhtA and RhtX were sufficient to allow the utilisation of rhizobactin 1021, it was decided to reconstitute the rhizobactin 1021 utilisation system in *S. meliloti* 102F34.

As previously described, the plasmid pPOC4 had been constructed to allow the expression of *rhtX* from an independent vector encoded *lac* promoter. Due to the lack of suitable broad host range expression vectors, it was decided to construct a plasmid that would allow for expression of *rhtA* from its own promoter. It was decided to use the vector pSUP104 for the construction of the required expression plasmid. The plasmid pSUP104 is a broad host range, low copy number plasmid (Priefer *et al*, 1985). The plasmid is mobilisable, although the *tra* functions have to be provided *in trans*. The vector encodes tetracycline resistance, which is a suitable antibiotic for selection in *S. meliloti*. The vector, however, is not particularly suitable for cloning due to its relatively large size and the absence of suitable restriction sites.

The expression of *rhtA* had previously been shown to be positively regulated by the AraC type regulator RhrA (Lynch *et al.*, 2001). In order to express *rhtA*, it was necessary therefore to also clone *rhrA* onto the plasmid. It was decided to directionally clone the region encoding *rhtA* and *rhrA* into the unique *Eco*R1 and *Xba*1 sites of pSUP104.

As the region encoding *rhr*A and *rht*A was considered too large for a single PCR amplification, it was decided to construct the plasmid encoding *rhrA* and *rhtA* using a two-stage PCR amplification process. Primers were designed to amplify *rhtA* and a portion of the promoter. The primer RhtA-F1 was designed to incorporate a unique

*Eco*R1 site to the PCR product. The reverse primer, RhtA-R1 was designed to incorporate a unique *Xba*1 site to the PCR product. The primers are shown in Figure 3.33.

Figure 3.33: Primers used for the amplification of a region encoding RhtA.

***Eco*R1**
RhtA-F1: 5' GAA TCC CCT GTT GAC GTT CGC ATG C 3'

***Xba*1**
RhtA-R1: 5' TCT AGA TTA AAA AAC CTT TCT CAG CGA GAC CGC G 3'

Total genomic DNA was prepared from *S. meliloti* 2011 and used as the template DNA in the PCR reaction. Following optimisation of the PCR reaction (Table 3.20), a specific 2.4 Kb PCR fragment was obtained and cloned into the pCR2.1 vector generating pCR2.4 E/Xb. The 2.4 Kb fragment was restricted from pCR2.4 E/Xb as an *Eco*R1/*Xba*1 fragment and cloned directionally into *Eco*R1/*Xba*1 restricted pSUP104 generating pSUP2.4 E/Xb.

Table 3.20: PCR Reaction Conditions For The Amplification Of The Region Encoding *rhtA*.

PCR Conditions	
Annealing Temp	55°C
Annealing Time	30 sec
Extension Time	3.5 min

Primers were designed to amplify the region encoding *rhrA* to the chromosomally encoded unique *Xho*1 site within *rhtA*. The primer RhrA-F was designed to incorporate a unique *Eco*R1 site to the PCR product. The reverse primer RhtA-R was designed to incorporate the chromosomal *Xho*1 site into the amplified PCR product. The primers are shown in Figure 3.34.

Figure 3.34: Primers used for the amplification of a region encoding *rhrA*.

*Eco*R1

RhrA-F: 5' GAA TTC TCA AGC GGC GGC TGC CAG CC 3'

*Xho*1

RhtA-R: 5' CTC GAG CGC GGA ATC GCC CAC G 3'

Total genomic DNA was prepared from *S. meliloti* 2011 and used as the template DNA in the PCR reaction. Following optimisation of the PCR reaction (Table 3.21), a specific 2.9 Kb PCR product was obtained and cloned into the pCR2.1 vector generating pCR2.9 E/X. The 2.9 Kb fragment was restricted from pCR2.9 E/X as an *Eco*R1/*Xho*1 fragment and cloned directionally into *Eco*R1/*Xho*1 restricted pSUP2.4 E/Xb generating pPOC5.

Table 3.21: PCR Reaction Conditions For The Amplification Of The Region Encoding *rhrA*.

PCR Conditions	
Annealing Temp	60°C
Annealing Time	30 sec
Extension Time	3.5 min

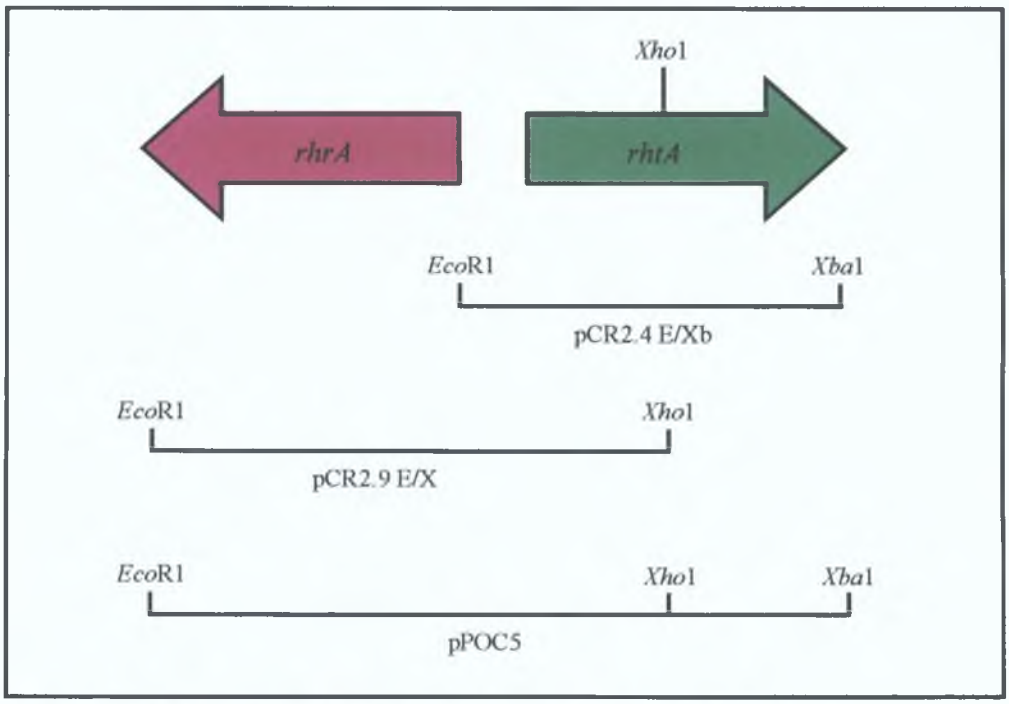

Figure 3.35: Plasmids Used In The Construction Of pPOC5.

The plasmid pPOC5 was introduced into *S. meliloti* 2011*rhrA*26 and *S. meliloti* 2011*rhtA*45 by triparental matings and the ability of the plasmid to complement the mutations was examined. The introduction of the plasmid into *S. meliloti* 2011*rhrA*26 and *S. meliloti* 2011*rhtA*45 conferred a phenotype similar to wild type *S. meliloti* 2011 on the mutants.

The plasmids pPOC5 and pPOC4 were introduced into *S. meliloti* 102F34 by triparental matings and selected using tetracycline and gentamicin resistance respectively. The ability of the transconjugants to utilise rhizobactin 1021 was analysed by the iron nutrition bioassay. The results are as indicated in Table 3.22.

Table 3.22: Analysis Of Rhizobactin 1021 Utilisation By *S. meliloti* 102F34.

S. meliloti	**Plasmid**	**Genotype**	**Rhizobactin 1021 Utilisaion**
102F34	-		-
102F34	pPOC5	$rhrA^+$, $rhtA^+$	-
102F34	pPOC4	$rhtX^+$	-
102F34	pPOC4/pPOC5	$rhrA^+$, $rhtA^+$, $rhtX^+$	+

Analysis of the result indicated that a *S. meliloti* 102F34 transconjugant expressing *rhtA* or *rhtX* separately did not confer upon the bacterium the ability to utilise rhizobactin 1021. However, when both genes were expressed, the ability to utilise rhizobactin 1021 was conferred upon the transconjugant (Figure 3.36). The result indicated that *rhtA* and *rhtX* were sufficient to allow for the utilisation of rhizobactin 1021 in *S. meliloti* 102F34, and that no other proteins encoded by either pPOC1 or pSyma were involved in rhizobactin 1021 utilisation.

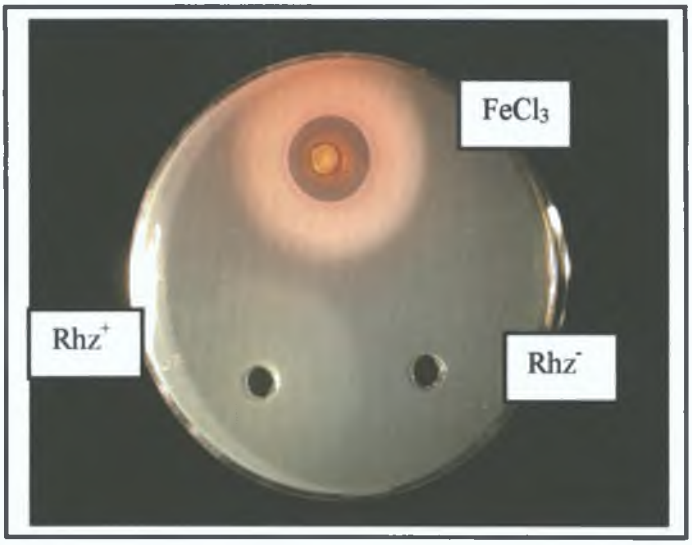

Figure 3.36: Rhizobactin 1021 Utilisation By *S. meliloti* 102F34 carrying pPOC4 and pPOC5. Ferric chloride ($FeCl_3$) was used as a positive control. Concentrated culture supernatant containing rhizobactin 1021 (Rhz^+) was prepared as described in Chapter 2. A concentrated culture supernatant (Rhz^-) prepared from a rhizobactin 1021 biosynthesis mutant was used as a negative control.

3.23: Siderophore Utilisation In *E. coli* and *S. meliloti*

Aerobactin is a citrate hydroxymate siderophore that is structurally similar to rhizobactin 1021. Utilisation of aerobactin in *E. coli* is mediated by the outer membrane receptor IutA and the inner membrane iron transport system encoded by the FhuCDB system (Chapter 1). Analysis of rhizobactin 1021 utilisation in *E. coli* indicated that utilisation of rhizobactin 1021 and of the structurally similar siderophore schizokinen, was also mediated by the outer membrane receptor, IutA (Lynch PhD Thesis, 1999). *E. coli* was analysed in order to determine if rhizobactin 1021 was transported via the inner membrane FhuCDB system. An *E. coli* strain, *E. coli* RK4375 was obtained from the *E. coli* Genetic Stock Centre, which was described as *fhuB478*::Tn*10* (Kadner *et al*, 1980). This mutation was constructed prior to the discovery of the *fhuC* and *fhuD* genes within the same operon, and it was therefore necessary to determine the precise gene within the *fhu* operon into which the Tn*10* had inserted.

In order to determine into which gene the Tn*10* had inserted, it was decided to complement the *fhuCDB* genes and to analyse the restoration of ferrichrome utilisation. Primers were designed that would allow the amplication of the *fhuCDB* genes in various combinations. It was decided to express the *fhu* genes from the pCR2.1 vector using the vector borne *lac* promoter. The forward primers were designed to include the ribosome binding sites for the individual genes. The primers are shown in Figure 3.37.

Figure 3.37: Primers For The Amplification Of The *fhuCDB* Genes.

FhuC-F: 5' GAA TTC GTG CCC ATT TC***A CAA G***TT GGC TGT TAT GC 3'

FhuD-F: 5' GAA TTC CTG CAC CT***G TGA G***TT TTG TTT ATT GAT GAG 3'

FhuD-R: 5' GGA TCC TCA CGC TTT ACC TCC GAT GGC GTT ATC C 3'

FhuB-R: 5' GGA TCC TTA ACG GCT CTG CTT TCT CAA CCA ATA GAT AA 3'

The ribosome-binding sites are highlighted and indicated in bold italics.

Total genomic DNA was prepared from *E. coli* H1443 as described in Chapter 2 and used as the template DNA in the PCR reaction. Following optimisation of the PCR reaction (Table 3.23-3.25), the amplified products, *fhuCDB*, *fhuCD* and *fhuDB* were cloned into the pCR2.1 vector generating pPC 3.5, pPC 2.9 and pPC 2.0 respectively.

Table 3.23: PCR Reaction Conditions For The Amplification Of *fhuCDB*

PCR Conditions	
Annealing Temp	70°C
Annealing Time	1 min
Extension Time	4.5 min

Table 3.24: PCR Reaction Conditions For The Amplification Of *fhuCD*

PCR Conditions	
Annealing Temp	70°C
Annealing Time	1 min
Extension Time	2.5 min

Table 3.25: PCR Reaction Conditions For The Amplification Of *fhuDB*

PCR Conditions	
Annealing Temp	70°C
Annealing Time	1 min
Extension Time	3.5 min

All three plasmids were transformed into *E. coli* RK4375 and the ability of the transformant to utilise ferrichrome was analysed.

Table 3.26: Analysis Of Ferrichrome Utilisation By *E. coli*

E. coli	Plasmid	Genotype	Ferrichrome Utilisation
RK4375	-		-
RK4375	pPC2.0	*fhuB478*::Tn*10*, *fhuDB*$^+$	-
RK4375	pPC2.9	*fhuB478*::Tn*10*, *fhuCD*$^+$	-
RK4375	pPC3.5	*fhuB478*::Tn*10*, *fhuCDB*$^+$	+

Examination of the result indicated that the strain carrying pPC3.5, but not those carrying pPC2.0 or pPC2.9 could complement the Tn*10* mutation. The result indicated that the transposon insertion in *E. coli* RK4375 was in *fhuC* and that it was having a polar effect on the downstream *fhuD* and *fhuB* genes.

A plasmid encoding IutA, pEN7, was introduced into *E. coli* RK4375 by transformation. The ability to utilise the citrate hydroxymate siderophores aerobactin and schizokinen and the hydroxymate siderophore, ferrichrome was examined (Table 3.27).

3.27: Analysis Of Siderophore Utilisation By *E. coli*.

E. coli Strain	Plasmid	Genotype	Rhizobactin 1021 Utilisaton	Schizokinen Utilisation	Aerobactin Utilisation	Ferrichrome Utilisation
H1443	-	*iutA*$^-$ *fhuC*$^+$	-	-	-	+
H1443	pEN7	*iutA*$^+$*fhuC*$^+$	+	+	+	+
RK4375	-	*iutA*$^-$ *fhuC*$^-$	-	-	-	-
RK4375	pEN7	*iutA*$^+$ *fhuC*$^-$	-	-	-	-

Analysis of the result confirmed that IutA was capable of mediating the utilisation of rhizobactin 1021 and schizokinen across the outer membrane. As expected, the transport of ferrichrome was shown to be independent of IutA across the outer membrane. Analysis of *E. coli* RK4375 indicated that the mutant was defective in the utilisation of all three citrate hydroxymate siderophores tested as well as in the utilisation of the hydroxymate siderophore ferrichrome. The introduction of the plasmid pEN7, which encodes the outer membrane receptor IutA, did not confer upon the mutant the ability to utilise any of the siderophores tested. The result indicated that similarly to aerobactin and ferrichrome, the utilisation of rhizobactin 1021 and schizokinen was dependent on the *fhu* system of *E. coli*.

Previous results had indicated that RhtX and RhtA were sufficient to allow the utilisation of rhizobactin 1021 in *S. meliloti* 102F34, a strain that does not produce or utilise rhizobactin 1021. The plasmid pPOC4 was introduced into *E. coli* RK4375 by transformation and the ability of the mutant to utilise the siderophores of interest was analysed (Table 3.28).

Table 3.28: Analysis Of Sideophore Utilisation By *E. coli*.

E. coli Strain	Plasmid	Genotype	Rhizobactin 1021 Utilisaton	Schizokinen Utilisation	Aerobactin Utilisation	Ferrichrome Utilisation
RK4375	-	*iutA⁻ fhuC⁻*	-	-	-	-
RK4375	pEN7	*iutA⁺ fhuC⁻*	-	-	-	-
RK4375	pPOC4	*fhuC⁻ rhtX⁺*	-	-	-	-
RK4375	pEN7 pPOC4	*iutA⁺ fhuC⁻ rhtX⁺*	+	+	-	-

Analysis of the results indicated that RhtX was capable of partially complementing FhuCDB in siderophore utilisation. Rhizobactin 1021 and the structurally similar siderophore schizokinen were both utilised in a strain expressing *iutA* and *rhtX*. However the same strain was incapable of transporting the citrate hydroxymate siderophore aerobactin. Further analysis indicated that the same strain was also incapable of utilising ferrichrome as an iron source. The results indicated that while RhtX could partially complement FhuCDB function, RhtX appeared to be a dedicated protein for the utilisation of rhizobactin 1021 and structurally similar siderophores.

Previous analysis of RhtX using the PSORT program (Nakai and Kanehisa, 1991) had indicated that RhtX was located in the inner membrane. The result of the siderophore utilisation bioassays indicated that RhtX appeared to be able to partially complement FhuC, an inner membrane associated protein, FhuD, a periplasmic binding protein, and FhuB, an integral inner membrane protein.

The ability of *S. meliloti* 102F34 expressing *rhtA* and *rhtX* to utilise various siderophores was analysed by iron nutrition bioassays. The results are described in Table 3.29.

3.29: Analysis Of Siderophore Utilisation By *S. meliloti* 102F34.

S. meliloti Strain	Plasmid	Genotype	Rhizobactin 1021 Utilisation	Schizokinen Utilisation	Aerobactin Utilisation	Ferrichrome Utilisation
102F34	-		-	-	-	+
102F34	pPOC4	*rhtX*	-	-	-	+
102F34	pPOC5	*rhrA rhtA*	-	-	-	+
102F34	pPOC4/ pPOC5	*rhtX rhrA rhtA*	+	+	-	+

Analysis of the results indicated that similarly to *E. coli*, transport of rhizobactin 1021 and schizokinen in a *S. meliloti* 102F34 transconjugant expressing *rhtA* and *rhtX*, was occurring via a common mechanism. Analysis also indicated that the expression of *rhtA* and *rhtX* did not confer upon the bacterium the ability to utilise aerobactin. In contrast to wild-type *E. coli*, the utilisation of ferrichrome appeared to occur via a mechanism that was independent of rhizobactin 1021 utilisation.

It had previously been shown that *S. meliloti* 2011 was not capable of utilising the citrate hydroxymate siderophore aerobactin (Lynch PhD Thesis, 1999). The ability of *S. meliloti* 2011 mutants to utilise various siderophores was analysed by iron nutrition bioassays. The abilities of the mutants *S. meliloti* 2011*rhtX*43, *S. meliloti* 2011*rhtA*45 and *S. meliloti* 2011*rhrA*26 to utilise schizokinen, aerobactin and ferrichrome was analysed. The indicator strain, *S. meliloti* 2011*rhbA*62 was used to analyse the utilisation of the various siderophores. The results are indicated in Table 3.30.

3.30: Analysis Of Siderophore Utilisation By *S. meliloti* 2011.

***S. meliloti* Strain**	**Rhizobactin 1021 Utilisation**	**Schizokinen Utilisation**	**Aerobactin Utilisation**	**Ferrichrome Utilisation**
2011*rhbA*62	+	+	-	+
2011*rhtX*43	-	-	-	+
2011*rhtA*45	-	-	-	+
2011*rhrA*26	-	-	-	+

Analysis of the results indicated that schizokinen was transported via RhtA and RhtX. The ability of *S. meliloti* to utilise aerobactin was examined and it was found that the bacterium was incapable of utilising the siderophore. As the outer membrane receptors for rhizobactin 1021 and aerobactin, RhtA and IutA respectively, display significant homology to each other, it was considered likely that the failure of *S. meliloti* 2011 to utilise aerobactin was due to the limited activity of RhtX. Ferrichrome transport was analysed, and it was found that ferrichrome was utilised in a manner independent of rhizobactin 1021 utilisation. Analysis of the *S. meliloti* 1021 genome sequence indicated that while there were two putative FhuA type proteins, FhuA1 and FhuA2, encoded in the genome, there were no significant homologues to the FhuCDB system present. Analysis of the region directly downstream of FhuA2

revealed the presence of a putative inner membrane iron transport system, encoded by *smc01658*, *smc01659* and possibly *smc01660*. The result indicated that ferrichrome transport at the inner membrane in *S. meliloti* 2011 was occurring via an alternative system to the FhuCDB system of *E. coli*.

3.24: *In silico* Analysis Of The *P. aeruginosa* Genome Sequence Encoding Pyochelin Utilisation

P. aeruginosa is an gram negative opportunistic human pathogen. As mentioned previously, *P. aeruginosa* produces two known siderophores, the complex peptidic siderophore pyoverdine and the salicylic acid based siderophore, pyochelin (Chapter 1). The cognate receptors for pyoverdine and pyochelin, FpvA and FptA respectively, which are located in the outer membrane, have been identified and characterised (Poole *et al.*, 1993; Ankenbauer *et al.*, 1992). The *P. aeruginosa* genome is predicted to encode a plethora of ferric siderophore receptors. However, despite the presence of these genes, there is a striking lack of clearly identifiable periplasmic and cytoplasmic membrane siderophore transport systems. To date, no proteins involved in siderophore mediated iron transport post the outer membrane have been experimentally identified in *P. aeruginosa*.

As previously described (Chapter 1), pyochelin is a salicylic acid based siderophore synthesised by *P. aeruginosa*. The outer membrane receptor for pyochelin, FptA, has been shown to be positively regulated by the AraC type regulator PchR. A putative ABC transport system, encoded by *pchH* and *pchI* (PA4223 and PA4222 respectively) was shown to be located in a region directly upstream of FptA (Reimann *et al.*, 2000). The PchHI system showed homology to the YptPQ system of *Y. pestis*, which has been shown to mediate yersiniabactin transport (Fetherston *et al*, 1999). However, mutants in the PchHI ABC transport system were unaffected in pyochelin utilisation (Reimann *et al.*, 2000)

Sequence analysis of the RhtX protein sequence by the BLASTP program (Altschul *et al*, 1997) lead to the identification of a homologue, PA4218, encoded within the *P. aeruginosa* genome sequence. *In silico* analysis indicated that PA4218 was encoded in a region directly downstream from *fptA*. Two other genes, PA4219 and PA4220, that had previously been described (Ankenbauer and Quan, 1994), were encoded in the region between *fptA* and PA4218 (Figure 3.38). The function of these proteins has not yet been determined.

Figure 3.38: Analysis Of The Pyochelin Regulon Of *P. aeruginosa*.

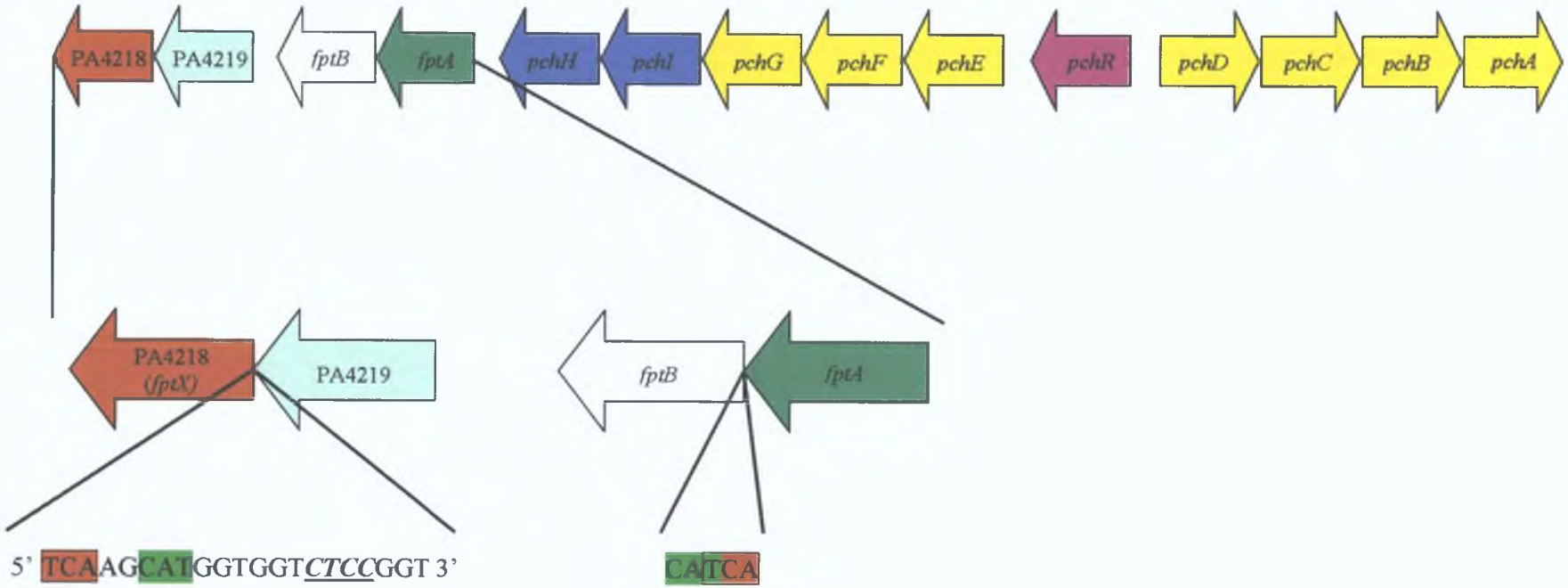

The genes known to be and predicted to be part of the pyochelin regulon are shown. The genes PA4218 and PA4219 and *fptA* and *fptB* appear to be translationally coupled. The overlapping regions are illustrated. The translational start site is indicated in green, while the translational stop codon is boxed and indicated in red. The predicted ribosome binding site for PA4218 is indicated in bold italics underlined.

3.25: *In silico analysis of PA4218*

PA4218 is located at position 4722857-4721613 on the *P. aeruginosa* chromosome. A putative ribosome binding site, GGAG, was identified upstream of the predicted translational start site for PA4218. The protein predicted to be encoded by PA4218 is 414 amino acids in length with a predicted molecular weight of 43.1 kDa and a pI of 9.43. The amino acid sequence of PA4218 is shown below in Figure 3.39.

Figure 3.39: Amino Acid Sequence Of PA4218.

MLELYRHRRLVITLALLYLSQGIPIGLAMDALPTLLRQDGAPLQALAFLPLVGLPWVV
KFLWAPWVDNHWSRRLGRRRSWILPMQCMVLACLLGLATLGLGVASAGWAVGLLALAS
LASATQDIATDGMAAEHFSGELLAKVNAVQIAGVMIGFFGGGAGSLILAGHFGQRTAF
LVMACVPLASLCCVLALGRGDPHELPPAPAAKASLLRFLRRPLAPSLLALALLSAMTA
VSGFGLSKLYLSDAGWALQDIGRLGMSGGLVTVFLGCGGGAWLVRRIGLWRGFALGVV
LAGCSALLWYLQAGRWLALSEGLAWTCVLIGSLATGITSVAILTAAMRFAGQGGQAGT
DVTAVQSTRDLGEMLASSFLVSLTAQIGYAGGFLTGSALAVLALLLALRLQAGEGRGE
WKGRAEEA

The amino acid sequence of PA4218 was compared against the NCBI database of protein sequences using the BLASTP program (Altschul *et al*, 1997). Sequence analysis of the PA4218 amino acid sequence indicated that the protein showed sequence homology to a family of proteins of unknown function. The most significant matches to PA4218 using the BLASTP program and their associated predicted biochemical data are listed in Table 3.31.

Table 3.31: Proteins Displaying Significant Homology To PA4218.

Protein	Homologue	Molecular Mass (kDa)	Accession	Identity (%)*
Rrub1580	*R. rubrum*	43.19	ZP_00014565	72 (84)
Rrub1561	*R rubrum*	47.25	ZP_00014546	35 (50)
RhtX	*S. meliloti* 1021	45.56	NP_436503	27 (42)
All4025	Nostoc sp. PCC 7120	43.73	NP_488065	25 (45)

*Identities (%) were calculated using the Genedoc program. Similarities are indicated in brackets.

The MultAlin (Corpet, 1988) and Genedoc programs were used to perform a global sequence alignment of PA4218 and *R. rubrum* Rrub1580, *R. rubrum* Rrub1561, *S. meliloti* 1021 RhtX and Nostoc sp. PCC7120 All4025. (Figure 3.40)

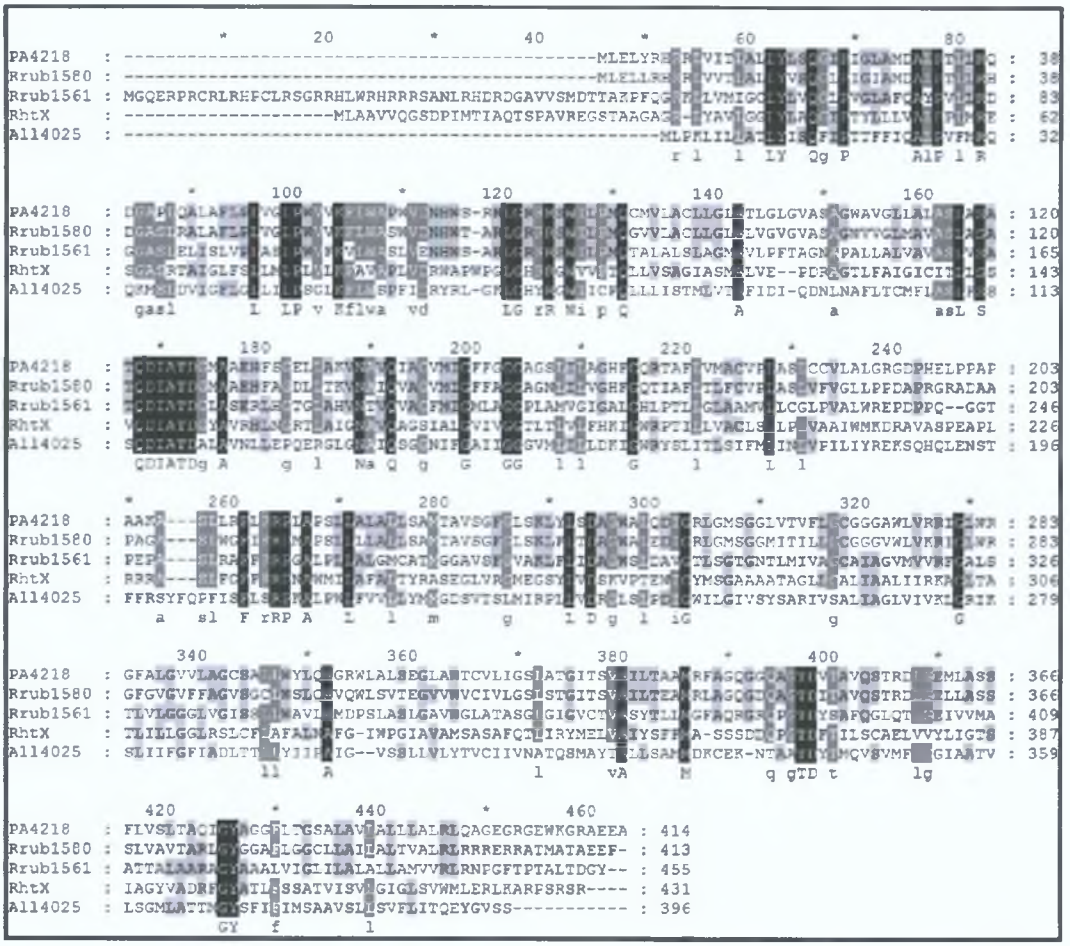

Figure 3.40: Multiple sequence alignment of PA4218; with *R. rubrum* Rrub1580, *R. rubrum* Rrub1561, *S. meliloti* 1021 RhtX and Nostoc sp. PCC 7120 All4025. Black indicates 100% conservation, dark grey indicates 80% conservation and light grey indicates 60% conservation.

The amino acid sequence of PA4218 was analysed using the PSORT program (Nakai and Kanehisa, 1991). Sequence analysis indicated that the protein was predicted to be located in the inner membrane.

3.26: *In silico analyis of PA4219*

PA4219 is located at position 4724034-4722850 on the *P. aeruginosa* chromosome. A putative ribosome binding site, GGAG, was identified upstream of the predicted translational start site for PA4219. The protein predicted to be encoded by PA4219 is 394 amino acids in length with a predicted molecular weight of 42.2 kDa and a pI of 11.31. The amino acid sequence of PA4219 is shown below in Figure 3.41.

Figure 3.41: Amino Acid Sequence Of PA4219.

MPALDLLLNLHKSLFVGFPGRVLVSLFGVSLLLLCLAGVLLHSRRWRDLRRWRRDRGL
RLALFDLHGLIGIWGLPWLLLFGFTGALSGLGALGTLLLAPVAYPQEPNRVFVELMGP
PPPAAEGRPLASRIDLDRLLAGDAVRAPGFVAQRLSLSHAGDVAGSVEIAGIRRGLPS
TANFERHRYRLADGTLLGERSSAQRGFWLRAFIAVQPLHFAQYQWLGPGWSAALRGLH
LAMGLGACLLCASGLYLWLQRRASAPDARVRLLQRLSQGFCAGLVAAAALLLLGLQLA
PSELLAGPWPGRLFLVLWAAAGLAALLLPGDWPLARGLLGVAGLACLAAAVAHLAPWL
MRGRLPALGPDLTLILCGALLIRHAWMQARAAAPPAHPRVTGDHHA

The amino acid sequence of PA4219 was compared against the NCBI database of protein sequences using the BLASTP program (Altschul *et al*, 1997). Sequence analysis of the PA4219 amino acid sequence revealed a significant degree of sequence identity to a protein of unknown function from *R. rubrum*. The most significant match to PA4219 using the BLASTP program and its associated predicted biochemical data is listed in Table 3.32.

Table 3.32: Proteins Displaying Significant Homology To PA4219.

Protein	Homologue	Molecular Mass (kDa)	Accession	Identities (%)
Rrub1581	*R. rubrum*	53.31	ZP_00014566	40 (52)

*Identities (%) were calculated using the Genedoc program. Similarities are indicated in brackets.

The MultAlin (Corpet, 1988) and Genedoc programs were used to perform a global sequence alignment of PA4219 and *R. rubrum* Rrub1581 (Figure 3.42).

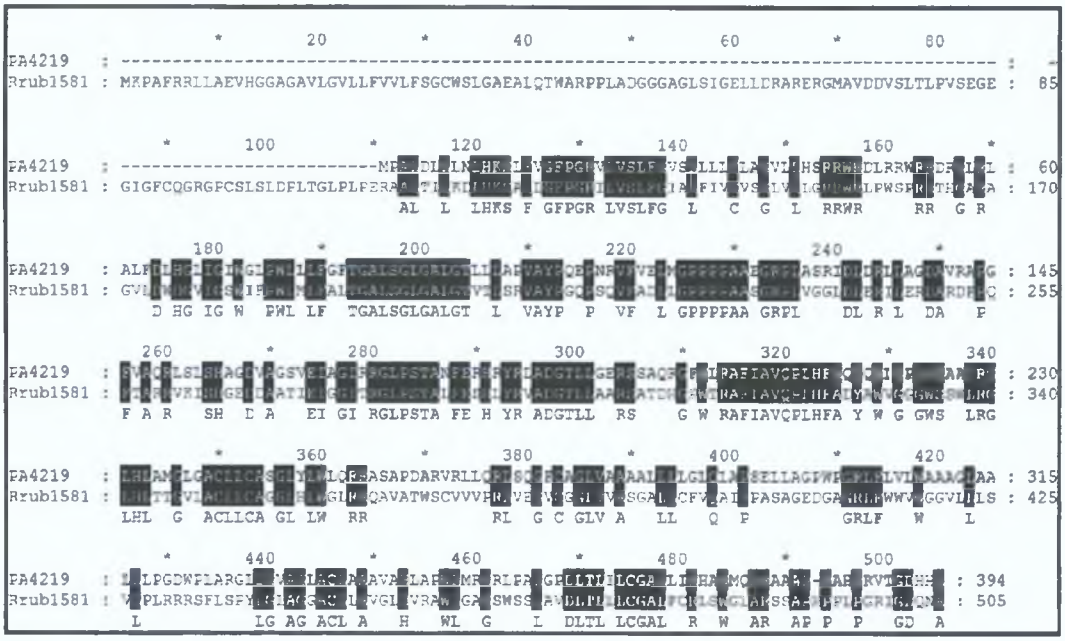

Figure 3.42: Multiple sequence alignment of PA4219; with *R. rubrum* Rrub1581. Black indicates 100% conservation.

The amino acid sequence of PA4219 was compared against a database of protein families in order to identify potential domains using the Pfam program (Chapter 2). Two domains of unknown function were identified within the protein sequence. The domains are indicated in Figure 3.43.

Figure 3.43: Identification Of Domains Within PA4219.

Legend

- Pfam-A Duf337
- Pfam-B 36635

The Pfam-A Duf337 motif is found in uncharacterised iron regulated membrane proteins. The function of the motif is not known. The function of the Pfam-B 36635 family is also unknown, but every member of this family is associated with the Pfam-A Duf337 domain.

The amino acid sequence of PA4219 was analysed using the PSORT program (Nakai and Kanehisa, 1991). Sequence analysis indicated that the protein was predicted to be located in the inner membrane.

3.27: *In silico analysis of fptB*

fptB is located at position 4724638-4724357 on the *P. aeruginosa* chromosome. A putative ribosome binding site, GGCG, was identified upstream of the predicted translational start codon. The protein predicted to be encoded by *fptB* is 93 amino acids in length with a predicted molecular weight of 9.56 kDa and a pI of 11.27. The amino acid sequence of FptB is shown below in Figure 3.44.

Figure 3.44: Amino Acid Sequence Of FptB.

MPRQSGFGWAWRVPLALAGSLAAATASGYLLTRGLPLDDPLERLYAGLFGALGVGLLL
LVGGLLARGPGNFAWRLGGSLLVLGLALWLLAGRG

The amino acid sequence of FptB was compared against the NCBI database of protein sequences using the BLASTP program (Altschul *et al*, 1997). Analysis of FptB indicated that the protein did not show any significant homology to any known protein. The amino acid sequence of FptB was subsequently compared against the NCBI database of protein sequences using the PSI-BLAST program (Altschul *et al*, 1997). Analysis of the FptB amino acid sequence revealed a degree of sequence identity to a protein of unknown function from *R. rubrum*. The most significant match to FptB using the PSI-BLAST program and its associated predicted biochemical data is listed in Table 3.33.

Table 3.33: Proteins Displaying Significant Homology To FptB.

Protein	Homologue	Molecular Mass (kDa)	Accession	Identities (%)
Rrub1582	*R. rubrum*	11.53	ZP_00014567	44 (54)

*Identities (%) were calculated using the Genedoc program. Similarities are indicated in brackets.

The MultAlin (Corpet, 1988) and Genedoc programs were used to perform a global sequence alignment of FptB and *R. rubrum* Rrub1582 (Figure 3.45).

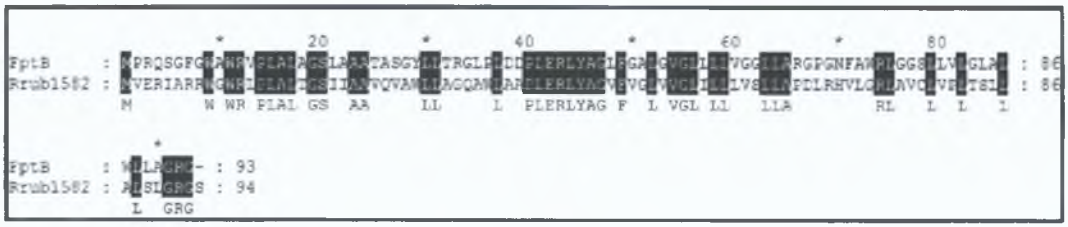

Figure 3.45: Multiple sequence alignment of FptB; with *R. rubrum* Rrub1582. Black indicates 100% conservation.

The amino acid sequence of FptB was analysed using the PSORT program (Nakai and Kanehisa, 1991). Sequence analysis indicated that the protein was predicted to be located in the inner membrane.

3.28: Determinatin Of Antibiotic Minimum Inhibitory Concentrations For *P. aeruginosa*

P. aeruginosa displays resistance to a wide range of commonly used laboratory antibiotics. The intrinsic antibiotic resistance of *P. aeruginosa* is in part afforded by the activity of multidrug efflux proteins. Analysis indicated that the minimum inhibitory concentrations (MICs) of commonly used antibiotics were significantly elevated for *P. aeruginosa* in comparison to *E. coli*. In order to successfully construct *P. aeruginosa* mutants it was necessary to determine the MICs for various commonly used antibiotics.

In order to determine the various antibiotic MICs of *P. aeruginosa*, cultures were grown in LB broth until early stationary phase and then plated at a range of dilutions on LB agar containing the antibiotic of interest. Only plates containing less than 100 cfu were examined when determining the antibiotic MICs as at higher cell densities cooperative degradation of the antibiotics can occur leading to inaccurate MIC results.

Analysis of the literature indicated that *P. aeruginosa* was intrinsically resistant to ampicillin and chloramphenicol at levels that were inhibitory to *E. coli*. As the various mutagenesis plasmids were to be introduced into *P. aeruginosa* by triparental matings, it was necessary to be able to counter select the *E. coli* donor cells. The plasmid pRK600 encodes the Tra functions necessary for mobilisation of the mutagenesis plasmids into *P. aeruginosa*. As pRK600 encodes chloramphenicol resistance, it was decided to use ampicillin to counter select the *E. coli* donor cells. *P. aeruginosa* was grown in LB broth as described above and plated on LB agar containing 100 μg/ml of ampicillin, a level known to be inhibitory to *E. coli*. Analysis of plates indicated that *P. aeruginosa* was capable of growing on LB agar containing a level of ampicillin that was inhibitory to *E. coli*.

As previously described, the suicide vector, pJQ200ks (Section 3.12) had been used in the generation of *S. meliloti* 2011 mutants. It was decided to use the pJQ200ks vector for the generation of *P. aeruginosa* mutants. In order to successfully introduce the mutagenesis plasmids into *P. aeruginosa* by triparental matings, it was necessary to be able to counter select *P. aeruginosa* recipients that had not received a plasmid.

Mutants were to be constructed by the insertion of the kanamycin cassette from pUC4K into various genes of interest. In order to successfully generate the *P. aeruginosa* mutants, it was necessary to select for the successful integration of the gentamicin resistant mutagenesis vector into the chromosome. Subsequently, it was necessary to be able to select for the loss of the vector and the retention of the kanamycin resistant mutagenesis cassette. *P. aeruginosa* was grown as described above and plated on LB agar containing the antibiotics at various concentrations. The results are indicated in Table 3.34.

Table 3.34: Determination Of *P. aeruginosa* MICs.

Antibiotic (μg/ml)	*P. aeruginosa* 01		*P. aeruginosa* CDC5	
	Gentamicin	Kanamycin	Gentamicin	Kanamycin
0	+	+	+	+
50	-	+	-	+
100	-	-	-	-
150	-	-	-	-
200	-	-	-	-
500	-	-	-	-

+ = Growth after 24 hours.

Analysis of the results indicated that *P. aeruginosa* was sensitive to all levels of gentamicin tested. After further incubation at room temperature for three days, no growth was apparent on any of the plates containing gentamicin. Analysis indicated that *P. aeruginosa* was sensitive to gentamicin even on plates containing high cell densities. *P. aeruginosa* was found to be resistant to the lowest level of kanamycin tested. Growth of *P. aeruginosa* on LB plates containing kanamycin at a level of 50 μg/ml was comparable to growth on LB plates not containing any antibiotics. When the plates were incubated at room temperature for a further three days, growth was apparent on all plates up to and including 200 μg/ml of kanamycin. Growth at a level of 500 μg/ml however appeared to be completely restricted. *P. aeruginosa* appeared to be increasingly resistant to kanamycin as cell densities increased. No difference in resistant levels was observed between the wild type *P. aeruginosa* PA01 strain and the pyoverdine mutant *P. aeruginosa* CDC5. As expected, *E. coli*, which was plated on identical media was sensitive to both antibiotics at all levels tested.

Analysis of the results indicated that a level of 50 μg/ml of gentamicin would be sufficient for the counter selection of *P. aeruginosa* cells during triparental matings. It was deemed inappropriate to use kanamycin for the counter selection of *P. aeruginosa* cells during triparental matings as the cell densities plated were quite high. Kanamycin was used at a level of 500 μg/ml during the screen for potential second recombinants that had successfully integrated the kanamycin cassette into the chromosome.

3.29: The Mutagenesis Of PA4218

As previously described (Section 3.12), the direct subcloning and subsequent mutagenesis of fragments of interest avoided the use of PCR amplification and the potential for Taq DNA polymerase generated mutations. In comparison to *S. meliloti* 1021, an ordered set of cosmid clones spanning the entire *P. aeruginosa* genome was available and consequently it was possible to devise a mutagenesis strategy that avoided the use of PCR. Analysis of the region encoding PA4218 indicated that the region of interest was encoded on a cosmid designated pMO 012405. The cosmid, which was harboured in *E. coli* S17-1 was obtained from the Pseudomonas Genetic Stock Centre. Restriction analysis of the cosmid was performed *in silico* using the sequence data available from the *Pseudomonas aeruginosa* Genome Site (Chapter 2).

Analysis of the region encoding PA4218 allowed the identification of a 3.6 Kb *Xho*1/*Xma*1 fragment with an internal *Sal*1 site, which was present within PA4218, into which an antibiotic resistance cassette could be inserted. An 8.8 Kb *Eco*R1 fragment encoding the 3.6 Kb region of interest was subcloned into pUC18 generating pUC8.8 E/E. The 3.6 Kb *Xho*1/*Xma*1 fragment was subsequently subcloned into pJQ200ks (Section 3.12) removing the vector borne *Sal*1 site and generating pOC3.6 X/Xm. The kanamycin cassette from pUC4K was excised as a *Sal*1 fragment and cloned into the unique *Sal*1 site of pOC3.6 X/Xm generating pOC3.6K X/Xm.

P. aeruginosa produces two siderophores, pyoverdine and pyochelin. In order to examine the effect of mutations on the pyochelin regulon, it was necessary to introduce the mutations into a pyoverdine deficient background. A pyoverdine biosynthesis mutant, *P. aeruginosa* CDC5, a kind gift from Dr. Keith Poole, was used for the generation of mutants in the pyochelin regulon. The plasmid pOC3.6K X/Xm was introduced into *P. aeruginosa* CDC5 by triparental mating and transconjugants were selected on LB agar containing ampicillin and gentamicin. Second recombinants were selected by growing a single first recombinant without antibiotic selection in LB broth until early stationary phase, and then by plating on LB agar containing 5% sucrose and kanamycin. In order to examine the efficacy of *sacB* expression in *P. aeruginosa*, the first recombinant was also plated on LB containing kanamycin. A comparison between both sets of LB plates indicated that the addition of sucrose to the

media was not having a clearly discernable effect on colony numbers. The level of sucrose in the media was increased to 10% but no difference in colony numbers was observed between the test and the control plates. As the SacB protein is toxic to cells even in the absence of sucrose, the *E. coli* host containing pOC3.6K X/Xm was plated on LB agar containing 5% sucrose and gentamicin and on LB containing gentamicin in order to eliminate the possibility that the *sacB* gene had been mutated. Analysis indicated that the *sacB* gene had not been affected.

It was concluded that the *sacB* gene of pJQ200ks was not being expressed or that the SacB protein was not functional in *P. aeruginosa*. In order to obtain the required mutant, it was necessary to screen for naturally occurring second recombinants. Although the previous results indicated that the addition of sucrose to the medium appeared to have no effect in selecting for loss of the vector, first recombinants that had been grown to early stationary phase in LB broth were nonetheless plated on LB containing 5% sucrose and kanamycin in case the sucrose selected at a low level for secondary recombinants. Individual colonies were subsequently screened for kanamycin resistance and gentamicin sensitivity. A potential mutant, *P. aeruginosa* PA4218km was identified in this way and selected for further analysis. Analysis of the potential mutant on LB agar indicated that the mutant was producing a blue pigmentation that was absent from wild type *P. aeruginosa*. This blue pigmentation shall be described in further detail in Section 3.35. On the basis of the homology of PA4218 with RhtX, and on the phenotypes described in the following sections, PA4218 was designated *fptX* for *f*erri*p*yochelin *t*ransport.

The genomic sequence in the region encoding *fptX* was examined to identify restriction sites that were deemed suitable for the confirmation of the potential mutant by Southern blot analysis (Chapter 2). The kanamycin cassette from pUC4K was inserted into a *Sal*1 site encoded within a larger 4.2 Kb *Xho*1 fragment (Figure 3.46) as an *Sal*1 fragment. Digestion of the mutant genomic DNA with *Xho*1 would generate one fragment as indicated in Figure 3.47. The plasmid pOC3K.6 X/Xm was labelled as described in Chapter 2 and used as a probe.

Figure 3.46: Analysis Of The Region Encoding *fptX* In *P. aeruginosa*.

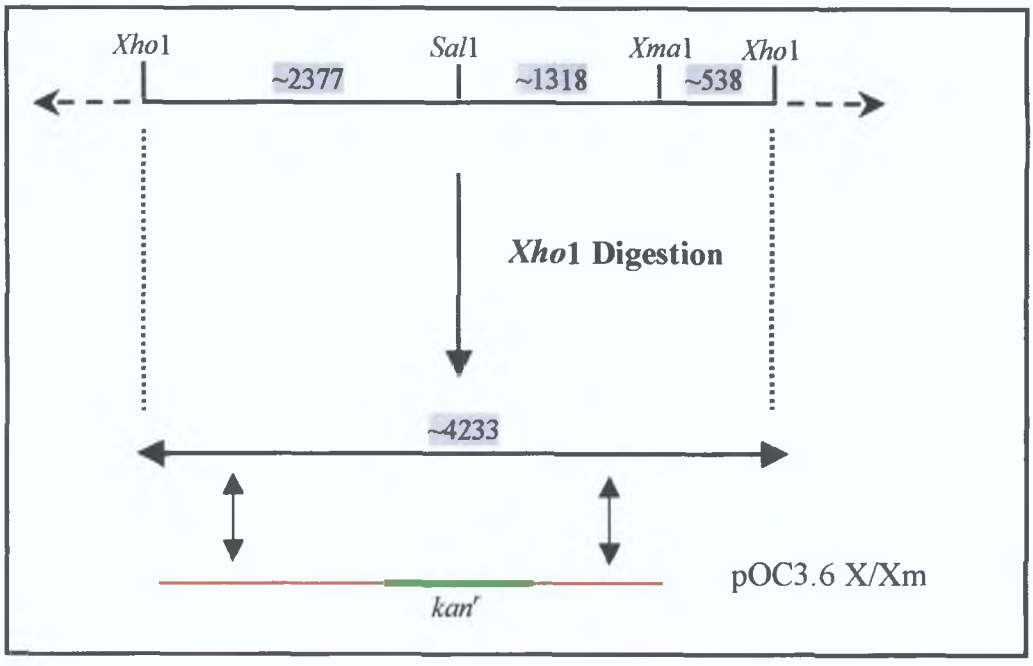

The predicted sizes of the digested fragments are highlighted in grey. The labelled probe is indicated in red, while the kanamycin cassette is highlighted in green. Regions of homology between the labelled probe and the digested fragments are indicated

Figure 3.47: Analysis Of The Region Encoding *fptX* In A Potential Mutant

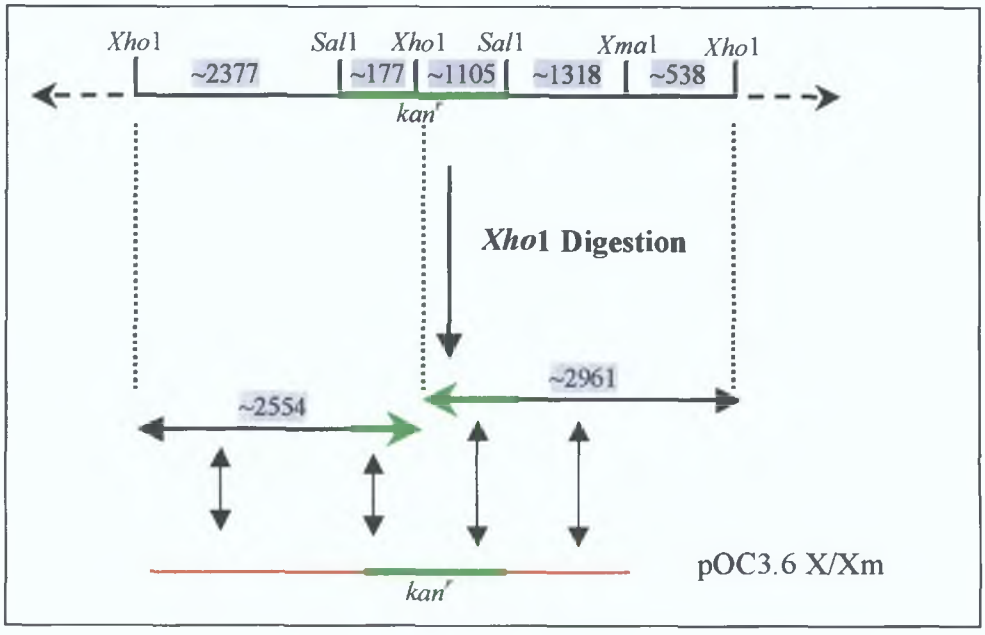

The predicted sizes of the digested fragments are highlighted in grey. The labelled probe is indicated in red, while the kanamycin cassette is highlighted in green. Regions of homology between the labelled probe and the digested fragments are indicated.

Genomic DNA was prepared from *P. aeruginosa* CDC5 and the potential mutant (Chapter 2), restricted with *Xho*1, transferred to nitrocellulose and probed with labelled plasmid as described in Chapter 2. Examination of the hybridisation result indicated that the kanamycin cassette had correctly integrated into the chromosome of *P. aeruginosa* (Figure 3.48).

Figure 3.48: Southern Blot Analysis Of *P. aeruginosa* CDC5 And The Kanamycin Cassette *fptX* Mutant.

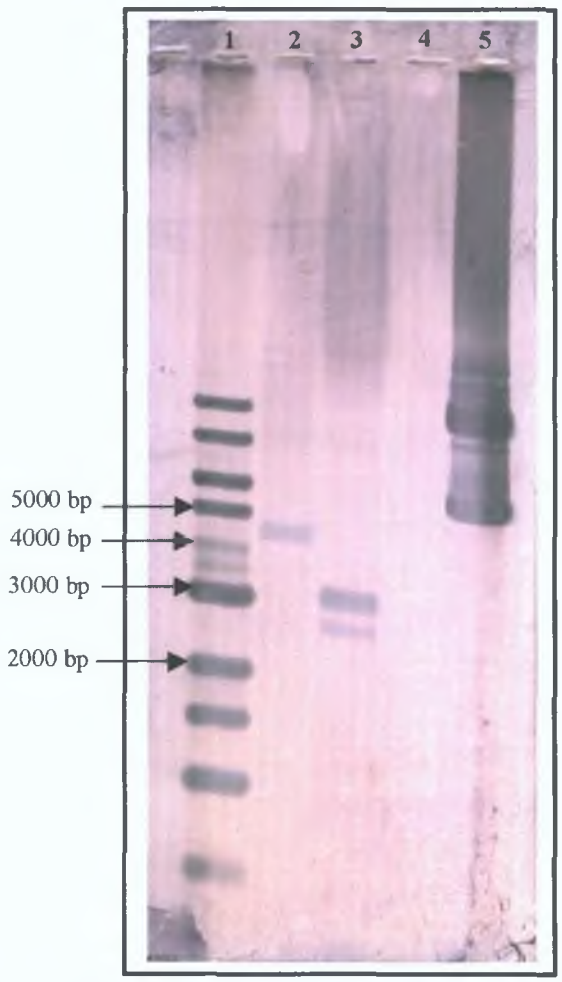

Legend

Lane 1: 1 Kb ladder (Section 2.28)

Lane 2: *P. aeruginosa* CDC5 *Xho*1

Lane 3: *P. aeruginosa* PA4218-km *Xho*1

Lane 5: pOC3.6K X/Xm

The mutant strain was named *P. aeruginosa* PA4218km. The phenotypic characterisation of the *S. meliloti* 2011*rhtX*1 is described in Section 3.32-3.35.

3.30: The Mutagenesis Of PA4219

Detailed sequence analysis of the region encoding PA4219 revealed the presence of a unique *Sma*1 site within the gene into which an antibiotic resistance cassette could be inserted. Analysis of the region encoding PA4219 enabled a strategy to be devised in which PA4219 could be mutated by successive cloning into various intermediate vectors thereby avoiding the use of PCR.

In order to mutate PA4219, a 3.6 Kb *Eco*R1/*Bam*H1 fragment was subcloned from pUC8.8 E/E into pUC18 generating pUC3.6 E/B. The 3.6 Kb fragment was restricted from pUC3.6 E/B as an *Eco*R1/*Hind*III fragment, using the vector encoded *Hind*III site, and then cloned into the pST Blue-1 vector generating pST3.6 E/H. The 3.6 Kb fragment was subsequently restricted from pST3.6 E/H as a *Pst*1/*Xba*1 fragment and cloned into pJQ200ks (Section 3.12) removing the vector borne *Sma*1 site and generating pOC3.6 P/Xb. The kanamycin cassette from pUC4K was excised as a *Hinc*II fragment and cloned into the unique *Sma*1 site of pOC3.6 P/Xb generating pOC3.6K P/Xb.

The plasmid pOC3.6K P/Xb was introduced into *P. aeruginosa* CDC5 by triparental mating and transconjugants were selected for on LB containing ampicillin and gentamicin. First recombinants that had been grown to early stationary phase in LB broth were plated on LB containing 5% sucrose and kanamycin. Individual colonies were subsequently screened for kanamycin resistance and gentamicin sensitivity. A potential mutant named *P. aeruginosa* PA4219km was identified in this way and selected for further analysis. The Southern blot analysis of *P. aeruginosa* PA4219km is described in Section 3.31.

3.31: The Mutagenesis Of *fptB*

Detailed sequence analysis of the region encoding *fptB* revealed the presence of a unique *Xho*1 site within the gene into which an antibiotic resistance cassette could be inserted. Similarly to PA4219, analysis of the region encoding *fptB* enabled a strategy to be devised in which *fptB* could be mutated by successive cloning into various intermediate vectors thereby avoiding the use of PCR.

The plasmid pUC3.6 E/B contains a unique *Xho*1 site that is located within the *fptB* coding determining sequence. The kanamycin cassette from pUC4K was excised as a *Sal*1 fragment and cloned into the unique *Xho*1 site of pUC3.6 E/B generating pUC3.6K E/B. The 3.6 Kb fragment with the inserted kanamycin cassette was excised as an *Eco*R1/ *Bam*H1 fragment and cloned into the pCR2.1 vector generating pCR3.6K E/B. The fragment was subsequently subcloned from pCR3.6K E/B as a *Bam*H1/*Xba*1 fragment using the vector encoded *Xba*1 site and directionally cloned into pJQ200ks (Section 3.12) generating pOC3.6K B/Xba.

The plasmid pOC3.6K B/Xba was introduced into *P. aeruginosa* CDC5 by triparental mating and transconjugants were selected for on LB containing ampicillin and gentamicin. First recombinants that had been grown to early stationary phase in LB broth were nonetheless plated on LB containing 5% sucrose and kanamycin. Individual colonies were subsequently screened for kanamycin resistance and gentamicin sensitivity. A potential mutant named *P. aeruginosa* PA4220km was identified in this way and selected for further analysis.

The genomic sequence in the region encoding *fptB* was examined to identify restriction sites that were deemed suitable for the confirmation of the potential mutant by Southern blot analysis (Chapter 2). The kanamycin cassette from pUC4K was inserted into an *Xho*1 site encoded within a larger 7.3 Kb *Xho*1 fragment (Figure 3.49) as an *Sal*1 fragment. Digestion of the mutant genomic DNA with *Xho*1 would generate two fragments as indicated in Figure 3.50. The plasmid pUC8,8 E/E was labelled as described in Chapter 2 and used as a probe. As pUC8.8 E/E extends over the entire region, three bands in total were predicted to be observed in the hybridisation (Figure 3.50).

Figure 3.49: Analysis Of The Region Encoding *fptB* In *P. aeruginosa*.

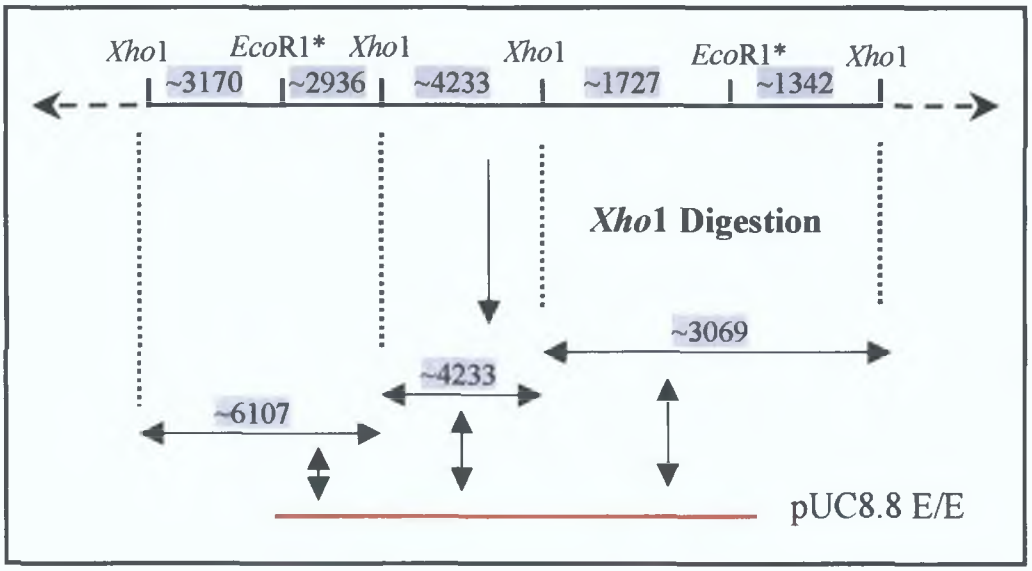

The predicted sizes of the digested fragments are highlighted in grey. The labelled probe is indicated in red, while the kanamycin cassette is highlighted in green. Regions of homology between the labelled probe and the digested fragments are indicated

Figure 3.50: Analysis Of The Region Encoding *fptB* A Potential Mutant

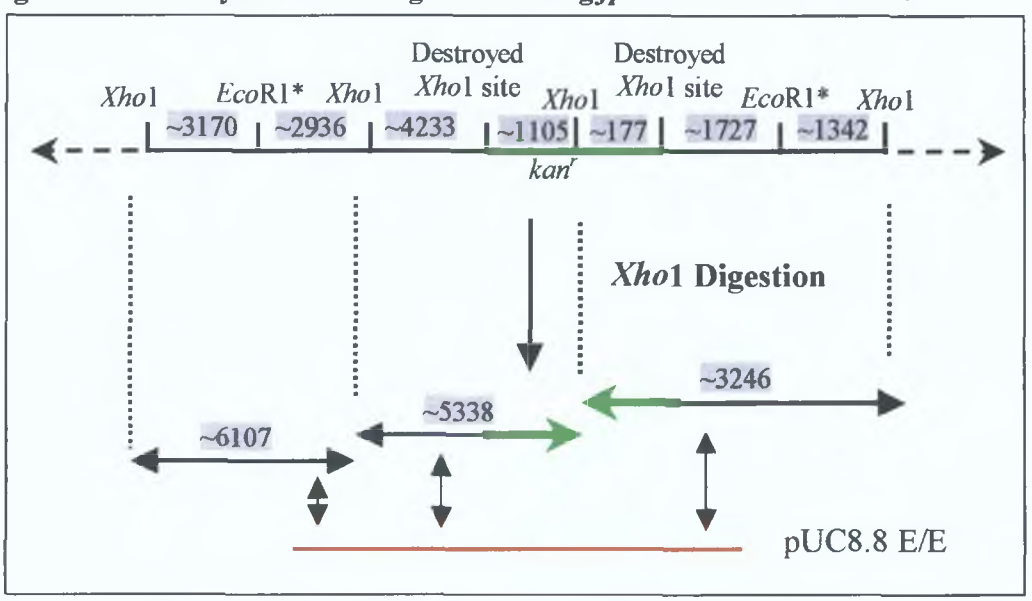

The predicted sizes of the digested fragments are highlighted in grey. The labelled probe is indicated in red, while the kanamycin cassette is highlighted in green. Regions of homology between the labelled probe and the digested fragments are indicated.

Genomic DNA was prepared from *P.aeruginosa* CDC5 and the potential mutant (Chapter 2), restricted with *Xho*1, transferred to nitrocellulose and probed with labelled plasmid as described in Chapter 2 (Figure 3.53).

The genomic sequence in the region encoding PA4219 was examined to identify restriction sites that were deemed suitable for the confirmation of the potential mutant by Southern blot analysis (Chapter 2). The kanamycin cassette from pUC4K was inserted into an *Sma*1 site encoded within a larger 4.2 Kb *Xho*1 fragment (Figure 3.51) as an *Hinc*II fragment. Digestion of the mutant genomic DNA with *Xho*1 would generate two fragments as indicated in Figure 3.52. The plasmid pUC8.8 E/E was labelled as described in Chapter 2 and used as a probe. As pUC8.8 E/E extends over the entire region, three bands in total were predicted to be observed in the hybridisation (Figure 3.52).

Figure 3.51: Analysis Of The Region Encoding PA4219 In *P. aeruginosa*.

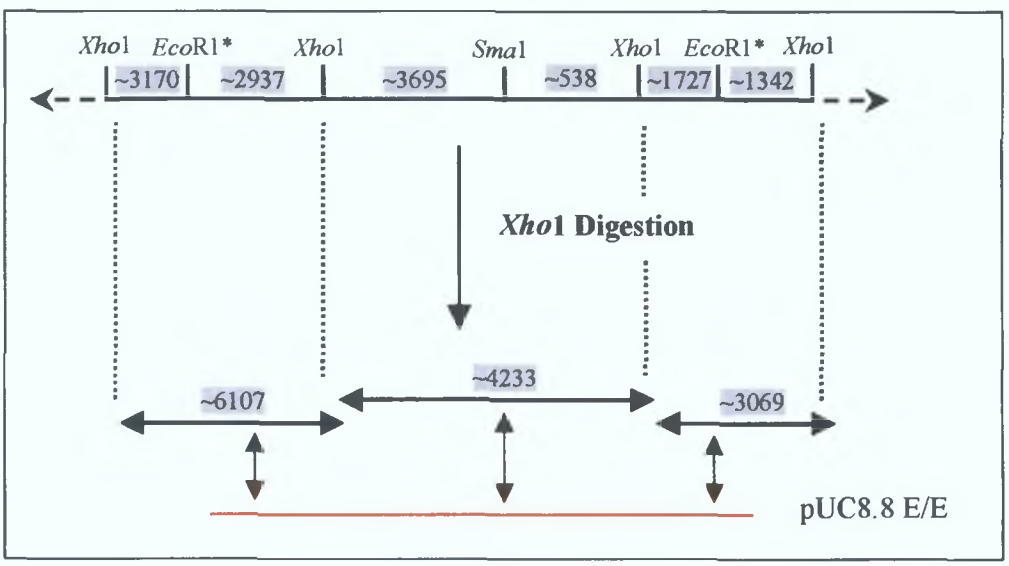

The predicted sizes of the digested fragments are highlighted in grey. The labelled probe is indicated in red, while the kanamycin cassette is highlighted in green. Regions of homology between the labelled probe and the digested fragments are indicated.

Figure 3.52: Analysis Of The Region Encoding PA4219 In A Potential Mutant.

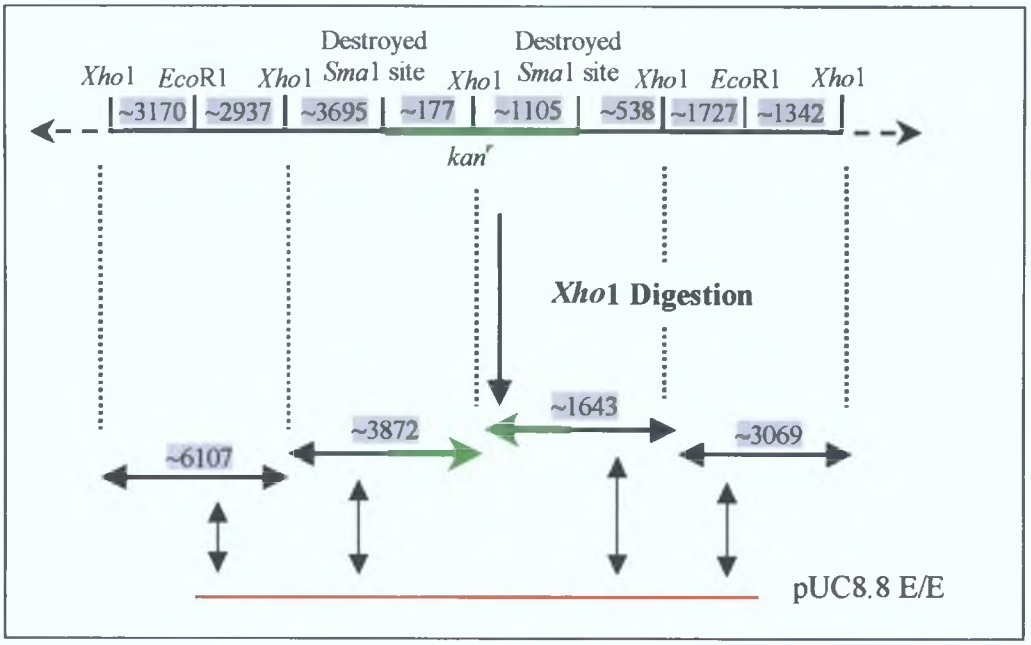

The predicted sizes of the digested fragments are highlighted in grey. The labelled probe is indicated in red, while the kanamycin cassette highlighted in green. Regions of homology between the labelled probe and the digested fragments are indicated.

Genomic DNA was prepared from *P. aeruginosa* CDC5 and the potential mutant (Chapter 2), restricted with *Xho*1, transferred to nitrocellulose and probed with labelled plasmid as described in Chapter 2 (Figure 3.53).

Figure 3.53: Southern Blot Analysis Of *P. aeruginosa* And The Kanamycin Cassette *fptB* And PA4219 Mutants.

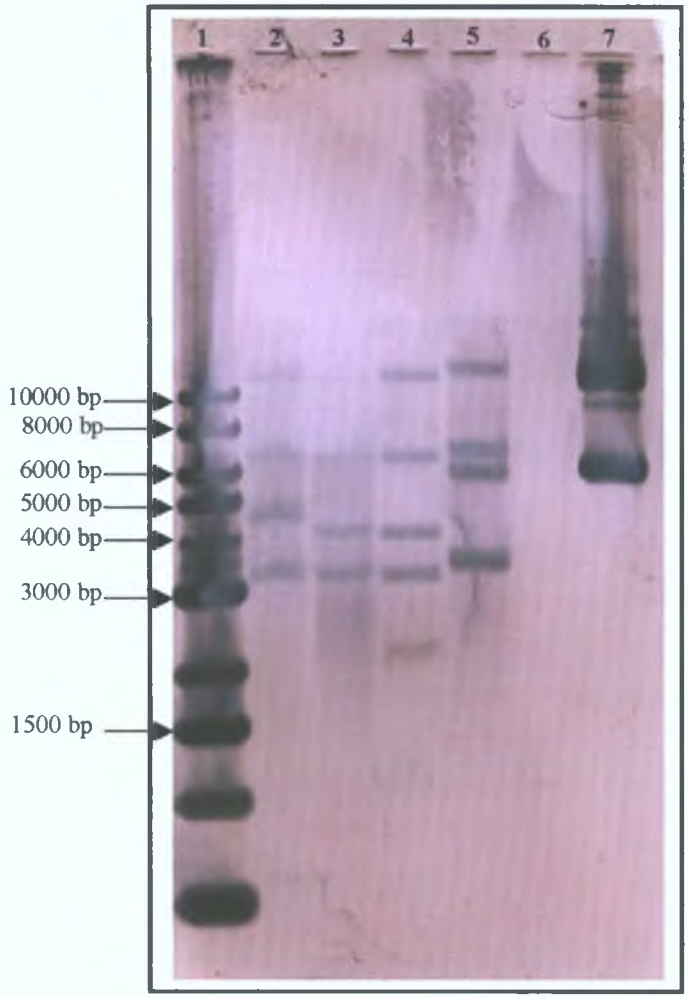

Legend

Lane 1: 1 Kb ladder (Section 2.28)

Lane 2: *P. aeruginosa* CDC5 *Xho*1

Lane 3: *P. aeruginosa* PA4219km *Xho*1

Lane 4: Not relevant to this work

Lane 5: *P. aeruginosa* PA4220km *Xho*1

Lane 7: pUC8.8 E/E

Analysis of the Southern blot indicated the presence of a >10 Kb present in all the strains analysed. Analysis of the pUC8.8 E/E plasmid indicated that the plasmid contained part of the phenazine biosynthesis operon located downstream from PA4218. *P. aeruginosa* encodes two phenazine biosynthesis operons. Analysis of the second operon revealed the presence of a 10.5 Kb *Xho*1 fragment spanning a substantial part of the operon. A comparison of the nucleotide sequences between both operons indicated that they showed extensive homology. The large >10 Kb band is therefore probably due to non specific hybridisation to the second phenazine biosynthesis operon.

Analysis also indicated that the *P. aeruginosa* PA4219km mutant did not appear to produce the predicted 1.6 Kb *Xho*1 fragment. Closer analysis of the predicted

restriction profile indicate that approximately 1.2 Kb of this fragment consisted of the kanamycin cassette with the remainder consisting of genomic DNA. The DNA loading in this lane was relatively poor, and coupled with the limited homology to the probe, the resulting hybridisation was possibly below the level of detection. The remainder of the restriction fragments are as predicted, and retention of the mutagenesis would have affected the restriction pattern of this region.

The results therefore indicated that both mutants had been correctly constructed. The *fptB* mutant strain was named *P. aeruginosa* PA4220km, while the PA4219 mutant strain was named *P. aeruginosa* PA4219km. The phenotypic characterisation of these strains is described in Section 3.32-3.35.

3.32: Analysis Of *P. aeruginosa* Growth Under Low Iron Conditions

P. aeruginosa CDC5 produces the siderophore pyochelin under low iron conditions. *P. aeruginosa* mutants defective in pyochelin biosynthesis or utilisation would be expected to show restricted growth under low iron conditions compared to *P. aeruginosa* CDC5. The chelator 2,2'dipyridyl displays an affinity for iron, and at high concentrations effectively removes available iron from the microbiological medium. The ability of *P. aeruginosa* and the cassette-generated mutants to grow on LB agar under low iron conditions was evaluated. *P. aeruginosa* cultures were grown until early stationary phase and a range of dilutions were then plated on LB agar with increasing concentrations of 2,2'dipyridyl. The plates were incubated at 37°C for 36 hours. Only plates where single colonies were clearly discernable were used in the analysis of the growth phenotype under low iron conditions. The results are shown in Table 3.35.

Table 3.35: Growth Of *P. aeruginosa* Mutants Under Low Iron Conditions.

P. aeruginosa	**Genotype**	**Concentration of 2,2'dipyridyl (mM)**				
		0	**0.5**	**1**	**1.5**	**2.0**
CDC5	*pvd-2*	+++++++	+++++++	++++++	++++	-
PA4218km	*pvd-2, fptX*	+++++++	++++	++	+	-
PA4219km	*pvd-2,* PA4219	+++++++	+++++	++++	++	-
PA4220km	*pvd-2, fptB*	+++++++	++++++	+++++	+++	-

The results indicated that *P. aeruginosa* CDC5 showed strong growth up to a level of 1 mM 2,2'dipryidyl. Growth of *P. aeruginosa* was completely inhibited at a level of 2 mM 2,2'dipyridyl. Analysis of *P. aeruginosa* PA4218km indicated that growth of the mutant was severely affected under iron limiting conditions. Growth of the mutant was severely affected at a level of 1 mM 2,2'dipyridyl. Growth of the *P. aeruginosa* mutant PA4219km was also affected under low iron conditions, but the effect was not as pronounced as that for mutant *P. aeruginosa* PA4218km. Growth of *P. aeruginosa* PA4220km was comparable to *P. aeruginosa* CDC5 at all levels tested.

3.33: Analysis Of Siderophore Utilisation By *P. aeruginosa* Pyochelin Mutants

The ability of *P. aeruginosa* pyochelin mutants to utilise siderophore was analysed by iron nutrition bioassays. *P. aeruginosa* mutants unaffected in siderophore utilisation show a characteristic halo of growth around a well containing the siderophore of interest.

Iron nutrition bioassays were performed on the *P. aeruginosa* pyochelin mutants as previously described (Chapter 2; Section 2.20). As indicated in section 3.32, growth of *P. aeruginosa* was inhibited at a level of 2 mM 2,2'dipyridyl. As such, the iron nutrition were performed with a final concentration of 2mM 2,2'dipyridyl. Three wells were cut out of the test plates and the various test solutions were added to individual wells. As a positive control, 50 µl of $FeCl_3$ was added to one of the wells. Pyochelin was prepared from *P. aeruginosa* CDC5 grown under iron deplete conditions as previously described (Chapter 2), and was added to one of the wells. As a negative control, *P. aeruginosa* CDC5 was grown under iron replete conditions, and the culture supernatant was prepared in a similar manner to that described for the pyochelin containing supernatant. A sample of this solution was added to the final well. The results of the iron nutrition bioassays are indicated in Table 3.36 below.

Table 3.36: Analysis Of Siderophore Utilisation In *P. aeruginosa*

***P. aeruginosa* Strain**	**Genotype**	**Pyochelin Utilisation**
CDC5	*pvd-2*	+
PA4218km	*pvd-2, fptX*	-
PA4219km	*pvd-2*, PA4219	+
PA4220km	*pvd-2, fptB*	+

P. aeruginosa CDC5 exhibited a pattern of growth through-out the plate. The strain was capable of producing and utilising pyochelin and was therefore able to overcome the conditions of iron limitation. Stronger growth of *P. aeruginosa* CDC5 was observed around the well containing pyochelin. Analysis of the results indicated that *P. aeruginosa* PA4218km was not producing a halo of growth around the well containing pyochelin. This indicated that the *P. aeruginosa* PA4218km mutant was affected in its ability to utilise pyochelin. The ability of *P. aeruginosa* PA4219km to

utilise pyochelin was also affected, although not to the same degree as *P. aeruginosa* PA4218km. A halo of growth was observed around the well containing pyochelin indicating that the kanamycin cassette in PA4219 was not having a polar effect on *fptX*. However growth through out the plate appeared to be affected and was weaker in comparison to wild type *P. aeruginosa* CDC5. The ability of *P. aeruginosa* PA4220km to utilise pyochelin appeared to be unaffected, and growth was comparable to wild type *P. aeruginosa* CDC5.

3.34: Analysis Of Siderophore Production By *P. aeruginosa* Pyochelin Mutants

The ability of *P. aeruginosa* pyochelin mutants to produce siderophore was analysed by the chrome azurol S (CAS) plate assay. Siderophore producing bacteria produce a distinctive orange halo around the colony that can indicate the effect of the mutation on siderophore production.

P. aeruginosa pyochelin mutants were spotted onto CAS plates along with wild type culture as previously described, (Chapter 2). The size and intensity of the halos produced are shown in Table 3.37.

Table 3.37: Analysis Of Siderophore Production In *P. aeruginosa*

***P. aeruginosa* Strain**	**Genotype**	**Halo**
CDC5	*pvd-2*	++
PA4218km	*pvd-2, fptX*	++++
PA4219km	*pvd-2*, PA4219	+++
PA4220km	*pvd-2, fptB*	+

++ = Wild type halo, +++ = Larger halo, + = Weaker halo.

Analysis of the results indicated that *P. aeruginosa* mutants PA4218km and PA4219km were affected in siderophore production. Both mutants had larger halos than those produced by wild type. As both mutants appeared to be affected in pyochelin utilisation, it is possible that the increase in halo size is due to an accumulation of siderophore in the medium. In contrast to *P. aeruginosa* mutants PA4218km and PA4219km, *P. aeruginosa* mutant PA4220km showed a decrease in siderophore production when compared to wild type. As *P. aeruginosa* PA4220km appeared to be unaffected in siderophore utilisation, the decrease in siderophore production was considered to be due to a reduction in biosynthesis or export of the siderophore, possibly by some unknown regulatory effect.

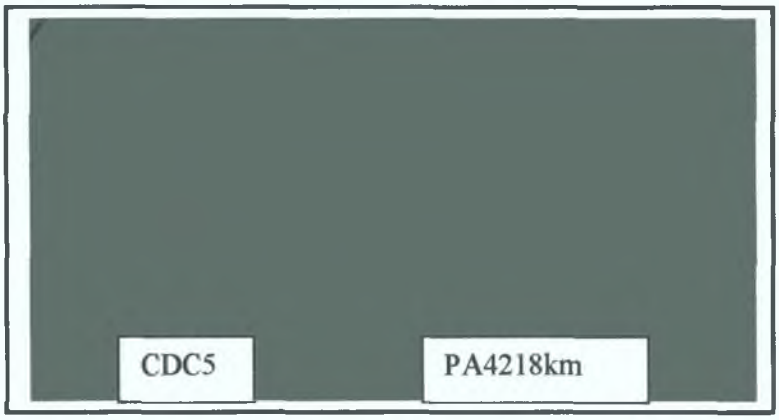

Figure 3.54: Analysis Of Siderophore Production By *P. aeruginosa* PA4218km. *P. aeruginosa* mutants were spotted on CAS plates and analysed as described in Chapter 2. The orange halo indicates siderophore production.

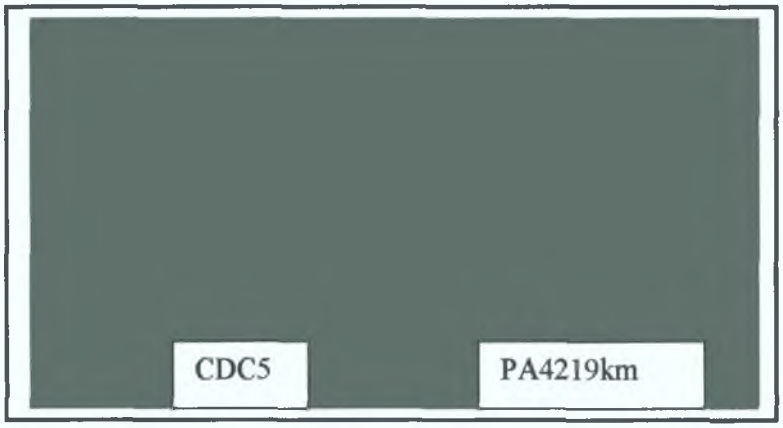

Figure 3.55: Analysis Of Siderophore Production By *P. aeruginosa* PA4219km. *P. aeruginosa* mutants were spotted on CAS plates and analysed as described in Chapter 2. The orange halo indicates siderophore production.

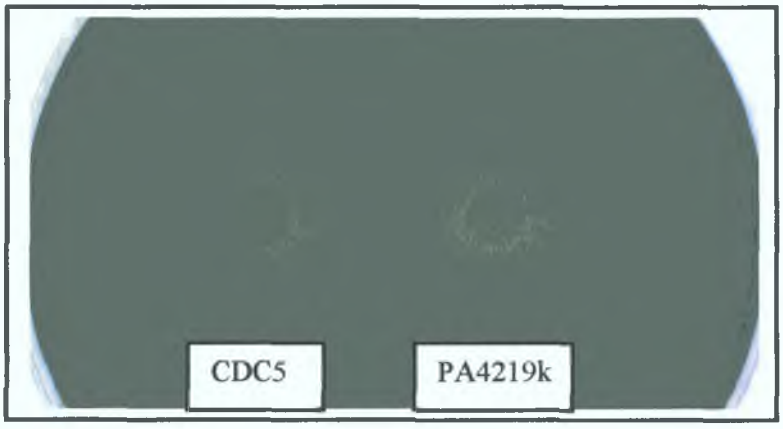

Figure 3.56: Analysis Of Siderophore Production By *P. aeruginosa* PA4220km. *P. aeruginosa* mutants were spotted on CAS plates and analysed as described in Chapter 2. The orange halo indicates siderophore production.

3.35: Phenotypic Analysis Of *P. aeruginosa* Cultures Under Low Iron Conditions

As previously described (Section 3.29), when *P. aeruginosa* PA4218km was grown on LB agar a difference was observed in the culture pigmentation in comparison to *P. aeruginosa* CDC5. A blue pigmentation appeared to be centred where culture growth was heaviest. The pyochelin regulon mutants were constructed in a strain, *P. aeruginosa* CDC5 that was defective in pyoverdine biosynthesis. Pyoverdine, a fluorescent siderophore, is the primary siderophore produced by *P. aeruginosa*. *P. aeruginosa* CDC5 was generated by chemical mutagenesis, and the resultant mutant was found to be a non-fluorescent strain defective in pyoverdine biosynthesis (Ankenbauer *et al*, 1986). *P. aeruginosa* has a high demand for iron, and it was hypothesised that the construction of a the PA4218km mutant in the pyochelin regulon had selected for a pyoverdine revertant. Although mutants in both siderophore systems had previously been generated, these mutants were constructed using mutagenesis cassettes and transposons and were considered stable. A plate containing the blue pigmentation was examined under UV light in order to determine if it was fluorescent. Analysis indicated that the pigment displayed a blue fluorescence.

As the blue pigment appeared where culture growth was heaviest, it was considered that the pigment was being produced in response to some form of nutrient limitation. As the only difference between the *P. aeruginosa* CDC5 and PA4218km were in iron acquisition systems, it was considered likely that the blue pigmentation was being produced in response to iron limitation. Various *P. aeruginosa* strains were streaked on LB agar and on LB agar containing 0.5 mM 2,2'dipyridyl in order to determine if they also produced the blue pigmentation. Two further mutants in the pyochelin regulon, *P. aeruginosa* DH119 and DH143, kind gifts from Dr. Keith Poole, were also streaked on LB agar in order to examine their pigmentation. Another mutant defective in the production of pyoverdine and pyochelin *P. aeruginosa* PALS128-17, a kind gift from Dr. Cornelia Reimann, was also examined for the production of the blue pigment. The results are described in Table 3.38.

Table 3.38: Analysis Of *P. aeruginosa* Pigmentation

P. aeruginosa Strain	Genotype	Pigmentation 0 mM 2,2'dipyridyl	Pigmentation 0.5 mM 2,2'dipyridyl
CDC5	*pvd-2*	Weak	Strong
PA4218km	*pvd-2, fptX*	Strong	Very stong
PA4219km	*pvd-2,* PA4219	Weak	Moderate
PA4220km	*pvd-2, fptB*	Weak	Moderate
DH119	*pvd-2, pchR*	Not present	Weak
DH143	*pvd-2, fptA*	Strong	Very strong
PALS128-17	*pvd, pchA or B*	Not present	Not present

Analysis indicated that all strains examined except the pyochelin biosynthesis mutant *P. aeruginosa* PALS128-17 and *P. aeruginosa* DH119, produced the blue pigmentation. The blue pigmentation seemed to be augmented in strains that were defective in pyochelin utilisation such as *P. aeruginosa* PA4218km and DH143. This result indicated that the blue pigmentation was due to an accumulation of pyochelin in the medium. In order to confirm that the compound was pyochelin, siderophore was prepared from *P. aeruginosa* PA01, CDC5, PA4218km and PALS128-17 and the ability of the compound to promote growth under iron limiting conditions was examined. The results are described in Table 3.39.

Table 3.39: Analysis Of Siderophore Utilisation By *P. aeruginosa*.

P. aeruginosa Strain	Genotype	PA01 siderophore	CDC5 siderophore	PA4218km siderophore	PALS128-17 siderophore
PA4218km	*pvd-2 fptX*	+	-	-	-
PALS128-17	*pvd pchA* or *B*	+	+	+	-

Siderophore was prepared from *P. aeruginosa* 01, CDC5, PA4218km and PALS128-17 as described previously (Chapter 2). As pyoverdine is the primary siderophore of *P. aeruginosa* PA01, the siderophore prepared from *P. aeruginosa* PA01 was expected to be composed mainly of pyoverdine but with some pyochelin also possibly present. *P. aeruginosa* CDC5 is defective in pyoverdine biosynthesis and only produces pyochelin. *P. aeruginosa* PA4218km appeared to be unaffected in pyochelin production and also produced the blue pigment. *P. aeruginosa* PALS128-17 is

defective in the biosynthesis of pyoverdine and pyochelin. Siderophores from all four strains were used to crossfeed *P. aeruginosa* PA4218km and PASL128-17. Examination of the results indicated that *P. aeruginosa* PA4218km was capable of utilising the siderophore produced by *P. aeruginosa* PA01 but not that produced by *P. aeruginosa* CDC5 and *P. aeruginosa* PA4218km. This result indicated that *P. aeruginosa* PA4218km was capable of utilising pyoverdine but not the compound produced by *P. aeruginosa* CDC5 and *P. aeruginosa* PA4218km. The siderophores produced by all four strains were examined by crossfeeding the *P. aeruginosa* PALS128-17 mutant, which is defective in the biosynthesis of both siderophores, but is unaffected in transport of both siderophores. Examination of the results indicated that the siderophores prepared from all four strains were capable of crossfeeding *P. aeruginosa* PALS128-17. Culture supernatants prepared from *P. aeruginosa* PALS128-17 did not crossfeed any of the strains tested.

The results indicated that the blue pigmentation was due to an accumulation of pyochelin in the medium and it did not result from reversion of the mutation that blocks pyoverdine production.

3.35: Discussion

S. meliloti 2011 the endosymbiont of *Medicago sativa* produces one known siderophore, the asymmetric citrate hydroxamate siderophore rhizobactin 1021 (Chapter 1). The transport of siderophores across the outer membrane has been found to be dependent on cognate outer membrane siderophore receptors. Transport across the periplasm and the cytoplasmic membrane has been found to be mediated by periplasmic binding protein-dependent transport systems (PBT) of the ABC superfamily (Chapter 1). The region encoding rhizobactin 1021 on pSyma has previously been characterised (Gill and Neilands, 1989; Reigh and O'Connell, 1993; Lynch *et al*, 2001). A 14.2 Kb region was sequenced and shown to encode a biosynthesis operon, an outer membrane receptor for rhizobactin 1021 and a transcriptional regulator of the AraC type that positively regulated the biosynthesis operon and the receptor gene (Lynch *et al*, 2001; Lynch, PhD Thesis 1999). Sequencing of a region directly upstream for the biosynthesis operon revealed the presence of an ORF, the predicted protein product of which showed low level sequence homology to signal transducers. A transposon insertion in the gene, termed *rhtX* was isolated and found to be defective in rhizobactin 1021 utilisation. Examination also revealed that siderophore production was also affected.

The region encoding the 5' end of the gene was subcloned and sequenced. *In silico* analysis indicated that the gene was predicted to encode an inner membrane type permease with 12 transmembrane domains and a molecular weight of 45.56 kDa. The protein displayed homology to YbtX, a protein of unknown function located within the yersiniabactin siderophore regulon of *Y. pestis* (Fetherston *et al*, 1999). Two proteins encoded proximally to YptX, YptP and YptQ display homology to ABC transporters with an export function, however these proteins have been implicated in siderophore utilisation in *Y. pestis*. In contrast, analysis of the region directly upstream of *rhtX* did not reveal the presence of any genes encoding proteins with a role in iron acquisition. Directly upstream of *rhtX* and transcribed in the opposite direction was a gene annotated Sma2335 in the published *S. meliloti* genome sequence. Immediately downstream of Sma2335 and orientated in the same direction, a putative potassium transport system, *kdp*, was located. *In silico* analysis of the genome sequence indicated that such a PBT was not encoded in the region located downstream from

rhbG. The phenotype associated with *S. melilot* 2011*rhtX*43 suggested that RhtX functioned in the utilisation of rhizobactin 1021. However, the associated siderophore production phenotype also suggested that RhtX possibly functioned in secretion of the siderophore. This appeared to be confirmed on the basis of complementation experiments involving two cosmids encoding *rhtX*.

The *S. meliloti* 2011*rhtX*43 mutant was complemented using a *S. meliloti* genebank, and two cosmids, pPOC1 and pPOC3 were isolated that complemented the mutation. The introduction of pPOC1 and pPOC3 into *S. meliloti* 2011*rhtX*43 resulted in a restoration of siderophore production and utilisation. The phenotypes conferred by both cosmids varied and restriction and complementation analysis indicated that they represented two independent cosmids containing a common 8.5 Kb *Eco*R1 fragment encoding *rhtX*. The cosmid pPOC1 was shown to encode the entire rhizobactin 1021 regulon, and its introduction into *S. meliloti* 2011*rhtX*43 resulted in a restoration of the wild type utilisation phenotype. Siderophore production was elevated in the transconjugant, but it was proposed that this was due to a cosmid copy number effect. The introduction of pPOC3 into *S. meliloti* 2011*rhtX*43 resulted in a partial restoration of siderophore utilisation. It was subsequently suggested that the partial restoration was possibly due to a titration effect of the RhrA regulator, which in contrast to pPOC1, was not encoded on the cosmid. The introduction of pPOC3 into *S. meliloti* 2011*rhtX*43 resulted in an increase in siderophore production as assayed by the CAS plate assay. The rhizobactin 1021 biosynthesis operon, *rhbABCDEF*, had previously been shown to be required for siderophore production (Lynch *et al*, 2001; Lynch, PhD Thesis 1999). Examination of pPOC3 indicated that the entire biosynthesis operon was not encoded on the cosmid, but extended to one of two centrally located *Eco*R1 sites within *rhbC*. This prompted the suggestion that RhtX was possibly involved in the secretion of rhizobactin 1021.

To confirm this hypothesis, it was decided to express *rhtX* from an independent promoter in *S. meliloti* 2011*rhtX*43 and to analyse the resultant phenotype. It was decided to express the protein from an independent promoter as this relieved *rhtX* from any possible RhrA regulation. The gene was cloned into the broad host range plasmid, pBBR1MCS-5 and mobilised into *S. meliloti* 2011*rhtX*43. Analysis of the transconjugant indicated that siderophore utilisation had been restored, but that

siderophore production remained impaired. The result suggest that RhtX was not involved in secretion of the siderophore, and that the increased halo observed was due to some effect of the biosynthesis proteins encoded by pPOC3. Analysis of the proposed biosynthesis pathway for rhizobactin 1021 indicated that RhbA and RhbB were involved in the synthesis of 1,3 diaminopropare, a precursor for rhizobactin 1021 biosynthesis. It was hypothesised that the synthesis of 1,3 diaminopropane was the rate limiting step in the production of rhizobactin 1021. As there was some siderophore production, and therefore RhbA, B, C, D, E and F present in *S. meliloti* 2011*rhtX*43, it was proposed that the extra copies of RhbA and RhbB would result in an increase in 1,3 diaminopropane production with a concomitant increase in siderophore biosynthesis. To confirm this hypopthesis, *rhbAB* were cloned into the pBBR1MCS-5 and introduced into *S. meliloti* 2011*rhtX*43. Examination of the transconjugant phenotype indicated an increase in siderophore as determined by the CAS plate assay. The result suggested that the production of 1,3 diaminopropane was the rate limiting step in rhizobactin 1021 biosynthesis and confirmed that RhtX was not involved in the secretion of the siderophore.

The production of siderophore in *S. meliloti* 2011*rhtX*43 suggested the presence of a promoter in the intergenic region between *rhtX* and *rhbA*. The biosynthesis operon had previously been shown to be positively regulated RhrA (Lynch *et al*, 2001). Examination of the region upstream of *rhtX* resulted in the identification of a putative binding site for RhrA. A similar sequence was found in the *rhrA/rhtA* intergenic region. Analysis of the intergenic region between *rhtX* and *rhbA* did not reveal the presence of a similar binding site. The result suggested that RhrA was exerting its effect of transcription of the biosynthesis genes from upstream of *rhtX*. The result also suggested that *rhtX* was also part of the biosynthesis operon. Analysis of the literature revealed that Tn*5lac* had been shown to display outward promoter activity (Wexler *et al*, 2001). It was hypothesised that the Tn*5lac* insertion in *rhtX* was resulting in low level transcription of the biosynthesis operon. To confirm that *rhtX* constituted part of the operon, it was decided to construct a polar mutation in *rhtX*. An omega element was introduced into *rhtX* by allelic exchange and phenotypic analysis of the mutant phenotype indicated that the mutant was defective in siderophore utilisation and production. This confirmed that *rhtX* formed part of an operon with *rhbABCDEF*.

In silico analysis of the Sma2335 gene indicated that it encoded a putative protein with a predicted molecular weight of 7.18 kDa that was predicted to be located in the inner membrane. A mutagenesis cassette was introduced into the gene by allelic exchange and phenotypic analysis of the mutant indicated that it was unaffected in siderophore utilisation and production.

As RhtX did not display any homology to proteins that had been shown to be involved in siderophore utilisation, it was hypothesised that proteins encoded proximal to the rhizobactin 1021 regulon could have a role in siderophore utilisation. This was despite *in silico* analysis that indicated that none of the proteins encoded in this region functioned in siderophore utilisation. A *S. meliloti* 2011 strain that had been cured of the pSyma plasmid (that encodes the rhizobactin 1021 regulon) was analysed for its ability to utilise rhizobactin 1021. Examination indicated that the strain was not capable of utilising the siderophore. The introduction of the cosmid pPOC1 however restored the ability of the strain to produce and utilise rhizobactin 1021. The result indicated that the genes encoded on pPOC1 were sufficient for production and utilisation of the siderophore, and that no other genes were encoded on pSyma that functioned in this regard. To identify the minimal requirements for rhizobactin 1021 transport, *rhtX* and *rhtA* (under the control of RhrA) were expressed in *S. meliloti* 102F34, a strain that does not produce or synthesise rhizobactin 1021. Expression of the proteins conferred upon the strain the ability to utilise the siderophore. As expected, the expression of *rhtX* or *rhtA* individually did not result in rhizobactin 1021 utilisation.

Rhizobactin 1021 is structurally similar to several citrate hydroxamate siderophores including schizokinen and aerobactin (Chapter 1). Previous analysis of xenosiderophore utilisation in *S. meliloti* 2011 indicated that the bacterium was capable of utilising schizokinen but not aerobactin as an iron source. Analysis indicated that schizokinen was utilised via the RhtA protein (Lynch, PhD Thesis 1999). Further analysis indicated that schizokinen utilisation was abolished in *S. meliloti* 2011*rhtX*43 and *S. meliloti* 2011*rhrA*26 indicating that the siderophore was used in a similar manner to rhizobactin 1021. The ability of *E. coli* to utilise rhizobactin 1021 and schizokinen had also previously been analysed and found to be dependent on the outer membrane receptor for aerobactin, IutA. Aerobactin transport

post the outer membrane is dependent upon the FhuCDB PBT system. An *E. coli* mutant was obtained that was annotated as having a Tn*10* insertion in *fhuB*. A personal correspondence with Wolfgang Köster revealed that the mutant had been constructed prior to the discovery of *fhuC* and *fhuD* and that the location of the transposon insertion was therefore not known. Complementation of the *fhuCDB* genes indicated that the Tn*10* insertion was located in *fhuC* and that it had a polar effect on the downstream *fhuDB* genes. Examination of rhizobactin 1021 and schizokinen utilisation in the mutant strain revealed that the utilisation phenotype had been abolished. As expected, the ability of the bacterium to utilise aerobactin and ferrichrome was also abrogated. A plasmid expressing *rhtX* was introduced into the mutant that also expressed *iutA* from a separate plasmid, and utilisation of rhizobactin 1021 and schizokinen was restored. The introduction of the plasmids did not confer upon the strain the ability to utilise aerobactin or ferrichrome. The result indicated that RhtX was capable of limited complementation of the FhuCDB system. Analysis of ferrichrome utilisation in *S. meliloti* 2011 and 102F34 indicated that utilisation occurred independently of RhtX. The result suggested that RhtX represented a novel type of acquisition protein that was capable of partially acting as an alternative to the FhuCDB system.

A homologue of RhtX was identified in the genome of the opportunistic human pathogen, *P. aeruginosa*. The gene, *fptX* (annotated PA4218 in the genome sequence), was located downstream from the pyochelin receptor gene, *fptA*. A mutagenesis cassette was introduced into the gene by allelic exchange and phenotypic examination of the resulting mutant indicated that it was affected in siderophore utilisation. Analysis of siderophore production indicated an increase as determined by the CAS plate assay, possibly due to the accumulation of siderophore extracellularly. The *fptX* gene appeared to be translationally coupled to a gene, encoding a protein of unknown function, PA4219. A PA4219 mutant displayed reduced growth under conditions of iron limitation, although the strain remained capable of utilising and producing pyochelin. Analysis of the region upstream of PA4219 revealed the presence of a heptamer, 5' CGAGGAA 3', that was identical to one of the heptamers described as being a putative binding site for PchR (Chapter 1). The presence of this heptamer in the promoter region suggested that PA4219 and *fptX* were possibly PchR regulated. An analysis of genes induced under conditions of iron depletion indicated that PA4219

and *fptX* were expressed and formed a transcriptional unit (Ochsner *et al*, 2002). Analysis of the promoter region of PA4219 did not reveal any sequences with significant homology to a Fur box, and it is therefore possible that the regulation of this operon under iron limiting conditions is through an intermediary protein.

Directly upstream of PA4219, and apparently coupled to *fptA* is a putative gene *fptB*. A mutant in the gene was constructed and analysis indicated that the mutant displayed reduced siderophore production, but that utilisation remained unaffected. A mutant in *fptA* showed reduced pyochelin production (Personal communication Dr. Cornelia Reimmann). It is likely that this phenotype is associated with a polar effect on *fptB*. The FptX, PA4219 and FptB proteins are all predicted to be located in the inner membrane. It is possible that they form a complex involved in the utilisation of pyochelin. Two domains were identified in PA4219 that also appear to be conserved in a putative ferrisiderophore reductase encoded within the *P. aeruginosa* genome (PA4513). While PA4219 is a smaller protein, it is possible that it functions to reduce the pyochelin on its own or in conjunction with FptX and/or FptB or with another reductase. The slight utilisation could be explained by the non-specific actions of other ferric reductases, the activity of which in general is non-specific. It is possible that FptB functions as a signal transducer, informing the cell of the efficiency of iron delivery by pyochelin. Mutants defective in FptX produce normal levels of pyochelin while mutants defective in FptA (with a possible polar effect on *fptB*) display reduced pyochelin production (Personal communication Dr. Cornelia Reimmann). It therefore seems unlikely that pyochelin directly interacts with PchR to activate it, but that PchR activity is somehow modulated by a mechanism involving FptB.

Analysis of the RhtX and its homologues indicated that the greatest level of homology is at the N-terminal region, which is predicted to be located in the cytoplasm. RhtX is not associated with any protein that may function as an energiser. It is possible that such an energiser is located elsewhere on the chromosome and may be a general energiser. Analysis of the sequence revealed the presence of a motif, QD(V/I)A, that appears to be conserved in these proteins. This motif is predicted to be located on a cytoplasmic loop and in the absence of an energising protein it is interesting to speculate that this represents a domain for such an interaction. It is of interest to note that a mutant isolated by Gill and Neilands (1989) had a transposon insertion in the C-

terminal region of *rhtX*. The resultant mutant was characterised by a greatly increased halo as determined by CAS plate analysis. A similar mutant isolated in this laboratory also exhibited a similar phenotype. Analysis of the C-terminal indicates the presence of motifs that may be responsible for the effect.

Analysis of the ferric citrate transport indicated that only iron and not the citrate iron complex was transported to the cytoplasm. As citrate forms the core of rhizobactin 1021, it is possible that RhtX functions by modifying the siderophore in some way and possibly transporting a derivative or free iron into the cytoplasm. Also, as aerobactin has been shown to be recycled, it is also of interest to determine if rhizobactin 1021 is similarly recycled and if so, is RhtX involved in the recycling process.

Of the homologues of RhtX identified, a significant number of them appear to be associated with AraC type regulators. It is tempting to speculate the RhtX may be involved in that activation of the regulators, possibly via its N-terminal, subsequently allowing them to bind to DNA.

Chapter 4

Analysis Of Haem Utilisation In *S. meliloti* 2011

4.1: Introduction

Rhizobia are nitrogen-fixing bacteria that are found free living in the soil or in a symbiotic relationship with leguminous plants (Chapter 1). Rhizobia display a high requirement for iron as many of the proteins involved in nitrogen fixation, such as nitrogenase and ferredoxin, require iron as a cofactor. The availability of iron in the soil is also potentially limiting due to the insolubility of ferric iron and also because rhizobia have to compete with other microorganisms for available iron. As previously described (Chapter 1; Chapter 3), *S. meliloti* 2011 produces one known siderophore, rhizobactin 1021 which has been shown not to be essential for symbiotic nitrogen fixation (Lynch *et al*, 2001), but is likely to contribute to the competitiveness of the bacterium when free living in the soil. The ability of *S. meliloti* 2011 to utilise various siderophores including ferrichrome, desferryl meyselate and schizokinen has also been characterised (Noya *et al*, 1997; Lynch, PhD Thesis 1999).

The ability of various animal pathogens to acquire iron from haem compounds has been determined (Chapter 1; reviewed by Genco and Dixon, 2001). Although they are not pathogenic, rhizobia interact with host organisms, where haem compounds are readily available during symbiosis. Analysis of a number of rhizobia including *S. meliloti*, *R. leguminosarum* and *B. japonicum* indicated that these organisms were capable of utilising haem, or the haem proteins haemoglobin and leghaemoglobin as sole iron sources (Chapter 1).

A number of the specific proteins involved in haem acquisition in rhizobia have been described. *In silico* analysis of the *S. meliloti* 2011 genome sequence enabled the identification of three putative haem acquistion loci. This chapter describes the analysis of the three putative haem acquisition loci in *S. melitoi* 2011. The mutagenesis and genetic characterisation of the three loci and the effect of these mutations on symbiotic nitrogen fixation in plants will also be described.

4.2: *In silico* Analysis Of The Putative Haem Utilisation Loci Of *S. meliloti* 2011

The ability of *S. meliloti* to utilise haem compounds as an iron source has previously been described. *S. meliloti* 2011 has been shown to be able to utilise haemoglobin, haemin and the plant symbiotic protein, leghaemoglobin (Noya *et al*, 1997; Lynch, PhD Thesis 1999). Of the three putative haem acquisition haem loci identified by *in silico* analysis, two were predicted to encode putative haem receptors, while the third locus was predicted to encode an inner membrane transport system for haem. All three putative haem acquisition loci were chromosomally encoded and located on different regions of the chromosome.

The two putative haem receptors, Smc04205 and Smc02726 showed homology to TonB dependent haem receptor proteins. Both proteins displayed homology to haem receptors found in both pathogenic and non-pathogenic microorganisms. The region encoding Smc04205 appeared to encode several proteins that were predicted to be involved in haem acquisition. The region encoding Smc02726 did not appear to encode any other proteins with a direct role in haem acquisition. Smc02726 has been found to be capable of binding haemin and has been designated ShmR (Chapter 1)(Battistoni *et al*, 2002). The third locus was predicted to encode an inner membrane transport system similar to the *hmu* system of *R. leguminosarum*. The putative *hmu* system was located close to the *S. meliloti* 2011 *tonB* homologue. The gene organisation at this third locus was similar to that described for *R. leguminosarum* (Chapter 1)(Wexler *et al.*, 2001).

4.3: Analysis Of The Smc04205 Locus

Smc04205 is located at position 2190347-2193001 on the *S. meliloti* 1021 chromosome. A number of proteins encoded in the vicinity of Smc04205 show homology to proteins involved in iron acquisition. Directly upstream of Smc04205 and orientated in the same direction a putative regulatory system, encoded by Smc04203 and Smc04204, is located that is similar to the *fecIR* ferric citrate regulatory system of *E. coli* (Chapter 1). Directly upstream of the Smc04203 and orientated in the opposite direction is Smc04202. Smc04202 is predicted to encode a putative transporter and is not predicted to be involved in haem utilisation. Directly downstream of Smc04205, Smc04206 is predicted to encode a protein that shows homology to rhizobiocins and haemolysins. Directly downstream of Smc04206, a putative toxin ATP dependent export system, encoded by Smc04207 and Smc04208 is located. Directly downstream of Smc04208 and orientated in the opposite direction is Smc04209. Smc04209 does not display homology to any known protein. A map of the region is shown in Figure 4.1.

Figure 4.1: Map Encoding Of The Region Encoding Smc04205.

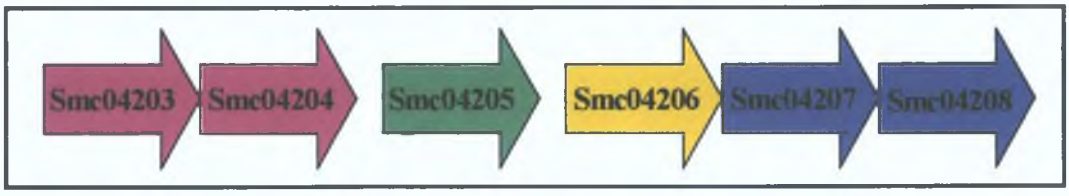

Legend

- Putative regulatory system
- Putative outer membrane haem receptor
- Putative rhizobiocin/haemolysin
- Putative ATP dependent export system

4.3.1: *In silico* Analysis Of The Genes Proximal To Smc04205

fecI

Smc04203 has been designated *fecI* on the *S. meliloti* 1021 Genome Homepage (Chapter 2). *fecI* is located at position 2188692-2189168 of the *S. meliloti* 1021 chromosome. A putative ribosome binding site, GGGGC, was identified upstream of the predicted translational start site. The protein predicted to be encoded by *fecI* is 159 amino acids in size with a predicted molecular weight of 18.3 kDa and a pI of 5.77. BLASTP analysis indicated that *fecI* is predicted to encode a putative RNA polymerase sigma factor. *fecI* shows strong identity to other putative ECF sigma factors such as Atu3387 from *A. tumefaciens* (40%) and Rrub1544 from *Rhodospirillum rubrum* (43%) as determined by BLASTP at NCBI.

fecR

Smc04204 has been designated *fecR* on the *S. meliloti* 1021 Genome Homepage (Chapter 2). *fecR* is located at position 2189161-2190222 of the *S. meliloti* 1021 chromosome. A putative ribosome binding site, AGGCA, was identified upstream of the predicted translational start site. The protein predicted to be encoded by *fecR* is 354 amino acids in size with a predicted molecular weight of 38.8 kDa and a pI of 5.58. BLASTP analysis indicated that *fecR* is predicted to encode a putative transmembrane acting signal transducer. *fecR* shows strong identity to other putative transmembrane acting signal transducers such as Atu3386 from *A. tumefaciens* (42%) and Rrub1543 from *R. rubrum* (35%) as determined by BLASTP at NCBI.

Smc04206

Smc04206 is located at position 2193379-2194176 of the *S. meliloti* 1021 chromosome. A putative ribosome binding site, AAGGA, was identified upstream of the predicted translational start site. The protein predicted to be encoded by Smc04206 is 266 amino acids in size with a predicted molecular weight of 27.5 kDa and a pI of 4.06. BLASTP analysis indicated that Smc02726 is predicted to encode a putative rhizobiocin, a rhizobial bacteriocin. Smc04206 shows strong identity to other putative rhizobiocins such as RczA from *R. leguminosarum* (31%) and RczA from *M. loti* (29%) as determined by BLASTP at NCBI.

Smc04207

Smc04207 is located at position 2194201-2196051 of the *S. meliloti* 1021 chromosome. A putative ribosome binding site, GGACT, was identified upstream of the predicted translational start site. The protein predicted to be encoded by Smc04207 is 617 amino acids in size with a predicted molecular weight of 65.7 kDa and a pI of 9.40. BLASTP analysis indicated that Smc02727 is predicted to encode a putative toxin secretion ATP-binding transport protein. Smc04207 shows strong identity to other putative toxin secretion ATP-binding transport proteins such as Atu3383 from *A. tumefaciens* (61%) and Mll1027 from *M. loti* (56%) as determined by BLASTP at NCBI.

Smc04208

Smc04208 is located at position 2196041-2197348 of the *S. meliloti* 1021 chromosome. A putative ribosome binding site, ACGGA, was identified upstream of the predicted translational start site. The protein predicted to be encoded by Smc04208 is 436 amino acids in size with a predicted molecular weight of 47.8 kDa. Analysis of Smc04208 using the PSORT program (Nakai and Kanehisa, 1991) indicated that the protein contained a 35 amino acid signal sequence typical for exported proteins. Cleavage of the signal sequence between the residues AWA-TT would result in a mature protein the predicted size of which is 44.4 kDa with a pI of 5.75. BLASTP analysis predicted that Smc02728 encodes a putative toxin secretion transmembrane protein. Smc04208 shows strong identity to other putative toxin secretion transmembrane proteins such as RspE from *A. tumefaciens* (57%) and Atu3382 from *A. tumefaciens* (57%) as determined by BLASTP at NCBI.

4.3.2: *In silico* Analysis Of Smc04205

Smc04205

Smc04205 is located at position 2190347-2193001 of the *S. meliloti* 1021 chromosome. A putative ribosome binding site, CGGGG, was identified upstream of the predicted translational start codon. The protein encoded by Smc04205 is 885 amino acids in length with a predicted molecular weight of 95.38 kDa. Analysis of Smc04205 using the PSORT program (Nakai and Kanehisa, 1991) indicated that the protein contains a 40 amino acid signal sequence typical for exported proteins.

Cleavage of the signal sequence between the residues LAA-QE would result in a mature protein the predicted size of which is 91.18 kDa with a pI of 4.82. The amino acid sequence and predicted signal sequence of Smc04205 is shown in Figure 4.2.

Figure 4.2: Amino Acid Sequence Of Smc04205

MAYGAASKRDTQFTTRYLRGFLLSTSAAIAVVCTAPQLAAQEIAATPQQSQAVRNFD
IPSQPLASALALFNRQSGIQISQAAAGRTSNVTTRAVRGRMTPEQALAQLLDGTGVH
YQFTANRAAVIGPAGDAGAPGSEEGATVLKRIVVTGKTGRNANSGAGFQGTPDWVYE
EPASVSVVSRDAVQSRAARNANDVLDSVAGVTSNRSEAQNPGIAINVRGLQDQNRVT
TMIDGARQDFQRAGHGASQRVYVDTAFLRSVEVEKGAVAGVGGAGSLGGAVNFRTVT
ADDIITPDRDRGVELNAETGTNAYYFNGSLIGAARFSEDFSVLGGISRKRVGDYDFG
QNGKSPLLDLAVTTAVDDSFLFSRLETFGTLLKVEGSPSDDFTFDLSWLRNDSEAIQ
GGLVFGDLRDDPQNYLNNTVSSSFEWDPDSELIDLKGRLWYNRVVNDELRDYTPRLP
ITYAMTSFGGSLDNTSRFETALGDLSLNYGGEAYSDNGKTTTPPLVDDQGFDEAYGY
KGLNPVGRRSMTSAFLNATLEHDDWLEVGAGLRYDRYRLKGFTEVGGRKPRYIVVPG
VCGYFYDDGECAYYDEDPVYGGGEAVLERVDIDKSGGALLPSARIAVMPFEGIQPFV
TYAHTYRPPSVMEALTSGGHPGDAIATYIPNPYLKPERGRTWELGINIARDGLFTAG
DSLRLKTVYFDRTIQDYITLGNGYFATFDKNLFQHVNLDGDTTMNGVEIEASYDMGS
AYVGASYTYLKTDYADTYSYSGPTASGTPLAASGNTPVPSVLFVPPENKFTLDAGIR
LFERKLVLGGRATYVSDSKPTVGQLAGLFNTAGYKVFDIYGSYSFSDSAKLRLAINN
VTDEQYAPALGAFYYPAPGRTATVSLNFKF

The amino acid sequence of Smc04205 was compared against the NCBI database of protein sequences using the BLASTP program (Altschul *et al*, 1997). Analysis of the Smc04205 amino acid sequence revealed a significant degree of sequence identity to the family of haem outer membrane receptors. The five most significant matches to Smc04205 identified using the BLASTP program and their associated predicted biochemical data are listed in Table 4.1 and illustrated in Figure 4.3.

Table 4.1: Proteins Displaying Significant Homology To Smc04205

Protein	Homologue	Molecular Mass (kDa)*	Accession Number	Identities (%)**
Atu3385	*A. tumefaciens* C58	99.69	NP_533882	37 (53)
HasR	*P. fluorescens* no. 33	101.18	BAA88490	26 (42)
HasR	*S. marcesens* SM365	98.28	CAA70172	26 (42)
HasR	*P. aeruginosa* PA01	97.86	NP_252098	25 (41)
YPO3923	*Y. pestis* CO92	93.50	NP_407367	22 (28)

*The predicted molecular mass (kDa) is calculated for the unprocessed protein.

**Identities (%) were calculated using the Genedoc program. Similarities are indicated in brackets.

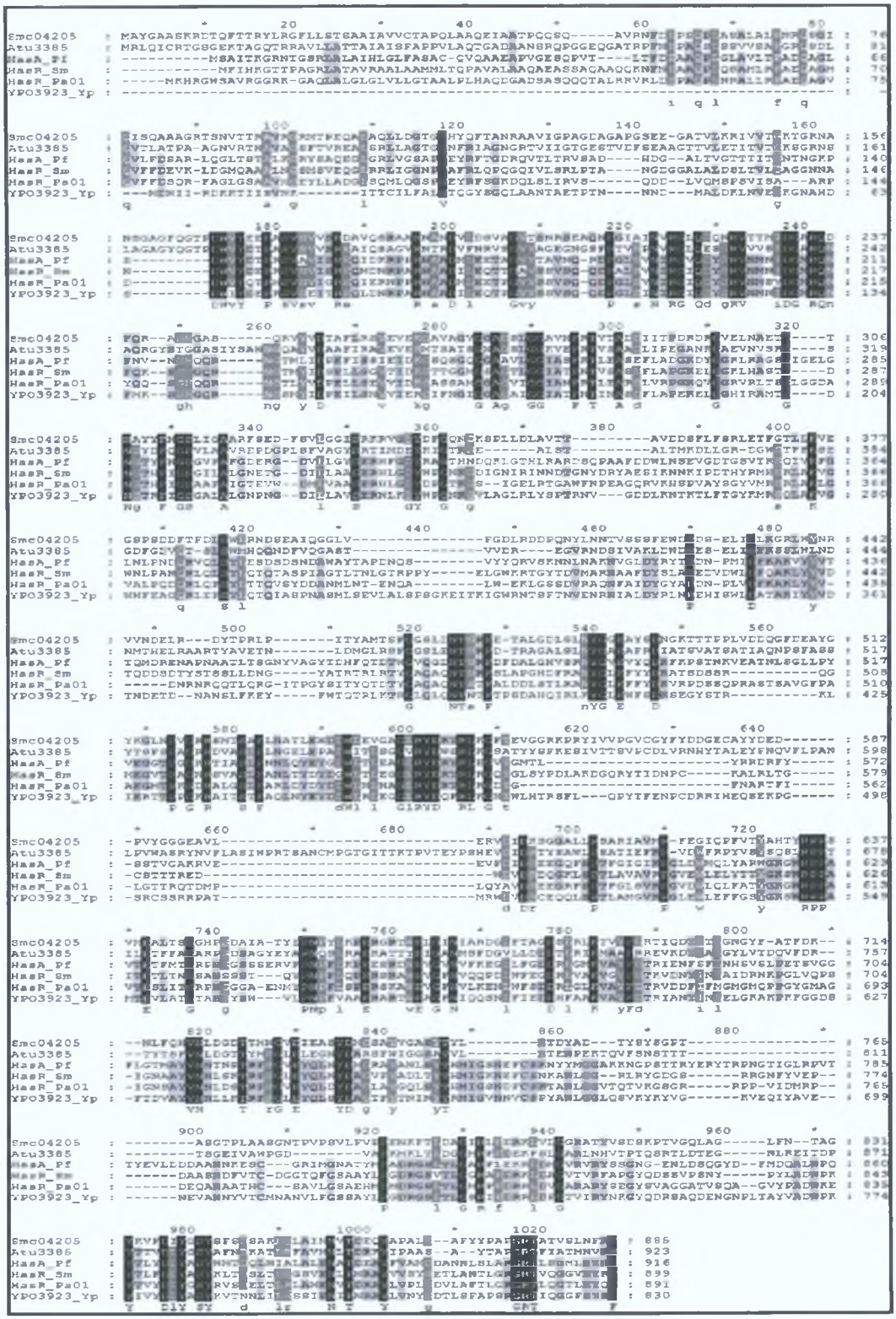

Figure 4.3: Multiple sequence aligenment of Smc04205; with *A. tumefaciens* C58 Atu3385, *P. fluorescens* no.33 HasR (HasR_Pf), *S. marcesens* SM365 HasR (HasR_Sm), *P. aeruginosa* PA01 HasR (HasR_Pa01) and *Y. pesitis* CO92 YPO3923 (YPO3923_Yp). Black indicates 100% conservation, dark grey indicates 83% conservation and light grey indicates 66% conservation.

The sequence of Smc04205 was analysed to determine if the protein contained the amino acid sequence motifs conserved among TonB-dependent receptors, previously designated regions I, II and III (Bitter *et al*, 1991). Region I is the 'TonB box' with the consensus sequence (D/E)TXXVXA(A/S) although this sequence is somewhat degenerate. Region I is typically located near the N-terminus of the protein (Bitter *et al*, 1991; Ankenbauer and Quan, 1994). Analysis of the N-terminal region of Smc04205 did not reveal the presence of a TonB motif in this region.

Region II is typically located in the C-terminal part of the protein and has the consensus sequence (F/I/L/M/V)XXX(I/L/V)XNLX(D/N)(K/R)XY. The amino acid sequence of Smc04205 was analysed and found to contain the motif LRLAINNVTDEQY at position 849-861.

Region III is typically located at a distance of 100 amino acids from region I. The region is characterised by the consensus sequence R(V/I)(D/E)(I/V)(I/V/L)(K/R)GXX(G/S/A)XXXGXXXXG(G/A)X(V/I). The amino acid sequence of Smc04205 was analysed and found to contain the motif SVEVEKGAVAGVGGAGSLGGAV at position 258-279.

Further analysis of the amino acid sequence of Smc04205 revealed the presence of the so-called FRAP-NPNL motif that is reported to be a common motif in haem receptors (Nienaber, 2001). The highly conserved histidine residue within the FRAP-NPNL is also conserved in Smc04205.

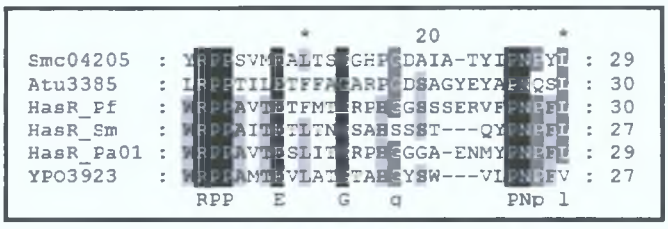

Figure 4.4: The FRAP-NPNL Motif Of Smc04205. Black indicates 100% conservation, dark grey indicates 83% conservation and light grey indicates 66% conservation.

The finding of the N-terminal signal sequence, the presence of the two characteristic 'TonB motifs' and the FRAP-NPNL motif suggest that Smc04205 is a TonB dependent haem outer membrane receptor.

4.4: The Mutagenesis Of Smc04205

As previously described (Chapter 3), the subcloning and subsequent mutatgenesis of of DNA fragments encoding various genes of interest was the method of choice when such a strategy was easily applicable. However, although a pLAFR1 based cosmid bank of *S. meliloti* 1021 was available, the cosmid bank was not ordered and it was considered that the isolation of the relevant cosmid encoding Smc04205 would be both laborious and time consuming. For that reason, it was decided to use PCR to amplify the region of interest for subsequent mutagenesis.

Sequence analysis of the Smc04205 gene revealed the presence of a unique *Bam*H1 site within the gene into which an antibiotic resistance cassette could be inserted. Two primers, Hem-F and Hem-R (Chapter 2) were designed to amplify a 2.7 Kb region of the *S. meliloti* 2011 genome encoding Smc04205, with the *Bam*H1 site centrally located. The forward primer Hem-F was designed so as to incorporate a unique *Apa*1 site into the PCR product. The region that the reverse primer was designed to prime contained a natural *Not*1 site, and this site was incorporated into the reverse primer. The unique *Apa*1 and *Not*1 sites in the PCR product were added to allow for the subsequent directional cloning of the 2.7 Kb fragment into pJQ200ks (Chapter 3), thereby removing the vector borne *Bam*H1 site.

Figure 4.5: **Primers For The Amplification Of A Region Encoding Smc04205.**

*Apa*1
Hem-F: 5' GGG CCC TCG ACG GCA CCG GGG GGG 3'

*Not*1
Hem-R: 5' GCG GCC GCT TCA CTC GAA CCA CTC TAG AAC T 3'

Restriction sites are underlined and indicated in blue.

Total genomic DNA was prepared from *S. meliloti* 2011 and used as the template DNA in the PCR reaction. Initial attempts to amplify the region encoding Smc04205 resulted in the amplification of several smaller non-specific PCR bands. The annealing temperature was increased, which lead to the elimination of some of the non-specific bands, but also lead to a decrease in the yield of the 2.7 Kb band.

The PCR reaction was optimised using a PCR optimisation kit (PCR Optimizer™ Kit, Invitrogen) in order to eliminate the non-specific PCR bands. The PCR optimisation kit allows the variation of magnesium concentration and pH within the PCR reaction. Varying the magnesium concentration and pH of the PCR reaction alters the specificity of priming, which eliminates non-specific products. Successive rounds of optimisation were performed until a specific PCR product was obtained.

Table 4.2: PCR Reaction Conditions For The Amplification Of The Region Encoding Smc04205

PCR Conditions	
Reaction Buffer (5X)	Buffer G*
Annealing Temp.	61°C
Annealing Time	1 min
Extension Time	3.5 min

*Buffer G: 12.5 mM $MgCl_2$, pH 9.0

Following optimisation of the PCR reaction, a specific 2.7 Kb PCR fragment was obtained and cloned into the pCR2.1 vector generating pCR2.7 A/N. The 2.7 Kb fragment was restricted from pCR2.7 A/N as an *Apa*1/*Not*1 fragment and cloned into pJQ200ks generating pOC2.7 A/N. The kanamycin cassette from pUC4K was inserted into the unique *Bam*H1 site of pOC2.7 A/N generating pOC2.7K A/N.

The plasmid pOC2.7K A/N was introduced into *S. meliloti* 2011 by triparental mating and transconjugants were selected on TY containing streptomycin and gentamicin. Second recombinants were selected by growing a single first recombinant without antibiotic selection in TY broth until early stationary phase, and then by plating on TY agar containing 5% sucrose and kanamycin. Individual colonies were screened for kanamycin resistance and gentamicin sensitivity. A potential mutant was identified in this way and selected for further analysis.

The genomic sequence in the region encoding Smc04205 was examined to identify restriction sites that were deemed suitable for the confirmation of the potential mutant by Southern blot analysis (Chapter 2). The kanamycin cassette was inserted into a

*Bam*H1 site encoded within a 4.6 Kb *Xho*1 fragment (Figure 4.6). As the kanamycin cassette from pUC4K encodes a unique *Xho*1 site, digestion of the mutant genomic DNA with *Xho*1 would generate two *Xho*1 fragments as indicated in Figure 4.7. The plasmid pOC2.7K A/N was labelled as described in Chapter 2 and used as a probe.

Figure 4.6: Analysis Of The Region Encoding Smc04205 In *S. meliloti* 2011

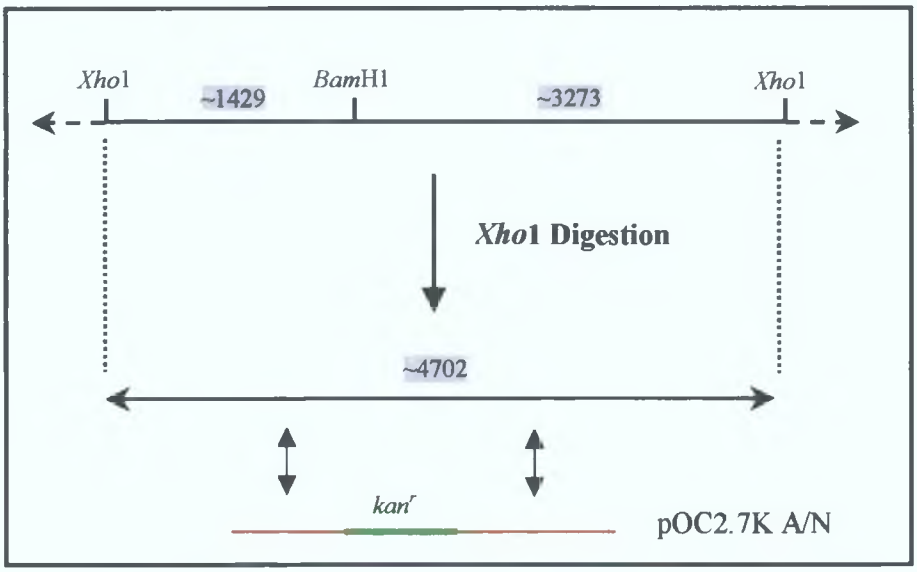

The predicted sizes of the digested fragments are highlighted in grey. The labelled probe is indicated in red, while the kanamycin cassette is highlighted in green. Regions of homology between the labelled probe and the digested fragments are indicated.

Figure 4.7: Analysis Of The Region Encoding Smc04205 In A Potential Mutant

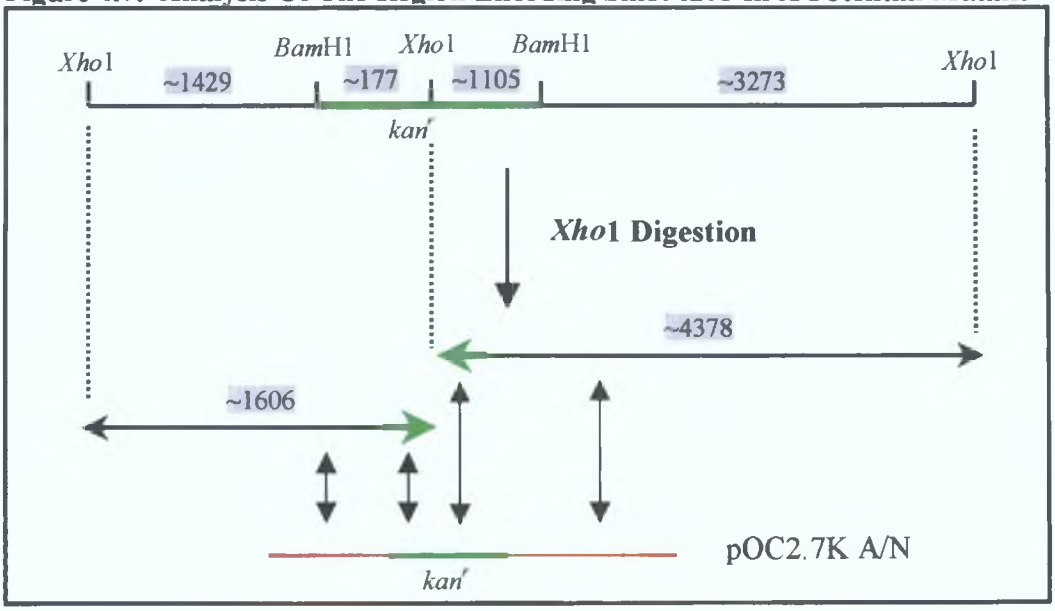

The predicted sizes of the digested fragments are highlighted in grey. The labelled probe is indicated in red, while the kanamycin cassette is highlighted in green. Regions of homology between the labelled probe and the digested fragments are indicated.

Genomic DNA was prepared from *S. meliloti* 2011 and the potential mutant (Chapter 2), restricted with *Xho*1, transferred to nitrocellulose and probed with labelled plasmid as described in Chapter 2. Examination of the hybridisation result indicated that the kanamycin cassette had correctly integrated into the chromosome of *S. meliloti* 2011 (Figure 4.8).

Figure 4.8: Southern Blot Analysis Of *S. meliloti* 2011 And *S. meliloti* 2011Smc04204km

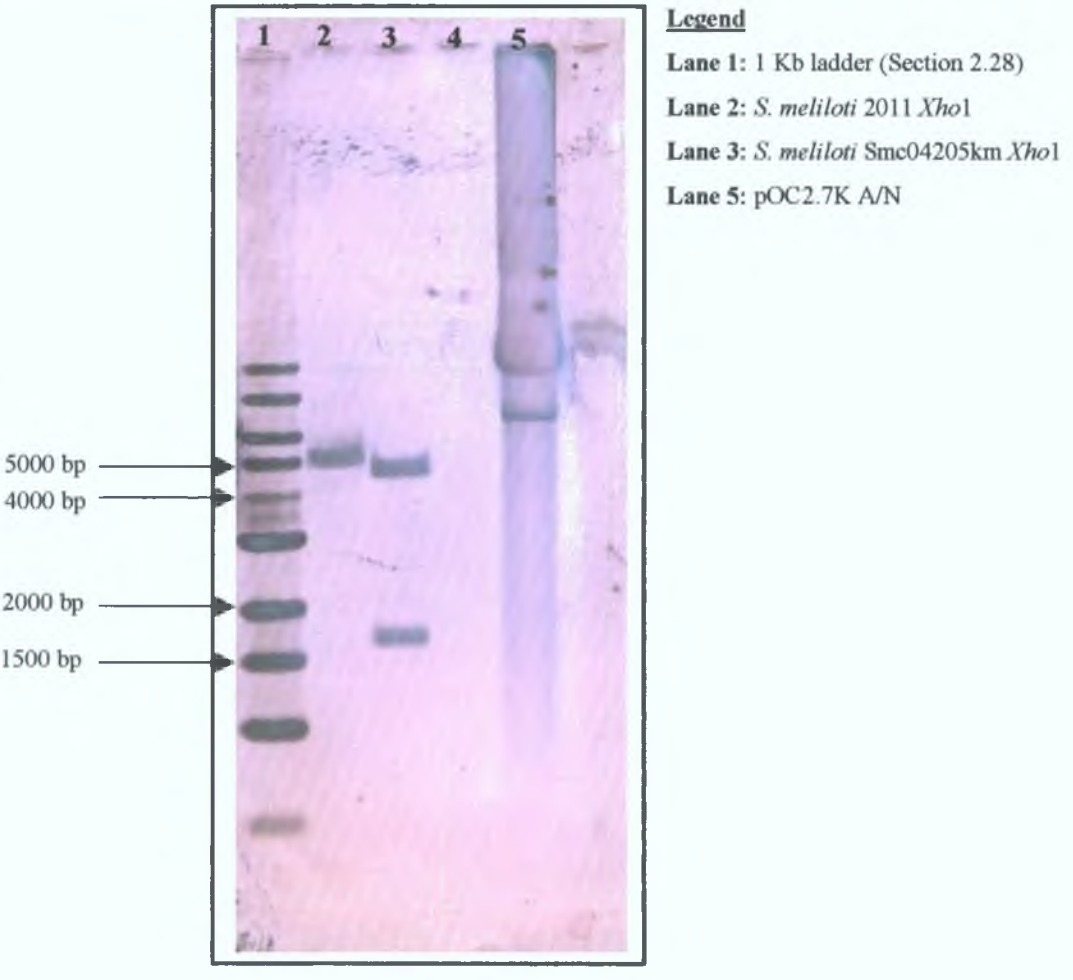

The mutant strain was named *S. meliloti* 2011Smc04205km. The phenotypic characterisation of the *S. meliloti* 2011Smc04205km is described in Section 4.10.

4.5: Analysis Of The Smc02726 Locus

Smc02726 is located at position 2578291-2576063 on the *S. meliloti* chromosome. Directly upstream of Smc02726 and orientated in the same direction is *trp*E(G) (Smc02725). The protein encoded by *trp*E(G) has been previously characterised and shown to encode anthranilate synthase. Anthranilate has been proposed to act as an *in planta* siderophore in *S. meliloti* (Chapter 1)(Barsomian *et al*, 1992). Directly downstream of Smc02726, and orientated in the opposite direction is a gene, Smc02727, encoding a protein of unknown function. None of the other proteins in the vicinity of Smc02726 show homology to proteins known to be involved in haem or iron acquisition. The iron utilisation locus in this region is predicted to consist of Smc02726 and possibly Smc02725. A map of the region is shown in Figure 4.9.

Figure 4.9: Map Of The Region Encoding Smc02726.

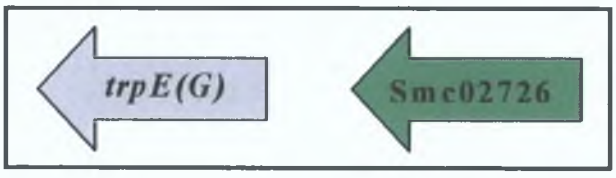

Legend

- Putative outer membrane haem receptor
- Anthranilate synthase

4.5.1: *In silco* Analysis Of The Genes Proximal To Smc02726

***trp*E(G)**

*trp*E(G) is located at position 2575786-2573600 of the chromosome. A putative ribosome binding site, GGAGC, was identified upstream of the predicted translational start site. The protein predicted to be encoded by *trp*E(G) is 729 amino acids in size with a predicted molecular weight of 80.5 kDa and a pI of 5.44. BLASTP analysis predicted that TrpE(G) is predicted to encode a putative anthranilate synthase. Smc02725 shows strong identity to other putative anthranilate synthase proteins such as TrpE(G) from *A. tumefaciens* (82%) and Mlr2774 from *M. loti* (75%) as determined by BLASTP at NCBI.

4.5.2: *In silico* Analysis Of Smc02726

Smc02726 is located at position 2578291-2576063 on the *S. meliloti* 1021 chromosome. A putative ribosome binding site, GGACT, was identified upstream of the predicted translational start codon. The protein encoded by Smc02726 is 743 amino acids in length with a predicted molecular weight of 80.57 kDa. Analysis of Smc02726 using the PSORT program (Nakai and Kanehisa, 1991) indicated that the protein contained a 27 amino acid signal sequence typical for exported proteins. Cleavage of the signal sequence between the residues VLA-QS would result in a mature protein the predicted size of which is 77.6 kDa with a pI of 4.71. The amino acid sequence and predicted signal sequence of Smc02726 is indicated in Figure 4.10.

Figure 4.10: Amino Acid Sequence Of Smc02726.

MLNRHHRLALLACTAAIFALPIPPVLAQSAPTETAAEGNANTTVLKKIVAKGDRLAG
AQRGGIADTPLATEIDAKTLEEKQVTDLDDLGRSVDAGINASRADFGINLRGLSGPR
IVTTIDGVPIPYISNSARQGAFASINANGGGDMFDFNSLSVVDIVRGADSSRGGSGM
LGGAVVLRTLEPEDVISDGKDWGAIFRSIYDSEDDSIAGSVAGAHRFGQTSVLFQGS
YRKGNERDNEGTVGGYGSARTEPNPTDFDQNNLLFKFRHELEGGHRIGLTAESFRRD
ADNDLRAEQGRRYKIGDYTGFEDRDRKRVSLDYDFEAASSDDFFSFARASLYWQDLE
RSSGSNGRTIADVPYGRDNSISNESVGFNGRAGKDFETGGFDHSLTFGLDVARSEWS
QYTSAVCPTPATCPALNNQSEVPDVRSMTVGAILEDRISVGDSAFALTPGLRFDWFQ
YDPQLNAGFESNTGSGIFGDLKARDGVRLSPKLLATYDVTPDVELFAQWSMAFRAPT
VDELYSRFYNPFGNYAQLGNPDLKPETGKGFEIGANFDTGELSGRVAAFHNIYDNFI
ETGDSINSDTGIREFKYANVNKARISGIELSALKTFDNGFNLHASLAYSYGKNEDEG
TRLRTVAPFKAIIGGGYSQETFGVDVSTTVSAAMPDDNDSETFDAPGYGLVDMTGWW
TPESFKGLRVEAGVYNIFDKKYFNALGVRGVDLASSSAQPRDFYSEPGRTFKVSLTQ
RF

The amino acid sequence of Smc02726 was compared against the NCBI database of protein sequences using the BLASTP program (Altschul *et al*, 1997). Analysis of the Smc02726 amino acid sequence revealed a significant degree of identity to the family of putative haem outer membrane receptors. The five most significant matches to Smc02726 identified using the BLASTP program and their associated predicted biochemical data are listed in Table 4.3 and illustrated in Figure 4.11.

Table 4.3: Proteins With Significant Homology To Smc02726.

Protein	Homologue	Molecular Mass (kDa)*	Accession Number	Identities (%)**
Atu2287	*A. tumefaciens* C58	82.92	NP_355244	46 (63)
BhuR	*B. avium* 4169	92.93	AAM28268	29 (45)
Pflu1071	*P. fluorescens* Pf0-1	95.20	ZP_00083834	22 (35)
Psyr1905	*P. syringae* pv. syringae B728a	93.91	ZP_00125613	21 (36)
PSPTO1284	*P. syringae* pv. tomato str. DC3000	93.86	NP_791113	21 (35)

*The predicted molecular mass (kDa) is calculated for the unprocessed protein.

**Identities (%) were calculated using the Genedoc program. Similarities are indicated in brackets.

Figure 4.11: Multiple sequence alignment of Smc02726; with *A. tumefaciens* C58 Atu2287, *B. avium* 4169 BhuR (BhuR_Ba), *P. fluorescens* Pf0-1 Pflu1071, *P. syringae* pv. syringae B728a Psyr1905 and *P. syringae* pv. tomato str. DC3000 PSPTO1284. Black indicates 100% conservation, dark grey indicates 83% conservation and light grey indicates 66% conservation.

As described in Section 4.3.2, the amino acid sequence of Smc02726 was analysed to determine if the protein contained the amino acid sequence motifs conserved among TonB-dependent receptors, previously designated regions I, II and III (Bitter *et al*, 1991). Region I is the 'TonB box' with the consensus sequence (D/E)TXXVXA(A/S) although this sequence is somewhat degenerate. Region I is typically located near the N-terminus of the protein (Bitter *et al*, 1991; Ankenbauer and Quan, 1994). Analysis of the N-terminal region of Smc02726 did not reveal the presence of a TonB motif.

As described in Section 4.3.2, region II is typically located in the C-terminal part of the protein and has the consensus sequence (F/I/L/M/V)XXX(I/L/V)XNLX(D/N)(K/R)XY. The amino acid sequence of Smc02726 was analysed and found to contain the motif VEAGVYNIFDKKY at position 694-706.

As described in Section 4.3.2, region III is typically located at a distance of 100 amino acids from region I. The region is characterised by the consensus sequence R(V/I)(D/E)(I/V)(I/V/L)(K/R)GXX(G/S/A)XXXGXXXXG(G/A)X(V/I). The amino acid sequence of Smc02726 was analysed and found to contain the motif VVDIVRGADSSRGGSGMLGGAV at position 155-176.

Further analysis of the amino acid sequence of Smc02726 revealed the presence of the so called FRAP-NPNL motif that is reported to be a common motif in haem receptors (Nienaber, 2001). The highly conserved histidine residue within the FRAP-NPNL is not conserved in Smc02726.

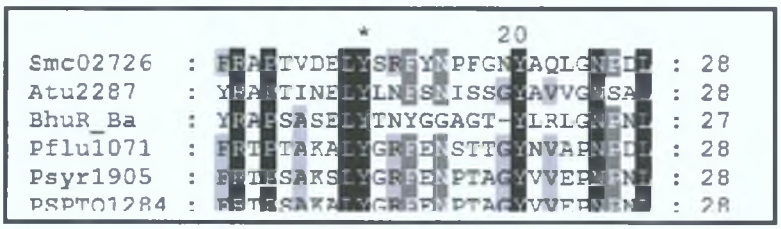

Figure 4.12: The FRAP-NPNL Motif Of Smc02726. Black indicates 100% conservation, dark grey indicates 83% conservation and light grey indicates 66% conservation.

The finding of the N-terminal signal sequence, the presence of the two characteristic 'TonB motifs' and the FRAP-NPNL motif suggest that Smc02726 is a TonB dependent haem outer membrane receptor.

4.6: The Mutagenesis Of Smc02726

Sequence analysis of Smc02726 indicated the presence of a unique *Bam*H1 site within the gene into which an antibiotic resistance cassette could be inserted. Two primers, HemR-F1 and HemR-R1 (Chapter 2) were designed to amplify a 2.2 Kb region of the *S. meliloti* 2011 genome encoding Smc02726. The forward primer was designed to incorporate a unique *Bgl*II site into the PCR product. The reverse primer was designed to incorporate a unique *Not*1 site into the PCR product. The unique *Bgl*II and *Not*1 sites in the PCR product were added to allow for the subsequent directional cloning of the 2.2 Kb fragment into pJQ200ks (Chapter 3). As *Bgl*II and *Bam*H1 have compatible cohesive ends, the cloning of the 2.2 Kb *Bgl*II/*Not*1 fragment into *Bam*H1/*Not*1 restricted pJQ200ks would result in the destruction of the vector borne *Bam*H1 site leaving only the unique *Bam*H1 site within Smc02726.

Figure 4.13: Primers For The Mutagenesis Of Smc02726

*Bgl*II

HemR-F1: 5' AGA TCT TGG GCG TCG GCG TCG GCC GAT CAT C3'

*Not*1

HemR-R1: 5' GCG GCC GCG CAA GCG ACG CAT GGA GGT TGA AGC CG 3'

Restriction sites are underlined and indicated in blue.

Total genomic DNA was prepared from *S. meliloti* 2011 and used as the template DNA in the PCR reaction. Following optimisation of the PCR reaction (Table 4.4), a specific 2.2 Kb PCR fragment was obtained and cloned into the pCR2.1 vector generating pCR2.2 N/Bg. The 2.2 Kb fragment was restricted from pCR2.2 N/Bg as a *Not*1/*Bgl*II fragment and cloned directionally into *Bam*H1/*Not*1 restricted pJQ200ks thereby destroying the vector borne *Bam*H1 site and generating pOC2.2 N/Bg. The kanamycin cassette from pUC4K was inserted into the unique *Bam*H1 site of pOC2.2 N/Bg generating pOC2.2K N/Bg.

Table 4.4: PCR Reaction Conditions For The Amplification Of The Region Encoding Smc02726.

PCR Conditions	
Annealing Temp	71°C
Annealing Time	1 min
Extension Time	3 min

The plasmid pOC2.2K N/Bg was introduced into *S. meliloti* 2011 by triparental mating and transconjugants were selected on TY containing streptomycin and gentamicin. Second recombinants were selected by growing a single first recombinant without antibiotic selection in TY broth until early stationary phase had been reached and then by plating on TY agar containing 5% sucrose and kanamycin. Individual colonies were then screened for kanamycin resistance and gentamicin sensitivity. A potential mutant was identified in this way and selected for further analysis.

The genomic sequence in the region encoding Smc02726 was examined to identify restriction sites that were deemed suitable for the confirmation of the potential mutant by Southern blot analysis (Chapter 2). The kanamycin cassette was inserted into a *Bam*H1 site encoded within a 4.2 Kb *Xho*1 fragment (Figure 4.14). The kanamycin cassette from pUC4K encodes a unique *Xho*1 site, thus digestion of the mutant genomic DNA with *Xho*1 would generate two *Xho*1 fragments to which the probe would hybridise. Digestion of the genomic DNA would also result in a 0.9 Kb *Xho*1 fragment directly downstream from the 4.2 Kb *Xho*1 fragment. As the probe also displays homology to this fragment, it would also be expected to hybridise with the probe (Figure 4.15). The plasmid pOC2.2K N/Bg was labelled as described in Chapter 2 and used as a probe.

Figure 4.14: Analysis Of The Region Encoding Smc02726 In *S. meliloti* 2011

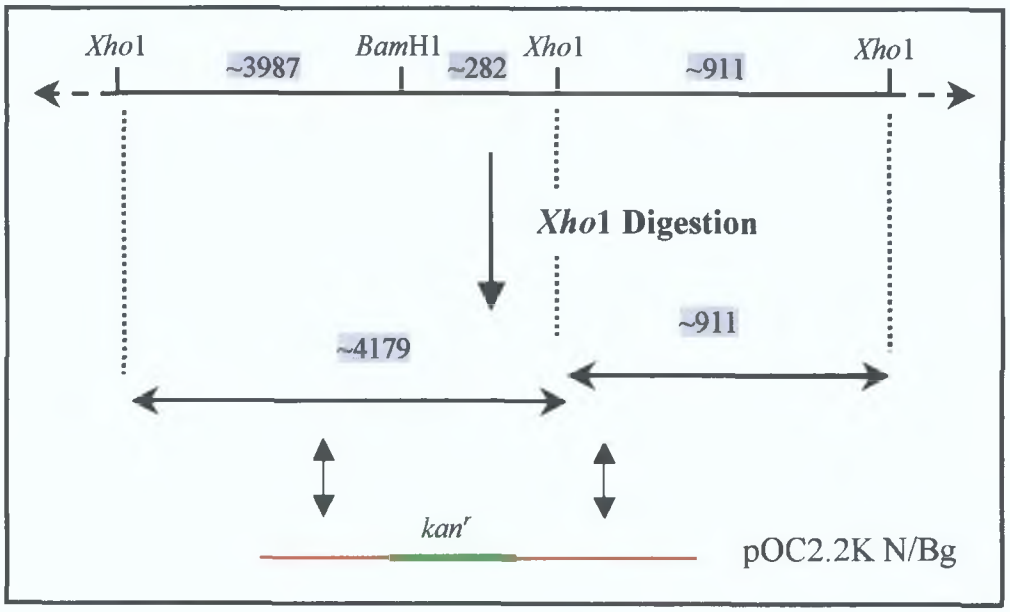

The predicted sizes of the digested fragments are highlighted in grey. The labelled probe is indicated in red, while the kanamycin cassette is highlighted in green. Regions of homology between the labelled probe and the digested fragments are indicated.

Figure 4.15: Analysis Of The Region Encoding Smc02726 In A Potential Mutant

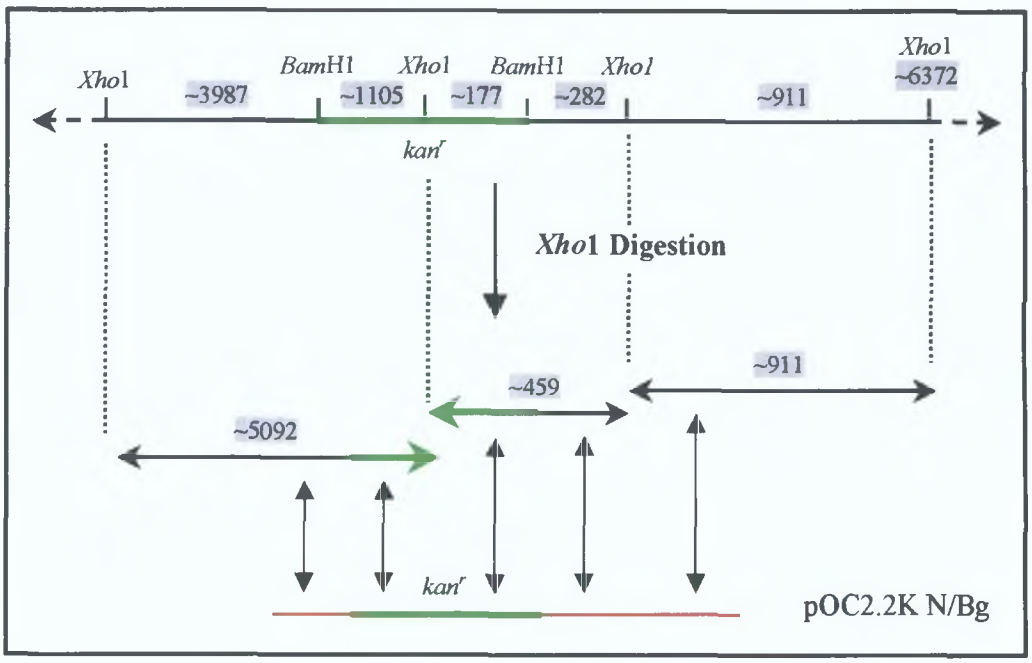

The predicted sizes of the digested fragments are highlighted in grey. The labelled probe is indicated in red, while the kanamycin cassette is highlighted in green. Regions of homology between the labelled probe and the digested fragments are indicated.

Genomic DNA was prepared from *S. meliloti* 2011 and the potential mutant (Chapter 2), restricted with *Xho*1, transferred to nitrocellulose and probed with labelled plasmid as described in Chapter 2. Examination of the hybridisation result indicated that the kanamycin cassette had correctly integrated into the chromosome of *S. meliloti* 2011 (Figure 4.16).

Figure 4.16: Southern Blot Analysis Of *S. meliloti* 2011 And *S. meliloti* 2011Smc02726km.

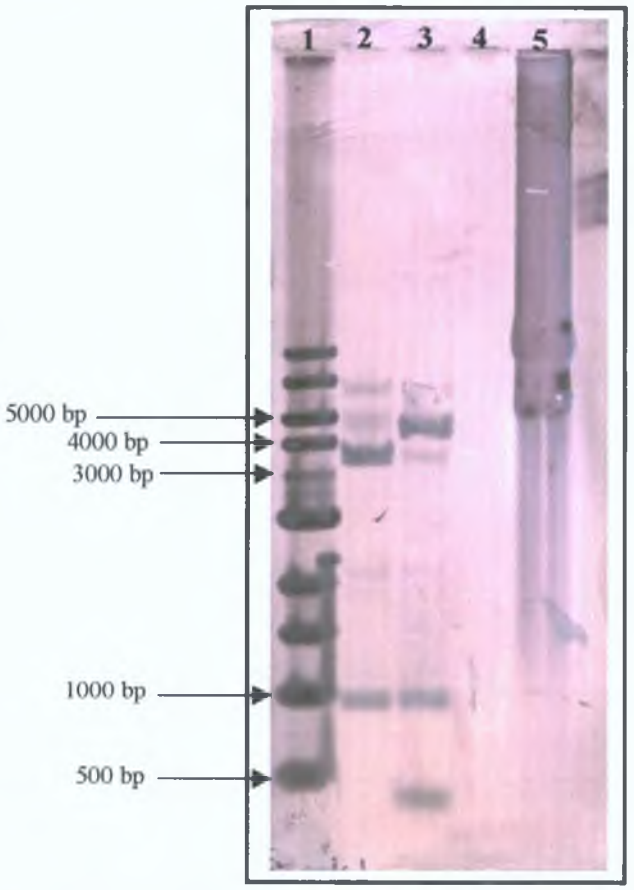

Legend

Lane 1: 1 Kb ladder (Section 2.28)

Lane 2: *S. meliloti* 2011 *Xho*1

Lane 3: *S. meliloti* Smc02726km *Xho*1

Lane 5: pOC2.2K N/Bg

The mutant strain was named *S. meliloti* 2011Smc02726km. The phenotypic characterisation of the *S. meliloti* 2011Smc02726km is described in Section 4.10.

4.7: Analysis Of The *hmu* Locus

Analysis of the *S. meliloti* 1021 genome sequence revealed a putative inner membrane haem transport system. The organisation of the genes in this region of the chromosome shows similarity to the characterised *hmu* system of *R. leguminosarum* (Chapter 1; Wexler *et al*, 2001). The genes encoding the *hmu* system are organised in the order *hmuSTUV*. There are very small gaps in between the genes suggesting that the genes are organised as an operon. Directly downstream of *hmuV* and transcribed in same orientation is Smc01509. Smc01509 is predicted to encode a protein of unknown function. Directly upstream of *hmuS* and transcribed in the same orientation is Smc01513. Directly upstream of Smc01513 and transcribed in the opposite orientation, a cluster of genes is located that includes the *S. meliloti* 1021 putative *tonB* gene. There are five predicted genes in the cluster; Smc01514, Smc01515 (*tonB*), Smc01516, Smc01517 and Smc01518. The functions of Smc01514, Smc01516, Smc01517 and Smc01518 are unknown although analysis of the Smc01514 and Smc01515 homologues in *R. leguminosarum* indicated that they were co-transcribed (Wexler *et al*, 2001). A map of the region is shown in Figure 4.17. In this section, only genes predicted to be involved in the transport of haem at the inner membrane will be discussed.

Figure 4.17: Map Of The Region Encoding *hmuT* And A Comparison With A Similar Region In *R. leguminosarum*

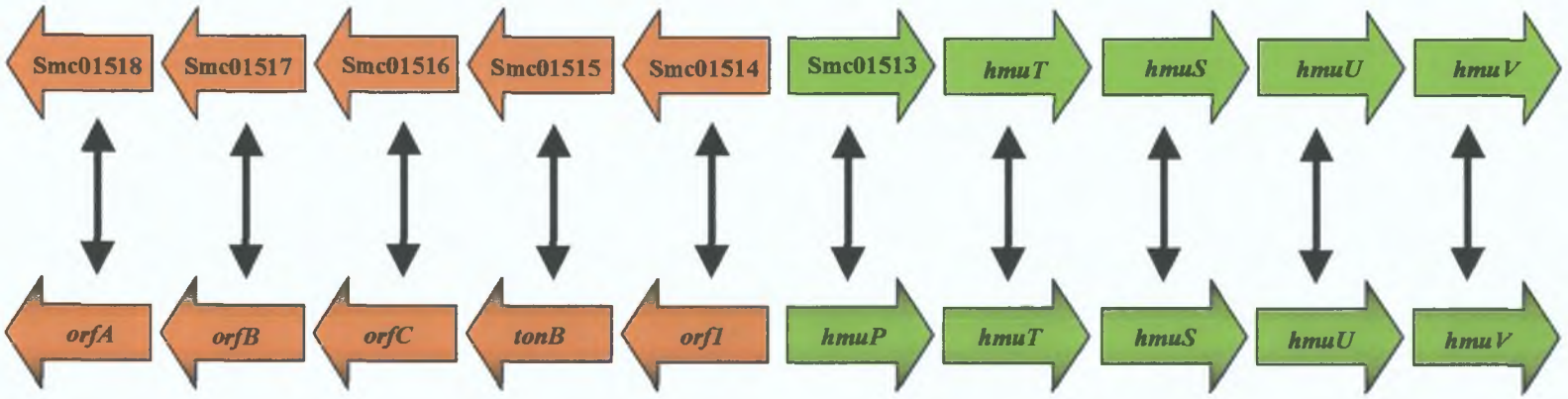

The genes predicted to be part of the *hmu* system of *S. meliloti* 2011 are indicated in green. The upstream *tonB* (Smc01515) locus is indicated in orange. The corresponding homologues (shaded) in *R. leguminosarum* (Wexler *et al*, 2001) are indicated by bi-directional arrows. The corresponding homologue of Smc01513 has been designated *hmuP* in *R. leguminosarum*. A number of the genes have overlapping junctions that are not indicated here.

4.7.1: *In silico* Analysis Of The Genes Proximal To *hmuT*

Smc01513

Smc01513 is located at position 2616325-2616462 of the *S. meliloti* 1021 chromosome. A putative ribosome binding site, CCGCA, was identified upstream of the predicted translational start site. The protein predicted to be encoded by Smc01513 is 46 amino acids in size with a predicted molecular weight of 5.32 kDa and a pI of 9.98. BLASTP analysis indicated that Smc01513 is predicted to encode a putative haemin uptake protein. Smc01513 shows strong identity to other putative haemin uptake proteins such as HmuP from *R. leguminosarum* (81%) and Mll1154 from *M. loti* (66%) as determined by BLASTP at NCBI.

hmuS

hmuS is located at position 2616470-2617534 of the *S. meliloti* 1021 chromosome. A putative ribosome binding site, AGCGA, was identified upstream of the predicted translational start site. The protein predicted to be encoded by *hmuS* is 355 amino acids in size with a predicted molecular weight of 39.27 kDa and a pI of 5.84. BLASTP analysis indicated that HmuS is predicted to encode a putative haemin degrading protein. HmuS shows strong identity to other putative haemin degrading proteins such as HmuS from *R. leguminosarum* (62%) and Mll1152 from *M. loti* (59%) as determined by BLASTP at NCBI.

hmuU

hmuU is located at position 2618550-2619647 of the *S. meliloti* 1021 chromosome. A putative ribosome binding site, AAGGC, was identified upstream of the predicted translational start site. The protein predicted to be encoded by *hmuU* is 366 amino acids in size with a predicted molecular weight of 37.60 kDa and a pI of 10.72. BLASTP analysis indicated that HmuU is predicted to encode a putative haemin transport system permease protein. HmuU shows strong identity to other putative haemin transport system permease proteins such as HmuU from *R. leguminosarum* (50%) and Mll1150 from *M. loti* (47%) as determined by BLASTP at NCBI.

hmuV

hmuV is located at position 2619659-2620444 of the *S. meliloti* 1021 chromosome. A putative ribosome binding site, CAGGG, was identified upstream of the predicted translational start site. The protein predicted to be encoded by *hmuV* is 262 amino acids in size with a predicted molecular weight of 27.85 kDa and a pI of 8.90. BLASTP analysis indicated that HmuV is predicted to encode a putative haemin transport system ATPase protein. HmuV shows strong identity to other putative haemin transport system ATPase proteins such as HmuV from *R. leguminosarum* (62%) and Mll1149 from *M. loti* (60%) as determined by BLASTP at NCBI.

4.7.2: *In silico* Analysis of *hmuT*

hmuT is located at position 2617595-2618542 on the *S. meliloti* 1021 chromosome. A putative ribosome binding site, CGGGA, was identified upstream of the predicted translational start codon. The protein predicted to be encoded by *hmuT* is 316 amino acids in length with a predicted molecular weight of 32.96 kDa. Analysis of HmuT using the PSORT program (Nakai and Kanehisa, 1991) indicated that the protein contained a 44 amino acid signal sequence typical for exported proteins. Cleavage of the signal sequence between the residues AMA-EV would result in a mature protein the predicted size of which is 28.13 kDa with a pI of 5.42. The amino acid sequence of HmuT is shown below. The predicted signal sequence is highlighted Figure 4.18.

Figure 4.18: Amino Acid Sequence Of HmuT

MMNGFAIRRLRRWEMALAAFALSAPFVLPSFAPGAPPFLRPAMAEVLEQPDTSRVVS
VGGAITEIIYALGEENRLVGRDSTSIYPEAATKLPDVGYMRQLAPEGVLAVNPTAIV
AVEGSGPPEALAVLKEANIPFTSVPETYDKDGIVNKIRAVGAFLGVKEKAETLAQSV
EKDLAAAMADSAARPQGERKRVLFILSTQGGRVLASGTGTAAAGIIELAGGVNAVGT
LPGYKALTEEAIIEAKPDVVLMMNRGGSHAAGPDELFALPALSLTPAAKNKALIRMD
GLHLLGFGPRTAGAIRELNAAIYGKKTNASQ

The amino acid sequence of HmuT was compared against the NCBI database of protein sequences using the BLASTP program (Altschul *et al*, 1997). Analysis of the HmuT amino acid sequence revealed a significant degree of sequence identity to the family of putative periplasmic haemin binding proteins. The five most significant matches to HmuT identified using the BLASTP program and their associated predicted biochemical data are listed in Table 4.5.

Table 4.5: Proteins Displaying Significant Homology To HmuT

Protein	Homologue	Molecular Mass (kDa)*	Accession Number	Identities (%)**
HmuT	*R. leguminosarum*	32.68	CAC34393	57 (57)
Mll1151	*M. loti*	30.25	NP_102804	48 (64)
Atu2460	*A. tumefaciens* C58	30.31	NP_533132	44 (59)
HmuT	*B. japonicum*	33.17	CAC38745	41 (58)
Rpal3393	*R. palustris*	25.45	ZP_00011692	29 (45)

*The predicted molecular mass (kDa) is calculated for the unprocessed protein.

**Identities (%) were calculated using the Genedoc program. Similarities are indicated in brackets.

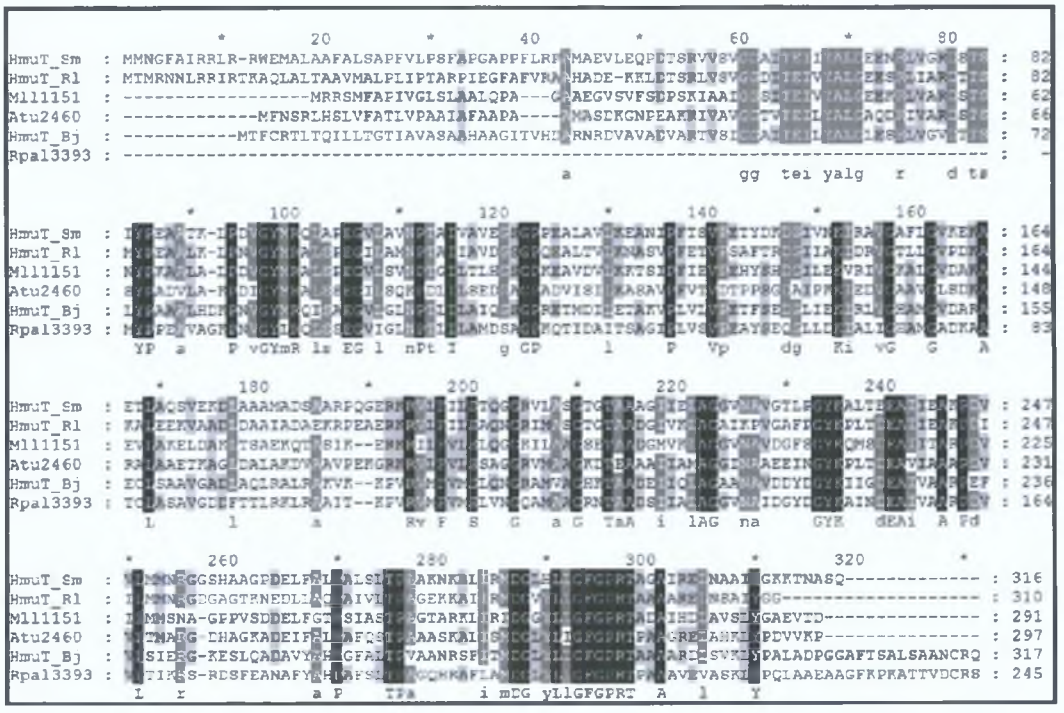

Figure 4.19: Multiple sequence alignment of *S. meliloti* 1021 HmuT (HmuT_Sm); with *R. leguminosarum* HmuT (HmuT_Rl), *M. loti* Mll1151, *A. tumefaciens* C58 Atu2460, *B. japonicum* HmuT (HmuT_Bj) and *R. palustris* Rpal3393. Black indicates 100% conservation, dark grey indicates 83% conservation and light grey indicates 66% conservation.

4.8: The Mutagenesis Of *hmuT*

Sequence analysis of *hmuT* revealed the presence of a unique *Xho*1 site within the gene into which an antibiotic resistance cassette could be inserted. Two primers, HmuT-F and HmuT-R (Chapter 2) were designed to amplify a 2.2 Kb region of the *S. meliloti* 2011 genome encoding *hmuT*, with the *Xho*1 site centrally located. The forward primer HmuT-F was designed so as to incorporate a unique *Sal*1 site into the PCR product. The reverse primer, HmuT-R was designed so as to incorporate a unique *Bam*H1 site into the PCR product. The unique *Sal*1 and *Bam*H1 sites in the PCR product were added to allow for the subsequent directional cloning of the 2.2 Kb fragment into pJQ200ks (Chapter 3). As *Sal*1 and *Xho*1 have compatible cohesive ends, the cloning of the 2.2 Kb *Sal*1/*Bam*H1 fragment into *Xho*1/*Bam*H1 restricted pJQ200ks would result in the destruction of the vector borne *Xho*1 site leaving only the unique *Xho*1 site within *hmuT*.

Figure 4.20: **Primers For The Amplification Of A Region Encoding *hmuT*.**

*Sal*1
HmuT-F: 5' GTC GAC GAA AGC GCC GTC CAC GAA AAG GTC GG 3'

*Bam*H1
HmuT-R: 5' GGA TCC ACG ATC AAA AGC ACC GCG CCG AGG CT 3'

Restriction sites are underlined and indicated in blue.

Total genomic DNA was prepared from *S. meliloti* 2011 and used as the template DNA in the PCR reaction. Following optimisation of the PCR reaction (Table 4.6), a specific 2.2 Kb PCR fragment was obtained and cloned into the pCR2.1 vector generating pCR2.2 S/B. The 2.2 Kb fragment was restricted from pCR2.2 S/B as a *Sal*1/*Bam*H1 fragment and cloned directionally into *Xho*1/*Bam*H1 restricted pJQ200ks generating pOC2.2 S/B. The kanamycin cassette from pUC4K was excised as a *Sal*1 fragment and inserted into the unique *Xho*1 site of pOC2.2 S/B generating pOC2.2K S/B.

Table 4.6: PCR Reaction Conditions For The Amplification Of The Region Encoding *hmuT*

PCR Conditions	
Annealing Temp	71°C
Annealing Time	1 min
Extension Time	3 min

The plasmid pOC2.2K S/B was introduced into *S. meliloti* 2011 by triparental mating and transconjugants were selected on TY containing streptomycin and gentamicin. Second recombinants were selected by growing a single first recombinant without antibiotic selection in TY broth until early stationary phase had been reached and then by plating on TY agar containing 5% sucrose and kanamycin. Individual colonies were then screened for kanamycin resistance and gentamicin sensitivity. A potential mutant was identified in this way and selected for further analysis.

The genomic sequence in the region encoding *hmuT* was examined to identify restriction sites that were deemed suitable for the confirmation of the potential mutant by Southern blot analysis (Chapter 2). The kanamycin cassette was inserted into an *Xho*1 encoded within a larger 7.8 Kb *Xho*1 fragment (Figure 4.21). The kanamycin cassette was inserted into the *Xho*1 site as a *Sal*1 fragment, thus destroying the site. The kanamycin cassette from pUC4K encodes a unique *Xho*1 site, and digestion of the mutant genomic DNA with *Xho*1 would generate two *Xho*1 fragments as indicated in Figure 4.22. The plasmid pOC2.2K X/B was labelled as described in Chapter 2 and used as a probe.

Figure 4.21: Analysis Of The Region Encoding *hmuT* In *S. meliloti* 2011

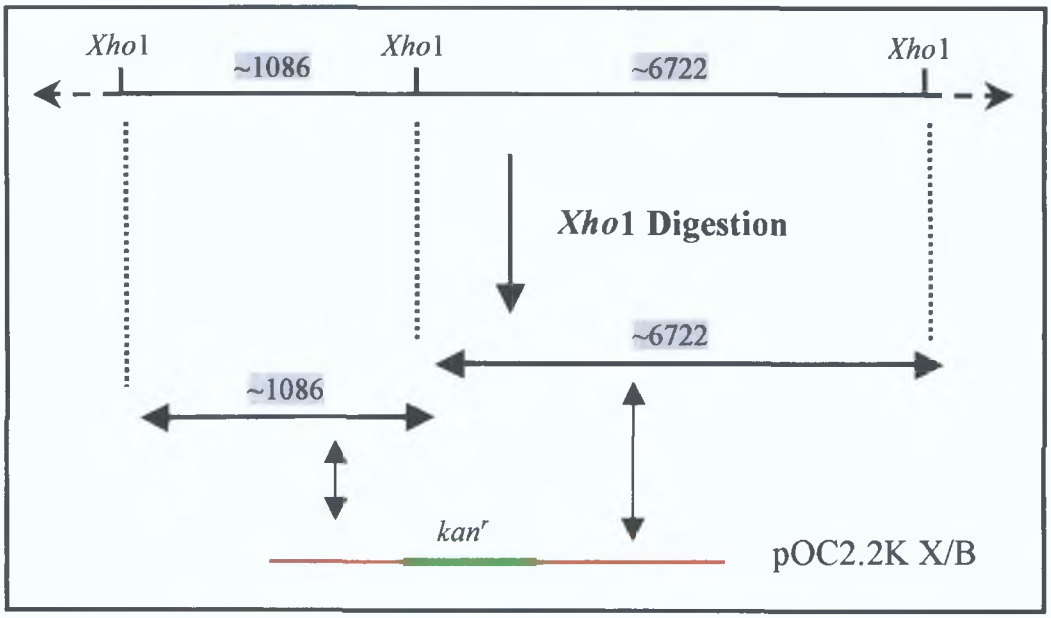

The predicted sizes of the digested fragments are highlighted in grey. The labelled probe is indicated in red, while the kanamycin cassette is highlighted in green. Regions of homology between the labelled probe and the digested fragments are indicated.

Figure 4.22: Analysis Of The Region Encoding *hmuT* In A Potential Mutant

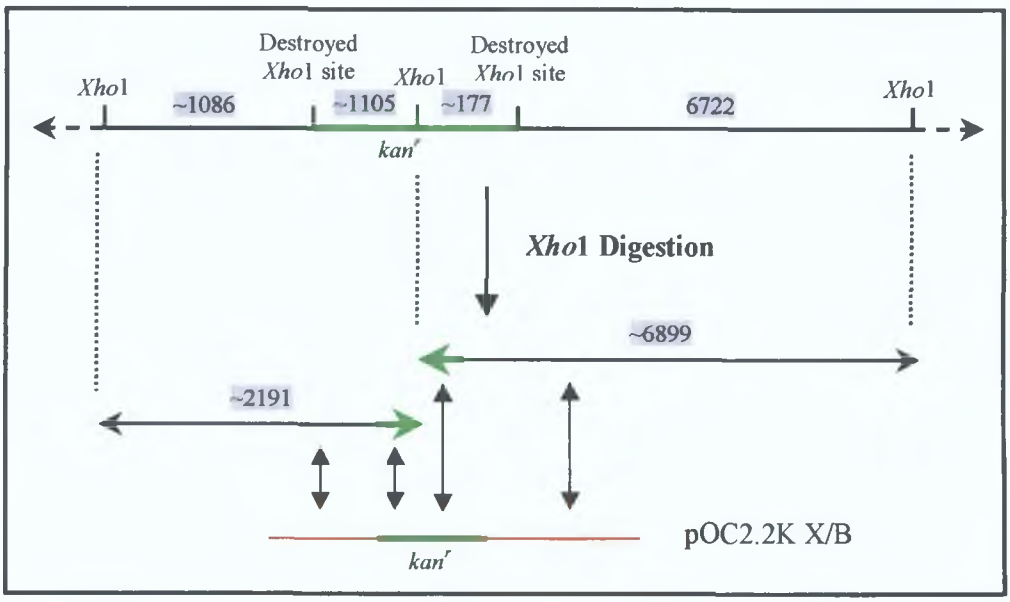

The predicted sizes of the digested fragments are highlighted in grey. The labelled probe is indicated in red, while the kanamycin cassette is highlighted in green.

Regions of homology between the labelled probe and the digested fragments are indicated.

Genomic DNA was prepared from *S. meliloti* 2011 and the potential mutant (Chapter 2, restricted with *Xho*1, transferred to nitrocellulose and probed with labelled plasmid as described in Chapter 2. Examination of the hybridisation result indicated that the kanamycin cassette had correctly integrated into the chromosome of *S. meliloti* 2011 (Figure 4.23).

Figure 4.23: Southern Blot Analysis Of *S. meliloti* 2011 And *S. meliloti* 2011*hmuT*-km.

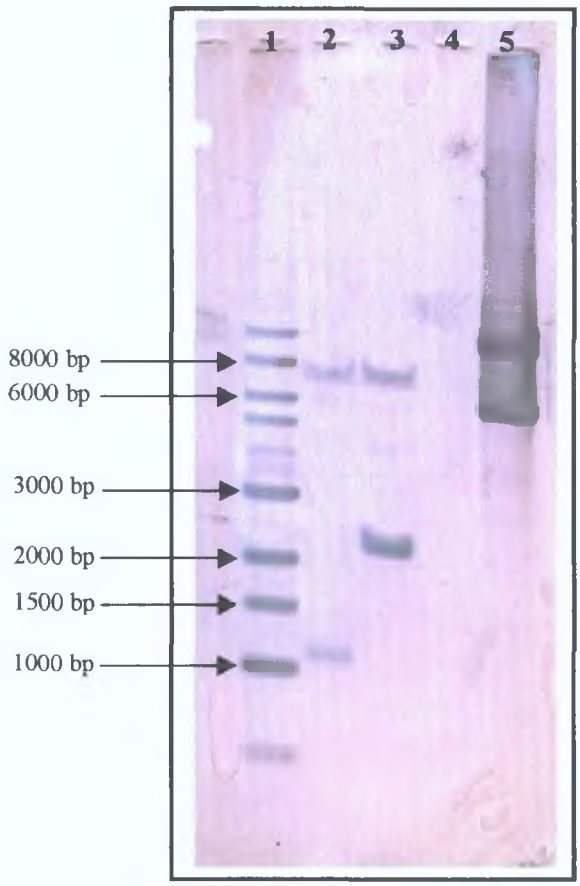

Legend

Lane 1: 1 Kb ladder (Section 2.28)

Lane 2: *S. meliloti* 2011 *Xho*1

Lane 3: *S. meliloti hmuT*-km *Xho*1

Lane 5: pOC2.2K X/B

The mutant strain was named *S. meliloti* 2011*hmuT*-km. The phenotypic characterisation of the *S. meliloti* 2011*hmuT*-km is described in Section 4.10.

4.9: Phenotypical Analysis Of *S. meliloti* 2011 Haem Mutants

In order to determine if *S. meliloti* 2011Smc04205km, 2011Smc02726km and 2011*hmuT*-km were affected in their ability to utilise various haem compounds, haem utilisation bioassays were performed on each mutant. All three haem mutants were generated from the parent strain *S. meliloti* 2011. *S. meliloti* 2011 is unaffected in rhizobactin 1021 production and utilisation and therefore is able to grow on low iron media. In order to minimise background growth and to determine the effect of the mutations on haem utilisation, 2,2' dipyridyl was added to TY agar to a final concentration of 400 μM. Haem utilisation bioassays were performed and the ability of the *S. meliloti* mutants to utilise the haem compounds haemoglobin and haemin was determined (Table 4.7)

Table 4.7: Phenotypical Analysis Of Haem Utilisation By *S. meliloti* 2011.

S. meliloti	**Haemoglobin Utilisation**	**Haemin Utilisation**
2011	+	+
2011Smc04205km	+	+
2011Smc02726km	-	-
2011*hmuT*-km	+	+

Analysis of the mutant phenotypes indicated that *S. meliloti* 2011Smc04205km was unaffected in its ability to utilise haemoglobin and haemin. The result indicated that *S. meliloti* 2011Smc02726km was unable to mediate haemoglobin or haemin acquisition (Figure 4.25). The ability of *S. meliloti* 2011*hmuT*-km to utilise both haem compounds remained unaffected, indicating that there is possibly another inner membrane haem transport system in *S. meliloti* 1021 that has yet to be identified.

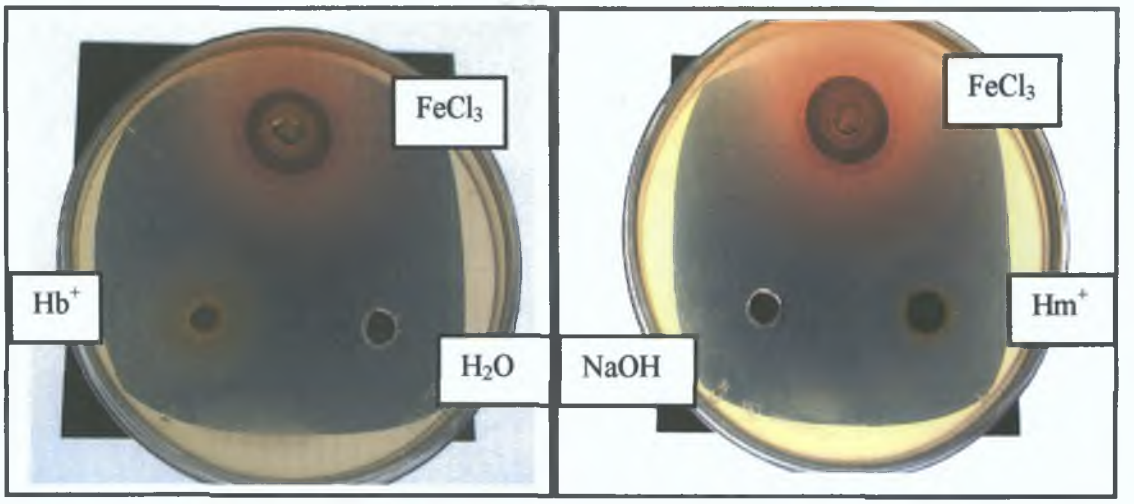

Figure 4.24: Analysis Of Haemoglobin (Hb^+) And Haemin (Hm^+) Utilisation By *S. meliloti* 2011. Ferric chloride ($FeCl_3$) was used as a positive control, while water (H_2O) and sodium hydroxide (NaOH) were used as negative controls for haemoglobin and haemin utilisation respectively.

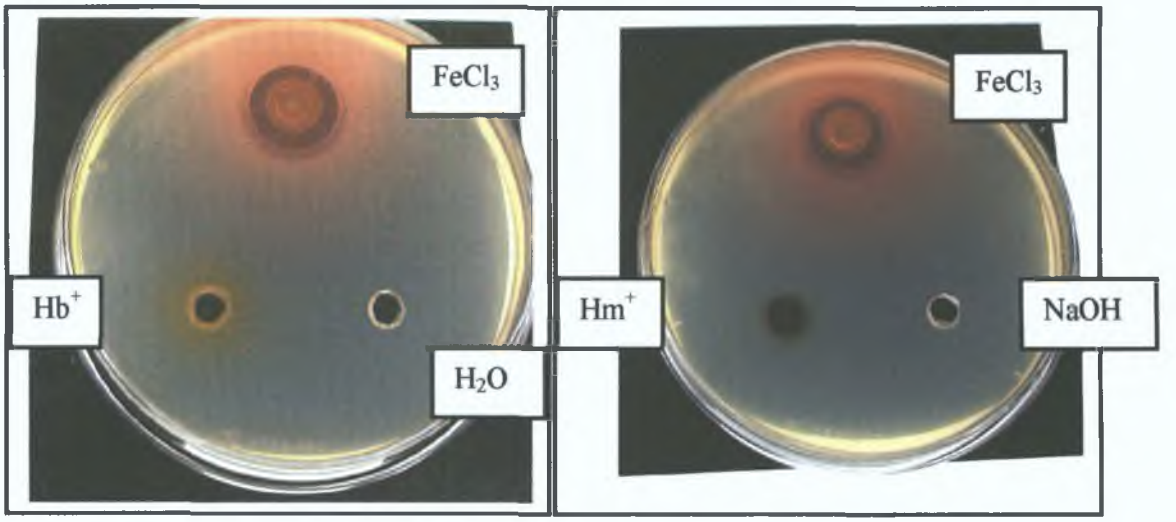

Figure 4.25: Analysis Of Haemoglobin (Hb^+) And Haemin (Hm^+) Utilisation By *S. meliloti* 2011Smc02726km. Ferric chloride ($FeCl_3$) was used as a positive control, while water (H_2O) and sodium hydroxide (NaOH) were used as negative controls for haemoglobin and haemin utilisation respectively.

4.10: Effect Of Haem Utilisation Mutations On Symbiotic Nitrogen Fixation

S. meliloti 2011 induces nodule formation and enters into a nitrogen fixing symbiosis with *Medicago sativa* (alfalfa). The ability of the mutant strains *S. meliloti* 2011Smc04205km, *S. meliloti* 2011Smc02726km and *S. meliloti* 2011*hmuT*-km to enter into an effective nitrogen fixing symbiotic relationship with *M. sativa* was examined. The effect of *S. meliloti* 2011 on plants was examined as a positive control. Uninoculated plants were examined as a negative control.

Following a thirty-day incubation the plants were analysed to determine if the mutants had induced nodulation. All the plants examined showed nodule formation. The nodules had a reddish hue indicating the presence of leghaemoglobin. The nodules were similar to those produced by *S. meliloti* 2011. The uninoculated plants did not show any nodule formation. No difference was observed between plants indicating that the haem mutations were not having noticeable effect on symbiosis.

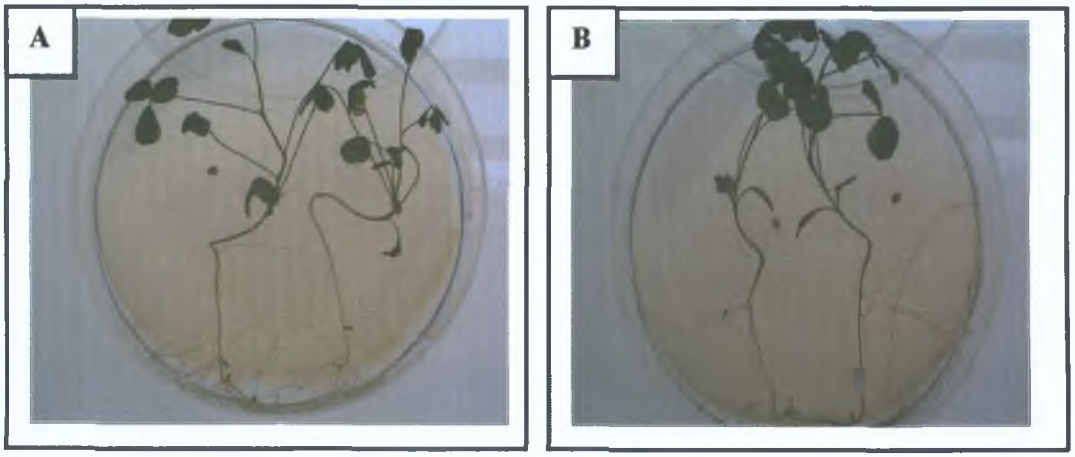

Figure 4.26: Analysis Of Nodulation Of *Medicago sativa* by *S. meliloti* 2011 (A) and *S. meliloti* 2011Smc04205km (B).

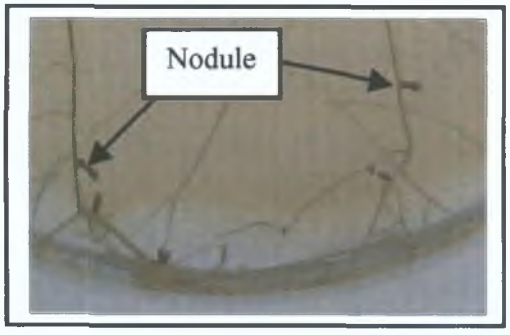

Figure 4.27: Nodules Produced By *S. meliloti* 2011 on *Medicago sativa*.

4.11: Discussion

S. meliloti 2011 synthesises the asymmetric citrate hydroxamate siderophore rhizobactin 1021 under conditions of iron limitation (Chapter 1). *S. meliloti* has also been shown to utilise several xenosiderophores including schizokinen, ferrichrome, and desferryl myselate (Noya *et al*, 1997; Lynch, PhD Thesis 1999). The ability of *S. meliloti* 2011 to utilise the haem compounds haemoglobin, haemin and leghaemoglobin as iron sources has also been reported (Noya *et al*, 1997; Lynch, PhD Thesis 1999). The ability to utilise haem compounds is usually associated with pathogenic microorgansims. The host environment is essentially an iron deplete environment with all available iron complexed with host proteins such as transferrin. Bacteria have consequently evolved mechanisms of acquiring iron from host proteins such as haemoglobin. Although *S. meliloti* 2011 is not pathogenic, it interacts with a host where haem compounds are readily available during symbiosis.

In silico analysis of the published *S. meliloti* 1021 genome sequence led to the identification of the three putative haem acquisition loci encoded on the chromosome of *S. meliloti* 2011 (Capela *et al*, 2001; personal observation). Two of the loci were predicted to encode putative haem receptors, while the third locus was predicted to encode a putative inner membrane haem transport system.

Examination of the Smc04205 protein sequence revealed the presence of a putative protein export signal sequence the cleavage of which results in a mature protein of 91.18 kDa. Analysis of the Smc04205 protein sequence revealed the presence of several motifs commonly found amongst haem dependent outer membrane receptors. Two 'TonB motifs' were identified corresponding to motifs TonB Region II and Region III (Bitter *et al*, 1991; Ankenbauer and Quan, 1994). Analysis of the N-terminal region did not reveal the presence of the TonB Region I motif, but as this sequence can be somewhat degenerate, the motif is not always readily identifiable. Further examination of the protein sequence revealed the presence of the FRAP-NPNL motif, commonly found amongst haem dependent outer membrane receptors. The histidine residue, which has been found to be functionally important (Bracken *et al*, 1999), is conserved in Smc04205. Further examination of the protein sequence revealed the presence of an N-terminal extension, similar to the extension found in the

FecA protein of E. coli (Chapter 1). Directly upstream of Smc04205 and orientated in the same direction, is a putative regulatory system annotated *fecIR* on the *S. meliloti* 1021 genome homepage. The *fecI* gene is predicted to encode a putative ECF function sigma factor while the *fecR* gene is predicted to encode a cytoplasmic transmembrane signal transduction protein. The presence of this putative regulatory system and the N-terminal extension suggest that the system possibly functions in a similar manner to the ferricitrate system of *E. coli*. Downstream of Smc04205 a putative gene of unknown function is located. BLASTP analysis indicated that the protein displayed homology to rhizobiocins and haemolysins. Directly downstream of Smc04206 a putative type I secretion system encoded by Smc04207 and Smc04208 is located. The proximity of the type I secretion system to Smc04206 suggest that they function in the export of this protein.

As previously described, haem acquisition systems can generally separated into three categories, depending on the factors that they involve (Chapter 1). The Smc04205 protein is predicted to form part of a type II haem acquisition system.

The Smc04205 gene was mutated by cassette mutagenesis and the resultant mutant phenotype was analysed. Analysis indicated that the mutant was unaffected in utilisation of haemoglobin or haemin.

The Smc04205 protein displays significant homology to several haem receptors that are associated with haemophore type proteins. As previously mentioned, haemophores are extracellular proteins that remove haem from haemoglobin and haemopexin and deliver the haem complex to an outer membrane receptor (Chapter 1). Analysis of the putative protein products encoded in the region containing Smc04205 did not reveal the presence of any proteins displaying homology to haemophores. Further examination of the *S. meliloti* genome sequence indicated that no proteins displaying homology to HasA were encoded within the genome. *In silico* BLASTP analysis indicated that Smc04206 displayed homology to rhizobiocin and haemolysin type proteins. Detailed analysis however indicated that the region of homology was limited and that Smc04206 was significantly smaller than these proteins. Detailed examination led to the identification of a protein of similar size to Smc04206 located directly downstream of the *A. tumefaciens* Smc04205 homologue,

Atu3385. The homologue, Atu3384 was located proximally to a type I secretion system similar to the system encode by Smc04207 and Smc04208. The gene encoding HasA proteins is also encoded proximally to type I secretion systems. *In silico* analysis of the region encoding YP03923 in *Y. pestis* revealed the presence of a putative type I secretion system located downstream from the putative haemophore. On the basis of the significant homology between the receptor proteins and the similar gene arrangements, it is tempting to speculate that Smc04206 represents a novel type of haemophore.

Analysis of the Smc04205 protein sequences and of those of its homologues indicated that they possessed N-terminal extensions with the exception of YPO3923. *In silico* analysis indicated that with the exception of YPO3923 and *P. fluorescens*, whose genome sequence is not yet available, the HasR homologues are located adjacent to putative regulatory systems similar to the *fecIR* system of *E. coli*. These systems consist of a cytoplasmic transmembrane signal transducer and and ECF function sigma factor, similar to the FecIR system of *E. coli*. Analysis of the regulatory system encoded by *hasI* and *hasS* in *S. marcescens* suggests that HasR is positively regulated by a signal transduction event involving haem loaded haemophore, the HasR protein and the HasIS regulatory system. This complex regulatory mechanism suggests that *S. marcescens* can respond to haem availability by upregulating the appropriate receptor.

The Smc02726 gene was identified by *in silico* analysis of the *S. meliloti* genome sequence. The Smc02726 gene is unlinked to any other gene encoding proteins with a role in haem acquisition. Examination of the Smc02726 protein sequence revealed the presence of a putative protein export signal sequence, the cleavage of which resulted in a mature protein of 77.6 kDa. Further examination of the protein sequence revealed the presence of several motifs commonly found amongst haem dependent outer membrane receptors. Two 'TonB motifs' corresponding to TonB Region II and TonB Region III were identified in the protein sequence. Examination of the N-terminal region of the protein did not reveal the presence of a TonB Region I motif, which as previously described, is somewhat degenerate, and not always identifiable. Further analysis of the protein sequence led to the identification of a FRAP-NPNL motif. Analysis of the sequence indicated that the highly conserved histidine residue

was not conserved. Directly downstream of Smc02726, the *trp*E(G) of *S. meliloti* 2011 is encoded. The *trp*E(G) of *S. meliloti* encodes an anthranilate synthetase, and functions in the initial stages of the tryptophan biosynthesis pathway (Barsomian *et al*, 1992). Anthranilate has previously been suggested to function as an *in planta* siderophore (Chapter 1).

The Smc02726 gene was mutated by cassette mutagenesis and the resulting mutant phenotype was examined. Analysis indicated that the mutant, *S. meliloti* Smc02726km was defective in the utilisation of haemoglobin and haemin.

As mentioned above, the *trp*E(G) gene of *S. meliloti* is located downstream of Smc02726. It had previously been suggested that anthranilate possibly functions as an *in planta* siderophore (Barsomian *et al*, 1992). Previous results indicated that *trp*E(G) is transcribed from a promoter located in the intergenic region between Smc02726 and *trp*E(G). It is therefore unlikely that the phenotype associated with Smc02726 is due to a polar effect on *trp*E(G). Analysis of the region encoding Smc02726 revealed that the gene order was similarly conserved in *A. tumefaciens*. Analysis of the *A. tumefaciens* genome sequence indicated that a homologue of *trp*E(G) was located downstream of the Smc02726 homologue, Atu2287. A putative protein of unknown function, Smc02727 located upstream of Smc02726, has a homologue encoded between Atu2287 and *trp*E(G) of *A. tumefaciens*. In the event of anthranilate functioning as a siderophore, it is tempting to speculate that its utilisation may be mediated via Smc02726 and other uncharacterised protein,s possibly including Smc02727.

In silico analysis of the region upstream and downstream of Smc02726 led to the identification of putative IS elements indicating that Smc02726 is located on a transposable element. It is not known if the IS elements are active, but the location of the haem receptor on this element indicates that the haem receptor was possibly introduced into *S. meliloti* by lateral gene transfer. Similarly it is also tempting to speculate that the presence of the haem receptor in the transposable element possibly confers a selective advantage to the recipient bacterium.

Analysis of *S. meliloti* 242 resulted in the identification of the protein product of the Smc02726 gene by MALDI-TOF analysis (Battistoti *et al*, 2003). The protein, which was designate ShmR, was shown to be capable of binding haemin, but not haemoglobin. The results described in this thesis suggest that haemoglobin utilisation is mediated by Smc02726 in *S. meliloti* 2011, but it is possible that there is another component involved in the utilisation, possibly in the release of haem iron from the protein moiety. It is also possible that the mechanism of transport in *S. meliloti* 242 is different to that described for *S. meliloti* 2011, although the two strains appear to show extensive homology. The highly conserved histidine residue located in the FRAP-NPNL motif is not conserved in Smc02726. The histidine residue of the HemR protein of *Y. enterocolotica* has been implicated in haem recognition and internalisation (Bracken *et al*, 1999). The absence of this residue in Smc02726 suggests that haem recognition and internalisation by Smc02726 may occur via a different mechanism.

The Smc02726 protein displays significant homology to BhuR, a haem receptor from *B. avium*. BhuR is required for efficient utilisation of haem and haem-containing proteins in this bacterium (Kirby *et al*, 2001). A homologue of BhuR identified in *B. petussis* and a mutant in the *bhuR* gene was shown to be defective in haemin and haemoglobin acquisition (Vanderpool and Armstrong, 2001). In contrast to Smc02726, the *bhuR* genes appear to be located beside inner membrane haem transport systems and also appear to be under the control of a regulatory system similar to the *fecIR* system of *E. coli* (Vanderpool and Armstrong, 2001; Kirby *et al*, 2001). In silico analysis indicated that in contrast to Smc02726, BhuR was shown to possess an N-terminal extension.

A putative inner membrane iron transport system similar to the *hmu* system of *R. leguminosarum* was identified on the chromosome of *S. meliloti* 2011. The *hmu* system is arranged in the order *hmuSTUV*. A putative gene, Smc01513, is located directly upstream of hmuS and is orientated in the same direction. A homologue of this gene has been designated *hmuP* in *R. leguminosarum*. The gaps between the individual genes in the *hmu* system are small indicating that they form an operon. Directly upstream of the *hmu* system, the *S. meliloti* TonB protein is encoded along with several proteins of unknown function

The *hmuT* gene was mutated by cassette mutagenesis and the resulting mutant phenotype was examined. Analysis indicated that the mutant, *S. meliloti hmuT*-km was unaffected in the utilisation of haemoglobin and haemin.

The gene organisation of the region encoding the *hmu* system is similar to that described for the region encoding the *hmu* system of *R. leguminosarum*. With the exception of TonB, the putative proteins encoded in both regions display significant homology to each other. *In silico* analysis indicated the presence of similar gene organisations in *M. loti* and *B. japonicum*. The *hmu* system homologue of *M. loti*, *hmuPSTUV* is located close to a putative haem receptor. A region downstream of the haem receptor encodes a putative TonB protein, while another TonB homologue is located elsewhere on the chromosome. Two other proteins encoded in this region display homology to Smc01518 and Smc01519 of *S. meliloti*. *In* silico analysis of the *B. japonicum* genome resulted in the identification of a *hmuTUV* system homologue. No significant homologues of HmuPS were identified. A TonB homologue encoded proximally to the *hmu* system has been shown to be required for haem uptake and acquisition from haemoglobin and leghaemoglobin. Homologues of ExbBD were also identified in this region as well as a protein displaying homology to Smc01518.

Similarly to results obtained with mutants deficient in haem acquisition in *R. leguminosarum* and *B. japonicum*, mutants defective in haem acquisition in *S. meliloti* are also unaffected in nodulation and appear to enter into an effective symbiosis with *Medicago sativa*. The results thus appear to indicate that the ability to acquire iron from haem is not essential for the formation of an effective symbiosis.

The absence of a clear phenotype associated with a mutation in *hmuT* indicates that *S. meliloti* 2011 possibly encodes a second mechanism for haem transport at the inner membrane. Mutations in the *hmu* system of *R. leguminosarum* and *B. japonicum* resulted in similar phenotypes also suggesting the presence of an alternative inner membrane transport system for haem in these organisms.

The absence of an Smc04205 utilisation phenotype is in contrast to the phenotypes associated with the homologues of this protein. It is possible that this system was not expressed under the conditions examined, and may only be induced under specific

conditions. Another possibility for the lack of an associated phenotype with *S. meliloti* Smc04205km mutant is that Smc04205 functions as a haem receptor for a different type of haem compound, possibly leghaemoglobin. It is possible that such a compound may be available in the nodule, and that Smc04205 plays a role in haem acquisition *in planta*. Analysis indicated that *S. meliloti* Smc04205km induced nodule formation and appeared to enter into an efficient symbiosis with *Medicago sativa*.

Mutants defective in Smc02726 appeared to form healthy nodules and the plants were similar to wild type. The result indicates that haem acquisition is not essential for an effective symbiosis.

Analysis with mutants defective in all types of iron acquisition examined also formed nodules and fixed iron, suggesting a novel mechanism for iron acquisition *in planta* (Unpublished results). It is possible that the haem acquisition systems of *S. meliloti* function when free living in oligotrophic soil conditions.

Chapter 5

Genetic Analysis And Characterisation Of Xenosiderophore Utilisation In *P. aeruginosa*

5.1: Introduction

As previously described, many bacteria are capable of the utilisation of heterologous or xenosiderophores (Chapter 1). Xenosiderophores may be defined as siderophores that can be utilised, but are not synthesised by a particular bacterium. The ability of bacteria to utilise xenosiderophores confers a competitive advantage on the bacteria and enables them to occupy extended ecological niches. *E. coli* for example has been found to be able to utilise a wide variety of xenosiderophores including ferrichrome, coprogen, and ferrioxamine B (Chapter 1). *Pseudomonas aeruginosa* an important opportunistic human pathogen synthesises two known siderophores, pyoverdine (Cox and Adams, 1985) and pyochelin (Cox, 1980). *P. aeruginosa* can also utilise various xenosiderophores including pyoverdines produced by other pseudomonads, enterobactin, ferrioxamine B, citrate and aerobactin (Chapter 1).

The ability of *P. aeruginosa* to utilise a wide variety of heterologous siderophores possibly enhances the organism's ability to acquire iron under a wide range of environmental conditions and also to compete with various other microorganisms for iron. The outer membrane receptors for pyoverdine, pyochelin and enterobactin in *P. aeruginosa* have been identified and cloned (Chapter 1). *In silico* analysis of the *P. aeruginosa* genome indicated that the genome encoded a number of putative siderophore outer membrane receptors, the ligands for which have yet to be identified.

In silico analysis of the *P. aeruginosa* genome also revealed an apparent lack of inner membrane siderophore transport systems (Köster, 2001; personal observation). A putative enterobactin inner membrane transport system has been identified, but has yet to be experimentally analysed. The apparent lack of clearly identifiable inner membrane siderophore transport systems possibly indicates that siderophore transport at the inner membrane occurs via a novel mechanism.

This chapter describes the identification of three further xenosiderophores that can be utilised by *P. aeruginosa*. The identification and characterisation of the outer membrane receptor for two of these xenosiderophores is also described.

5.2: Rhizobactin 1021 Utilisation In *Pseudomonas aeruginosa*

The ability of *P. aeruginosa* to utilise rhizobactin 1021 was examined in the pyoverdine and pyochelin mutant *P. aeruginosa* DH119, and in the *fptX* mutant, *P. aeruginosa* PA4218km. These strains were chosen for examination, as the lack of functional siderophore regulons results in limited growth under conditions of iron deprivation, and allow xenosiderophore utilisation to be more clearly analysed. Siderophore utilisation bioassays were performed on *P. aeruginosa* DH119 and PA4218km and it was determined that a concentration of 2 mM 2,2'dipyridyl was sufficient to induce conditions of iron limitation. *P. aeruginosa* DH119 and PA4218km were crossfed with rhizobactin 1021 and the ability to utilise the siderophore was analysed by the siderophore utilisation bioassay. Analysis of the result indicated that *P. aeruginosa* DH119 was capable of utilising rhizobactin 1021 as an iron source. *P. aeruginosa* PA4218km was also found to be capable of utilising rhizobactin 1021 (Table 5.1; Figure 5.1 and 5.2).

Table 5.1: Utilisation Of Rhizobactin 1021 By *P. aerugionsa*

***P.* aeruginosa Strain**	**Genotype**	**Rhizobactin 1021 Utilisation**
DH119	*pvd-2, pchR*	+
PA4218km	*pvd-2, fptX*	+

In addition to indicating that *P. aeruginosa* was capable of utilising the xenosiderophore rhizobactin 1021 as an iron source, the result also indicated that the RhtX homologue, FptX, was not involved in the utilisation of rhizobactin 1021 in *P. aeruginosa*. This indicated that rhizobactin 1021 transport in *P. aeruginosa* was occurring via a different mechanism to that described for *S. meliloti* 2011.

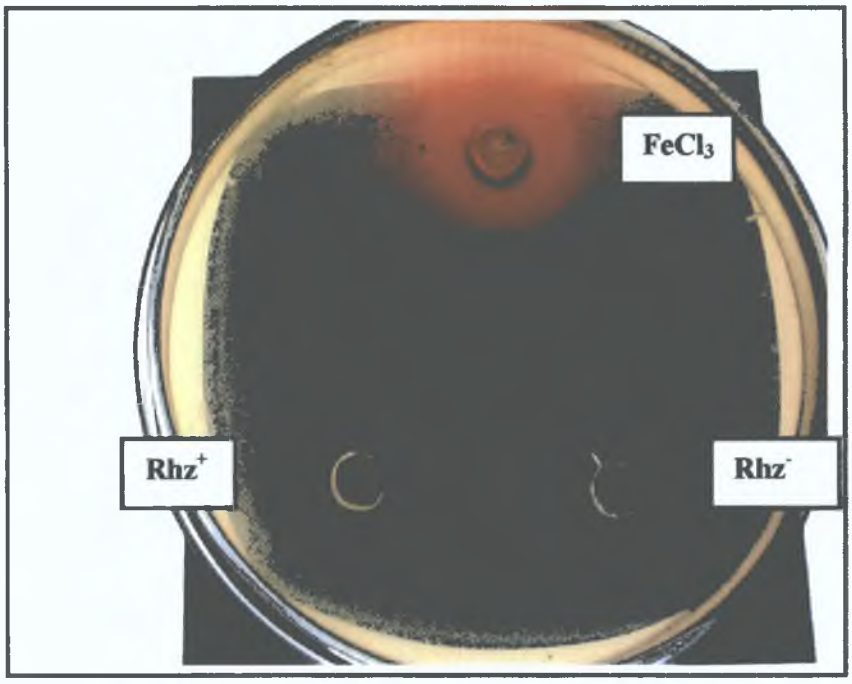

Figure 5.1: Rhizobactin 1021 Utilisation By *P. aeruginosa* DH119. Ferric chloride ($FeCl_3$) was used as a positive control. Concentrated culture supernatant containing rhizobactin 1021 (Rhz^+) was prepared as described in Chapter 2. A concentrated culture supernatant (Rhz^-) prepared from a rhizobactin 1021 biosynthesis mutant was used as a negative control.

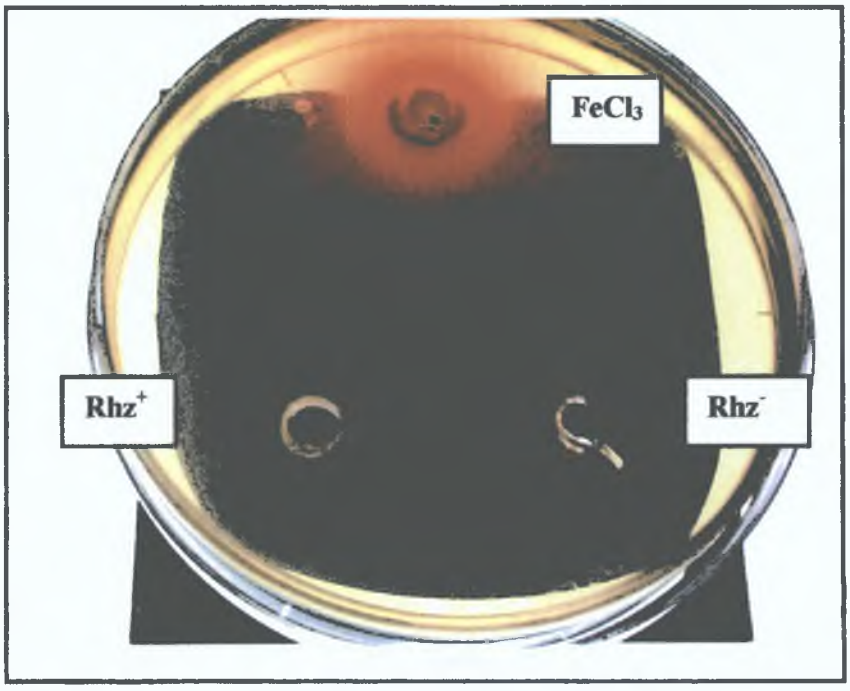

Figure 5.2: Rhizobactin 1021 Utilisation By *P. aeruginosa* PA4218km. Ferric chloride ($FeCl_3$) was used as a positive control. Concentrated culture supernatant containing rhizobactin 1021 (Rhz^+) was prepared as described in Chapter 2. A concentrated culture supernatant (Rhz^-) prepared from a rhizobactin 1021 biosynthesis mutant was used as a negative control.

5.3: Citrate Hydroxymate Siderophore Utilisation In *P. aeruginosa*

Rhizobactin 1021 displays structural similarities to various citrate hydroxymate siderophores, amongst them, schizokinen and aerobactin. The ability of *P. aeruginosa* to utilise citrate hydroxymate siderophores structurally similar to rhizobactin 1021 was analysed. Schizokinen, a siderophore produced by *B. megaterium* is identical in its core structure to rhizobactin 1021, which differs only by the addition of an (E)-2-decanoic acid at one of its distal ends (see Figure 5.3). Aerobactin is produced by *Aeromonas* sp. and various strains of pathogenic *E. coli* and *Shigella* sp. Aerobactin, which is structurally similar to rhizobactin 1021 is a known virulence factor and has been found to be an important virulence determinant even in strains that produce other siderophores (Chapter 1).

Figure 5.3: Structure Of Various Citrate Hydroxymate Siderophores

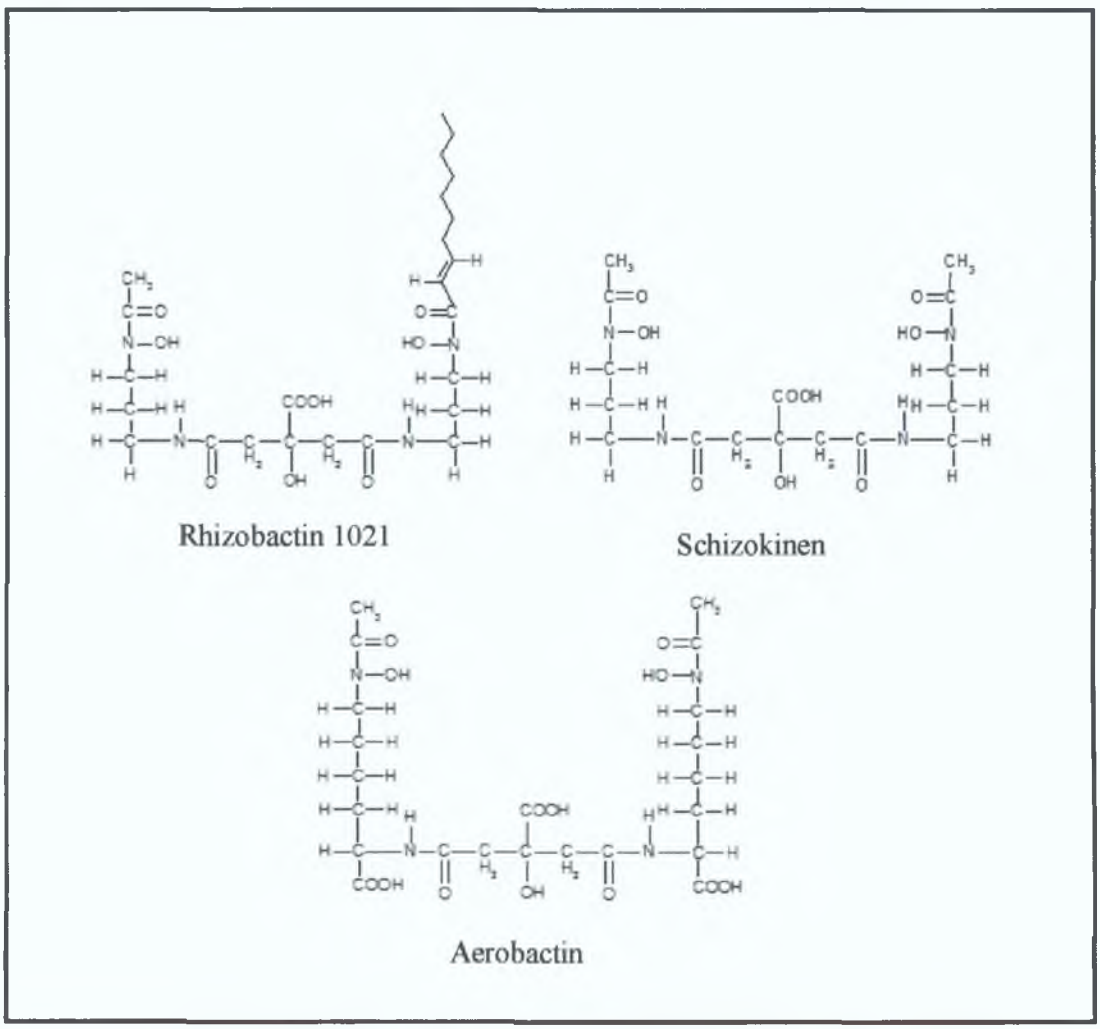

The ability of *P. aeruginosa* to utilise aerobactin has previously been reported (Liu and Shokrani, 1978). The ability of *P. aeruginosa* DH119 and PA4218km to transport schizokinen and aerobactin was analysed by the siderophore utilisation bioassay. The results indicated that *P. aeruginosa* DH119 and PC4218km could both utilise schizokinen and aerobactin as iron sources (Table 5.2).

Table 5.2: Utilisation Of Schizokinen And Aerobactin by *P. aeruginosa*

***P. aeruginosa* Strain**	**Genotype**	**Schizokinen Utilisation**	**Aerobactin Utilisation**
DH119	*pvd-2, pchR*	+	+
PA4218km	*pvd-2, fptX*	+	+

The result indicated that *P. aeruginosa* was capable of utilising various citrate hydroxymate siderophores as iron sources. Analysis of the ligand specificity of heterologously expressed *rhtX* in *E. coli* indicated that RhtX was not capable of mediating the transport of aerobactin (Chapter 3). The result indicated that FptX was not mediating the transport of schizokinen and aerobactin in *P. aeruginosa*.

5.4: *In silico* Analysis Of The *P. aeruginosa* Genome Sequence

In *E. coli*, the aerobactin receptor, IutA, functions as the outer membrane receptor for the structurally similar siderophores schizokinen and rhizobactin 1021 (Lynch, PhD Thesis 1999). The utilisation of rhizobactin 1021 and schizokinen in *S. meliloti* 2011 has been found to be dependent on the outer membrane receptor RhtA (Lynch *et al*, 2001). *In silico* analysis of the *P. aeruginosa* genome sequence using the protein sequence for the rhizobactin 1021 outer membrane receptor, RhtA, enabled the identification of two putative proteins with significant homology to RhtA. The two proteins, PA4675 and PA1365, showed 44% and 29% identity to RhtA respectively as calculated by BLASTP at the *P. aeruginosa* Genome Homepage.

In *S. meliloti* 2011, rhizobactin 1021 transport is mediated by the RhtX permease. *In silico* analysis of the *P. aeruginosa* genome sequence indicated that FptX displayed the highest homology to RhtX. Analysis of the *fptX* mutant *P. aeruginosa* PA4218km however, indicated that FptX was not involved in the transport of citrate hydroxymate siderophores. In *E. coli* the transport of aerobactin is mediated via the *fhuCDB* system. The *P. aeruginosa* genome sequence was analysed but no FhuD homologue and only weak FhuB and FhuC homologues were identified. The *in silico* analysis indicated that the transport of citrate hydroxymate siderophores at the inner membrane in *P. aeruginosa* was occurring via a novel mechanism.

5.5: Analysis Of The PA4675 Locus

PA4675 is located at position 5243177-5245405 on the *P. aeruginosa* chromosome. No other proteins encoded in the vicinity of PA4675 show homology to any known protein involved in siderophore mediated iron transport. Directly downstream of PA4675, and orientated in the opposite direction is a putative carbonic anhydrase (PA4676). Directly upstream of PA4675 a putative gene, PA4674 that is divergently expressed from PA4675, is encoded. PA4674 does not display homology to any known protein involved in siderophore mediated iron transport. The iron utilisation locus in this region is predicted to consist solely of PA4675.

Analysis Of PA4675

PA4675 is 2226 base pairs in length. A putative ribosome binding site, CTCC, was identified upstream of the predicted translational start codon. The protein encoded by PA4675 is 742 amino acids in length with a predicted molecular weight of 80.9 kDa. Analysis of PA4675 using the PSORT program (Nakai and Kanehisa, 1991) indicated that the protein contains a 28 amino acid signal sequence typical for exported proteins. Cleavage of the signal sequence between the residues ALA-AD results in a mature protein the predicted size of which is 78 kDa with a pI of 5.21. The amino acid sequence of PA4675 is shown below. The predicted signal sequence is highlighted (Figure 5.4).

Figure 5.4: Amino Acid Sequence Of PA4675.

MPRSIPLRPAPLALSLSLFASFSAPALAADPVEQQMVVIGSRAPTSISELPGTVWVI
EREQLDQQTQAGVPLKEALGQLIPGLDIGSQGRTNNGQNLRGRSVLVMIDGVSLNSS
RGISRQFDSIDPFNIERIEVMSGASAVYGGGATGGIINIVTKKGVGGDTRFNTELGA
RSGFQSHEDHDLRAAQSISGGNDLFNGRLAIAYQKNGAAYDGSGDQVLTDITQTDLQ
YNRSVDLMGSLGFTFANGHSLDLGLQYYDSGYDGDRGLDLGRNFDALRGRAPYSIKG
GVDLDREPESKRHQFNATYHAPEVLGHDLYLQAYYRNEKMAFNPFPTIRYSNTGAIN
YGTSYYSASQQDTDYYGMKLALVKTWERASLTYGVDLDREKFTSDQMLFNLPLAAAS
GGLVASEQAKLGRYPDIDTDSRAFFLQGSWKATDDLTLSAGVRRQSMSTDVSDFVAA
NQQILIANGLGKTADAVPGGSKDYDVNLVNVGAIYKLNLQQQVWANYSEGFELPDPA
KYYGFGRYGAADGNGHYPLLQGVSVNDSPLDGIKTKQVELGWRHTDGALDTQVAAFY
SWSDKSIKYDSKTLAVLQQDTKKRNYGLEGQATYWLDDHWQVGVNGLAIRSQEKVDG
RWLKQDVTSASPSKAGAFVGWKDDQRSLRLQGVRTFNLNDEPGNKIDGYALFDLLGT
QALPVGTLTAGIQNLLDKDYTTVWGQRAQVYYGGLAPAGLFDYKGRGRTYSLTYSVE
F

The amino acid sequence of PA4675 was compared against the NCBI database of protein sequences using the BLASTP program (Altschul *et al*, 1997). Sequence analysis of the PA4675 amino acid sequence revealed a significant degree of sequence identity to the family of putative aerobactin outer membrane receptors. The five most significant matches to PA4675 using the BLASTP program and their associated predicted biochemical data are listed in Table 5.3.

Table 5.3: Proteins Displaying Significant Homology To PA4675

Protein	Homologue	Molecular Mass (kDa)*	Accession	Homology (% Identity)**
S4056	*S. flexneri* 2a str. 2457T	80.96	NP_839219	46 (64)
IutA	*E. coli* CFT073	84.05	NP_755498	45 (62)
SF3719	*S. flexneri* 2a str. 301	84.05	NP_709458	44 (62)
IutA	*Escherichia fergusonii*	80.69	AAL01550	44 (63)
PP2193	*P. putida* KT130	89.79	NP_744342	43 (56)

*The predicted molecular mass (kDa) is calculated for the unprocessed protein.

**Identities (%) were calculated using the Genedoc program. Similarities are indicated in brackets.

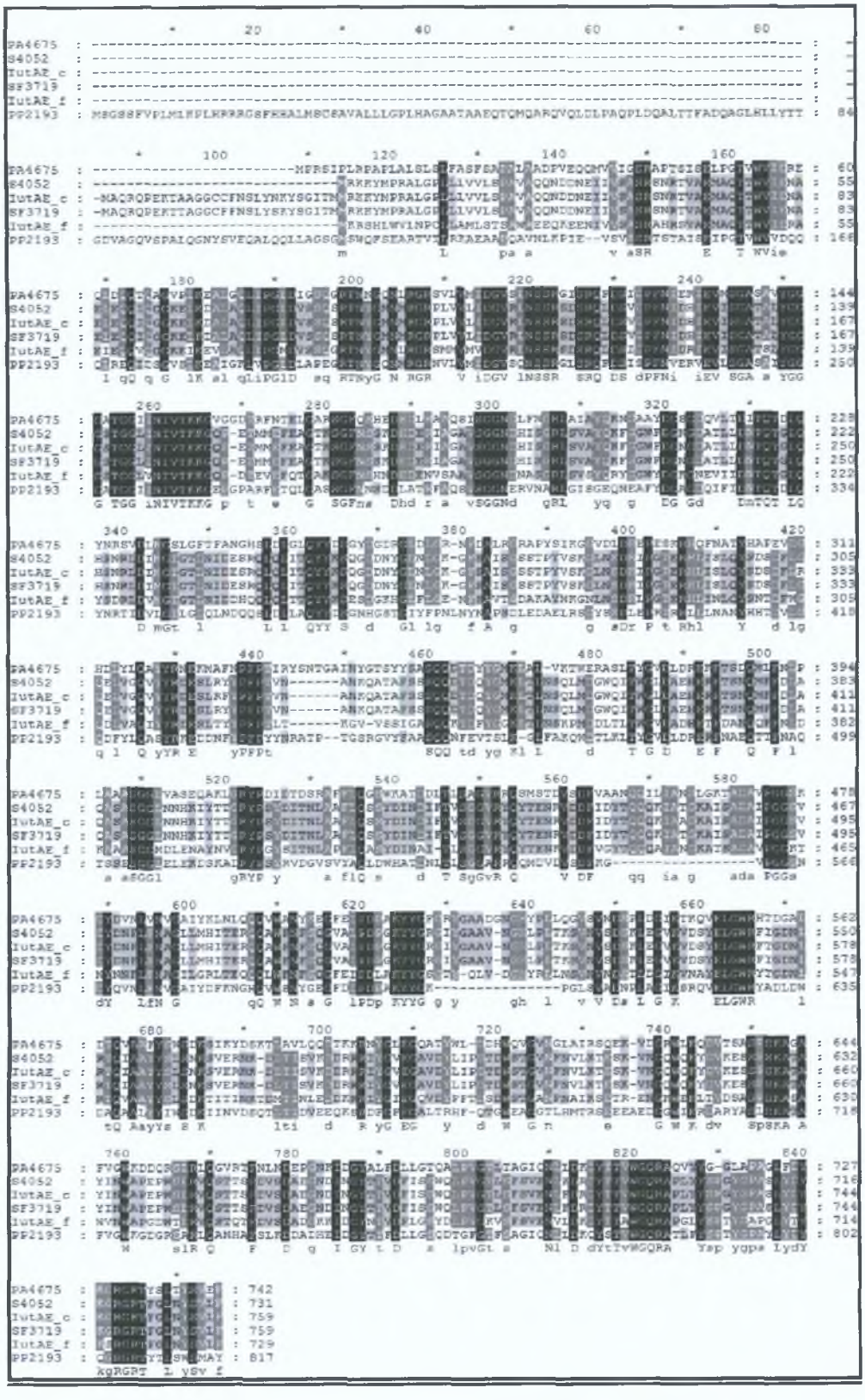

Figure 5.3: Multiple sequence alignment of PA4675; with S4052 from *S. flexneri* 21 str. 2457T, IutA from *E. coli*, SF3719 from *S. flexneri* 21 str. 301, IutA from *E. fergusonii* and PP2193 from *P. putida* KT130. Black indicates 100% conservation, dark grey indicates 83% conservation and light grey indicates 66% conservation.

The amino acid sequence of PA4675 was analysed to determine if the protein contained the amino acid sequence motifs conserved among TonB-dependent receptors, previously designated regions I, II and III (Bitter *et al*, 1991). Region I is the 'TonB box' with the consensus sequence (D/E)TXXVXA(A/S) although this sequence is somewhat degenerate. Region I is typically located near the N-terminus of the protein (Bitter *et al*, 1991; Ankenbauer and Quan, 1994). A weak 'TonB box' like motif, GTVWVIER, was located at amino acid positions 24-31 of the mature PA4675 protein. A multiple sequence alignment of Region I of the highest homologues to PA4675 was analysed to determine if the same degenerate sequence was present. All of the sequences showed weak homology to the Region I consensus sequence, but showed good homology amongst each other (Figure 5.6).

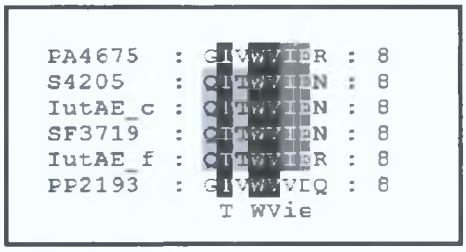

Figure 5.6: TonB Region I Motif. Black indicates 100% conservation, dark grey indicates 83% conservation and light grey indicates 66% conservation.

Region II is typically located in the C-terminal part of the protein and has the consensus sequence (F/I/L/M/V)XXX(I/L/V)XNLX(D/N)(K/R)XY. The amino acid sequence of PA4675 was analysed and found to contain the motif LTAGIQNLLDKDY at position 692-704, which completely matches the region II consensus sequence.

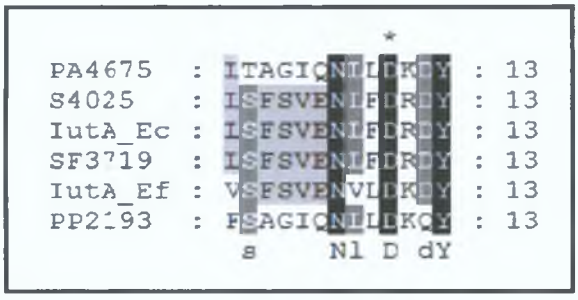

Figure 5.7: TonB Region II Motif. Black indicates 100% conservation, dark grey indicates 83% conservation and light grey indicates 66% conservation.

Region III is typically located at a distance of 100 amino acids from region I. The region is characterised by the consensus sequence R(V/I)(D/E)(I/V)(I/V/L)(K/R)GXX(G/S/A)XXXG XXXXG(G/A)X(V/I). The amino acid sequence of PA4675 was analysed and found to contain the motif RIEVMSGASAVYGGGATGGIIN at position 131-152.

Figure 5.8: TonB Region III Motif. Black indicates 100% conservation, dark grey indicates 83% conservation and light grey indicates 66% conservation.

The finding of the N-terminal signal sequence and the presence of the three characteristic 'TonB motifs' suggest that PA4675 is a TonB dependent outer membrane receptor.

5.6: The Mutagenesis Of PA4675

Analysis of the region encoding PA4675 indicated that the region of interest was encoded on a cosmid designated pMO 010918. The cosmid, which was harboured in *E. coli* S17-1 was obtained from the Pseudomonas Genetic Stock Centre. Restriction analysis of the cosmid was performed *in silico* using the sequence data available on the *Pseudomonas aeruginosa* Genome Homepage (www.pseudomonas.com). Analysis of the region encoding PA4675 allowed the identification of a 3.4 Kb *Xho*1/*Xma*1 fragment with an internal *Bam*H1 site that was located within PA4675. The *Bam*H1 site was deemed suitable for the insertion of an antibiotic resistance cassette.

A 6 Kb *Eco*R1 fragment encoding the region of interest was subcloned into pUC18 generating pUC6.0 E/E. The unique *Bam*H1 site in the suicide vector pJQ200ks (Chapter 3) was destroyed generating pOC200. The 3.4kb *Xho*1/*Xma*1 fragment was subcloned into pOC200 generating pOC3.4 X/Xm. The kanamycin cassette from pUC4K was excised as a *Bam*H1 fragment and cloned into the unique *Bam*H1 site of pOC3.4 X/Xm generating pOC3.4K X/Xm.

To counter select the *E. coli* donor, it was decided to utilise the tetracycline resistance afforded to *P. aeruginosa* DH119 by virtue of the tetracycline resistance omega cassette inserted into *pchR*. Analysis of the literature suggested that 50 µg/ml was a suitable level of antibiotic to use. The plasmid pOC3.4K X/Xm was introduced into *P. aeruginosa* DH119 by triparental mating and transconjugants were selected on LB with tetracycline and gentamicin. As previously described (Chapter 3), the *sacB* gene of pJQ200ks may not be expressed in *P. aeruginosa*. Nonetheless, sucrose was added to the medium in case it enhanced the selection of second recombinants. Second recombinants were selected by plating on LB with 5% sucrose and kanamycin. Individual colonies were then screened for kanamycin resistance and gentamicin sensitivity. A potential mutant was identified in this way and selected for further analysis.

The genomic sequence of the region encoding PA4675 was examined to identify restriction sites that were deemed suitable for the confirmation of the potential mutant by Southern blot analysis (Chapter 2). The kanamycin cassette was inserted into a *Bam*H1 site encoded within a 5.3 Kb *Xho*1 fragment (Figure 5.9). The kanamycin cassette from pUC4K encodes a unique *Xho*1 site, thus digestion of the mutant genomic DNA with *Xho*1 would generate two *Xho*1 fragments to which the probe would hybridise (Figure 5.10). The plasmid pOC3.4K X/Xm was labelled as described in Chapter 2 and used as a probe.

Figure 5.9: Analysis Of The Region Encoding PA4675 In *P. aeruginosa* DH119

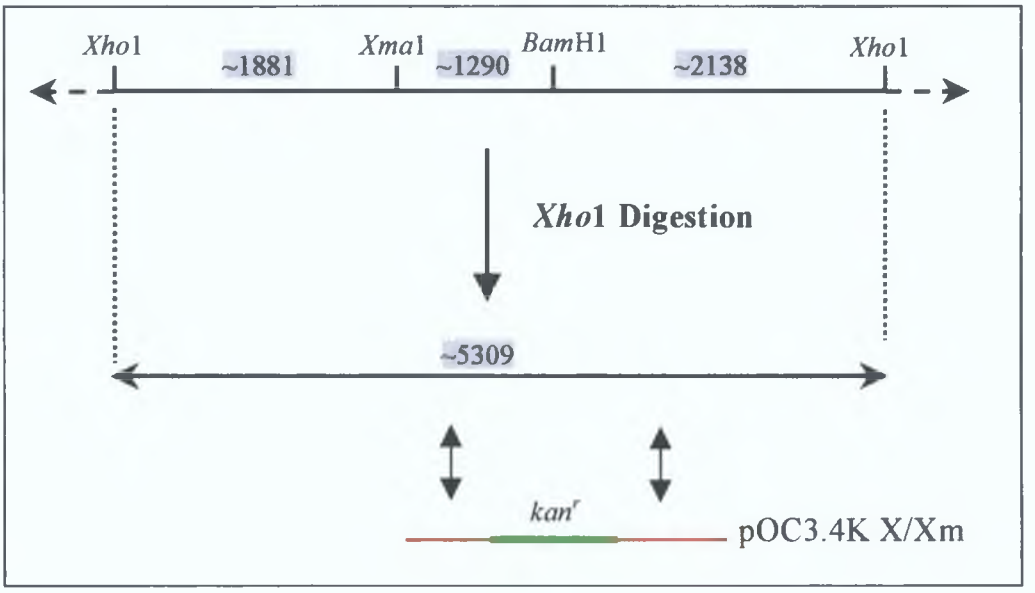

The predicted sizes of the digested fragments are highlighted in grey. The labelled probe is indicated in red, while the kanamycin cassette is highlighted in green. Regions of homology between the labelled probe and the digested fragments are indicated.

Figure 5.10: Analysis Of The Region Encoding PA4675 In A Potential Mutant

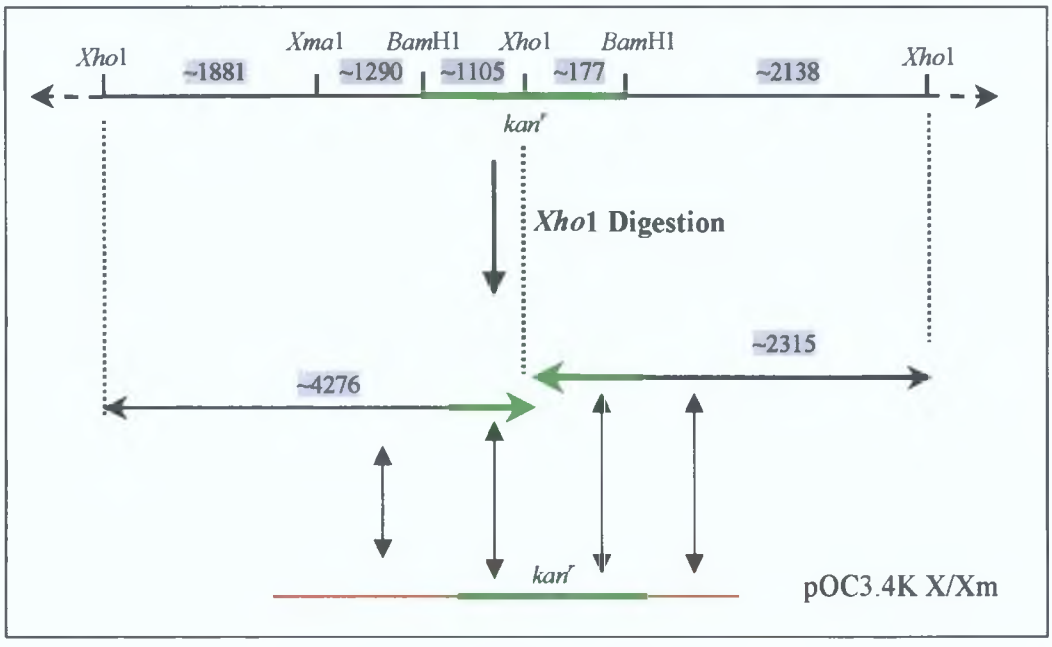

The predicted sizes of the digested fragments are highlighted in grey. The labelled probe is indicated in red, while the kanamycin cassette is highlighted in green. Regions of homology between the labelled probe and the digested fragments are indicated.

Genomic DNA was prepared from *P. aeruginosa* and the potential mutant (Chapter 2), restricted with *Xho*1, transferred to nitrocellulose and probed with labelled plasmid as described in (Chapter 2). Examination of the hybridisation result revealed that one of the predicted *Xho*1 fragments was larger in the control and in the potential mutant. This was unexpected, even more so as the banding pattern was as expected with apparently the correct size shift expected between the two larger fragments (Figure 5.11).

Figure 5.11: Southern Blot Analysis Of *P. aeruginosa* DH119 And *P. aeruginosa* PA4675km.

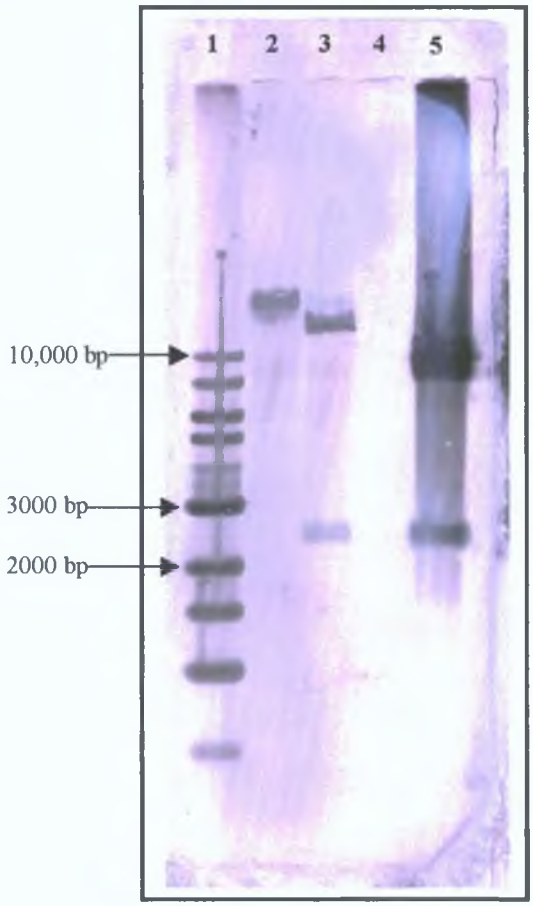

Legend

Lane 1: 1 Kb ladder (Section 2.28)

Lane 2: *P. aeruginosa* DH119 *Xho*1

Lane 3: *P. aeruginosa* PA4675km *Xho*1

Lane 5: pOC3.4K X/Xm *Xho*1

The result was unexpected and indicated that the sequence in the region encoding PA4675 in *P. aeruginosa* PA01 was at variance with the genomic sequence of *P. aeruginosa* DH119, which was itself a *P. aeruginosa* PA01 derivative. It was decided to carry out a more detailed Southern blot of the region encoding PA4675 in order to determine if there were was any other differences with the *P. aeruginosa* PA01 genomic sequence. Digests were designed that would give a diagnostic restriction pattern of the area encoding PA4675, to determine if the major restriction sites were present. Genomic DNA was digested with *Eco*R1, *Bam*H1 and *Xho*1. The predicted digests for *P. aeruginosa* DH119 and the mutant are shown in Figure 5.12 and 5.13.

Figure 5.12: Analysis Of The Region Encoding PA4675 In *P. aeruginosa* DH119

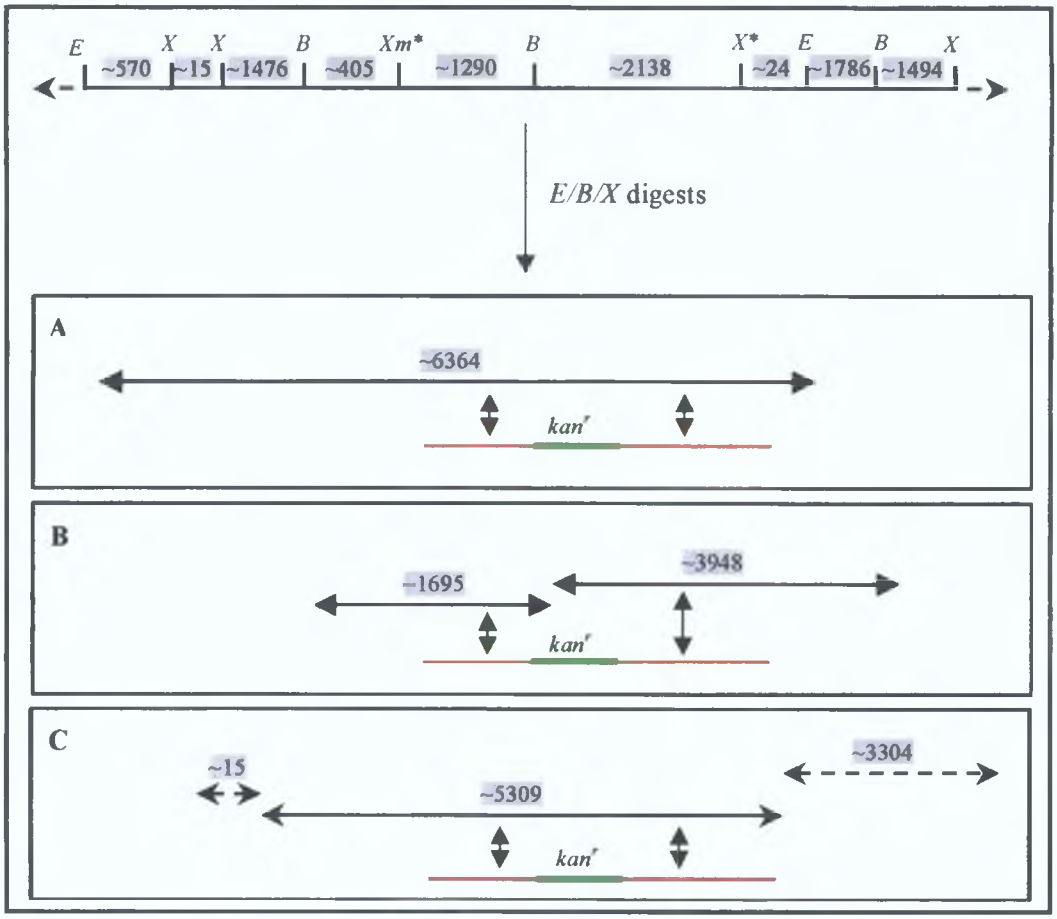

*Eco*R1, *E*; *Bam*H1, *B*; *Xho*1, *X*; *Xma*1, *Xm*. * Genomic region encoded in the probe. The probe also encodes the kanamycin cassette (green). **A:** Predicted *Eco*R1 fragments; **B:** Predicted *Bam*H1 fragments; C: Predicted *Xho*1 fragments. The *Xho*1 fragments directly adjacent to the central 5.3 Kb *Xho*1 fragment are indicated.

Figure 5.13: Analysis Of The Region Encoding PA4675 In A Potential Mutant

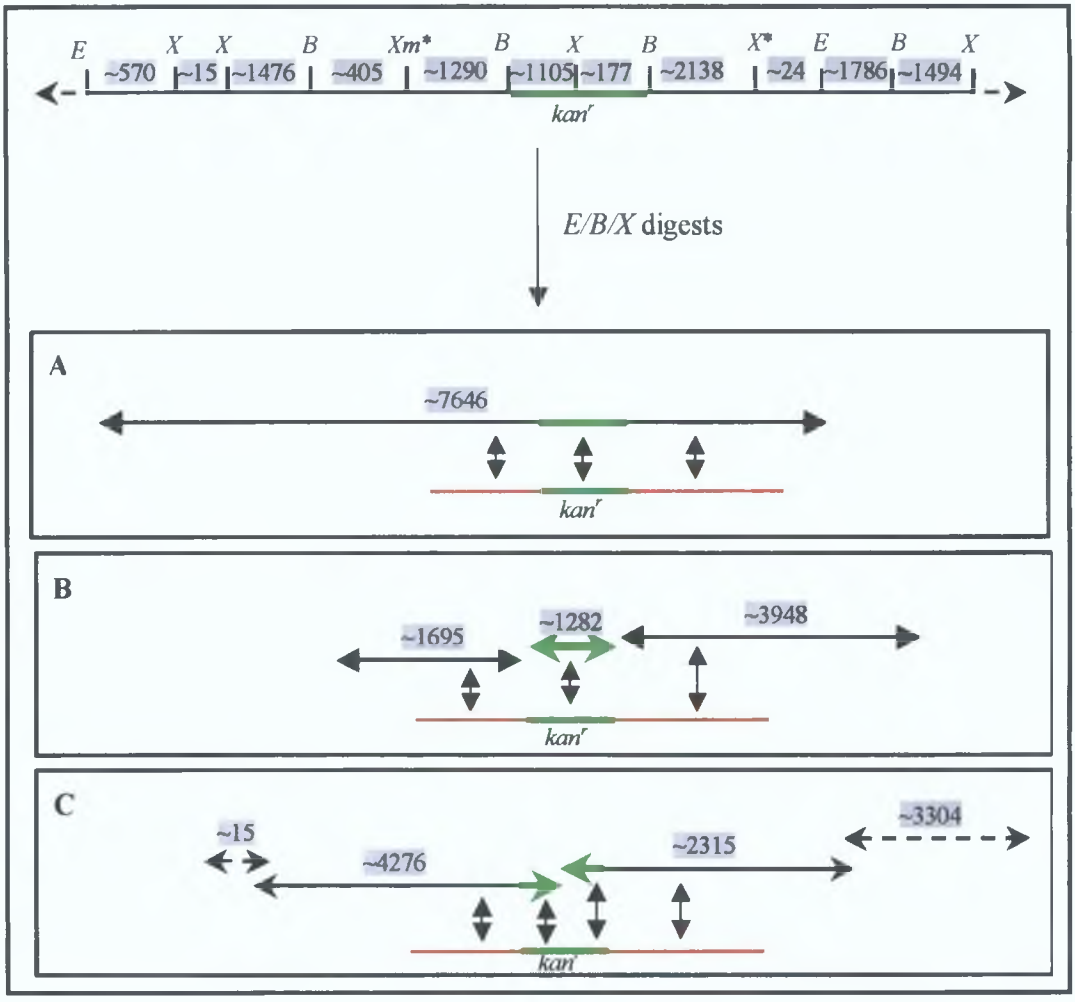

*Eco*R1, *E*; *Bam*H1, *B*; *Xho*1, *X*; *Xma*1, *Xm*. * Genomic region encoded in the probe. The probe also encodes the kanamycin cassette (green). **A:** Predicted *Eco*R1 fragments; **B:** Predicted *Bam*H1 fragments; C: Predicted *Xho*1 fragments. The *Xho*1 fragments directly adjacent to the central 5.3 Kb *Xho*1 fragment are indicated.

Genomic DNA from *P. aeruginosa* DH119 and the potential mutant was restricted with *Eco*R1, *Bam*H1 and *Xho*1, transferred to nitrocellulose and probed with labelled plasmid as described in Chapter 2. Examination of the hybridisation result revealed that the *Eco*R1 and *Bam*H1 fragments were as predicted. However the *Xho*1 hybridised fragments were similar to those previously observed (Figure 5.14).

Figure 5.14: Extended Southern Blot Analysis Of *P. aeruginosa* DH119 And *P. aeruginosa* PA4675km.

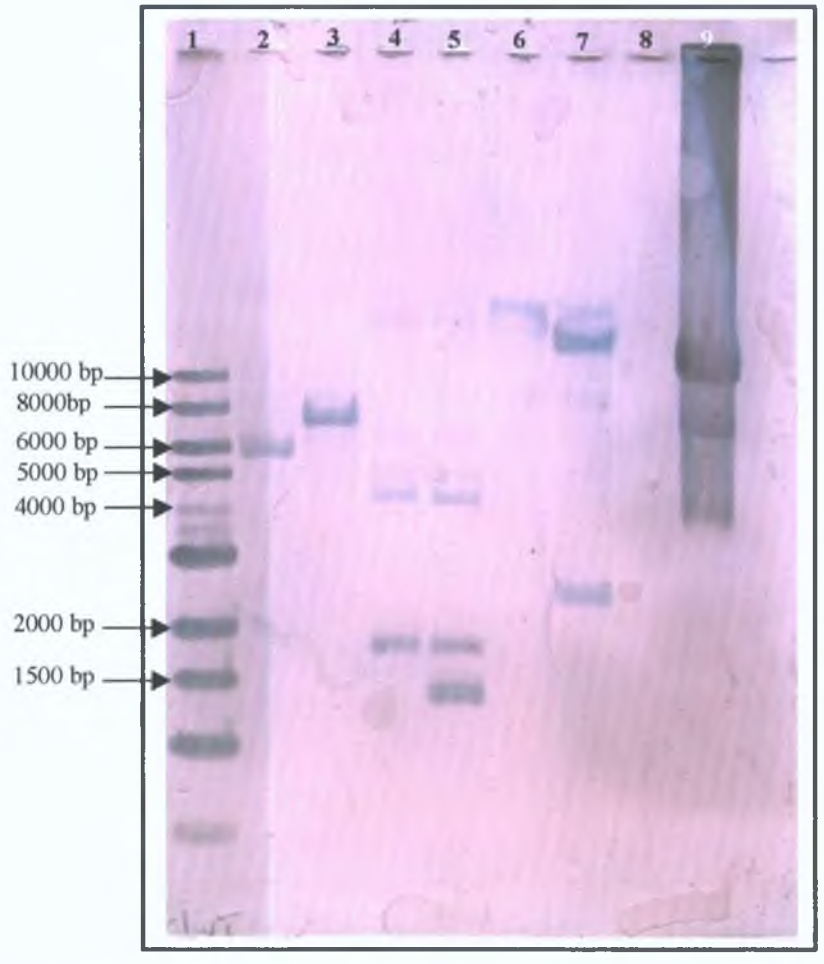

Lane 1: 1 Kb ladder (Section 2.28)

Lane 2: *P. aeruginosa* DH119 *Eco*R1

Lane 3: *P. aeruginosa* PA4675km *Eco*R1

Lane 4: *P. aeruginosa* DH119 *Bam*H1

Lane 5: *P. aeruginosa* PA4675km *Bam*H1

Lane 6: *P. aeruginosa* DH119 *Xho*1

Lane 7: *P. aeruginosa* PA4675km *Xho*1

Lane 9: pOC3.4K X/Xm

The *Eco*R1 and *Bam*H1 digests suggested that the mutation had been correctly constructed. It was considered possible that the anomalous result with *Xho*1 was possibly due to a variation in the laboratory strain *P. aeruginosa* PA01 compared to wild type *P. aeruginosa* PA01, or to an error in the genome sequence.

The mutant strain was named *P. aeruginosa* PA4675km. The phenotypic characterisation of *P. aeruginosa* PA4675km is described in Section 5.10.

5.7: The Identification Of PA1365

In silico analysis of the *P. aeruginosa* genome indicated that a second putative receptor protein which displayed significant homology to RhtA was encoded within the genome. PA1365 is located at 1476384-1478825 of the *P aeruginosa* chromosome. A number of proteins encoded in the vicinity of PA1365 show homology to proteins involved in siderophore mediated iron transport. Directly upstream of PA1365 and orientated in the same direction is a putative regulatory system similar to the *fecIR* ferric citrate regulatory system of *E. coli*. Directly upstream of the putative regulatory system genes, PA1363 and PA1364, is another putative gene, PA1362 that is transcribed in the same direction as PA1363 and PA1363. Upstream of PA1362 and orientated in the opposite direction is PA1361. PA1361 is predicted to encode a putative efflux protein that does not display homology to proteins known to be involved in iron acquisition. Directly downstream of PA1365 and orientated in the opposite direction is PA1366. PA1366 does not display homology to any known protein.

Figure 5.15: Analysis Of The Region Encoding PA1365

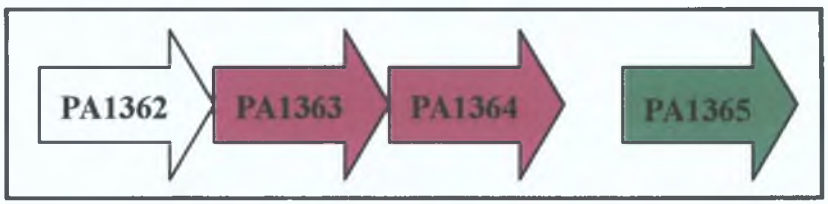

5.7.1: *In silico* Analysis Of The Genes Proximal To PA1365

PA1362

PA1362 is located at 1474391-1474714 of the chromosome. A putative ribosome binding site, AGGA, was identified upsteam of the predicted translational start site. The protein predicted to be encoded by PA1362 is 108 amino acids in size with a predicted molecular weight of 11.6 kDa and a pI of 4.74. BLASTP analysis indicated that PA1362 shows homology to two proteins, PA0819 (83%) and PA2422 (51%), of unknown function encoded within the *P. aeruginosa* genome as determined by BLASTP at NCBI.

PA1363

PA1363 is located at 1474727-1475467 of the chromosome. A putative ribosome binding site, GGAG, was identified upstream of the predicted translational start site. The protein predicted to be encoded by PA1363 is 247 amino acids with a predicted molecular weight of 27.21 kDa and a pI of 8.84. BLASTP analysis indicated that PA1363 is predicted to encode an putative extra cytoplasmic sigma factor (ECF). PA1363 shows strong identity to other putative ECF sigma factors such as RSc2918 from *R. solanacearum* (52%) and Avin3366 from *Azotobacter vinelandii* (43%) as determined by BLASTP at NCBI.

PA1364

PA1365 is located at 1475464-1476306 of the chromosome. A putative ribosome binding site, CGAG, was identified upstream of the predicted translational start site. The protein predicted to be encoded by PA1364 is 281 amino acids with a predicted molecular weight of 30.78 kDa and a pI of 10.19. BLASTP analysis indicated that PA1364 is predicted to encode a putative transmembrane acting signal transducer. PA1364 has strong identity to other putative transmembrane acting signal transducer such as RSc2919 from *R. solanacearum* (41%) and Pflu4793 from *P. fluorescens* Pf0-1 (38%) as determined by BLASTP at NCBI.

5.7.2: *In silico* Analysis Of PA1365

PA1365

PA4675 is located at position 1476384-1478825 on the chromosome. A putative ribosome binding site, AGGA, was identified upstream of the predicted translational start site for PA1365. The protein encoded by PA1365 is 813 amino acids in length with a predicted molecular weight of 89.1 kDa. Analysis of PA1365 using the PSORT program (Nakai and Kanehisa, 1991) indicated that the protein contained a 27 amino acid signal sequence typical for exported proteins. Cleavage of the signal sequence between the residues AGQ-QE resulted in a mature protein the predicted size of which is 86.2 kDa with a pI of 4.99. The amino acid sequence of PA1365 is shown below. The predicted signal sequence is highlighted (Figure 5.16)

Figure 5.16: Amino Acid Sequence Of PA1365

MHFSLRSRHLRPSLLASSLLLAVSAQGQEKLDVDLPAAPLGQAINALAQQSSVQILF
AGDLGAGRQAPALKGRFTPEEALRQLLRDSGLKAQARDEHTFIVVPASEAAVPATQA
RSEPLDMEQMEITASRTSSDLVSATRQSTVIEHAQLEELRQGSDSLATVLAKAVPGM
SDSSRTITEYGQTLRGRSMLVMVDGVPLNTNRDSSRNLANIDPALIERIEVIRGSSA
IYGSGATGGIISITTRPAGGENRAETRLSATSPLTRLGSDGLGGQFQQYFAGSLGAL
DYSFDFGTRHVGASYDAHGDRIAPEPSQGDLFDSNVYNIGGKLGLRIDENQRVQLAL
SHYDARQDTDYATDPRVARLPPGSVPANAIKGLELDEQNRIRNTLANLEYENLDILG
SRLSAQLYYRDYFTRFTPFDARAVSTRGGNVDQIMQNSEVFGSRLTLRTPLGESGNT
ELVWGGDYNQERSDMPLDVFDPAAYDASGGLVFDKIGKLTYMPPLRTRSAGAFAQLQ
HRFDEHWSIDGGLRYEYSTAEFDDFIPLSESKAASPVTVKGGDLDYDAVLSNLGIVY
SPVAGQEIYASFSQGFQLPDVGIQLRNARRGFDIGSSNLEPVKTNNYELGWRGAIGG
NTLGSLALFYTTSKLGDVQSFNNGLILTRTKERIYGVEASADWLSDDEVWGAGGSAT
WMRGREKPDGKDWQDMTGYRVPPLKLTAYLQYKPDADWNNRLQATFFDSKDYRLDGV
ESFGRRQVSTYTTVDLVSQYRITPDDQLSLGIQNLFNRDYYPLYSQLLRNNNNTSHL
PAPGTVLTASYTHNW

The amino acid sequence of PA1365 was compared against the NCBI database of protein sequences using the BLASTP program (Altschul *et al*, 1997). Sequence analysis of the PA1365 amino acid sequence revealed a significant degree of sequence identity to the family of putative siderophore outer membrane receptors. The five most significant matches to PA4675 using the BLASTP program and their associated predicted biochemical data are listed in Table 5.4.

Table 5.4: Proteins Displaying Significant Homology To PA1365

Protein	Homologue	Molecular Mass (kDa)*	Accession Number	Identity (%)**
Reut3763	*Ralstonia metalidurans*	91.16	ZP_00024780	62 (77)
Rsp0416	*R. solanacearum*	87.43	NP_521977	61 (76)
AleB	*R. metalidurans*	91.73	CAA66129	52 (66)
Alr0397	Nostoc sp PCC7120	94.33	NP_484441	33 (50)
Sll1206	Synechocystis sp PCC6803	91.66	NP_439914	33 (50)

*The predicted molecular mass (kDa) is calculated for the unprocessed protein.

**Identities (%) were calculated using the Genedoc program. Similarities are indicated in brackets.

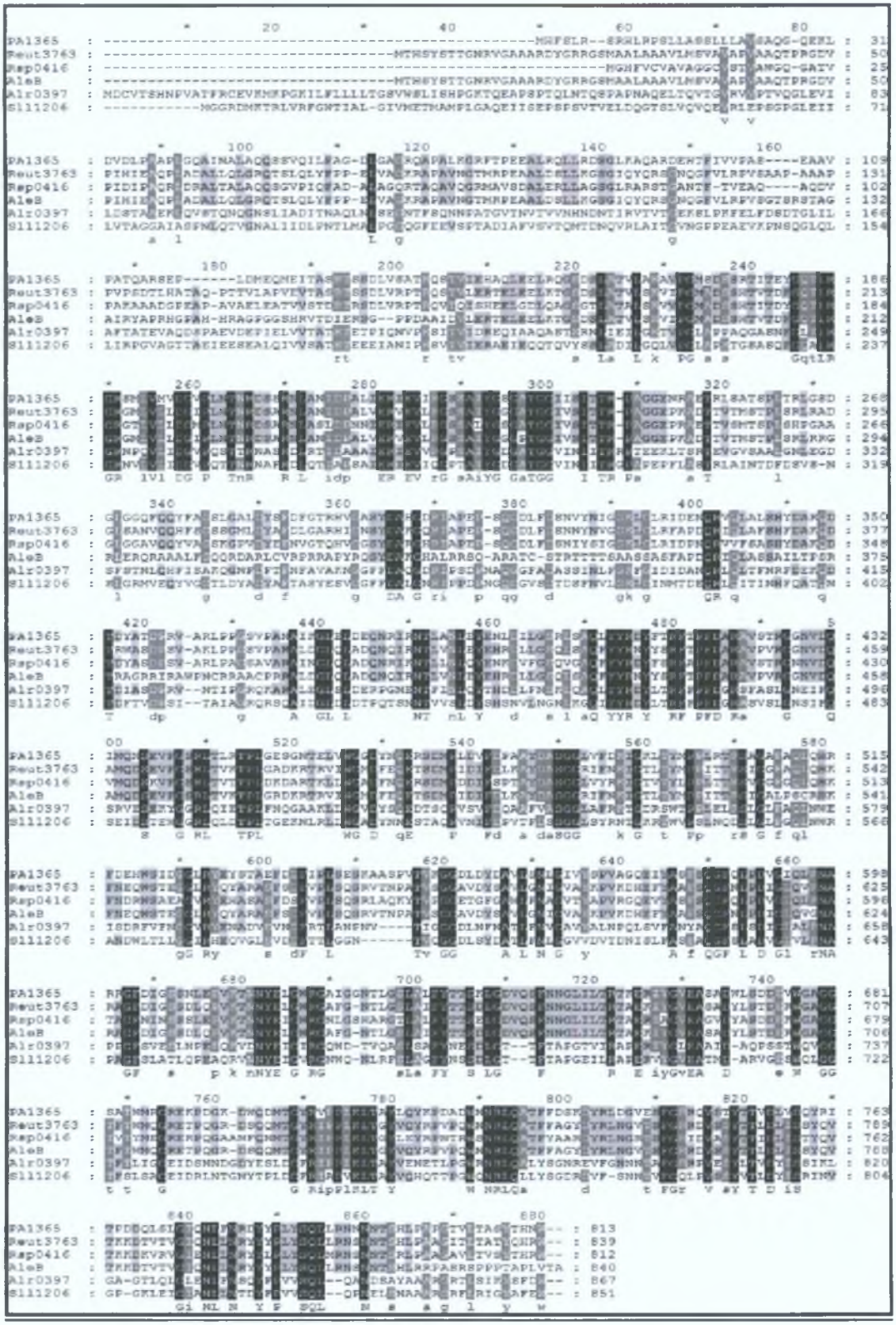

Figure 5.17: Multiple sequence aligenment of PA1365; with Reut3763 from *R. metalidurans*, Rsp0416 from *R. solanacearum*, AleB from *R. metalidurans*, Alr0397 from Nostoc sp PCC7120 and Sll1206 from Synechocystis sp PCC6803. Black indicates 100% conservation, dark grey indicates 83% conservation and light grey indicates 66% conservation.

The amino acid sequence of PA1365 was analysed to determine if the protein contained the amino acid sequence motifs conserved among TonB-dependent receptors, previously designated regions I, II and III (Bitter *et al*, 1991). Region I is the 'TonB box' with the consensus sequence (D/E)TXXVXA(A/S) although this sequence is somewhat degenerate. Region I is typically located near the N-terminus of the protein (Bitter *et al*, 1991; Ankenbauer and Quan, 1994). Analysis of the N-terminal region of PA1365 did not reveal the presence of a TonB motif in this region.

Region II is typically located in the C-terminal part of the protein and has the consensus sequence (F/I/L/M/V)XXX(I/L/V)XNLX(D/N)(K/R)XY. The amino acid sequence of PA1365 was analysed and found to contain the motif LSLGIQNLFNRDY at position 769-781, which completely matches the region II consensus sequence.

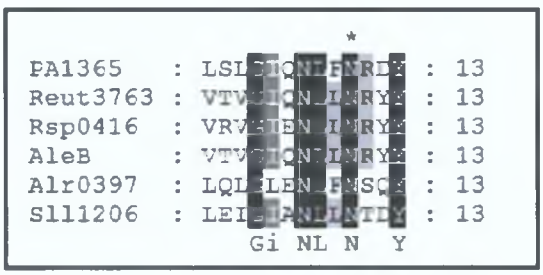

Figure 5.18: TonB Region II Motif. Black indicates 100% conservation, dark grey indicates 83% conservation and light grey indicates 66% conservation.

Region III is typically located at a distance of 100 amino acids from region I. The region is characterised by the consensus sequence R(V/I)(D/E)(I/V)(I/V/L)(K/R)GXX(G/S/A)XXXGXXXXG(G/A)X(V/I). The amino acid sequence of PA1365 was analysed and found to contain the motif RIEVIRGSSAIYGSGATGGIIS at position 219-240.

Figure 5.19: TonB Region III Motif. Black indicates 100% conservation, dark grey indicates 83% conservation and light grey indicates 66% conservation.

The finding of the N-terminal signal sequence and the presence of two characteristic 'TonB motifs' suggest that PA1365 is a TonB dependent outer membrane receptor.

5.8: The Mutagenesis Of PA1365

Analysis of the region encoding PA1365 indicated that the region of interest was encoded on a cosmid designated pMO 010141. The cosmid, which was harboured in *E. coli* S17-1 was obtained from the Pseudomonas Genetic Stock Centre. Restriction analysis of the cosmid was performed *in silico* using the sequence data available on the *Pseudomonas aeruginosa* Genome Homepage (www.pseudomonas.com). Analysis of the region encoding PA1365 allowed the identification of a 4kb *Apa*1/*Bam*H1 fragment with an internal *Xho*1 site that was located within PA1365. The *Xho*1 site was deemed suitable for the insertion of an antibiotic resistance cassette.

Analysis of the cosmid sequence indicated that the *Apa*1 site was possibly dcm methylated. Host restriction and modification encompass a number of elements such as DNA methyltransferases that act to protect the host DNA from restriction from the corresponding restriction endonucleases. The Dcm methylase which is encoded by the *dcm* gene, methylates the cytosine residue, at the C^5 position, in the sequence CCWGG, where W = A/T. The methylated Apa1 site of the 4 Kb *Apa*1/*Bam*H1 fragment is shown in Figure 5.20.

Figure 5.20: Methylated *Apa*1 site in pMO 010141.

The *Apa*1 site is indicated in blue writing while the site of methylation is indicated in red.

Cosmid pMO 010141 was isolated from *E. coli* S17-1 and restricted with *Apa*1. Examination of the restriction profile indicated that the *Apa*1 site was indeed dcm methylated. To ensure complete restriction of the cosmid with *Apa*1 it was necessary to transform pMO 010141 into the *E. coli dcm* mutant, *E. coli* BL21. As the transformation of large DNA fragments can result in deletions or rearrangements of the DNA, pMO 010141 from *E. coli* BL21 was prepared and restricted with *Xho*1 and *Bam*H1. The restriction profile of pMO 010141 prepared from *E. coli* BL21 was

identical to that prepared from *E. coli* S17-1 indicating that no deletions or rearrangements of the cosmid DNA had occurred.

The 4kb *Apa*I/*Bam*HI fragment was isolated and cloned into pJQ200ks (Chapter 3) removing the vector borne *Xho*I site and generating pOC4.0 A/B. The plasmid pOC4.0 A/B was restricted with *Xho*I and the kanamycin cassette from pUC4K was inserted into the *Xho*I site as a *Sal*I fragment generating pOC4.0K A/B. The plasmid pOC4.0K A/B was introduced into *P. aeruginosa* DH119 by triparental mating and transconjugants were selected on LB with tetracycline and gentamicin. Second recombinants were selected by plating on LB with 5% sucrose and kanamycin. Individual colonies were then screened for kanamycin resistance and gentamicin sensitivity. A potential mutant was identified in this way and selected for further analysis.

The genomic sequence in the region encoding PA1365 was examined to identify restriction sites that were deemed suitable for the confirmation of the potential mutant by Southern blot analysis (Chapter 2). The kanamycin cassette was inserted into an *Xho*I site encoded within a 4.0 Kb *Apa*I/*Bam*HI fragment (Figure 5.21) as a *Sal*I fragment, thus destroying the *Xho*I site. However, as the kanamycin cassette from pUC4K encodes a unique *Xho*I site, digestion of the mutant genomic DNA with *Xho*I would generate two *Xho*I fragments as indicated in Figure 5.22. The plasmid pOC4.0K A/B was labelled as described in Chapter 2 and used as a probe.

Figure 5.21: Analysis Of The Region Encoding PA1365 In *P. aeruginosa*.

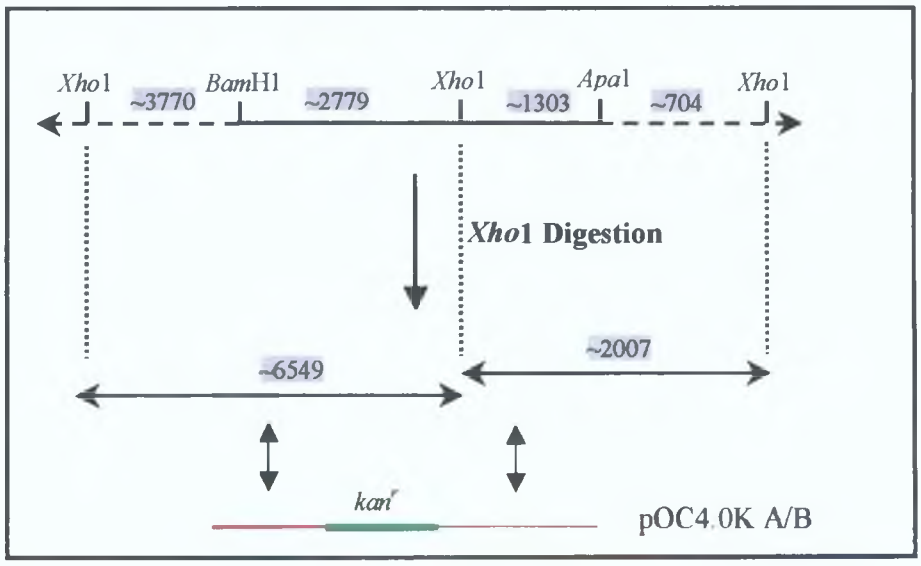

The predicted sizes of the digested fragments are highlighted in grey. The labelled probe is indicated in red, while the kanamycin cassette is highlighted in green. Regions of homology between the labelled probe and the digested fragments are indicated.

Figure 5.22: Analysis Of The Region Encoding PA1365 In A Potential Mutant

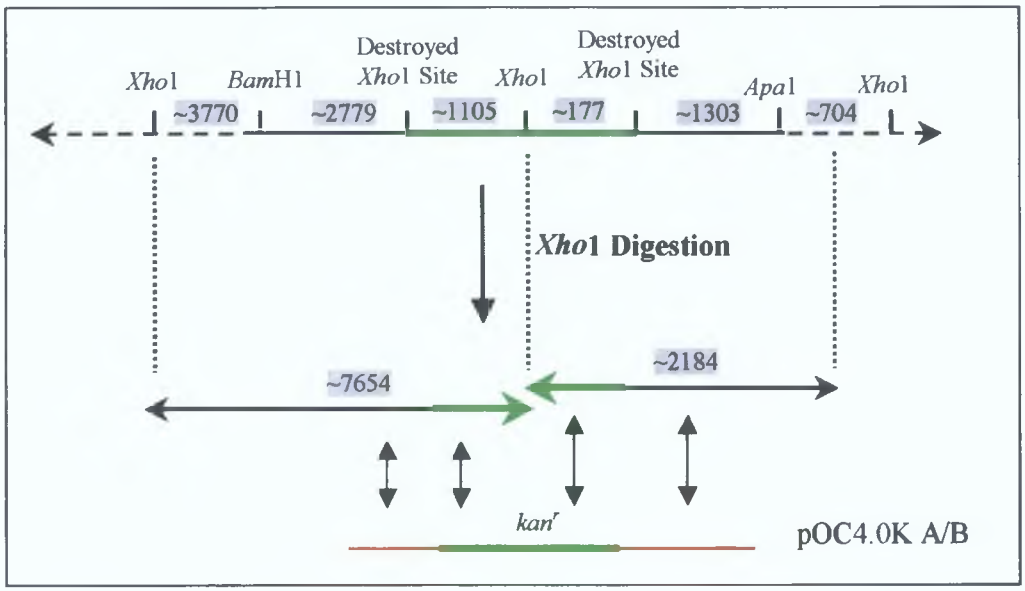

The predicted sizes of the digested fragments are highlighted in grey. The labelled probe is indicated in red, while the kanamycin cassette is highlighted in green. Regions of homology between the labelled probe and the digested fragments are indicated.

Genomic DNA was prepared from *P. aeruginosa* and the potential mutant (Chapter 2), restricted with *Xho*1, transferred to nitrocellulose and probed with labelled plasmid as described in Chapter 2. Examination of the hybridisation result indicated that the kanamycin cassette had correctly integrated into the chromosome of *P. aeruginosa* (Figure 5.23).

Figure 5.23: Southern Blot Analysis Of *P. aeruginosa* DH119 And *P. aeruginosa* PA1365km.

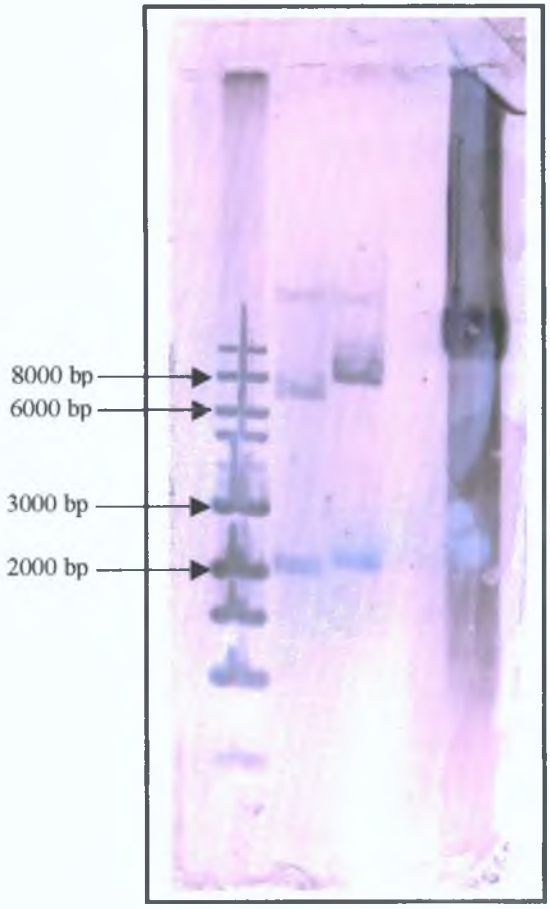

Legend

Lane 1: 1 Kb ladder (Section 2.28)

Lane 2: *P. aeruginosa* DH119 *Xho*1

Lane 3: *P. aeruginosa* PA1365km *Xho*1

Lane 5: pOC4.0K A/B

The mutant strain was named *P. aeruginosa* PA1365km. The phenotypic characterisation of *P. aeruginosa* PA1365km is described in Section 5.10.

5.9: Phenotypic Analysis Of *P. aeruginosa* PA4675km And PA1365km

To determine if *P. aeruginosa* PA4675km and PA1365km were affected in their ability to utilise the citrate hydroxymate siderophores rhizobactin 1021, schizokinen and aerobactin, siderophore utilisation bioassays were performed on each mutant. *P. aeruginosa* PA4675km and PA1365km were generated from the parent strain *P. aeruginosa* DH119 (Heinrichs and Poole, 1993). *P. aeruginosa* DH119 is affected in pyoverdine biosynthesis and is also affected in the production and utilisation of pyochelin. Siderophore utilisation bioassays were performed on the *P. aeruginosa* mutants, and their ability to utilise citrate hydroxymate siderophores was analysed. Table 5.5.

Table 5.5: Citrate Hydroxamate Utilisation By P. aeruginosa

***P. aeruginosa* Strain**	**Genotype**	**Rhizobactin 1021 Utilisation**	**Schizokinen Utilisation**	**Aerobactin Utilisation**
DH119	*pvd-2, pchR*	+	+	+
PA4675km	*pvd-2, pchR*, PA4675	-	-	-
PA1365km	*pvd-2, pchR*, PA1365	+	+	+

Analysis of the mutant phenotypes indicated that *P. aeruginosa* PA4675km was affected in its ability to utilise all three citrate hydroxymate siderophores tested. Mutant *P. aeruginosa* PA1365km however remained unaffected in its ability to utilise the three siderophores (Table 5.5). The result indicated that PA4675 is the outer membrane receptor for the citrate hydroxymate siderophores tested. PA4675 was redesignated *chtA* (citrate hydroxymate transport). The ability of ChtA to mediate the transport of rhizobactin 1021, schizokinen and aerobactin is similar to that described for IutA in *E. coli*. The result indicated that IutA and its homologues are capable of mediating the transport of structurally similar citrate hydroxymate siderophores.

5.10: Siderophore Transport Via ChtA Is TonB1 Mediated

Receptor mediated ligand uptake across the outer membrane of Gram negative bacteria is an energy dependent process that is dependent upon the function of the TonB protein. Two TonB homologues, TonB1 and TonB2, have been identified and experimentally characterised in *P. aeruginosa* (Poole *et al*, 1996; Takese *et al*, 2000; Zhao and Poole, 2000). Analysis of *P. aeruginosa tonB* mutants indicated that siderophore mediated iron transport is primarily dependent on TonB1 function. *P. aeruginosa tonB2* mutants are also affected in iron utilisation, but to a much lesser extent than *P. aeruginosa tonB1* mutants (Zhao and Poole, 2000).

The ability of a *tonB* mutant of *P. aeruginosa* to utilise various citrate hydroxymate siderophores was analysed by the siderophore utilisation bioassay (see Table 5.6). A *P. aeruginosa tonB* mutant, which is a PA01 derivative, was kindly provided by Dr. Keith Poole.

Table 5.6: Citrate Hydroxamate Siderophore Utilisation By *P. aeruginosa*

***P. aeruginosa* Strain**	**Rhizobactin 1021 Utilisation**	**Schizokinen Utilisation**	**Aerobactin Utilisation**
DH119	+	+	+
K1040	-	-	-

Analysis of the siderophore utilisation bioassay results indicated that siderophore mediated iron transport via the outer membrane receptor ChtA was TonB1 dependent. The result is consistent with previous results in *P. aeruginosa* that indicated that TonB1 is the primary energy transducer to TonB dependent outer membrane proteins in *P. aeruginosa*.

5.11: Ferrichrome Transport In *P. aeruginosa*

In silico analysis of the *P. aeruginosa* genome sequence indicated that there was an apparent lack of clearly identifiable siderophore inner membrane transport systems encoded within the genome (Köster, 2001; personal observation). As previously described, in *S. meliloti* 2011, the transport of the citrate hydroxymate siderophores rhizobactin 1021 and schizokinen is mediated via the RhtX permease (Chapter 3). A homologue of RhtX was identified in *P. aeruginosa* and the corresponding mutant, PA4218km was found to be defective in pyochelin transport (Chapter 3), while transport of the citrate hydroxymate siderophores rhizobactin 1021, schizokinen and aerobactin in PA4218km remained unaffected (Section 5.2 and 5.3). In *E. coli*, transport of rhizobactin 1021, schizokinen and aerobactin is mediated at the inner membrane by the FhuCDB system (Chapter 3). *In silico* analysis of the *P. aeruginosa* genome sequence revealed that there was no FhuD homologue and only a weak FhuB (15% identity to PA2914) homologue present in the genome. A putative protein was identified displaying 38% identity to FhuC (PA4158), but this protein displays 70% identity to FepC. PA4158 is encoded proximal to other putative Fep inner membrane transport proteins, and considering the relative specificity of inner membrane siderophore transport systems (Chapter 1), it is unlikely that this protein functions in hydroxamate/citrate hydroxamate utilisation. Analysis indicated that a putative outer membrane receptor for ferrichrome, FhuA, was encoded within the genome.

To determine if *P. aeruginosa* was capable of mediating the transport of ferrichrome, a siderophore utilisation bioassay was performed using strains DH119 and PA4218km.

Table 5.7: Ferrichrome Utilisation By *P. aeruginosa*.

***P. aeruginosa* Strain**	**Ferrichrome Utilisation**
DH119	+
PA4218km	+

Analysis of the result indicated that strains *P. aeruginosa* DH119 and PA4218km could both utilise the xenosiderophore ferrichrome, as an iron source. The result also indicated that *P. aeruginosa* was capable of mediating the transport of ferrichrome in the absence of a clearly identifiable *fhuBCD* system. The absence of a clearly identifiable FhuBCD system in *P. aeruginosa* indicated that the utilisation of citrate hydroxamates is occurring via an alternative transport system . Overall the results for ferrichrome and the citrate hydroxymate siderophores indicate that siderophore mediated transport at the inner membrane in *P. aeruginosa* is occurring via a novel mechanism.

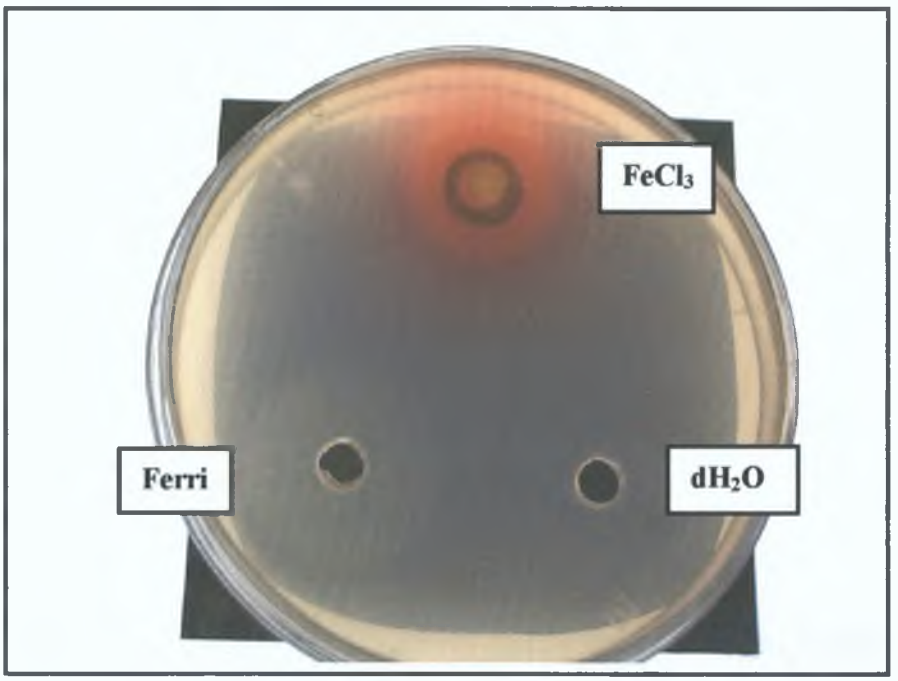

Figure 5.24: Ferrichrome Utilisation By *P. aeruginosa* DH119. Ferric chloride ($FeCl_3$) was used as a positive control. Ferrichrome (Ferri) was resuspended in ultra pure water. Sterile ultra pure water (dH_2O) was used as a negative control.

5.12: Discussion

P. aeruginosa produces two siderophores under conditions of iron limitation; pyoverdine and pyochelin (Chapter 1). The cognate outer membrane receptors for pyoverdine and pyochelin, FpvA and FptA respectively, have been identified and characterised. As previously described, many bacteria have been found to utilise siderophores that they do not themselves produce, termed xenosiderophores. The ability of an organism to utilise xenosiderophores possibly confers a competitive advantage on the bacterium, enabling it to survive in extended ecological niches. *In silico* analysis of the *P. aeruginosa* genome sequence led to the identification of 34 putative TonB dependent receptors, many of whose ligands are unidentified (Köster, 2001). The plethora of putative siderophore outer membrane receptors encoded by *P. aeruginosa* and the ability of the organism to utilise several xenosiderophores reflects the ecological range of this organism

The ability of *P. aeruginosa* to utilise various xenosiderophores has previously been described (Chapter 1). Aerobactin, a known virulence factor, has been shown to be utilised by *P. aeruginosa* (Liu and Shokrani, 1978). *In silico* analysis of the *P. aeruginosa* genome sequence resulted in the identification of a putative protein, ChtA displaying significant homology to RhtA, the outer membrane receptor for rhizobactin 1021 in *S. meliloti* 2011. Further detailed analysis indicated that *P. aeruginosa* encodes a further protein, PA1365, which also displays significant homology to RhtA. On the basis of the significant homology between the receptors coupled to the fact that *S. meliloti* 2011 and *P. aeruginosa* can occupy the same ecological niche, it was decided to examine the ability of *P. aeruginosa* to utilise the xenosiderophore rhizobactin 1021.

A *P. aeruginosa* strain, DH119, impaired in pyoverdine and pyochelin biosynthesis was used for the analysis of xenosiderophores utilisation. The defect in siderophore production inhibits growth in iron deplete media resulting in reduced background growth and enabling accurate analysis of xenosiderophore utilisation. Examination indicated that *P. aeruginosa* DH119 was capable of utilising rhizobactin 1021 as an iron source. Rhizobactin 1021 utilisation had previously been shown to be mediated

by the RhtX permease in *S. meliloti* 2011 (Chapter 3). A homologue of RhtX, FptX, was found to mediate the utilisation of pyochelin in *P. aeruginosa*. Although rhizobactin 1021 and pyochelin are structurally dissimilar, the RhtX and FptX proteins display significant homology to each other (41% identity as calculated by BLASTP at NCBI). Due to this significant homology, the ability of FptX to mediate the utilisation of rhizobactin 1021 was examined. An *fptX* mutant was found to be unimpaired in rhizobactin 1021 utilisation. The ability of *P. aeruginosa* to utilise schizokinen, which is structurally similar to rhizobactin 1021 was examined. *P. aeruginosa* was found to be capable of utilising schizokinen. Further analysis indicated that FptX was not required for the utilisation of either schizokinen or aerobactin.

As described above, two putative receptors designated ChtA and PA1365, identified in the *P. aeruginosa* genome sequence displayed significant homology to RhtA. The ChtA protein was analysed against the database of proteins at NCBI and was found to display significant homology to IutA type receptors from various *Escherichia* and *Shigella* sp. (Chapter 5). In *E. coli* the utilisation of the citrate hydroxamate siderophores aerobactin, schizokinen and rhizobactin 1021 is mediated by the IutA outer membrane receptor (Chapter 3). The genes encoded in the region adjacent to *cht*A were analysed but were determined to be unlikely to encode proteins that functioned in siderophore mediated iron acquisition. Examination of the ChtA protein sequence enabled the identification of a putative protein export signal sequence commonly found amongst outer membrane proteins. Cleavage of the predicted signal sequence results in a protein with a predicted size of 78 kDa, typical for siderophore outer membrane receptors. Analysis of the protein sequence resulted in the identification of the three 'TonB motifs' corresponding to regions I, II and III, commonly found amongst TonB dependent receptors (Bitter *et al*, 1991; Ankenbauer and Quan, 1994). The presence of the N-terminal sequence and the 'TonB motifs' suggested that ChtA was a TonB dependent outer membrane receptor.

Analysis of PA1365 against the database of proteins at NCBI revealed that PA1365 displayed homology to uncharacterised putative siderophore receptors from *Ralstonia* sp. and to IutA type receptors from Nostoc sp. PCC7120 and Synechocystis sp. PCC6803. PA1365 also shows strong homology to a receptor from *R. metalidurans*

(formerly *Acaligenes eutropha*) that had previously been characterised. AleB was found to transport a phenolate type siderophore whose structure has not yet been elucidated (Gilis *et al*, 1996). Examination of the PA1365 protein sequence indicated the presence of a protein export signal sequence, the cleavage of which results in a protein product the predicted size of which is 86.2 kDa. Analysis of the PA1365 protein sequence resulted in the identification of two 'TonB motifs' corresponding to regions II and III. The N-terminal TonB region I motif was not identified although this sequence is somewhat degenerate and not always clearly identifiable. The presence of the N-terminal export signal sequence and the TonB motifs suggested that PA1365 was a TonB dependent outer membrane receptor. Analysis of the PA1365 protein sequence indicated the presence of an N-terminal extension, similar to the extension found in proteins such as FecA and FpvA. This N-terminal extension is involved in signal transduction via a transmembrane regulatory system from the outer membrane to the cytoplasm (Chapter 1). A putative regulatory system was identified in the region directly upstream from PA1365. The proteins, PA1363 and PA1364 were predicted to encode a putative ECF sigma factor and a cytoplasmic transmembrane acting signal transducer. Directly upstream of PA1363, a putative gene encoding a protein product of unknown function was encoded. Analysis indicated that there were very small gaps between PA1362, PA1363 and PA1364, indicating that they possibly formed an operon. The identification of a putative regulatory system adjacent to PA1365 and the presence of an N-terminal extension sequence in PA1365 suggest that PA1365 is regulated by this system. Several of the proteins displaying homology to PA1365 also possess N-terminal extensions and are encoded adjacent to putative regulatory systems.

The *chtA* gene and the PA1365 gene were mutated by the cassette mutagenesis and the resulting mutant phenotypes were examined. Analysis indicated that the *chtA* mutant, *P. aeruginosa* PA4675km was defective in the utilisation of aerobactin, schizokinen and rhizobactin 1021. Analysis of the PA1365 mutant, *P. aeruginosa* PA1365km revealed that the mutant was unaffected in the utilisation of aerobactin, schizokinen and rhizobactin 1021. This result indicated that ChtA is a common receptor for utilisation of the citrate hydroxamate siderophores described above in *P. aeruginosa*.

Ochsner *et al* (2001) described the global analysis of gene expression in response to iron starvation. Analysis of the results indicated that expression of *chtA* and PA1365 were not induced under conditions of iron limitation. Complex regulatory systems have been shown to be present in *P. aeruginosa* that allow for expression of the receptor gene only in the presence of the cognate siderophore. Expression of the ferricitrate system in *E. coli* is positively mediated by the presence of exogenous ferricitrate in a signal transduction cascade involving FecIR and FecA. The presence of an N-terminal extension on PA1365 and a putative regulatory system, encoded by PA1363 and PA1364 and predicted to be similar to the FecIR system of *E. coli* possibly indicate that the expression of PA1365 is regulated by the regulatory system. In the absence of the cognate siderophore, it is possible that PA1365 is not maximally expressed, and that the level of expression falls below the detection level threshold used by Ochsner *et al* (2001).

The absence of a clearly identifiable regulator proximal to PA4675 indicated that the gene was possibly directly regulated by Fur. However, PA4675 did not appear to be expressed under the conditions of iron limitation examined. Analysis of the promoter region of PA4675 led to the identification of two putative Fur boxes. Fur Box 1, which was located approximately 300 – 320 bp upstream from the PA4675 translational start site displayed 63% homology to the *E. coli* Fur box consensus sequence. Fur Box 2, which was located approximately 55 – 65 bp upstream from the PA4675 translational start site displayed 73% homology to the *E. coli* Fur box consensus sequence. Examination of the fur boxes indicated that Fur Box 2 exhibited a characteristic inverted repeat, while Fur Box 1 did not, suggesting that this first Fur box may have limited Fur-binding ability. Several genes in *P. aeruginosa* are positively regulated by PvdS (Chapter 1). Examination of the promoter region of *chtA* did not reveal the presence of an Iron Starvation box (IS box) that is characteristically found in the promoters of PvdS regulated genes. Analysis of gene expression in a *pvdS* deletion mutant of *P. aeruginosa* indicated that PvdS does not regulate *chtA* (Ochsner *et al*, 2001). The absence of detectable *chtA* transcription under conditions of iron limitation possibly indicates that *chtA* may be under the control of an as yet unidentified regulator and may need to be induced by the addition of the cognate siderophore.

In *E. coli* the utilisation of citrate hydroxamate siderophores aerobactin, schizokinen and rhizobactin 1021 is dependent on the FhuCDB inner membrane iron transport system (Chapter 1 and Chapter 3). *In silico* analysis of the *P. aeruginosa* genome sequence indicated the absence of a clearly identifiable FhuBCD system homologue. A homologue of FhuC, PA4158 was identified in the genome sequence and displayed 38% identity to FhuC. This protein however displays 78% identity to FepC and is located adjacent to a putative Fep inner membrane transport system and is thus unlikely to function in hydroxamate utilisation. No FhuD homologue was identified within the genomic sequence of *P. aeruginosa* while only a weak FhuB homolgue (15% identity to PA2914) was identified. In *S. meliloti* 2011, the utilisation of schizokinen and rhizobactin 1021 is dependent on the RhtX protein. A mutant defective in the production of the RhtX homologue FptX was found to be unimpaired for citrate hydroxamate utilisation. The lack of activity of FptX for citrate hydroxamate transport and the absence of a clearly identifiable FhuBCD system suggest that citrate hydroxamate transport at the inner membrane of *P. aeruginosa* occurs via a novel mechanism. *In silico* analysis of the *P. aeruginosa* genome indicates that *P. aeruginosa* does not appear to encode readily identifiable inner membrane siderophore transport systems. The lack of such systems indicates that *P. aeruginosa* possibly encodes 'novel' type transporters similar to FptX for pyochelin utilisation (Chapter 3). Alternatively, iron may be released in the periplasm and transported to the cytoplasm by metal transport proteins specific for ferrous or ferric iron.

Siderophore mediated iron acquisition requires active transport against a concentration gradient, and consequently is an energy dependent process. Energy is transduced to the outer membrane by a complex of proteins termed the TonB complex (Chapter 1). Two homologues of TonB, TonB1 and TonB2 have been identified in *P. aeruginosa* (Poole *et al*, 1994; Zhao and Poole, 2000). Mutants defective in TonB1 production are severely affected in iron acquisition. Mutants defective in TonB2 are not as severely affected, indicating partial redundancy for this protein. Analysis of citrate hydroxamate utilisation by a *P. aeruginosa* TonB1 mutant, K1040 indicated that siderophore utilisation had been abolished. The result indicates that TonB1 is involved in energy transduction to ChtA.

Southern blot analysis of the region encoding *chtA* in *P. aeruginosa* DH119 revealed that *chtA* appeared to be encoded on a larger *Xho*1 fragment than that predicted from the genome sequence. Detailed Southern blot analysis of the region encoding *chtA* in *P. aeruginosa* DH119 and *P. aeruginosa* PA4675km indicated that the 6 Kb *Eco*R1 and 3.9 Kb and 1.6 Kb *Bam*H1 fragments that spanned the gene and the adjacent regions upstream and downstream correlated with the predicted sizes from the genome sequence. Further analysis of the *Xho*1 digest suggested that the anomaly in the *Xho*1 sites was located in a region upstream of *chtA* as the Southern blot indicated that the downstream *Xho*1 site was intact. As the upstream Xho1 site(s) are located within the 6 Kb *Eco*R1 fragment, the analysis suggested a possible inaccuracy in the genomic sequence.

P. aeruginosa has been shown to utilise a variety of xenosiderophores including enterobactin and its breakdown products as well as several siderophores of fungal origin (Chapter 1). While pyochelin is an active transporter of iron, cells producing pyoverdine appear to produce very little pyochelin (Heinrichs *et al*, 1991). Similarly, the presence of enterobactin leads to a concomitant reduction in pyoverdine and pyochelin production (Poole *et al*, 1990; Dean and Poole, 1993). It therefore seems that *P. aeruginosa* appears to have a hierarchy of siderophore usage in which the most efficient chelator of iron is preferentially utilised. This feature of *P. aeruginosa* possibly reflects a strategy whereby energy is conserved by scavenging siderophores produced by other organisms ensuring that siderophore chelated iron is still available to the bacterium. The wide distribution of *P. aeruginosa* is also possibly reflected in the range of xenosiderophores that it can utilise, and also in the range of ferrisiderophore receptors that it encodes. The ability of *P. aeruginosa* to utilise aerobactin is intriguing as aerobactin is produced by various important pathogens such as *E. coli* and *Shigella* sp. which often colonise the same sites as *P. aeruginosa*. The ability of aerobactin to effectively deliver iron in an infection situation possibly enhances the virulence of the bacteria. Information about siderophore usage during mixed infections is limited, and could lead to alternative therapies.

A number of other organisms have been reported to utilise aerobactin, although the receptors involved have yet to be identified. Analysis of xenosiderophores utilisation in *P. putida* indicated that the bacterium could utilise both enterobactin and aerobactin

(Loper and Henkels, 1999). Similarly analysis of the draft genome sequence revealed the presence of a ChtA homologue encoded within the genome. *Vibrio parahaemolyticus*, an estuarine pathogen was shown to encode an IutA homologue and to be capable of utilising aerobactin (Funahashi *et al*, 2003). Southern blot analysis indicated that *iutA* homologues were widely distributed amongst clinical and environmental *V. parahaemolyticus* isolates.

The relative non-specificity of siderophore outer membrane receptors makes them attractive as targets for siderophore antibiotic conjugate therapy. The widespread distribution of specific siderophore receptors across various species will also possibly result in effective directed treatment of infections. As siderophore receptors are found at the cell surface, they often induce antibody production, which consequently makes them good targets for vaccine production. Antibodies directed against siderophore outer membrane receptors in *A. baumannii* blocked siderophore utilisation and were also bactericidal (Goel and Kapil, 2001). Similarly FetA in *Nesseria* represents a good vaccine target as indicated by antibody production in various patients (Black *et al*, 1986). Phase variant regulation of this receptor however, possibly indicates that a combination of outer membrane targets may be required for the production of an effective vaccine.

Concluding Remarks

6.0: Concluding Remarks

E. coli is regarded as a model organism and consequently, the mechanisms of siderophore mediated iron acquisition have been well studied. *E. coli* encodes six TonB dependent siderophore outer membrane receptors and three inner membrane siderophore iron transport systems; the *fhu*, *fep* and *fec* systems, of which the *fhu* system is best characterised. The *fhu* system represents a classic PBT transport system consisting of a periplasmic binding protein, an inner membrane permease and an inner membrane associated ATPase.

A region of *S. meliloti* 2011 encoding proteins involved in rhizobactin 1021 biosynthesis, regulation and outer membrane transport was identified (Lynch *et al*, 2001; Lynch, PhD Thesis, 1999). Also identified was a gene, *rhtX*, encoding a protein showing weak homology to AmpG, a protein involved in cell wall recycling. Characterisation of RhtX indicated that it was involved in the utilisation of rhizobactin 1021 in *S. meliloti* 2011. The expression of *rhtA* and *rhtX in trans* in *S. meliloti* 102F34, a strain not producing or utilising rhizobactin 1021 indicated that RhtA and RhtX were sufficient to confer upon this strain the ability to utilise rhizobactin 1021.

Analysis of rhizobactin 1021 and schizokinen utilisation in *E. coli* indicated that they were utilised via IutA and FhuCDB in a manner similar to that described for aerobactin. The expression of *rhtX* in an *E. coli fhuC* mutant restored rhizobactin 1021 and schizokinen utilisation, indicating that RhtX was capable of the partial complementation of the FhuCDB system. While RhtX is predicted to be an inner membrane permease, it does not contain any of the motifs usually associated with permeases associated with PBT systems suggesting that RhtX is a novel protein and possibly functions by a novel mechanism.

The ability of *P. aeruginosa* to utilise aerobactin has previously been reported (Liu and Shokrani, 1978). Further analysis indicated that *P. aeruginosa* was capable of utilising both rhizobactin 1021 and schizokinen as iron sources. *In silico* analysis resulted in the identification of two receptors displaying significant homology to IutA type receptors. Mutants were constructed in both putative receptor genes and it was

determined that PA4675 (ChtA) was the outer membrane receptor for rhizobactin 1021, schizokinen and aerobactin. Further analysis indicated that the utilisation of the citrate hydroxamate siderophore was not mediated by the RhtX homologue, FptX. *In silico* analysis indicated that *P. aeruginosa* did not encode significant FhuCDB homologues. It was thus proposed that the utilisation of citrate hydroxamate siderophores at the inner membrane in *P. aeruginosa* was occurring via a novel mechanism.

A proposed model for citrate hydroxamate utilisation in *E. coli*, *S. meliloti* 2011 and *P. aeruginosa* is illustrated below.

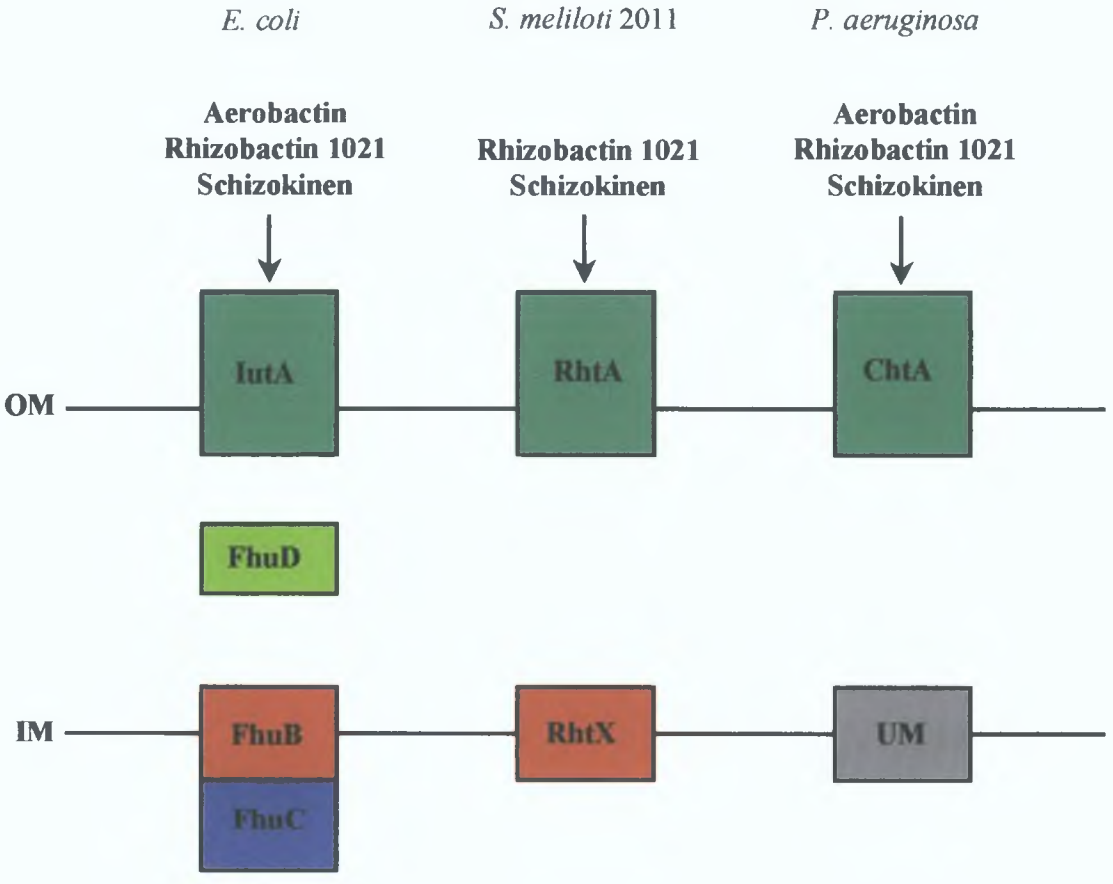

Figure 6.1: Citrate hydroxamate utilisation in *E. coli*, *S. meliloti* 2011 and *P. aeruginosa*. In *E. coli*, the utilisation of aerobactin, rhizobactin 1021 and schizokinen is mediated at the outer membrane (OM) by IutA. It is subsequently transported via FhuD to the inner membrane (IM) where it is subsequently transported to the cytoplasm by a process involving both FhuB and FhuC. In *S. meliloti* 2011, the utilisation of rhizobactin 1021 and schizokinen is mediated at the outer membrane by RhtA. Utilisation is subsequently mediated by RhtX, possibly at the inner membrane. No other components have yet been identified that function in this system. In *P. aeruginosa*, the utilisation of aerobactin, rhizobactin 1021 and schizokinen is mediated at the outer membrane by ChtA. The siderophores are subsequently utilised by an unknown mechanism (UM).

References

- Abdul-Tehrani, H., Hudson, A. J., Chang, Y. S., Timms, A. R., Hawkins, C., Williams, J. M., Harrison, P. M., Guest, J. R. and Andrews, S. C. (1999) Ferritin mutants of *Escherichia coli* are iron deficient and growth impaired, and *fur* mutants are iron deficient. J. Bacteriol. 181: 1415-1428
- Adjimani, J. P. and Emery, J. (1987) Iron uptake in *Mycelia sterilia* EP-76. J. Bacteriol. 169: 3664-3668.
- Ahmer, B. M. M., Thomas, M. G., Larsen, R. A. and Postle, K. (1995) Characterization of the *exbBD* operon of *Escherichia coli* and the role of ExbB and ExbD in TonB function and stability. J. Bacteriol. 177: 4742-4747
- Alexeyev, M. K., Shokolenko, I. N. and Croughan, T. P. (1995) Improved antibiotic-resistance gene cassettes and omega elements for *Escherichia coli* vector construction and *in vitro* deletion/insertion mutagenesis. Gene 160: 63-67
- Almiron, M., Link, A. J. and Furlong, D. (1992) A novel DNA-binding protein with regulatory and protective roles in starved *Escherichia coli*. Genes Dev. 6: 2646-2654
- Althaus, E. W., Outten, C. E., Olson, K. E., Cao, H. and O'Halloran, T. V. (1999) The ferric uptake regulation (Fur) repressor is a zinc metalloprotein. Biochemistry 38: 6559-6569
- Altschul, S. F., Madden, T. L., Schaffer, A. A., Zhang, J., Zhang, Z., Miller, W. and Lipman D. J. (1997) Gapped BLAST and PSI-BLAST: a new generation of protein database search programs. Nucl. Acids Res. 25: 3389-3402
- Andrews, S. C. (1998) Iron storage in bacteria. Adv. Microb. Phys. 40: 281-351
- Andrews, S. C., Le Brun, N. E., Barynin, V., Thomson, A. J., Moore, G. R., Guest, J. R. and Harrison, P. M. (1995) Site-directed replacement of the coaxial heme ligands of bacterioferritins generates heme-free variants. J. Biol. Chem. 270: 23268-23274
- Andrews, S. C., Robinson, A. K. and Rodríguez-Quinones, F. (2003) Bacterial iron homeostasis. FEMS Microbiol. Review. 27: 215-237
- Angerer, A., Enz, M., Ochs, M. and Braun, V. (1995) Transcriptional regulation of ferric citrate transport in *Escherichia coli* K-12. FecI belongs to a

new subfamily of sigma 70-type factors that respond to extracytoplasmic stimuli. Mol. Microbiol. 18: 163-174

- Ankenbauer, R. G. (1992) Cloning of the outer membrane high affinity Fe(III) pyochelin receptor of *Pseudomonas aeruginosa*. J. Bacteriol. 174: 4401-4409
- Ankenbauer, R. G. and Quan, H. N. (1994) FptA, the Fe(III)-pyochelin receptor of *Pseudomonas aeruginosa*: a phenolate siderophore receptor homologous to hydroxymate siderophore receptors. J. Bacteriol. 176: 307-319
- Ankenbauer, R. L., Hanne, F. and Cox, C. D. (1986) Mapping of mutations in *Pseudomonas aeruginosa* defective in pyoverdin production. J. Bacteriol. 167: 7-11
- Arceneaux, J. E. L. and Byers, B. R. (1980) Ferrisiderophore reductase activity in *Bacillus megaterium*. J. Bacteriol. 141: 715-721
- Ardon, O., Nudleman, R., Caris, C., Libman, J., Shazner, A., Chen, Y. and Hadar, Y. (1998) Iron uptake in *Ustilago maydis*: Tracking the iron path. J. Bacteriol. 180: 2021-2026
- Ardon, O., Weizman, H., Libman, J., Shazner, A., Chen, Y. and Hadar, Y. (1997) Iron uptake in *Ustilago maydis*: studies with fluorescent ferrichrome analogues. Microbiology 143: 3625-3631
- Bagg, A. and Neilands, J. B. (1987) Ferric uptake regulation protein acts as a repressor, employing iron(II) as a cofactor to bind the operator of an iron transport operon in *Escherichia coli*. Biochemistry 30: 5471-5477
- Baichoo, N., Wang, T., Ye, R. and Helmann, J. D. (2002) Global analysis of the *Bacillus subtilis* Fur regulon and the iron starvation stimulon. Mol. Microbiol. 45: 1613-1629
- Barloy-Hubler, F., Capela, D., Barnett, M. J., Kalman, S., Federspiel, N. A., Long, S. A. and Galibert, F. (2000) High-resolution physical map of the *Sinorhizobium meliloti* 1021 pSyma megaplasmid. J. Bacteriol. 182: 1185-1189
- Barnett, M. J., Fisher, R. F., Jones, T., Komp, C., Abola, A. P., Barloy-Hubler, F., Bowser, L., Capela, D., Gailbert, F., Gouzy, J., Gurjal, M, Hong, A, Huizar, L., Hyman, R. W., Kahn, D., Kahn, M. L., Kalman, S., Keating, D. H., Palm, C. Peck, M. C., Surzycki, R., Wells, D. H., Yeh, K-C, Davis, R. W., Federspiel, N. A. and Long, S. R. (2001) Nucleotide sequence and predicted

functions of the entire *Sinorhizobium meliloti* pSymA megaplasmid. Proc. Natl. Acad. Sci. U. S. A.. 98: 9883-9888

- Barsomian, G. D., Urzainqui, A., Lohman, K. and Walker, G. C. (1992) *Rhizobium meliloti* mutants unable to synthesize anthranilate display a novel symbiotic phenotype. J. Bacteriol. 174: 4416-4426
- Barton, I. L., Johnson, G. V., Schitoskey, K. and Wertz, M. (1996) Siderophore-mediated iron metabolism in growth and nitrogen fixation by alfalfa nodulated with *Rhizobium meliloti*. J. Plant. Nutr. 19: 1201-1210.
- Barton, L. L., Fekete, F. A., Vester, C. R., Gill, P. R. and Neilands, J. B. (1992) Physiological characteristics of *Rhizobium meliloti* 1021 Tn5 mutants with altered rhizobactin activities. J. Plant Nutr. 15: 2145-2156.
- Bateman, A., Birney, E., Cerruti, L., Durbin, R., Etwiller, L., Eddy, S. R., Grittiths-Jones, S., Howe, K. L., Marshall, M. and Sonnhammer, E. L. L. (2002) The Pfam protein families database. Nucl. Acids. Res. 30: 276-280
- Battistoni, F., Platero, R., Duran, R., Cervenansky, C. Battistoni, J., Arias, A. and Fabiano, E. (2002) Identification of an iron-regulated, hemin-binding outer membrane protein in *Sinorhizobium meliloti*. Appl. Environ. Microbiol. 68: 5877-5881
- Beare, P. A., Raewyn, J. F., Martin, L. W. and Lamont, I. L. (2003) Siderophore-mediated cell signalling in *Pseudomonas aeruginosa*: divergent pathways regulate virulence factor production and siderophore receptor synthesis. Mol. Microbiol. 47: 195-207
- Bekra, R. M. and Vasil, M. L. (1982) Phospholipase C (heat-labile hemolysin) of *Pseudomonas aeruginosa*: purification and preliminary characterization. J. Bacteriol. 152: 239-245
- Bell, P. E., Nau, C. D., Browun, J. T., Konisky, J. and Kadner, R. J., (1990) Genetic suppression demonstrates interaction of TonB protein with outer membrane transport proteins in *Escherichia coli*. J. Bacteriol. 172: 3826-3829.
- Bergman, K., Gulash-Hofee, M., Hovestadt, R. E., Larosiliere, R. C., Ronco, P. G. and Su, L. (1988) Physiology of behavioral mutants of *Rhizobium meliloti*: evidence for a dual chemotaxis pathway. J. Bacteriol. 170: 3249-3254.

- Beringer, J. E. (1974) R factor transfer in *Rhizobium leguminosarum*. J. Gen. Micro. 84: 188-198
- Bindereif, A. and Neilands, J. B. (1985) Promoter mapping and transcriptional regulation of the iron assimilation system of plasmid ColV-K30 in *Escherichia coli* K-12. J. Bacteriol. 162: 1039-1046
- Birmboim, H. and Doly, J. (1979) A rapid alkaline extraction procedure for screening recombinant plasmid DNA. Nucleic Acids Res. 7: 1513-1523
- Bitter, W., Marugg, J. D., de Weger, L. A., Tommassen, J. and Weisbeek, P. J., (1991) The ferric-pseudobactin receptor PupA of *Pseudomonas putida* WCS358: homology to TonB dependent *Escherichia coli* receptors and specificity of the protein. Mol. Micorbiol. 5: 647-655
- Black, J. R., Dyer, D. W., Thompson, M. K. and Sparling, P. F. (1986) Human immune response to iron-repressible outer membrane proteins of *Neisseria meningitides*. Infect. Immun. 54: 710-713
- Blumer, C., Heeb, S., Pessi, G. and Haas, D. (1999) Global GacA-steered control of cyanide and exprotease production in *Pseudomonas fluorescens* involves specific ribosome binding sites. Proc. Natl. Acad. Sci. U. S. A. 96: 14073-14078
- Bosch, M., Garrido, E., Llagostera, M., Pérez de Rozas, A. M., Badiola, I. and Barbé, J. (2002) *Pasteurella multocida exbB*, *exbD* and *tonB* genes are physically linked but independently transcribed. FEMS Microbiol. Lett. 210: 201-208
- Boyd, J., Oza, M. N. and Murphy, J. R. (1990) Molecular cloning and DNA sequence analysis of a diphtheria toxin iron-dependent regulatory element (*dtxR*) from *Corynebacterium diphtheriae*. Proc. Natl. Acad. Sci. U. S. A. 87: 5968-5972
- Boyer, R. F., McArthur, J. S. and Cary, T. M. (1990) Plant phenolics as reductants for ferritin iron release. Phytochemistry 29: 3717-3719
- Bracken, C. S., Baer, M. T., Abdur-Rashid, A., Helmes, W. and Stojilkovic, I. (1999) Use of heme-protein complexes by the *Yersinia enterocolitica* HemR receptor: histidine residues are essential for receptor function. J. Bacteriol. 181: 6063-6072

- Bradbeer, C. (1993) The proton motive force drives the outer membrane transport of cobalamin. J. Bacteriol. 175: 3146-3150.
- Braun, M., Killmann, H. and Braun, V. (1999) The beta barrel domain of FhuAΔ5-160 is sufficient for TonB-dependent FhuA activities of *Escherichia coli*. Mol. Micorbiol. 33: 1037-1049
- Braun, V. (1989) The structurally related *exbB* and *tolQ* genes are interchangeable in conferring *tonB*-dependent colicin, bacteriophage, and albomycin sensitivity. J. Bacteriol. 178: 6387-6390
- Braun, V. (1995) Energy-coupled transport and signal transduction through the Gram-negative outer membrane via TonB-ExbB-ExbD-dependent receptor proteins. FEMS Microbiol. Rev. 16: 295-307
- Braun, V. (1999) Active transport of siderophore-mimicking antibacterials across the outer membrane. Drug. Res. Up. 2: 363-369
- Braun, V. and Braun, M. (2002) Iron transport and signalling in *Escherichia coli*. FEBS Lett. 529: 78-85
- Braun, V. and Herrmann, C. (1993) Evolutionary relationship of uptake systems for biopolymers in *Escherichia coli*: cross-complementation between the TonB-ExbB-ExbD and TolA-TolQ-TolR proteins. Mol. Microbiol. 8: 261-268
- Braun, V., Brazel-Faisst, C. and Schneider, R. (1984) Growth stimulation of *Escherichia coli* in serum by iron (III) aerobactin. Recycling of aerobactin. FEMS Microbiol. Lett. 21: 99-103
- Braun, V., Gaisser, S., Herman, C., Kampfenkel, K., Killman, H. and Traub, I. (1996) Energy coupled transport across the outer membrane of *Escherichia coli*: ExbB binds ExbD and TonB *in vitro*, and leucine 132 in the periplasmic region and aspartate 25 in the transmembrane region are important for ExbD activity. J. Bacteriol. 178: 2836-2845
- Braun, V., Hantke, K. and Köster, W. (1998) Bacterial iron transport: mechanisms, genetics, and regulation. Met. Ions Biol. Syst. 35: 67-145
- Brewer, S., Tolley, M., Trayer, I. P., Barr, G. C., Dorman, C. J., Hannavy, K., Higgins, C. F., Evans, J. S., Levine, B. A. and Wormald, M. R. (1990) Structure and function of X-Pro dipeptide repeats in the TonB protein of *Salmonella typhimurium* and *Escherichia coli*. J. Mol. Biol. 216: 883-895

- Brickman, T. J. and Armstrong, S. K. (1999) Essential role of the iron-regulated outer membrane receptor FauA in alcaligin siderophore-mediated iron uptake in *Bordetella* species. J. Bacteriol. 181: 5958-5966
- Brown, K. A. and Ratledge, C. (1975) Iron transport in *Mycobacterium smegmatis*: ferrimycobactin reductase NAD(P)H: ferrimycobactin oxidoreductase, the enzyme releasing iron from its carrier. FEBS Lett. 53: 262-266
- Buchanan, S. K., Smith, B. S., Venkatramani, L., Xia, D., Esser, L., Palnitkar, M., Chakraborty, R., van der Helm, D and Deisenhofer, J. (1999) Crystal structure of the outer membrane active transporter FepA from *Escherichia coli*. Nat. Struct. Biol. 6: 56-63
- Budzikiewicz, H. (2001) Siderophore-antibiotic conjugates used as Trojan horses against *Pseudomonas aeruginosa*. Curr. Top. Med. Chem. 1: 73-82
- Buyer, J. S. and Leong, J. (1986) Iron transport-mediated antagonism between plant growth-promoting and plant deleterious *Pseudomonas* strains. J. Biol. Chem. 261: 791-794
- Byers, B. R., Powell, M. V. and Lankford, C. E. (1967) Iron-chelating hydroxamic acid (schizokinen) active in initiation of cell division in *Bacillus megaterium*. J. Bacteriol. 93: 286-294
- Cadieux, N. and Kadner, R. J. (1999) Site-directed disulfide bonding reveals an interaction site between energy-coupling protein TonB and BtuB, the outer membrane colbalamin transporter. Proc. Natl. Acad. Sci. U. S. A. 96: 10673-10678
- Cadieux, N., Bradbeer, C. and Kadner, R. J., (2000) Sequence changes in the Ton box region of BtuB affect its transport activities and interaction with the TonB protein. J. Bacteriol. 182: 5954-5961
- Callaham, D. A. and Torrey, J. G. (1981) The structural basis for infection of root hairs of *Trifolium repens* by *Rhizobium*. Can. J. Bot. 59: 1647-1664
- Capela, D., Barloy-Hubler, F., Gouzy, J., Bothe, G., Ampe, F., Batut, J., Boistard, P., Becker, A., Boutry, M., Cadieu, E., Dréano, S., Gloux, S, Godrie, T., Goffeau, Kahn, D., Kiss, E., Lelaure, V., Masuy, D., Pohl, T., Portetelle, D., Pühler, A., Purnelle, B., Ramsperger, U., Renard, C., Thebault, P., Vandenbol, M., Weidner, S. and Gailbert, F. (2001) Analysis of the

chromosome sequence of the legume symbiont *Sinorhizobium meliloti* strain 1021. Proc. Natl. Acad. Sci. U. S. A.. 98: 9877-9882

- Carson, K. C., Holliday, S., Glenn, A. R. and Dilworth, M. J. (1992) Siderophore and organic acid production in root nodule bacteria. Arch. Microbiol. 157: 264-271
- Carson, S. D. B., Klebba, P. E., Newton, S. M. C. and Sparling, P. F. (1999) Ferric enterobactin binding and utilization by *Neisseria gonorrhoeae*. J. Bacteriol. 181: 2895-2901
- Carson, S. D. B., Stone, B., Beucher, M., Fu, J. and Sparling, P. F. (2000) Phase variation of the gonococcal siderophore receptor FetA. Mol. Micro. 36: 585-593
- Carter, R. A., Worsley, P. S., Sawers, G., Challis, G. L., Dilworth, M. J., Carson, K. C., Lawerence, J. A., Wexler, M., Johnston, A. W. B. and Yeoman, K. H. (2002) The *vbs* genes that direct the synthesis of the siderophore vicibactin in *Rhizobium leguminosarum*: their expression in other genera requires ECF σ factor RpoI. Mol. Microbiol 44: 1153-1166
- Chang, C. S., Mosser, A., Plückthun, A., Wlodawer, A. (2001) Crystal structure of the dimeric C-terminal domain of TonB reveals a novel fold. J. Biol. Chem. 276: 27535-27540
- Chen, W. and Kuo, T. (1993) A simple and rapid method for preparation of gram-negative bacterial genomic DNA. Nucleic Acids. Res. 21: 2260
- Chenault, S. S. and Earhart, C. F. (1991) Organization of genes encoding membrane proteins of the *Escherichia coli* ferrienterobactin permease. Mol. Microbiol. 5: 1405-1413
- Chu, G. C. Katakura, K., Zhang, X., Yoshida, T. and Ikeda-Saito, M. (1999) Heme degradation as catalysed by a recombinant bacterial heme oxygenase (HmuO) from *Corynebacterium diphtheriae*. J. Biol. Chem. 274: 21319-21325
- Clarke, S. E., Stuart, J., and Sanders-Loehr, J. (1987) Induction of siderophore activity in Anabaena spp. and its moderation of copper toxicity. Appl. Environ. Microbiol. 53: 917-922
- Clarke, T. E., Ku, S. Y., Dougan, D. R., Vogel, H. J. and Tari, L. W. (2000) The structure of the ferric siderophore binding protein FhuD complexed with gallichrome. Nat. Struct. Biol. 7: 287-291

- Cornelis, P. and Matthijs, S. (2002) Diversity of siderophore-mediated iron uptake systems in fluorescent pseudomonads: not only pyoverdines. Env. Microbiol. 4: 787-798
- Corpet, F. (1988) Multiple sequence alignment with hierarchical clustering. Nucl. Acids Res. 16: 10881-10890
- Coulton, J. W. Mason, P., Cameron, D. R., Carmel, G., Jean, R. and Rode, H. N. (1986) Protein fusions of β-galactosidase to the ferrichrome-iron receptor of *Escherichia coli* K-12. J. Bacteriol. 165: 181-190.
- Coulton, J. W., Mason, P., and DuBow, M. S. (1983) Molecular cloning of the ferrichrome-iron receptor of *Escherichia coli* K-12. J. Bacteriol. 156: 1315-1321.
- Cox, C. D. (1980a) Iron reductase in *Pseudomonas aeruginosa*. J. Bacteriol. 141: 199-204
- Cox, C. D. (1980b) Iron uptake with ferripyochelin and ferric citrate by *Pseudomonas aeruginosa*. J. Bacteriol. 142: 581-587
- Cox, C. D. (1982) Effect of pyochelin on the virulence of *Pseudomonas aeruginosa*. Infect. Immun. 36: 17-23
- Cox, C. D. and Adams, P. (1985) Siderophore activity of pyoverdine for *Pseudomonas aeruginosa*. Infect Immun. 48: 130-138
- Cox, C. D. and Graham, R. (1979) Isolation of an iron-binding compound from *Pseudomonas aeruginosa*. J. Bacteriol. 137: 357-364.
- Cox, C. D., Rinehart, K. L., Moore, M. L. and Cook, J. C. (1981) Pyochelin: novel structure of an iron-chelating growth promoter for *Pseudomonas aeruginosa*. Proc. Natl. Acad. Sci. U. S. A. 78: 4256-4260.
- Coy, M. and Neilands, J. B. (1991) Structural dynamics and functional domains of the Fur protein. Biochemistry 30: 8201-8210
- Crosa, J. H. (1997) Signal transduction and transcriptional and posttranscriptional control or iron regulated genes in bacteria. Microbiol. Mol. Biol. Rev 61: 319-336
- Crosa, J. H. and Walsh, C. T. (2002) Genetics and assembly line enzymology of siderophore biosynthesis in bacteria. Microbiol. Mol. Biol. Rev. 66: 223-249

- de Lorenzo, V., Bindereif, A., Paw, B. H. and Neilands, J. B. (1986) Aerobactin biosynthesis and transport genes of plasmid ColV-K30 in *Escherichia coli* K-12. J. Bacteriol. 165: 570-578.
- de Lorenzo, V., Giovannini, F., Herrero, M. and Neilands, J. B. (1988a) Metal ion regulation of gene expression: Fur repressor-operator interaction at the promoter region of the aerobactin system of pColV-K30. J. Mol. Biol. 203: 875-884
- de Lorenzo, V., Herrero, M. and Neilands, J. B. (1988b) IS1-mediated mobility of the aerobactin system of pColV-K30 in *Escherichia coli*. Mol. Gen. Genet. 213: 487-490
- de Lorenzo, V., Wee, S., Herrero, M. and Neilands, J. B. (1987) Operator sequences of the aerobactin operon of plasmid ColV-K30 binding the ferric uptake regulation (*fur*) repressor. J. Bacteriol. 169: 2624-2630
- de Luca, N. G., Wexler, M., Pereira, M. J., Yeoman, K. H. and Johnston, A. W. B. (1998) Is the *fur* gene of *Rhizobium leguminosarum* essential? FEMS Microbiol. Lett. 168: 289-295
- Dean, C. R. and Poole, K. (1993) Cloning and characterization of the ferric enterobactin receptor gene (*pfeA*) of *Pseudomonas aeruginosa*. J. Bacteriol. 175: 317-324
- Dean, C. R. and Poole, K. (1993) Expression of the ferric enterobactin receptor (PfeA) of *Pseudomonas aeruginosa*: involvement of a two-component regulatory system. Mol. Microbiol. 8: 1095-1103
- Dean, C. R., Neshat, S. and Poole, K. (1996) PfeR, an enterobactin-responsive activator of ferric enterobactin receptor gene expression in *Pseudomonas aeruginosa*. J. Bacteriol. 178: 5361-5369
- Dekkers, L. C., Phoelich, C. C., Van der Fits, L. and Lugtenberg, B. J. J. (1998) A site-specific recombinase is required for competitive root colonization by *Pseudomonas fluorescens* WCS365. Proc. Natl. Acad. Sci. U. S. A. 95: 7051-7056
- Demain, A. L. and Fang, A. (2000) The natural functions of secondary metabolites. Adv. Biochem. Eng. Biotechnol. 69: 1-39

- Dennis, J. J., Lafontaine, E. R. and Solol, P. A. (1996) Identification and characterization of the *tolQRA* genes of *Pseudomonas aeruginosa*. J. Bacteriol. 178: 7059-7068
- Der Vartanian, M. (1988) Differences in excretion and efficiency of the aerobactin and enterochelin siderophores in a bovine pathogenic strain of *Escherichia coli*. Infect. Immun. 56: 413-418
- Diarra, M. S., Lavoie, M. C., Jaques, M., Darwish, I., Dolence, E. K., Dolence, J. A., Ghosh, A., Ghosh, M., Miller, M. J. and Malouin, F. (1996) Species selectivity of new siderophore-drug conjugates that use specific iron uptake for entry into bacteria. Antimicrob. Agents. Chemother. 40: 2610-2617
- Dilworth, M. J., Carson, K. C., Giles, R. G. F., Byrne, L. T. and Glenn, A. R. (1998) *Rhizobium leguminosarum* bv. *viciae* produces a novel cyclic trihydroxamate siderophore, vivibactin. Microbiology 144: 781-791
- Dinh, T., Paulsen, I. T. and Saier, M. H. Jr. (1994) A family of extracytoplasmic proteins that allow transport of large molecules across the outer membranes of gram-negative bacteria. J. Bacteriol. 176: 3825-3831
- Ditta, G., Stanfield, S., Corbin, D. and Helsinki, D. R. (1980) Broad host range DNA cloning system for Gram negative bacteria: Construction of a gene bank of *Rhizobium meliloti* 77: 7347-7351
- Dorsey, C. W., Tolmasky, M. E., Crosa, J. H. and Actis, L. A. (2003) Genetic organization of an *Acinetobacter baumannii* chromosomal region harbouring genes releated to siderophore biosynthesis and transport. Microbiol. 149: 1227-1238
- Dreschel, H. and Jung, G. (1998) Peptide siderophores. J. Pept. Sci. 4: 147-181
- Dubrac, S. and Touati, D. (2000) Fur positive regulation of iron superoxide dismutase in *Escherichia coli*: functional analysis of the *sodB* promoter. J. Bacteriol. 182: 3802-3808
- Earhart, C. F. (1996) *In: Escherichia coli* and *Salmonella* cellular and molecular biology. (Neidhardt, F. C. ed) ASM Press, Washington D. C. pp 1075-1090
- Eich-Helmerich, K. and Braun, V. (1989) Import of biopolymers into *Escherichia coli*: nucleotide sequences of the *exbB* and *exbD* genes are

homologous to those of the *tolQ* and *tolR* genes, respectively. J. Bacteriol. 171: 5117-5126

- Ernst, J. F., Bennett, R. L. and Rothfield, L. I. (1978) Constitutive expression of the iron-enterochelin and ferrichrome uptake systems in a mutant strain of *Salmonella typhimurium*. J. Bacteriol. 135: 928-934
- Escolar, L., Pérez-Martín, J. and de Lorenzo, V. (1998) Binding of the Fur (ferric uptake regulator) repressor of *Escherichia coli* to arrays of the GATAAT sequence. J. Mol. Biol. 283: 537-547
- Escolar, L., Pérez-Martín, J. and de Lorenzo, V. (1999) Opening the iron box: transcriptional metalloregulation by the Fur protein. J. Bacteriol. 181: 6223-6229
- Escolar, L., Pérez-Martín, J. and de Lorenzo, V. (2000) Evidence of an unusually long operator for the Fur repressor in the aerobactin promoter of *Escherichia coli*. J. Biol. Chem. 275: 24709-24714
- Evans, J. S., Levine, B. A., Trayer, I. P., Dorman, C. J. and Higgins, C. F. (1986) Sequence-imposed structural constraints in the TonB protein of *E. coli* FEBS Lett. 208: 211-216.
- Fabiano, E., Gill, P. R., Noya, F., Bagnasco, P., Delafuente, L. and Arias, A. (1995) Siderophore-mediated iron transport iron acquisition mutants in *Rhizobium meliloti* 242 and its effect on the nodulation kinetics of alfalfa nodules. Symbiosis 19: 197-211
- Fabiano, E., Gualtieri, G., Pritsch, C., Polla, G. and Arias, A. (1994) Extent of high-affinity iron transport systems in field isolates of Rhizobia. Plant and Soil 164: 177-185
- Fellay, R., Frey, J. and Krisch, H. (1987) Interposon mutagenesis of soil and water bacteria: a family of DNA fragments designed for *in vitro* insertional mutagenesis of Gram-negative bacteria. Gene 52: 147-154
- Ferguson, A. D. and Deisenhofer, J. (2002) TonB-dependent receptors-structural perspectives. Biochim. Biophys. Acta. 1565: 318-332
- Ferguson, A. D., Braun, V., Fiedler, H. -P., Coulton, J. W., Diederichs, K. and Welte, W. (2000) Crystal structure of the antibiotic albomycin in complex with the outer membrane transporter FhuA. Protein Sci. 9: 956-963

- Ferguson, A. D., Chakraborty, R., Smith, B. S., Esser, L., van der Helm, D. and Deisenhofer, J. (2002) Structural basis of gating by the outer membrane transporter FecA. Science 295: 1715-1719
- Ferguson, A. D., Hofmann, E., Coulton, J.W., Diederichs, K and Welte, W. (1998) Siderophore-mediated iron transport: Crystal structure of FhuA with bound lipopolysaccharide. Science 282: 2215-2220
- Ferguson, A. D., Kodding, J. W., Coulton, K., Diederichs, K., Braun, V. and Welte, W. (2001) Active transport of an antibiotic rifamycin derivative by the outer-membrane transporter FhuA. Structure 9: 707-716
- Fetherston, J. D., Bertolino, V. J. and Perry, R. D. (1999) YptP and YbtQ: two ABC transporters required for iron uptake in *Yersinia pestis*. Mol. Microbiol. 32: 289-299
- Finan, T.M., Kunkel, B., De Vos, G.F. and Signer, E.R. (1986) Second symbiotic megaplasmid in Rhizobium meliloti carrying exopolysaccharide and thiamine synthesis genes. J. Bacteriol. 167: 66-72.
- Fischer, R., Günter, K. and Braun, V. (1989) Involvement of ExbB and TonB in transport across the outer membrane of *Escherichia coli*: phenotypic complementation of *exb* mutants by overexpressed *tonB* and physical stabilization of TonB by ExbB. J Bacteriol. 171: 5127-5134
- Fisher, E. Strehlow, B. Hartz, D. Braun, V. (1990) Soluble and membrane-bound ferrisiderophore reductases of *Escherichia coli* K-12. Arch. Microbiol. 153: 329-336
- Fisher, R. F. and Long, S. R. (1992) *Rhizobium*-plant signal exchange. Nature 357: 655-660.
- Fontecave, M., Covès, J. and Pierre, J. –L. (1994) Ferric reductases or flavin reductases. Biometals 7: 3-8
- Friedman, A. M., Long, S. R., Brown, S. E., Buikema, W. J., Ausubel, F.M. (1982) Construction of a broad host range cosmid cloning vector and its use in the genetic analysis of *Rhizobium* mutants. Gene 18: 289-296
- Frustaci, J. M. and O' Brian, M. R. (1992) Characterization of a *Bradyrhizobium japonicum* ferrochelatase mutant and isolation of the *hemH* gene. J. Bacteriol. 174:4223-4229.

- Funahashi, T., Tanabe, T., Aso, H., Nakao, H., Fujii, Y., Okamoto, K., Narimatsu, S. and Yamamoto, S. (2003) An iron-regulated gene required for utilization of aerobactin as an exogenous siderophore in *Vibrio parahaemolyticus*. Microbiology 149: 1217-1225
- Furrer, J. L. Sanders, D. N., Hook-Barnard, I. G. and McIntosh, M. A. (2002) Export of the siderophore enterobactin in *Escherichia coli*: involvement of a 43 kDa membrane exporter. Mol. Microbiol. 44: 1225-1234
- Galibert, F., Finan, T. M., Long, S. R., Puhler, A., Abola, P., Ampe, F., Barloy-Hubler, F., Barnett, M. J., Becker, A., Boistard, P., Bothe, G., Boutry, M., Bowser, L., Buhrmester, J., Cadieu, E., Capela, D., Chain, P., Cowie, A., Davis, R. W., Dreano, S., Federspiel, N. A., Fisher, R. F., Gloux, S., Godrie, T., Goffeau, A., Golding, B., Gouzy, J., Gurjal, M., Hernandez-Lucas, I., Hong, A., Huizar, L., Hyman, R. W., Jones, T., Kahn, D., Kahn, M. L., Kalman, S., Keating, D. H., Kiss, E., Komp, C., Lelaure, V., Masuy, D., Palm, C., Peck, M. C., Pohl, T. M., Portetelle, D., Purnelle, B., Ramsperger, U., Surzycki, R., Thebault, P., Vandenbol, M., Vorholter, F. J., Weidner, S., Wells, D. H., Wong, K., Yeh, K. C. and Batut, J. (2001) The composite genome of the legume symbiont *Sinorhizobium meliloti*. Science 293: 668-672
- Garg, R. P., Vargo, C. J., Cui, X. Y. and Kurtz, D. M. (1996) A [2Fe-2S] protein encoded by an open reading frame upstream of the *Escherichia coli* bacterioferritin gene. Biochemistry 35: 6297-6301
- Gehring, A. M., Bradley, K. A. and Walsh, C. T. (1997) Enterobactin biosynthesis in *Escherichia coli*: isochorismate lyase (EntB) is a bifunctional enzyme that is phosphopantetheinylated by EntD and then acylated by EntE using ATP and 2,3-dihydroxybenzoate. Biochemistry 36: 8495-8503
- Genco, C. A. and Dixon, D. W. (2001) Emerging strategies in microbial haem capture. Mol. Microbiol. 39: 1-11
- Gensberg, K., Hughes, K. and Smith, A. W. (1992) Siderophore-specific induction of iron uptake in *Pseudomonas aeruginosa*. J. Gen. Microbiol. 138: 2381-2387
- Ghosh, A. and Miller, M. J. (1993) Synthesis of novel citrate-based siderophores and siderophore-β-lactam conjugates. Iron transport-mediated drug delivery systems. J. Org. Chem. 58: 7652-7659

- Ghosh, A., Ghosh, M., Niu, C., Malouin, F., Möllmann, U. and Miller, M. J. (1996) Iron transport-mediated drug delivery using mixed-ligand siderophore-β-lactam conjugates. Chemistry and Biology 3: 1011-1019
- Ghosh, M. and Miller, M. J. (1996) Synthesis and *in vitro* antibacterial activity of spermidine-based mixed catechol- and hydroxamate-containing siderophore-vancomycin conjugates. Bioorg. Med. Chem. 4: 43-48
- Gibson, F. and Magrath, D. I. (1969) The isolation and characterization of a hydroxamic acid (aerobactin) formed by *Aerobacter aerogens* 62-I. Biochim. Biophys. Acta. 192: 175-184
- Gilis, A., Khan, M. A., Cornelis, P., Meyer, J. M., Mergeay, M. and van der Lelie, D. (1996) Siderophore-mediated iron uptake in *Alcaligens eutrophus* CH43 and identification of *aleB* encoding the ferric iron-Alcaligin E receptor. J. Bacteriol. 178: 5499-5507
- Gill, P. R. and Neilands, J. B. (1989) Cloning a genomic region required for a high-affinity iron-uptake system in *Rhizobium meliloti* 1021. Mol. Micro. 3: 1183-1189.
- Goel, V. K and Kapil, A. (2001) Monoclonal antibodies against the iron regulated outer membrane proteins of *Acinetobacter baumannii* are bactericidal. BMC Microbiology 1: 16
- Gorbacheva, V. Y., Faundez, G., Godfrey, H. P. and Cabello, F. C. (2001) Restricted growth of *ent*(-) and *tonB* mutants of *Salmonella enterica* serovar Typhi in human Nomo Mac 6 monocytic cells. FEMS Microbiol. Lett. 196: 7-11
- Gotoh, N., Tsujimoto, H. Poole, K., Yamagishi, J. –I. and Nishino, T. (1995) The outer membrane protein OprM of *Pseudomonas aeruginosa* is encoded by *oprK* of the *mexA-mexB-oprK* multidrug resistance operon. Antimicrob. Agents. Chemother. 39: 2567-2569
- Gottesman, S. (2002) Stealth regulation: biological circuits with small RNA switches. Genes Dev. 16: 2829-2842
- Griffiths, G. L., Sigel, S. P., Payne, S. M. and Neilands, J. B. (1984) Vibriobactin, a siderophore from Vibrio cholerae. J. Biol. Chem. 259: 383-385

- Griggs, D. W. and Konisky, J. (1989) Mechanism for iron regulated transcription of the *Escherichia coli* cir gene: metal-dependent binding of Fur protein to promoters. J. Bacteriol. 171: 1048-1054
- Groeger, W. and Köster, W. (1998) Transmembrane topology of the two FhuB domains representing the hydrophobic components of bacterial ABC transporters involved in the uptake of siderophores, haem and vitamin B_{12}. Microbiology 144: 2759-2769
- Gross, R. F., Engelbrecht, F. and Braun, V. (1984) Genetic and biochemical characterisation of the aerobactin synthesis operon on pColV. Mol. Gen. Genet. 196: 74-80
- Gross, R. F., Engelbrecht, F. and Braun, V. (1985) Identification of the genes and their polypeptide products responsible for aerobactin synthesis by pColV plasmids. Mol. Gen. Genet. 201: 204-212
- Gruer, M. J. and Guest, J. R. (1994) Two genetically-distinct and differentially-regulated aconitases (AcnA and AcnB). Microbiology 140: 2531-2541
- Guerinot, M. L. (1994) Microbial Iron Transport. Annu. Rev. Microbiol. 48: 743-772
- Guerinot, M. L. and Chelm, B. K. (1986) Bacterial δ-aminolevulinic acid synthase is not essential for leghemoglobin formation in the soybean/*Bradyrhizobium japonicum* symbiosis. Proc. Natl. Acad. Sci. U.S.A. 83: 1837-1841.
- Guerinot, M. L.(1993) *In* : Iron chelation in plants and soil microorganisms. (Barton, L. L. and Hemming, B.C. eds.) Academic Press, California. pp197-217.
- Guerinot, M. L., Maidl, E. J. and Plessner, O. C. (1990) Citrate as a siderophore in *Bradyrhizobium japonicum*. J. Bacteriol. 172: 3298-3303.
- Günter, K and Braun, V. (1990) *In vivo* evidence for FhuA outer membrane interaction with the TonB inner membrane protein of *Escherichia coli*. FEMS Microbiol. Lett. 274: 85-88.
- Guo, H., Naser, S. A., Ghobrial, G. and Phanstiel IV, O. (2002) Synthesis and biological evaluation of new citrate-based siderophores as potential probes for the mechanism of iron uptake in bacteria. J. Med. Chem. 45: 2056-2063

- Hall, H. K. and Foster, J. W. (1996) The role of Fur in the acid tolerance response of *Salmonella typhimurium* is physiologically and genetically separable from its role in iron acquisition. J. Bacteriol. 178: 5683-5691
- Hamood, A. N., Colmer, J. A., Ochsner, U. A. and Vasil, M. L. (1996) Isolation and characterization of a *Pseudomonas aeruginosa* gene, *ptxR*, which positively regulates exotoxin A production. Mol. Microbiol. 21: 97-110
- Hamza, I., Chauhan, S., Hassett, R. and O'Brian, M. R. (1998) The bacterial Irr protein is required for coordination of heme biosynthesis with iron availability. J. Biol. Chem. 273: 21669-21674
- Hancock, R. E. and Chapple, D. S. (1999) Peptide antibiotics. Antimicrob. Agents. Chemother. 43: 1317-1323
- Hannavy, K., Barr, G. C., Dorman, C. J., Adamson, J., Mazengera, L. R., Gallagher, M.P., Evans, J.S., Levine, B. A., Trayer, L. P. and Higgins, C. F. (1990) TonB protein of *Salmonella typhimurium*: a model for signal transduction between membranes. J. Mol. Biol. 216: 897-210
- Hanson, M. S., Slaughter, C. and Hansen, E. J. (1992) The *hbpA* gene of *Haemophilus influenzae* type *b* encodes a heme-binding lipoprotein conserved among heme-dependent *Haemophilus* species. Infect. Immun. 60: 2257-2266
- Hantke, K. (1984) Cloning of the repressor protein gene of iron-regulated systems in *Escherichia coli* K-12. Mol. Gen. Genet. 197: 337-341
- Hantke, K. (1987) Selection procedure for deregulated iron transport mutants (*fur*) in *Escherichia coli* K-12: Fur not only affects iron metabolism. Mol. Gen. Genet. 210: 135-139
- Hantke, K. (1990) Dihydroxybenzoylserine: a siderophore for *E. coli*. FEMS Microbiol. Lett. 67: 5-8
- Hantke, K. (2001) Iron and metal regulation in bacteria. Curr. Opin. Microbiol. 4: 172-177
- Harding, R. A. and Royt, P. W. (1990) Acquisition of iron from citrate by *Pseudomonas aeruginosa*. J. Gen. Microbiol. 136: 1859-1867
- Härle, C., Insook, K., Angerer, A. and Braun, V. (1995) Signal transfer through three compartments: transcription initiation of the *Escherichia coli* ferric citrate transport system from the cell surface. EMBO J 14: 1430-1438

- Hartmann, A. and Braun, V. (1980) Iron transport in *Escherichia coli*: Uptake and modification of ferrichrome. J. Bacteriol. 143: 246-255
- Heinisch, L., Wittmann, S., Stoiber, T., Berg, A., Ankel-Fuchs, D. and Möllmann, U. (2002) Highly antibacterial active aminoacyl penicillin conjugates with acylated bis-catecholate siderophores based on secondary diamino acids and related compounds. J. Med. Chem. 45: 3032-3040
- Heinrichs, D. E. and Poole, K. (1993) Cloning and sequence analysis of a gene (*pchR*) encoding an AraC family activator of pyochelin and ferripyochelin receptor synthesis in *Pseudomonas aeruginosa*. J. Bacteriol. 175: 5882-5889
- Heinrichs, D. E. and Poole, K. (1996) PchR, a regulator of ferric pyochelin receptor gene (*fptA*) expression in *Pseudomonas aeruginosa*, functions both as an activator and as a repressor. J. Bacteriol. 178: 2586-2592
- Heinrichs, D., Young, E. L. and Poole, K. (1991) Pyochelin-mediated iron transport in *Pseudomonas aeruginosa*: involvement of a high-molecular-mass outer membrane protein. Infect. Immun. 59: 3680-3684
- Heller, K. J., Kadner, R. J., and Günter, K. (1998) Suppression of the *btuB*451 mutation by mutations in the *tonB* gene suggests a direct interaction between TonB and TonB dependent receptor proteins in the outer membrane of *Escherichia coli*. Gene 64: 147-153
- Henderson, D. P. and Payne, S. M. (1994) *Vibrio cholera* iron transport systems: roles of heme and siderophore iron transport in virulence and identification of a gene associated with multiple iron transport systems. Infect. Immun. 62: 5120-5125
- Higgins, C. F. (1992) ABC transporters: from microorgansims to man. Annu. Rev. Cell. Biol. 8: 67-113
- Higgs, P. A., Larsen, R. A. and Postle, K. (2002a) Quantification of known components of the *Escherichia coli* TonB energy transduction system: TonB, ExbB, ExbD and FepA. Mol. Microbiol. 44: 271-281
- Higgs, P. I., Letain, T. E., Merrian, K. K., Burke, N. S., Park, H., Kang, C. and Postle, K. (2002b) TonB interacts with nonreceptor proteins in the outer membrane of *Escherichia coli*. J. Bacteriol. 184: 1640-1648

- Higgs, P. I., Myers, P.S. and Postle, K. (1998) Interactions in the TonB-dependent energy transduction complex: ExbB and ExbD form homomultimers. J. Bacteriol 180: 6031-6038
- Höfte, M. (1993) *In* : Iron chelation in plants and soil microorganisms. (Barton, L. L. and Hemming, B. C. eds.) Academic Press, California. pp 3-26.
- Holmes, D. S. and Quigley, M. (1981) A rapid boiling method for the preparation of bacterial plasmids. Anal. Biochem. 114:193-197.
- Horbung, J. M., Jones, H. A. and Perry, R. D. (1996) The *hmu* locus of *Yersinia pestis* is essential for utilization of free haemin and haem-protein complexes as iron sources. Mol. Microbiol. 20: 725-739
- Howard, S. P. Herrmann, C., Stratilo, C. W. and Braun, V. (2001) *In vivo* synthesis of the periplasmic domain of TonB inhibits transport through the FecA and FhuA iron siderophore transporters of *Escherichia coli*. J. Bacteriol. 183: 5885-5895.
- Howard, S. P., Meiklejohn, H. G., Shivak, D. and Jahagirdar, R. (1996) A TonB-like protein and a novel membrane protein containing an ATP-binding cassette function together in exotoxin secretion. Mol. Microbiol. 22: 595-604
- Hussein, S., Hantke, K. and Braun, V. (1981) Citrate-dependent iron transport system in *Escherichia coli* K-12. Eur. J. Biochem. 117: 431-437.
- Idei, A., Kawai, E., Akatsuka, H. and Omori, K. (1999) Cloning and characterization of the *Pseudomonas fluorescens* ATP-binding cassette exporter, Has DEF, for the heme acquisition protein HasA. J. Bacteriol. 181: 7545-7551
- Ilari, A., Stefanini, S., Chiancone, E. and Tsernoglou, D. (2000) The dodecameric ferritin from *Listeria innocua* contains a novel intersubunit iron-binding site. Nat. Struct. Biol. 7: 38-43
- Inoue, H., Nojima, H. and Okayama, H. (1990) High efficiency transformation of *Escherichia coli* with plasmids. Gene 96: 23-28
- Jacobs, C., Huang, L., Bartowsky, E., Normark, S. and Park, J. T. (1994) Bacterial cell wall recycling provides cytosolic muropeptides as effectors for β-lactamase induction. EMBO J. 13: 4684-4694

- Jacquarmet, L., Aberdam, D., Adrait, A., Hazemann, J. L., Latour, J. M. and Michaud-Soret, I. (1998) X-ray absorption spectroscopy of a new zinc site in the Fur protein from *Escherichia coli*. Biochemistry 37: 2564-2571
- Jadhav, R. S. and Desai, A. (1994) Role of siderophore in iron uptake in cowpea *Rhizobium* GN1 (peanut isolate): Possible involvement of iron repressible outer membrane proteins. FEMS Micro. Lett. 155: 185-190
- Jalal, M. A., Hossain, M. B., van der Helm, D., Sanders-Loehr, J., Actis, A. and Crosa, J. H. (1989) Structure of anguibactin, a unique plasmid-related bacterial siderophore from the fish pathogen *Vibrio anguillarum*. J. Am. Chem. Soc. 111: 292-296.
- Jarostk, G. P., Sanders, J. D., Cope, L. D. Muller-Eberhard, U. and Hansen, E. J. (1994) A functional *tonB* is required for both utilization of heme and virulence expression by *Haemophilus influenzae* type b. Infect. Immun. 62: 2470-2477
- Jaskula, J. C., Letain, T. E., Roof, S. K., Skare, J. T. and Postle, K. (1994) Role of the TonB amino terminus in energy transduction between membranes. J. Bacteriol. 176: 2326-2338
- Jensen, H. L. (1942) Nitrogen fixation in leguminous plants. I. Proc. Linn. Soc. N.S.W. 98-108
- Kadner, R. J. (1990) Vitamin B_{12} transport in *Escherichia coli*: energy coupling between membranes. Mol. Microbiol. 4: 2027-2033
- Kadner, R. J., Heller, K., Coulton, J. W. and Braun, V. (1980) Genetic control of hydroxamate mediated iron uptake in *Escherichia coli*. J. Bacteriol. 143: 256-264
- Kampfenkel, K. and Braun, V. (1992) Membrane topology of the *Escherichia coli* ExbD protein. J. Bacteriol. 174: 5485-5487.
- Kampfenkel, K. and Braun, V. (1993a) Membrane topologies of the TolQ and TolR proteins of *Escherichia coli*: inactivation of TolQR by a missense mutation in proposed first transmembrane segment. J. Bacteriol. 175: 4485-4491
- Kampfenkel, K. and Braun, V. (1993b) Topology of the ExbB protein in the cytoplasmic membrane of *Escherichia coli*. J. Biol. Chem. 268: 6050-6057

- Karlsson, M., Hannavy, K. and Higgins, C. F. (1993) ExbB acts as a chaperone-like protein to stabilize TonB in the cytoplasm. Mol. Microbiol 8: 389-369
- Killmann, H., Herrmann, C., Torun, A., Jung, G. and Braun, V. (2002) TonB of *Escherichia coli* activates FhuA through interaction with the β-barrel. Microbiol. 148: 3497-3509
- Kim, I., Stiefel, A., Plantör, S., Angerer, A. and Braun, V. (1997) Transcription induction of the ferric citrate transport genes via the N-terminus of the FecA outer membrane protein, the Ton system and the electrochemical potential of the cytoplasmic membrane. Mol. Microbiol. 23: 333-344
- Kirby, A. E., Metzger, D. J., Murphy, E. R. and O' Connell, T. D. (2001) Heme utilization in *Bordetella avium* is regulated by RhuI, a heme-responsive extracytoplasmic function sigma factor. Infect. Immun. 69: 6951-6961.
- Klebba, P. E., Mc Intosh, M. A. and Neilands, J. B. (1982) Kinetics of biosynthesis of iron-regulated membrane proteins in *Escherichia coli*. J. Bacteriol. 149: 880-888.
- Kline, T., Fromhold, M., McKennon, T. E., Cai, S., Treiberg, J., Ihle, N., Sherman, D., Schwan, W., Hickey, M. J., Warrener, P., Witte, P. R., Brody, L. L., Goltry, L., Barker, L. M., Anderson, S. U., Tanaka, S. K., Shawar, R. M., Nguyen, L. Y., Langhorne, M., Bigelow, A., Embuscado, L. and Naeemi, E. (2000) Antimicrobial effects of novel siderophores linked to β-lactam antibiotics. Bioorg. Med. Chem. 8: 73-93
- Ko, M. P., Huang, P. –Y., Huang, J. -S. and Barker, K. R. (1987) The occurrence of phytoferritin and its relationship to effectiveness of soybean nodules. Plant. Physiol. 83: 299-305.
- Konopka, K. and Neilands, J. B. (1984) Effect of serum albumin on siderophore mediated utilization of transferrin iron. Biochemistry 23: 2122-2127
- Köster, W. (1997) *In*: Bioinorganic chemistry, transition metals in biology and their coordination chemistry. (Trautwein, A. X. ed) Wiley-VCH. pp56-68
- Köster, W. (2001) ABC transporter-mediated uptake of iron, siderophores, heme and vitamin B_{12}. Res. Microbiol. 152: 291-301

- Köster, W. and Böhm, B. (1992) Point mutations in 2 conserved glycine residues within the integral membrane protein FhuB affect iron(III) hydroxamate transport. Mol. Gen. Genet. 232: 399-407
- Köster, W. and Braun, V. (1990) Iron(III) hydroxamate transport of *Escherichia coli*: restoration of iron supply by coexpression of the N- and C-terminal halves of the cytoplasmic membrane protein FhuB cloned on separate plasmids. Mol. Gen. Genet. 223: 379-384
- Kovach, M. E., Elzer, P. H., Hill, D. S., Robertson, G. T., Farris, M. A. Roop II, R. M. and Peterson, K. M. (1995) Four new derivatives of the broad-host range cloning vector pBBR1MCS, carrying different antibiotic-resistance cassettes. Gene 166: 175-176
- Kovach, M. E., Philips, R. W., Elzer, P. H., Roop II, R. M. and Peterson, K. M. (1994) pBBR1MCS: a broad-host-range cloning vector. BioTechniques 16: 800-802
- Lafontaine, E. R. and Solol, P. A. (1998) Effects of iron and temperature on expression of the *Pseudomonas aeruginosa tolQRA* genes: role of the ferric uptake regulator. J. Bacteriol. 180: 2836-2841.
- Lamont, I. L., Beare, P. A., Ochsner, U., Vasil, A. I. and Vasil, M. L. (2002) Siderophore-mediated signalling regulates virulence factor production in *Pseudomonas aeruginosa*. Proc. Natl. Acad. Sci. U. S. A. 99: 7072-7077
- Larsen, R. A. and Postle, K. (2001) Conserved residues Ser(16) and His(20) and their relative positioning are essential for TonB activity, cross-linking of TonB with ExbB, and the ability of TonB to respond to proton motive force. J. Biol. Chem. 276: 8111-8117
- Larsen, R. A., Foster-Hartnett, D., McIntosh, M. A. and Postle, K. (1997) Regions of *Escherichia coli* TonB and FepA proteins essential for *in vivo* physical interactions. J. Bacteriol. 179: 3213-3221.
- Larsen, R. A., Myers, P. S., Skare, J. T., Seachord, C. L., Darveau, R. P. and Postle, K. (1996) Identification of TonB homologs in the family Enterobacteriaceae and evidence for conservation of TonB-dependent energy transduction complexes. J. Bacteriol 178: 1363-1373

- Larsen, R. A., Thomas, M. G. and Postle, K. (1999) Protonmotive force, ExbB and ligand-bound FepA drive conformational changes in TonB. Mol. Microbiol. 31: 1809-1824.
- Larsen, R. A., Thomas, M. T., Wood, G. E. and Postle, K. (1994) Partial suppression of an *Escherichia coli* TonB transmembrane domain mutation (ΔV17) by a missense mutation in ExbB. Mol. Microbiol. 13: 627-640.
- Larsen, R. A., Wood, G. E. and Postle, K. (1993) The conserved proline-rich motif is not essential for energy transduction by *Escherichia coli* TonB protein. Mol. Micro. 10: 943-953
- Lavrrar, J. L., Christoffersen, C. A. and McIntosh, M. A. (2002) Fur-DNA interactions at the bi-directional *fepDGC-entS* promoter region in *Escherichia coli*. J. Mol. Biol. 322: 983-995
- Lawlor, K. M. and Payne, S. M. (1984) Aerobactin genes in *Shigella* spp. J. Bacteriol. 160: 266-272
- Lawlor, K. M., Daskaleros, P. A., Robinson, R. E. and Payne, S. M. (1987) Virulence of iron transport mutants of *Shigella flexneri* and utilization of host iron compounds. Infect. Immun. 55: 594-599
- Le Cam, E., Fréchon, D., Barray, M., Fourcade, A. and Delain, E. (1994) Observation of binding and polymerization of Fur repressor onto operator-containing DNA with electron and atomic force microscopes. Proc. Natl. Acad. Sci. U. S. A. 91: 11816-11820
- Le Vier, D. A. and Guerinot, M. L. (1996) Iron uptake by symbiosomes from soybean root nodules. Plant Physiol. 111:893-900.
- Lee, B. C. (1995) Quelling the red menace: haem capture by bacteria. Mol. Microbiol. 18: 383-390
- Leong, S. A., Ditta, G. S. and Helinski, D. R. (1982) Heme biosynthesis in *Rhizobium*. Identification of a cloned gene coding for delta-aminolevulinic acid synthetase from *Rhizobium meliloti*. J. Biol. Chem. 257: 8724-8730
- Letain, T. E. and Postle, K. (1997) TonB protein appears to transduce energy by shuttling between the cytoplasmic membrane and the outer membrane in gram-negative bacteria. Mol. Microbiol. 24: 271-283
- Létoffé, S., Ghigo, J. M. and Wandersman, C. (1994) Secretion of the *Serratia marcescens* HasA protein by an ABC transporter. J. Bacteriol. 176: 5372-5377

- Létoffé, S., Nato, F., Goldberg, M. E. and Wandersman, C. (1999) Interactions of HasA, a bacterial haemophore, with haemoglobin and with its outer membrane receptor HasR. Mol. Microbiol. 33: 546-555
- Létoffé, S., Onori, K. and Wandersman, C. (2000) Functional characterization of the HasA (PF) haemophore and its truncated and chimeric variants; determination of a region involved in binding to the hemphore receptor. J. Bacteriol. 182: 4401-4405
- Létoffé, S., Redeker, V. and Wandersman, C. (1998) Isolation and characterization of an extracellular haem-binding protein from *Pseudomonas aeruginosa* that shares function and sequence similarities with the *Serratia marcesens* HasA haemophore. Mol. Microbiol. 28: 1223-1234
- Levinson, G. and Gutman, G. A. (1987) Slipped-strand mispairing: a major mechanism for DNA sequence evolution. Mol. Biol. Evol. 4: 203-221
- Lewin, A. C., Doughty, P. A., Flegg, L., Moore, G. R. and Spiro, S. (2002) The ferric uptake regulator of *Pseudomonas aeruginosa* has no essential cysteine residues and does not contain a structural zinc ion. Microbiology 148: 2449-2456
- Li, X. –Z., Nikaido, H. and Poole, K. (1995) Role of MexA-MexB-OprM in antibiotic efflux in *Pseudomonas aeruginosa*. Antimicrob. Agents. Chemother. 39: 1948-1953
- Libbenga, K.R. and Harkes, P.A.A. (1973) Initial proliferation of cortical cells in the formation of root nodules in *Pisum sativum*. Planta 144: 17-28.
- Litwin, C. M. and Calderwood, S. B. (1993) Role of iron in regulation of virulence genes. Clin. Microbiol. Rev. 6: 137-149
- Liu, P. V. and Shokrani, F. (1978) Biological activities of pyochelins: iron chelating agents of *Pseudomonas aeruginosa*. Infect. Immun. 22: 878-890
- Locher, K., Rees, B., Koebnik, R., Mitschler, A., Moulinier, L., Rosenbusch, J. P. and Moras, D. (1998) Transmembrane signalling across the ligand-gated FhuA receptor: crystal structures of free and ferrichrome-bound states reveal allosteric changes. Cell 95: 771-778
- Long, S. R. (1989) Rhizobium-legume nodulation: life together in the underground. Cell 56: 203-214.

- Loper, J. E. and Buyer, J. S. (1991) Siderophores in microbial interactions on plant surfaces. Mol. Plant-Microb. Interact. 4: 5-13
- Lynch, D. (1999) Genetic analysis of iron uptake in *Sinorhizobium meliloti* 2011. PhD Thesis, Dublin City University
- Lynch, D., O'Brien, J., Welch, T., Clarke, P., Ó Cuív, P., Crosa, J. H. and O'Connell, M. (2001) Genetic organization of the region encoding regulation, biosynthesis, and transport of rhizobactin 1021 a siderophore produced by *Sinorhizobium meliloti*. J. Bacteriol. 183: 2576-2585
- Machuca, A. and Milagres, A. M. F. (2003) Use of CAS-agar plate modified to study the effect of different variables on the siderophore production by *Aspergillus*. Lett. App. Micro. 36: 177-181
- Mademidis, A., Killmann, H., Krass, W., Flechsler, I., Jung, G. and Braun, V. (1997) ATP-dependent ferric hydroxamate transport system in *Escherichia coli*: periplasmic FhuD interacts with a periplasmic and with a transmembrane/cytoplasmic region of the integral membrane protein FhuB, as revealed by competitive peptide mapping. Mol. Microbiol. 26: 1109-1123
- Marger, M., and Saier, J. M. H. (1993) A major superfamily of transmembrane facilitators that can catalyse uniport, symport, and antiport. Trends Biochem. Sci. 18: 13-20
- Martinez, J. L., Delgado-Iribarren, A. and Banquero, F. (1990) Mechanisms of iron acquisition and bacterial virulence. FEMS Microbiol. Rev. 6: 45-56.
- Martinez, J. L., Herrero, M. and DeLorenzo, V. (1994) The organisation of intercistronic regions of the aerobactin operon of pColV-K30 may account for the differential expression of the *iucABCD iutA* genes. J. Mol. Biol. 238: 288-293
- Masuda, N., Sakagawa, E. and Ohya, S. (1995) Outer membrane proteins responsible for multiple drug resistance in *Pseudomonas aeruginosa*. Antimicrob. Agents. Chemother. 39: 645-649
- McDougall, S. and Neilands, J. B. (1984) Plasmid- and chromosome-encoded aerobactin synthesis in enteric bacteria: insertion sequences flank operon in plasmid-mediated systems. J. Bacteriol. 159: 300-305
- Meade, H.M., Long, S.R., Ruvkin, G.B., Brown, S.E. and Ausubel, F.M. (1982) Physical and genetic characterization of symbiotic and auxotrophic

mutants of *Rhizobium meliloti* induced by transposon Tn5 mutagenesis. J. Bacteriol. 149: 114-122

- Menzl, K., Maier, E., Chakraborty, T. and Benz, R. (1996) HlyA hemolysin of *Vibrio cholerae* O1 biotype El Tor: identification of the haemolytic complex and evidence for the formation of anion-selective ion-permeable channels. Eur. J. Biochem. 240: 646-654
- Merianos, H. J., Cadieux, N., Lin, C. H., Kadner, R. J. and Cafiso, D. S. (2000) Substrate-induced exposure of an energy-coupling motif of a membrane receptor. Nat. Struct. Biol. 7: 205-209
- Merrick, M. J. (1992) *In*: Biological Nitrogen Fixation. (Stacey, G., Burris, R. H. and Evans, H. J. eds) Chapman and Hall New York, pp 835-876
- Meyer, J. M. (1992) Exogenous siderophore-mediated iron uptake in *Pseudomonas aeruginosa*: possible involvement of porin OprF in iron translocation. J. Gen. Microbiol. 138: 951-958
- Milagres, A. M. F., Machuca, A. and Napoleão, D. (1999) Detection of siderophore production from several fungi and bacteria by a modification of chrome azurol S (CAS) agar plate assay. J. Micro. Meth. 37: 1-6
- Minnick, A. A., McKee, J. A., Dolence, E. K. and Miller, M. J. (1992) Iron-transport-mediated antibacterial activity of and development of resistance to hydroxamate and catechol siderophore-carbacephalosporin conjugates. Antimicro. Agents Chemother. 36: 840-850
- Modi, M., Shah, K. S. and Modi, V. V. (1985) Isolation and characterisation of catechol-type siderophore from cowpea *Rhizobium* RA-1. Arch. Microbiol. 141: 156-158
- Moeck, G. S. and Letellier, L. (2001) Characterization of *in vitro* interactions between a truncated TonB protein from *Escherichia coli* and the outer membrane receptors FhuA and FepA. J. Bacteriol. 183: 2755-2764
- Moeck, G. S., Coulton, J. W. and Postle, K. (1997) Cell envelope signalling in *Escherichia coli*: Ligand binding to the ferrichrome iron receptor FhuA promotes interaction with the energy transducing protein TonB. J. Biol. Chem. 272: 28391-28397

- Moore, D. G. and Earhart, C. F. (1981) Specific inhibition of *Escherichia coli* enterochelin uptake by a normal human serum immunoglobulin. Infect. Immun. 31: 631-635
- Moss, J. E., Cardozo, T. J., Zychlinsky, A. and Groisman, E. A. (1999) The *selC*-associated SHI-2 pathogenicity island of *Shigella flexneri*. Mol. Microbiol. 33: 74-83
- Mossialos, D., Ochsner, U., Baysse, C., Chablain, P., Pirnay, J. –P., Koedan, N., Budzikiewicz, H., Fernàndez, D. U., Schäfer, M., Ravel, J. and Cornelis, P. (2002) Identification of new, conserved, non-ribosomal peptide synthetases from fluorescent pseudomonads involved in the biosynthesis of the siderophore pyoverdine. Mol. Microbiol. 45: 1673-1685
- Muffler, A. Traulsen, D. D., Fischer, D., Lange, R. and Hengge-Aronis, R. (1997) The RNA-binding protein HF-1 plays a global regulatory role which is largely, but not exclusively, due to its role in expression of the sigmaS subunit of RNA polymerase in *Escherichia coli*. J. Bacteriol. 179: 297-300
- Muffler, A., Fischer, D. and Hengge-Aronis, R. (1996) The RNA-binding protein HF-1, known as a host factor for phage Qbeta RNA replication, is essential for *rpoS* translation in *Escherichia coli*. Genes Dev. 10: 1143-1151
- Muller, K. Matzanke, B. F., Schunemann, V., Trautwein, A. X. and Hantke, K. (1998) FhuF, an iron-regulated protein of Escherichia coli with a new type of [2Fe-2S] center. Eur. J.Biochem. 258: 1001-1008
- Mulligan, J. T. and Long, S. R. (1985) Induction of *Rhizobium meliloti nodC* expression by plant exudate requires *nodD*. Proc. Natl. Acad. Sci. U. S. A. 82: 6609-6613.
- Murray, A. P. and Miller, M. J. (2003) The preparation of a fully differentiated "multiwarhead" siderophore precursor. J. Org. Chem. 68: 191-194
- Nakai, K. and Kanehisa, M. (1991) Expert system for predicting protein localization sites in Gram-negative bacteria. PROTEINS: Structure, Function, and Genetics 11: 95-110.
- Nassif, X., Mazert, M. C., Mounier, J. and Sansonetti, P. J. (1987) Evaluation with an *iuc*::Tn*10* mutant of the role of aerobactin production in the virulence of *Shigella flexneri*. Infect. Immun. 55: 1963-1969

- Neilands J.B, Konopka, K., Schwyn, B., Coy, M., Francis, R.T., Paw, B.H. and Bagg, A. (1987) *In* : Iron transport in microbes, plants and animals. (Winkelmann, G., van der Helm, D. and Neilands, J.B. eds.) VCH, New York. pp 3-33.
- Neilands, J. B. and Leong, S. A. (1986) Siderophores in relation to plant growth and disease. Ann. Rev. Plant. Physiol. 37: 187-208
- Neilands, J.B. (1981) Microbial iron compounds. Ann. Rev. Biochem. 50: 715-731.
- Nielsen, H., Engelbrecht, J., Brunak, S. and von Heijne, G. (1997) Identification of prokaryotic and eukaryotic signal peptides and prediction of their cleavage sites. Protein Engineering 10: 1-6
- Nienaber, A., Hennecke, H. and Fischer, H. M. (2001) Discovery of a haem uptake system in the soil bacterium *Bradyrhizobium japonicum.* Mol. Microbiol. 41: 787-800
- Nikaidi, H and Saier, M. H. (1992) Transport proteins in bacteria: common themes in their design. Science 258: 937-941
- Nikaido, H. (1996) Multidrug efflux pumps of Gram-negative bacteria. J. Bacteriol. 178: 5853-5859
- Nikaido, H. and Hall, J. A. (1998) Overview of bacterial ABC transporters. Meth. Enz. 292: 3-20
- Noya, F., Arias, A. and Fabiano, E. (1997) Heme compounds as iron sources for nonpathogenic *Rhizobium* species. J. Bacteriol. 179: 3076-3078
- Nudelman, R., Ardon, O., Hadar, Y., Chen, Y., Libman, J. and Shazner, A. (1998) Modular fluorescent-labelled siderophore analogues. J. Med. Chem. 41: 1671-1678
- O' Hara, G. W., Dilworth, M. J., Boonkerd, N. and Parkpian, P. (1988) Iron-deficiency specifically limits nodule development in peanut inoculated with *Bradyrhizobium* sp. New Phytol. 108: 51-57
- O'Brien, E. G. and Gibson, F. (1970) The structure of enterochelin and related 2,3-dihydroxy-N-benzoyl serine conjugates from *Escherica coli.* Biochim. Biophys. Acta. 215: 393-402.
- O'Brien, E. G., Cox, G. B. and Gibson, F. (1971) Enterochelin hydrolysis and iron metabolism in *Escherichia coli.* Biochim. Biophys. Acta. 237: 537-549

- Occhino, D. A., Wyckoff, S. L., Henderson, D. P., Wrona, T. J. and Payne, S.M. (1998) *Vibrio cholera* iron transport: haem transport genes are linked to one of two sets of *tonB, exbB, exbD* genes. Mol. Microbiol. 29: 1493-1507
- Ochs, M., Veitinger, S., Kim, I., Welz, I., Angerer, A. and Braun, V. (1995) Regulation of citrate-dependent iron transport of *Escherichia coli*: FecR is required for transcription activation by FecI. Mol. Microbiol. 15: 119-132
- Ochsner, U. A. and Vasil. M. L. (1996) Gene repression by the ferric uptake regulator in *Pseudomonas aeruginosa*: cycle selection of iron-regulated genes. Proc. Natl. Acad. Sci. U. S. A. 93: 4409-4414
- Ochsner, U. A., Johnson, Z. and Vasil, M. L. (2000) Genetics and regulation of two distinct haem-uptake systems, *phu* and *has*, in *Pseudomonas aeruginosa*. Microbiol. 146: 185-198
- Ochsner, U. A., Johnson, Z., Lamont, I. L., Cunliffe, H. E. and Vasil, M. L. (1996) Exotoxin A production in *Pseudomonas aeruginosa* requires the iron-regulated *pvdS* gene encoding an alternative sigma factor. Mol. Microbiol. 21: 1019-1028
- Ochsner, U. A., Snyder, A., Vasil, A. I. and Vasil, M. L. (2002) Effects of the twin-arginine translocase on secretion of virulence, stress response, and pathogenesis. Proc. Natl. Acad. Sci. U. S. A. 99: 8312-8317
- Ochsner, U. A., Wilderman, P. J., Vasil, A. I. and Vasil, M. A. (2002) GeneChip® expression analysis of the iron starvation response in *Pseudomonas aeruginosa*: identification of novel pyoverdine biosynthesis genes. Mol. Microbiol. 45: 1277-1287
- Okujo, N., Sakakibara, Y., Yoshida, T. and Yamamoto, S. (1994) Structure of acinetoferrin, a new citrate-based dihydroxamate siderophore from *Acinetobacter haemolyticus*. Biometals 7: 170-176
- Ong, S. A., Peterson, T. and Neilands, J. B. (1979) Agrobactin, a siderophore from *Agrobacterium tumefaciein*. J. Biol. Chem. 254: 1860-1865.
- Pao, S. S., Paulsen, I. T., Saier, J. and Saier, M. H. (1998) Major facilitator superfamily. Microbiol. Mol. Biol. Rev. 62: 1-34
- Patel, H. N., Chakraborty, R. N. and Desai, S. B. (1988) Isolation and partial characterization of phenolate siderophore from *Rhizobium leguminosarum* IARI102. FEMS Microbiol. Lett. 56: 131-134

- Patzer, S. I. and Hantke, K. (1999) SufS is a NifS-like protein, and SufD is necessary for stability of the [2Fe-2S] FhuF protein in *Escherichia coli*. J. Bacteriol. 181: 3307-3309
- Payne, S. M. (1993) Iron acquisition in microbial pathogenesis. Trends Microbiol. 1: 66-69
- Persmark, M., Expert, D. and Neilands, J. B. (1989) Isolation, characterization, and synthesis of chrysobactin, a compound with siderophore activity from *Erwinia chrysanthemi*. J. Biol. Chem. 264: 3187-3193.
- Persmark, M., Pittman, P., Buyer, J. S., Schwyn, B., Gill, P. R. and Neilands, J. B. (1993) Isolation and structure of rhizobactin 1021, a siderophore from the alfalfa symbiont *Rhizobium meliloti* 1021. J. Am. Chem. Soc. 115: 3950-3956
- Peterson, T. and Neilands, J. B. (1979) Revised structure of a catecholates sperimidine siderophore. Tet. Lett. 50: 4805-4808
- Pierce, J. R., Pickett, C. L. and Earhart, C. F. (1983) Two *fep* genes are required for ferrienterochelin uptake in *Escherichia coli* K-12 J. Bacteriol. 155: 330-336.
- Platero, R. A., Jaureguy, M., Battistoni, F. J. and Fabiano, E. R. (2003) Mutations in *sitB* and *sitD* genes affect manganese-growth requirements in *Sinorhizobium meliloti*. FEMS Micro. Lett. 218: 65-70
- Pollack, J. R. and Neilands, J. B. (1970) Enterobactin, an iron transport compound from *Salmonella typhimurium*. Biochem. Biophys. Res. Commun. 38: 989-992.
- Poole, K. (1994) Bacterial multidrug resistance-emphasis on efflux mechanisms and *Pseudomonas aeruginosa*. J. Antimicrob. Agents. Chemother. 34: 453-456
- Poole, K. and Braun, V. (1988) Iron regulation of *Serratia marcescens* hemolysin gene expression. Infect. Immun. 56: 2967-2971
- Poole, K. and McKay, G. A. (2003) Iron acquisition and its control in *Pseudomonas aeruginosa*: Many roads lead to Rome. Frontiers in Bioscience 8: 661-686
- Poole, K., Heinrichs, D. E. and Neshat, S. (1993a) Cloning and sequence analysis of an EnvCD homologue in *Pseudomonas aeruginosa*: regulation by

iron and possible involvement in the secretion of the siderophore pyoverdine. Mol. Microbiol. 10: 529-544

- Poole, K., Kreves, K., McNally, C. and Neshat, S. (1993b) Multiple antibiotic resistance in *Psedomonas aeruginosa*: evidence for involvement of an efflux operon. J. Bacteriol. 175: 7363-7372
- Poole, K., Neshat, S., Krebes, K., and Heinrichs, D. E. (1993) Cloning and nucleotide sequencing analysis of the pyoverdin receptor gene *fpvA* of *Pseudomonas aeruginosa*. J. Bacteriol. 175: 4597-4604
- Poole, K., Young, L. and Neshat, S. (1990) Enterobactin mediated iron transport in *Pseudomonas aeruginosa*. J. Bacteriol. 172: 6991-6996
- Poole, K., Zhao, Q., Neshat, S., Heinrichs, D. E. and Dean, C. R. (1996) The *Pseudomonas aeruginosa tonB* gene encodes a novel TonB protein. Microbiol. 142: 1449-1458
- Postle, K. (1993) TonB protein and energy transduction between membranes. J. Bioenerg. Biomemb. 25: 591-601
- Postle, K. (2002) Close before opening. Science 295: 1658-1659
- Postle, K. and Skare, J. T. (1988) *Escherichia coli* TonB protein is exported from the cytoplasm without proteolytic cleavage of its amino terminus. J. Biol. Chem. 263: 11000-11007
- Pradel, E., Guiso, N., Menozii, F. D. and Locht, C. (2000) *Bordetella pertussis*, TonB, a Bvg-independent virulence determinant. Infect. Immun. 68: 1919-1927
- Priefer, U. B., Simon, R. and Puehler, A. (1985) Extension of the host range of *Escherichia coli* vectors by incorporation of RSF1010 replication and mobilisation functions. J. Bacteriol. 163: 324-330
- Purdy, G. E. and Payne, S. M. (2001) The SHI-3 iron transport island of *Shigella boydii* 0-1392 carries the genes for aerobactin synthesis and transport. J. Bacteriol. 183: 4176-4182
- Putman, M. vanVeen, H. W. and Konings, W. N. (2000) Molecular properties of multidrug transporters. Microbiol. Mol. Biol. Rev. 64: 672-693
- Qi, Z. and O'Brian, M. R. (2002) Interaction between the bacterial iron response regulator and ferrochelatase mediates genetic control of heme biosynthesis. Mol. Cell. 9: 155-162

- Qi, Z., Hamza, I. and O'Brian, M. R. (1999) Heme is an effector molecule for iron-dependent degradation of the bacterial iron response regulator (Irr) protein. Proc. Natl. Acad. Sci. U. S. A. 96: 13056-13061
- Quail, M. A., Jordan, P., Grogan, J. M., Butt, J. N., Lutz, M., Thomson, A. J., Andrews, S. C. and Guest, J. R. (1996) Spectroscopic and voltammetric characterisation of the bacterioferritin-associated ferredoxin of *Escherichia coli*. Biochem. Biophys. Res. Commun. 229: 635-642
- Quandt, J. and Hynes, M.F. (1993) Versitile suicide vectors which allow direct selection for gene replacement in Gram-negative bacteria. Gene 127: 15-21
- Ratledge, C. (1971) Transport of iron by mycobactin in *Mycobacterium smegmatis*. Biochem. Biophys. Res. Commun. 45: 856-861
- Ratledge, C. (1987) *In* : Iron transport in microbes, plants and animals. (Winkelmann, G., van der Helm, D. and Neilands, J.B. eds.) VCH, New York. pp 207-221.
- Ratledge, C. and Dover, L. G. (2000) Iron metabolism in pathogenic bacteria. Annu. Rev. Microbiol. 54: 881-941
- Ratliff, M., Zhu, W., Deshmukh, R., Wilks, A. and Stojiljkovic, I. (2001) Homologues of neisserial heme oxygenase in gram-negative bacteria: degradation of heme by the product of the *pigA* gene of *Pseudomonas aeruginosa*. J. Bacteriol. 183: 6394-6403
- Rédly, G. A. and Poole, K. (2003) Pyoverdine-mediated regulation of FpvA synthesis in *Pseudomonas aeruginosa*: Involvement of a probable extracytoplasmic-function sigma factor, FpvI. Mol. Microbiol. 185: 1261-1265
- Reeves, S. A., Torres, A. G. and Payne, S. M. (2000) TonB is required for intracellular growth and virulence of *Shigella dysenteriae*. Infect. Immun. 68: 6329-6336.
- Reidl, J. and Mekalanos, J. J. S. (1996) Lipoprotein e(P4) is essential for hemin uptake by *Haemophilus influenzae*. J. Exp. Med. 183:621-629
- Reigh, G. (1991) Analysis of siderophore production by *Rhizobium meliloti* 220-5. PhD Thesis, Dublin City University.

- Reigh, G. and O'Connell, M. (1993) Siderophore-mediated iron transport correlates with the presence of specific iron-regulated proteins in the outer membrane of *Rhizobium meliloti*. J. Bacteriol. 175: 94-102
- Reimmann, C., Patel, H. M., Serino, L., Barone, M., Walsh, C. T. and Haas, D. (2001) Essential PchG-dependent reduction in pyochelin biosynthesis of *Pseudomonas aeruginosa*. J. Bacteriol. 183: 813-820
- Reimmann, C., Serino, L., Beyeler, M. and Haas, D. (1998) Dihydroaeruginoic acid synthetase and pyochelin synthetase, products of the *pchEF* genes, are induced by extracellular pyochelin in *Pseudomonas aeruginosa*. Microbiology 144: 3135-3148
- Rioux, C. R., Jordan, D. C. and Rattray, J. B. M. (1986) Iron requirement of *Rhizobium leguminosarum* and secretion of anthranilic acid during growth on an iron-deficient medium. Arch. Biochem. 248: 175-182
- Robertson, J. G., Lyttleton, P., Bullivant, S. and Grayston, G. F. (1978) Membranes in lupin root nodules. The role of Golgi bodies in the biogenesis of infection threads and peribacteroid membranes. J. Cell Sci. 30: 129-149.
- Rohrbach, M. R., Braun, V. and Köster, W. (1995) Ferrichrome transport in *Escherichia coli* K-12: altered substrate specificity of mutated periplasmic FhuD and interaction of FhuD with the integral membrane protein FhuB. J. Bacteriol. 177: 7186-7193
- Römheld, V. (1987) *In*: Iron transport in microbes, plants and animals. (Winklemann, G., van der Helm, D. and Neilands, J. B. eds.) VCH, New York. pp 353-374
- Roosenberg II, J. M., Lin, Y.-M., Lu, Y. and Miller, M. J. (2000) Studies and syntheses of siderophores, microbial iron chelators, and analogs as potential drug delivery agents. Curr. Med. Chem. 7: 159-197
- Roy, N. Bhattacharyya, P. and Chakrabartty, P. K. (1994) Iron acquisition during growth in an iron deficient medium by *Rhizobium* sp. isolated from *Cicer arietinum*. Microbiology 140: 2811-2820
- Saier, M. H., Tam, R., Reizer, A. and Reizer, J. (1994) Two novel families of bacterial membrane proteins concerned with nodulation, cell division, and transport. Mol. Microbiol. 11: 841-847

- Sánchez-Contreras, M., Maritn, M., Villacieros, M., O'Gara, F., Bonilla, Ildefonso, B. and Rivilla, R. (2002) Phenotypic selection and phase variation occur during alfalfa root colonization by *Pseudomonas fluorescens* F113. J. Bacteriol. 184: 1587-1596
- Sangwan, I. and O' Brian, M.R. (1991) Evidence for an inter-organismic heme biosynthetic pathway in symbiotic soybean root nodules. Science 251: 1220-1222.
- Schalk, I. J., Abdallah, M. A. and Pattus, F. (2002) Recycling of pyoverdin on the FpvA receptor after ferric pyoverdine uptake and dissociation in *Pseudomonas aeruginosa*. Biochemistry 41: 1663-1671
- Schalk, I. J., Hennard, C., Dugave, C., Poole, K., Abdallah, M. A. and Pattus, F. (2001) Iron-free pyoverdine binds to its outer membrane receptor FpvA in *Pseudomonas aeruginosa*: a new mechanism for membrane iron transport. Mol. Microbiol. 39: 351-360
- Schöffler, H. and Braun, V. (1989) Transport across the outer membrane of *Escherichia coli* K12 via the FhuA receptor is regulated by the TonB protein of the cytoplasmic membrane. Mol. Gen. Genet. 217: 378-383
- Schultz-Hauser, G., Köster, W., Schwarz, H. and Braun, V. (1992) Iron(III) hydroxamate transport in *Escherichia coli* K-12: FhuB-mediated membrane association of the FhuC protein and negative complementation of *fhuC* mutants. J. Bacteriol. 174: 2305-2311
- Schwyn, B. and Neilands, J. B. (1987) Universal chemical assay for the detection and determination of siderophores. Anal. Biochem. 160: 47-57
- Scott, D. C., Cao, Z., Qi, Z., Bauler, M., Igo, J. D., Newton, S. M. C. and Klebba, P. E., (2001) Exchangeability of N termini in the ligand gated porins of *Escherichia coli*. J. Biol. Chem. 276: 13025-13033
- Screen, J., Moya, E., Blagbrough, I. S. and Smith, A. W. (1995) Iron uptake in *Pseudomonas aeruginosa* mediated by N-(2,3-dihydroxybenzoyl)-L-serine and 2,3-dihydroxybenzoic acid. FEMS Microbiol. Lett. 127: 145-149
- Seliger, S. A., Mey, A. Valle, A. and Payne, S. (2001) The two TonB systems of *Vibrio cholera*: redundant and specific functions. Mol. Microbiol. 39: 801-812

- Serino, L., Reimmann, C., Baur, H., Beyeler, M., Visca, P. and Haas, D. (1995) Structural genes for salicylate biosynthesis from chorismate in *Pseudomonas aeruginosa*. Mol. Gen. Genet. 249: 217-228
- Serino, L., Reimmann, C., Visca, P., Beyeler, M., Chiesa, V. D. and Hass, D. (1997) Biosynthesis of pyochelin and dihydroaeruginoic acid requires the iron-regulated *pchDCBA* operon in *Pseudomonas aeruginosa*. J. Bacteriol. 179: 248-257
- Shea, C. M. and McIntosh, M. A. (1991) Nucleotide sequence and genetic organization of the ferric enterobactin transport system: homology to other periplasmic binding protein-dependent systems in *Escherichia coli*. Mol. Microbiol. 5: 1415-1428
- Shen, J., Meldrum, A. and Poole, K. (2002) FpvA receptor involvement in pyoverdine biosynthesis in *Pseudomonas aeruginosa*. J. Bacteriol. 184: 3268-3275
- Simon, R. (1984) High frequency mobilization of gram-negative bacterial replicons by the *in vivo* constructed Tn5-*mob* transposon. Mol. Gen. Genet. 196: 413-420.
- Skare, J. T. and Postle, K. (1991) Evidence for a TonB-dependent energy transduction complex in *Escherichia coli*. Mol. Microbiol. 5: 2883-2890
- Skare, J. T., Ahmer, B. M. M., Seachord, C. L., Darveau, R. P. and Postle, K. (1993) Energy transduction between membranes-TonB, a cytoplasmic membrane protein, can be chemically cross-linked *in vivo* to the outer membrane FepA. J. Biol. Chem. 268: 16302-16308
- Smith, M. J. and Neilands, J.B. (1984) Rhizobactin, a siderophore from *Rhizobium meliloti*. J. Plant. Nut. 7: 449-458.
- Smith, M. J., Shoolery, J. N., Schwyn, B., Holden, I. and Neilands, J. B. (1985) Rhizobactin, a structurally novel siderophore from *Rhizobium meliloti*. J. Am. Chem. Soc. 107: 1739-1743
- Sokol, P.A. (1984) Production of ferripyochelin outer membrane receptor by *Pseudomonas* species. FEMS Microbiol. Lett. 23: 313-317.
- Sriyosachati, S. and Cox, C. D. (1986) Siderophore-mediated iron acquisition from transferrin by *Pseudomonas aeruginosa*. Infect. Immun. 52: 885-891

- Stanley, J., Dowling, D. N. and Broughton, W. J. (1988) Cloning of *hemA* from *Rhizobium* sp. NGR234 and symbiotic phenotype of a gene-directed mutant in diverse legume genera. Mol. Gen. Genet. 215: 32-37.
- Staudenmaier, H., Van Howe, B., Yaraghi, Z. and Braun, V. (1989) Nucleotide sequences of the *fecBCDE* genes and locations of the proteins suggest a periplasmic-binding-protein-dependent transport mechanism for iron(III) dicitrate in *Escherichia coli*. J. Bacteriol. 171: 2622-2633
- Stevens, J. B., Carter, R. A., Hussain, H., Carson, K. C., Dilworth, M. J. and Johnston, A. W. B. (1999) The *fhu* genes of *Rhizobium leguminosarum*, specifying siderophore uptake proteins: *fhuDCB* are adjacent to a pseudogene version of *fhuA*. Microbiology 145: 593-601
- Stintzi, A., Cornelis, P., Hohnadel, D., Meyer, J. –M., Dean, C., Poole, K., Kourambas, S. and Krishnapillai, V. (1996) Novel pyoverdine biosynthesis gene(s) of *Pseudomonas aeruginosa* PAO. Microbiology 142: 1181-1190
- Stintzi, A., Johnson, Z., Stonehouse, M., Ochsner, U., Meyer, J. –M., Vasil, M. L. and Poole, K. (1999) The *pvc* cluster of *Pseudomonas aeruginosa*: role in synthesis of the pyoverdine chromophore and regulation by PtxR and PvdS. J. Bacteriol. 181: 4118-4124
- Stinzi, A., Barnes, C., Xu, J. and Raymond, K. N. (2000) Microbial iron transport via a siderophore shuttle: a membrane ion transport paradigm. Proc. Natl. Acad. Sci. U. S. A. 97: 10691-10696
- Stobner, J. A. and Payne, S. M. (1988) Iron-regulated hemolysin production and utilization of heme and haemoglobin by *Vibrio cholerae*. Infect. Immun. 56: 2891-2895
- Stojiljkovic, I. A. and Hantke, K. (1995) Functional domains of the *Escherichia coli* ferric uptake regulator protein (Fur). Mol. Gen. Genet. 247: 199-205
- Stojiljkovic, I., Baumler, A. J. and Hantke, K. (1994) Fur regulon in gram-negative bacteria. Identification and characteheization of new iron-regulated *Escherichia coli* genes by a Fur titration assay. J. Mol. Biol. 236: 531-545
- Stojilkovic, I. and Hantke, K. (1992) Hemin uptake system of *Yersinia enterocolitica*: similarities with other TonB-dependent systems in gram-negative bacteria. EMBO J. 11: 4359-4367

- Stover, C. K., Pham, X. Q., Erwin, A. L., Mizoguchi, S. D., Warrener, P., Hickey, M. J., Brinkman, F. S., Hufnagle, W. O., Kowalik, D. J., Lagrou, M., Garber, R. L., Goltry, L., Tolentino, E., Westbrock-Wadman, S., Yuan, Y., Brody, L. L., Coulter, S. N., Folger, K. R., Kas, A., Larbig, K., Lim, R., Smith, K., Spencer, D., Wong, G. K., Wu, Z., Paulsen, I. T., Reizer, J., Saier, M. H., Hancock, R.E., Lory, S. and Olson, M. V. (2000) Complete genome sequence of *Pseudomonas aeruginosa* PA01, an opportunistic pathogen. Nature 406: 959-964
- Struyvé, M., Moons, M. and Tommassen, J. (1991) Carboxyl-terminal phenylalanine is essential for the correct assembly of a bacterial outer membrane protein. J. Mol. Biol. 218: 141-148
- Szeto, W. W., Nixon, B. T., Ronson, C. W. and Ausubel, F. M. (1987) Identification and characterization of the *Rhizobium meliloti ntrC* gene: *R. meliloti* has separate regulatory pathways for activation of nitrogen fixation genes in free-living and symbiotic cells. J. Bacteriol. 169: 1423-1432.
- Tait, G. H. (1975) The identification and biosynthesis of siderochromes formed by *Micrococcus denitrificans*. Biochem. J. 146: 191-204
- Takagi, S. (1987) *In*: Iron chelation in plants and soil microorganisms. (Barton, L. L. and Hemming, B. C. eds.) Academic Press, California. pp 111-131
- Takase, H., Nitanai, H., Hoshino, K. and Otani, T. (2000a) Impact of siderophore production on *Pseudomonas aeruginosa* infections in immunosuppressed mice. Infect. Immun, 68: 1834-1839
- Takase, H., Nitanai, H., Hoshino, K. and Otani, T. (2000b) Requirement of the *Pseudomonas aeruginosa tonB* gene for high-affinity iron acquisition and infection. Infect. Immun. 68: 4498-4504
- Thompson, J. M., Jones, H. A. and Perry, R. D. (1999) Molecular characterization of the hemin uptake locus (*hmu*) from *Yersinia pestis* and analysis of *hmu* mutants for hemin and hemoprotein utilization. Infect. Immun. 67: 3879-3892
- Todd, J. D., Wexler, M., Sawers, G., Yeoman, K. H., Poole, P. S. and Johnston, A. W. B. (2002) RirA, an iron-responsive regulator in the symbiotic bacterium *Rhizobium leguminosarum*. Microbiology 148: 4059-4071

- Tolmasky, M. E., Wertheimer, A. and Crosa, J. H. (1994) Characterization of the *Vibrio anguillarum fur* gene: role in regulation of expression of the FatA outer membrane protein and catechols. J. Bacteriol. 176: 213-220
- Torres, A. G., Redford, P., Welch, R. A. and Payne, S. M. (2001) TonB-dependent systems of uropathogenic *Escherichia coli*: Aerobactin and heme transport and TonB are required for virulence in the mouse. Infect. Immun. 69: 6179-6185
- Traub, J., Gaisser, S. and Braun, V. (1993) Activity domains of the TonB protein. Mol. Microbiol. 8: 409-423
- Tsolis, R. M., Baumler, A. J., Heffron, F. and Stojiljkovic, I. (1996) Contribution of TonB- and Feo-mediated iron uptake to growth of *Salmonella typhimurium* in the mouse. Infec. Immun. 64: 4549-4556.
- Tsuda, M., Miyazaki, H. and Nakazawa, T. (1995) Genetic and physical mapping of genes involved in pyoverdine production in *Pseudomonas aeruginosa* PAO. J. Bacteriol. 177: 423-431
- Tsui, H. C., Leung, H. C. and Winkler, M. E. (1994) Characterization of broadly pleiotropic phenotypes cause by an *hfq* insertion mutation in *Escherichia coli* K-12. Mol. Microbiol. 13: 35-49
- Tuckman, M. and Osburne, M. S. (1992) *In vivo* inhibition of TonB-dependent processes by a TonB box consensus pentapeptide. J. Bacteriol. 174: 320-323
- Usher, K. C., Özkan, E., Gardner, J. and Deisenhofer, J. (2001) The plug domain of FepA, a TonB-dependent transport protein from *Escherichia coli*, binds its siderophore in the absence of the transmembrane barrel domain. Proc. Natl. Acad. Sci. U. S. A. 98: 10676-10681
- Vanderpool, C. K. and Armstrong, S. K. (2001) The *Bordetella bhu* locus is required for heme iron utilization. J. Bacteriol. 183: 4278-4287
- Vasil, M. L. and Ochsner, U. A. (1999) The response of *Pseudomonas aeruginosa* to iron: genetics, biochemistry and virulence. Mol. Microbiol. 34: 399-413
- Vasil, M. L., Kabat, D. and Iglewski, B. H. (1977) Structure-activity relationships of an exotoxin of *Pseudomonas aeruginosa*. Infect. Immun. 16: 353-361

- Verma, D. and Long, S. (1983) The molecular biology of *Rhizobium*-legume symbiosis. Int. Rev. Cytol. Suppl. 14: 211-245
- Vieira, J and Messing, J. (1982) The pUC plasmids, an M13mp7-derived system for insertion mutagenesis and sequencing with synthetic universal primers. Gene 19: 259-268
- Visca, P., Civero, A., Sanfilippo, V. and Orsi, N. (1993) Iron-regulated salicylate synthesis by *Pseudomonas aeruginosa* spp. J. Gen. Micro. 139: 1995-2001
- Visca, P., Colotti, G., Serino, L., Verzili, D., Orsi, N and Chiancone, E. (1992) Metal regulation of siderophore synthesis in *Pseudomonas aeruginosa* and functional effects of siderophore-metal complexes. Appl. Environ. Microbiol. 58: 2886-2893
- Visca, P., Leoni, L., Wilson, M. J. and Lamont, I. L. (2002) Iron transport and regulation, cell signalling and genomics: lessons from *Escherichia coli* and *Pseudomonas*. Mol. Microbiol. 45: 1177-1190
- Vokes, S. A., Reeves, S. A., Torres, A. G. and Payne, S. M. (1999) The aerobactin iron transport system genes in *Shigella flexneri* are present within a pathogenicity island. Mol. Microbiol. 33: 63-73
- Wacek, T. and Brill, W. J. (1976) Simple, rapid assay for screening nitrogen fixing ability in soybean. Crop. Sci. 16: 519-522
- Waldbeser, L. S., Chen, Q. and Crosa, J. H. (1995) Antisense RNA regulation of the *fatB* iron transport protein gene in *Vibrio anguillarum*. Mol. Microbiol. 17: 747-756
- Waldbeser, L. S., Tolmasky, M. E., Actis, L. A. and Crosa, J. H. (1993) Mechanisms for negative regulation by iron of the *fatA* outer membrane protein gene expression in *Vibrio anguillarum* 775. J. Biol. Chem. 268: 10433-10439
- Walsh, C. T., Liu, J., Rusnak, F. and Sakaitani, M. (1990) Molecular studies on enzymes in chorismate metabolism and the enterobactin biosynthesis pathway. Chem. Rev. 90: 1105-1129
- Wandersman, C. and Stojilkovic, I. (2000) Bacterial heme sources: the role of heme, hemoprotein receptors and hemophores. Curr. Opin. Microbiol. 3: 215-220

- Wang, J., Lory, S., Ramphal, R. and Jin, S. (1996) Isolation and characterization of *Pseudomonas aeruginosa* genes inducible by respiratory mucus derived from cystic fibrosis patients. Mol. Microbiol. 22: 1005-1012
- Wang, J., Mushegian, A., Lory, S. and Jin, S. (1996) Large-scale isolation of candidate virulence genes of *Pseudomonas aeruginosa* by *in vivo* selection. Proc. Natl. Acad. Sci. U. S. A. 93: 10434-10439
- Wang, Q. X. and Phanstiel IV, O. (1998) Total synthesis of acinetoferrin. J. Org. Chem. 63: 1491-1495
- Warner, P. J. Willians, P. H. Bindereif, A. and Neilands, J. B. (1981) ColV plasmid-specified aerobactin synthesis by invasive strains of *Escherichia coli* Infect. Immun. 33: 540-545
- Wassarman, K. M., Repoila, F., Rosenow, C., Storz, G. and Gottesman, S. (2001) Identification of novel small RNAs using comparative genomics and microarrays. Genes Dev. 15: 1637-1651
- Welkie, G. W. and Miller, G. W. (1993) *In* : Iron chelation in plants and soil microorgansims. (Barton, L. L. and Hemming, B. C. eds.) Academic Press, California. pp 345-369.
- Wexler, M., Yeoman, K. H., Stevens, J. B., deLuca, N. G., Sawers, G. and Johnston, A. W. B. (2001) The *Rhizobium leguminosarum tonB* genes is required for the uptake of siderophore and haem as sources of iron. Mol. Microbiol. 41: 801-816
- Wilderman, P. J., Vasil, A. I., Johnson, Z., Wilson, M. J., Cunliffe, H. E., Lamont, I. L. and Vasil, M. L. (2001) Characterization of an endoprotease (PrpL) encoded by a PvdS-regulated gene in *Pseudomonas aeruginosa*. Infect. Immun. 69: 5385-5394
- Williams, P. H. (1979) Novel iron uptake system specified by ColV plasmids: an important component of the virulence of invasive strains of *Escherichia coli*. Infect. Immun. 26: 925-932
- Williams, P. H. and Carbonetti, N. H. (1986) Iron, siderophores, and the pursuit of virulence: independence of the aerobactin and enterochelin uptake systems in *Escherichia coli*. Infect. Immun. 51: 942-947

- Williams, P. H. and Warner, P. J. (1980) ColV plasmid mediated, colicin V-independent iron uptake system of invasive strains of *Escherichia coli*. Infect. Immun. 29: 411-416
- Wilson, M. J., McMorran, B. J. and Lamont, I. L. (2001) Analysis of promoters recognized by PvdS, an extracytoplasmic-function sigma factor protein from *Pseudomonas aeruginosa*. J. Bacteriol. 183: 2151-2155
- Winkelmann, G. and Huschka, H.G. (1987). *In* : Iron transport in microbes, plants and animals. (Winkelmann, G., van der Helm, D. and Neilands, J.B. eds.) VCH, New York. pp 317-336.
- Wittenberg, J. B., Wittenberg, B. A., Day, D. A., Udvardi, M. K. and Appleby, C. A. (1996) Siderophore-bound iron in the peribacteroid space of soybean root nodules. Plant and Soil 178: 161-169.
- Wittnamam, S., Schnabelrauch, M., Scherlitz-Hofmann, I., Möllmann, U., Ankel-Fuchs, D. and Heinisch, L. (2002) New synthetic siderophores and their β-lactam conjugates based on diamino acids and dipeptides. Bioorg. Med. Chem. 10: 1659-1670
- Wooldridge, K. G., Morrissey, J. A. and Williams, P. H. (1992) Transport of ferric-aerobactin into the periplasm and cytoplasm of Escherichia coli K12: role of envelope-associated proteins and effect of endogenous siderophores. J. Gen. Microbiol. 138: 597-603
- Yamamoto, S., Okujo, N. and Sakakibara, Y. (1994) Isolation and structure elucidation of acinetobactin, a novel siderophore from *Acinetobacter baumanii*. Arch. Microbiol. 162: 249-254
- Yeoman, K. H., deMay, A. G., Luca, N. G., Stuckey, D. B. and Johnston, A. W. B. (1999) A putative ECF sigma factor gene, *rpoI*, regulates siderophore production if *Rhizobium leguminosarum*. Mol. Plant-Microbe. Interact. 12: 994-999
- Yeoman, K. H., Wisniewski-Dye, F., Timony, C., Stevens, J. B., deLuca, N. G., Downie, J. A. and Johnston, A. W. B. (2000) Analysis of the *Rhizobium leguminosarum* siderophore-uptake gene *fhuA*: differential expression in free-living bacteria and nitrogen-fixing bacteroids and distribution of an *fhuA* pseudogene in different strains. Microbiology 146: 829-837

- Zhao, G. H., Ceci, P., Ilari, A., Giangiacomo, L., Laue, T. M., Chiancone, E. and Chasteen, N. D. (2002) Iron and hydrogen peroxide detoxification properties of DNA-binding proteins from starved cells – A ferritin like DNA-binding protein of *Escherichia coli*. J. Biol. Chem. 277: 27689-27696
- Zhao, Q. and Poole, K. (2000) A second *tonB* gene in *Pseudomonas aeruginosa* is linked to the *exbB* and *exbD* genes. Microbiol. 184: 127-132
- Zhao, Q. and Poole, K. (2002) Mutational analysis of the TonB1 energy coupler of *Pseudomonas aeruginosa*. J. Bacteriol. 184: 1503-1513
- Zhao, Q., Li, X. –Z., Mistry, A., Srikumar, R., Zhang, L., Lomovskaya, O. and Poole, K. (1998) Influence of the TonB energy-coupling protein on efflux-mediated multidrug resistance in *Pseudomonas aeruginosa*. Antimicrob. Agents. Chemother. 42: 2225-2231
- Zheng, M., Doan, B., Schneider, T. D. and Storz, G. (1999) OxyR and SoxRS regulation of *fur*. J. Bacteriol. 181: 4639-4643
- Zhu, W., Arceneaux, J. E. L., Beggs, M. L., Byers, B. R., Eisenach, K. D. and Lundrigan, M. D. (1998) Exochelin genes in *Mycobacterium smegmatis*: identification of an ABC transporter and two non-ribosomal peptide synthetase genes. Mol. Micro. 29: 629-639
- Zimmermann, L., Hantke, K. and Braun, V. (1984) Exogenous induction of the iron dicitrate transport system of *Escherichia coli*. J. Bacteriol. 159:271-277